INFORMATION TO USERS

This manuscript has been reproduced from the microfilm master. UMI films the text directly from the original or copy submitted. Thus, some thesis and dissertation copies are in typewriter face, while others may be from any type of computer printer.

The quality of this reproduction is dependent upon the quality of the copy submitted. Broken or indistinct print, colored or poor quality illustrations and photographs, print bleedthrough, substandard margins, and improper alignment can adversely affect reproduction.

In the unlikely event that the author did not send UMI a complete manuscript and there are missing pages, these will be noted. Also, if unauthorized copyright material had to be removed, a note will indicate the deletion.

Oversize materials (e.g., maps, drawings, charts) are reproduced by sectioning the original, beginning at the upper left-hand corner and continuing from left to right in equal sections with small overlaps.

Photographs included in the original manuscript have been reproduced xerographically in this copy. Higher quality 6" x 9" black and white photographic prints are available for any photographs or illustrations appearing in this copy for an additional charge. Contact UMI directly to order.

Bell & Howell Information and Learning
300 North Zeeb Road, Ann Arbor, MI 48106-1346 USA
800-521-0600

UMI®

University of Alberta

Iron in wastewater: Effect on quartz sleeve scale

By

Jason Marc Topnik ©

A thesis submitted to the Faculty of Graduate Studies and Research in partial fulfillment of the requirements for the degree of Master of Science

In

Environmental Science

Department of Civil and Environmental Engineering

Edmonton, Alberta

Fall 1999

National Library of Canada
Bibliothèque nationale du Canada

Acquisitions and Bibliographic Services
Acquisitions et services bibliographiques

395 Wellington Street
Ottawa ON K1A 0N4
Canada

395, rue Wellington
Ottawa ON K1A 0N4
Canada

Your file Votre référence

Our file Notre référence

The author has granted a non-exclusive licence allowing the National Library of Canada to reproduce, loan, distribute or sell copies of this thesis in microform, paper or electronic formats.

L'auteur a accordé une licence non exclusive permettant à la Bibliothèque nationale du Canada de reproduire, prêter, distribuer ou vendre des copies de cette thèse sous la forme de microfiche/film, de reproduction sur papier ou sur format électronique.

The author retains ownership of the copyright in this thesis. Neither the thesis nor substantial extracts from it may be printed or otherwise reproduced without the author's permission.

L'auteur conserve la propriété du droit d'auteur qui protège cette thèse. Ni la thèse ni des extraits substantiels de celle-ci ne doivent être imprimés ou autrement reproduits sans son autorisation.

0-612-47108-X

Canada

University of Alberta

Library Release Form

Name of Author: Jason Marc Topnik

Title of Thesis: Iron in wastewater: Effect on quartz sleeve scale

Degree: Master of Science

Year this Degree Granted: 1999

Permission is hereby granted to the University of Alberta Library to reproduce single copies of this thesis and to lend or sell copies for private, scholarly, or scientific research purposes only.

The author reserves all other publication and other rights in association with the copyright in the thesis, and except as hereinbefore provided, neither the thesis nor any substantial portion thereof may be printed or otherwise reproduced in any material form whatever without the author's prior written permission.

Permanent Address:
203 11011-86th Avenue
Edmonton, Alberta
T6G-0X1

Date: September 8, 1999

University of Alberta

Faculty of Graduate Studies and Research

The undersigned certify that they have read, and recommend to the Faculty of Graduate Studies and Research for acceptance, a thesis entitled Iron in wastewater: Effect on quartz sleeve scale submitted by Jason Marc Topnik in Partial fulfillment of the requirements for the degree of Master of Science in Environmental Science.

Daniel W. Smith – Supervisor

Ian D. Buchanan – Co-Supervisor

Jeremy J. Leonard

Date: September 1 1999

Dedicated to my loving wife,

Melissa Marie Topnik

It was her love and support that truly made this thesis what it is.

As well, I would like to thank my parents,

Ms. Ellie Topnik; and,

Dr. Brian Topnik Ph.D., P.Eng.

It was because of their encouragement that I pursued this Masters of Science degree and if it were not for their unending emotional, and financial support, I would not be completing this degree.

I love and thank you all.

Abstract

Bench scale analysis was conducted on 20 L of activated sludge which was spiked with high concentrations of iron (either reagent grade ferrous or waste ferrous). The activated sludge was aerated and analyzed for total and ferrous iron every two hours for a total of three times. The total iron concentrations were found to decrease over the six hour aeration period to approximately 0.35 mg/L. Filtered effluent total iron concentrations were found to be approximately 0.10 mg/L. Ultraviolet light quartz sleeve analyses was performed in which quartz glass coupons 10 mm x 10 mm in size were heated to 50 °C and exposed to effluents with iron concentrations of 1.5 mg/L total iron. Samples were exposed for 24 and 48 hours after which time they were analyzed for iron scale deposits using a scanning electron microscope and the inductive couple plasma (ICP) technique. The scanning electron microscope provided evidence that scaling was occurring. Most scale build-up was due to calcium scale as well as clay particles. Iron was found to be present on all quartz glass coupons in varying percentages. The amount of iron scale that may be present is unlikely to hinder the disinfection ability of the WWTP provided that the cleaning mechanism removes all residue and iron scale deposits.

Acknowledgments

The author wishes to express his sincere appreciation to Dr. Daniel W. Smith and Dr. Ian D. Buchanan for their guidance, encouragement and understanding throughout the experimental investigations and preparation of this manuscript. Without their support, the completion of this project would not have been possible.

The author would also like to thank Mr. Nick Cherunka for his assistance in the development of the experimental procedure and setup of the experimental equipment. As well, his timely suggestions and discussions were invaluable in the completion of the project.

The author would also like to acknowledge Mrs. Maria Demeter for her unending support and help throughout the experimental analysis, as well as her countless suggestions, for which I am truly grateful.

A thank you is also extended to Gary Solonynko and Debra Long for their support during the experimental portion of the project, for without their help this project would still be in the analysis phase.

Finally, I would like to thank the Gold Bar Wastewater Treatment Plant Staff for their cooperation and assistance throughout the project. Financial support for this project was provided by the City of Edmonton.

Table of Contents

1.0 Introduction _____ *1*

1.1 Gold Bar Wastewater Treatment Plant Processes _____ **2**

1.2 Previous anaerobic digester study _____ **4**

1.3 Cause for concern _____ **5**

2.0 Project objectives _____ *7*

3.0 Literature Review _____ *8*

3.1 Disinfection _____ **8**

3.2 Criteria needed for disinfection _____ **10**

3.3 Mechanisms of disinfection _____ **13**

3.4 Wastewater disinfection processes _____ **14**

3.4.1 Chemical agents _____ 14

3.4.2 Mechanical Agents _____ 16

3.4.3 Radiation _____ 16

3.5 Ultraviolet light radiation _____ **17**

3.5.1 Mechanism of UV destruction _____ 17

3.5.1.1 Electromagnetic radiation _____ 18

3.5.1.2 Electromagnetic spectrum _____ 19

3.5.1.3 Ultraviolet light radiation spectrum _____ 20

3.5.1.4 UV damage to DNA and RNA _____ 21

3.6 Microbial repair after exposure to UV _____ **24**

3.6.1 Photo-reactivation 24

3.6.2 Dark reactivation 27

3.6.3 SOS repair 27

3.7 UV mercury quartz lamps 28

3.7.1 Low pressure mercury lamps 28

3.7.2 Medium pressure lamps 29

3.8 Effect of suspended solids on UV performance 31

3.8.1 The Lambert-Beer law 33

3.8.2 UV absorbance and transmittance 34

3.9 Iron characteristics 36

3.10 Quartz lamp fouling 38

3.10.1 Classification of Fouling 39

3.10.2 Fouling events 41

3.10.3 Mineral scales 43

3.10.4 Iron and possible scale formation 44

4.0 Methods and Materials 47

4.1 Materials 47

4.2 Analytical techniques 48

4.2.1 Total sulfide measurement 48

4.2.2 Ferrous and Ferric iron determination 49

4.2.3 TSS analysis 50

4.3 Experimental protocol 51

4.3.1 Digester sludge experiment protocol 51

4.3.1.1 Experiment A: Digester sludge 51

4.3.1.2 Experiment B: Digester sludge 52

4.3.2 Activated sludge experimental protocol 53

4.3.2.1 Experiment A: Activated sludge 53

4.3.2.2 Experimental arrangement for experiment A 55

4.3.2.3 Experiment B: Activated sludge 58

4.3.2.4 Experimental arrangement for experiment B 58

4.3.3 Wastewater Treatment plant influent and effluent analysis 60

4.3.4 Iron quartz sleeve scaling experiment 61

4.3.4.1 Quartz scale experimental procedure 61

4.3.4.2 Iron scale determination 62

4.3.4.3 Experimental arrangement for quartz sleeve experiments 64

5.0 Results and Discussion ***69***

5.1 Current treatment plant iron concentrations 69

5.2 Iron determination on treatment plant influent and effluents 71

5.3 Sulfide analysis 73

5.4 Aerated return activated sludge (RAS) iron analysis experiment A 75

5.5 Aerated mixed liquor iron analysis experiment B. 79

5.6 Comparison of 0.45 μm filtered and 0.2 μm filtered effluents in experiment B 83

5.7 pH analysis of experiment B 85

5.8 TSS and iron / TSS ratio analysis of Experiment B 86

5.9 Combined experiments A and B. 89

5.9.1 Statistical comparison of experiments A and B for all samples of total and ferrous irons ____ 91

5.10 Quartz scale analysis ____ **93**

5.10.1 Transmittance data for quartz glass pieces ____ 96

5.10.2 Scanning electron microscope x-ray defraction ____ 98

5.10.3 Inductive coupled plasma analysis on quartz scale ____ 100

6.0 Conclusion ____ ***105***

7.0 Recommendations ____ ***107***

8.0 References ____ ***108***

Appendix A. Data for Sulfide Analysis ____ ***112***

Appendix B. Iron Experiment A. Data and Graphs ____ ***118***

Appendix C. Iron Experiment B. Data and Graphs ____ ***133***

Appendix D. TSS Data for Experiment B ____ ***152***

Appendix E. Iron Experiment B, pH Data ____ ***160***

Appendix F. Data for Raw Influent, Treated Effluent, RAS and Mixed Liquor ____ ***166***

Appendix G. Iron Experiment A and B Combined Graphs ____ ***175***

Appendix H. Iron Scale Data ____ ***190***

Appendix I. Quantitative Analysis Data for Quartz Glass Piece ____ ***196***

Appendix J. Transmittance Data for Quartz Glass Pieces ____ ***238***

List of Tables

Table 1. Infectious agents potentially present in raw domestic wastewater 9

Table 2. Comparison of ideal and actual characteristics of commonly used disinfectants 12

Table 3. Absorbance and transmittance data for different levels of treatment ... 35

Table 4. Iron complexes found in natural water conditions at equilibrium 38

Table 5. Materials for all experiments conducted..... 47

Table 6. Experimental arrangement for experiment A: Digester sludge. Control sample. 55

Table 7. Experimental arrangement for experiment A: Activated sludge, Control sample 55

Table 8. Experimental arrangement for experiment A: Digester sludge, Ferrous sample. 56

Table 9. Experimental arrangement for experiment A: Activated sludge, Ferrous solution sample 56

Table 10. Experimental arrangement for experiment A: Digester sludge, Waste solution sample. 57

Table 11. Experimental arrangement for experiment A: Activated sludge, Waste solution sample 57

Table 12. Experimental arrangement for experiment B: Digester sludge, Control sample. 58

Table 13. Experimental arrangement for experiment B: Activated sludge, Control sample 59

Table 14. Experimental arrangement for experiment B: Digester sludge, Ferrous sample. 59

Table 15. Experimental arrangement for experiment B: Activated sludge, Ferrous solution sample 59

Table 16. Experimental arrangement for experiment B: Digester sludge, Waste solution sample. 60

Table 17. Experimental arrangement for experiment B: Activated sludge, Waste solution sample 60

Table 18 Experimental arrangement for 1.5 mg/L trials 64

Table 19 Experimental arrangement for 3.0 mg/L trial 64

Table 20 Experimental arrangement for treated effluent 64

Table 21. Data for total iron in plant influent and effluent 70

Table 22. Total iron data for treatment plant influent and effluents 71

Table 23. TSS data for supernatant treatment plant influent and effluents 71

Table 24. Ratio data for treatment plant influent and effluents 72

Table 25. Total S^{-2} data for the duration of the sulfide experiment 74

Table 26. Statistical analysis of 0.45 μm and 0.2 μm samples, (control) 84

Table 27. Statistical analysis of 0.45 μm and 0.2 μm samples, (ferrous solution) 85

Table 28. Statistical analysis of 0.45 μm and 0.2 μm samples, (waste solution) 85

Table 29 Statistics of experiment A and B control sample 92

Table 30 Statistics of experiment A and B ferrous sample 92

Table 31 Statistics of experiment A and B waste sample 93

Table 32. Transmittance data 1.5 mg/L sample at 24 hours exposure, experiment 1 96

Table 33. Quantitative analysis data of particle 1 on 1.5 mg/L Experiment 1 at 48 hours 100

Table 34. 1.5 mg/L sample, experiment 2 at 24 hours 101

Table 35. Percent of iron associated with quartz lamp sleeve scale using ICP analyses. 102

Table 36. Percent of iron found in all x-ray defraction analyses. 103

List of Figures

Figure 1. Flow schematic for Gold Bar Wastewater Treatment Plant 4

Figure 2. Absorption spectrum of Nucleic acids with comparison to *E. coli* killing 22

Figure 3. Thymine dimer 23

Figure 4. Particle shading and incomplete penetration 32

Figure 5. Estimated lamp sleeve fouling rate 46

Figure 6. Calibration line for iron analysis 50

Figure 7. Aeration of mixed liquor 54

Figure 8. Heating column used to heat quartz glass pieces to 50 °C. 65

Figure 9. Tank used to hold mixed liquor during aeration 66

Figure 10. Volume of mixed liquor at the completion of settling 67

Figure 11. Batch Reactor set up used in scale experiment 68

Figure 12 Close up of quartz glass coupons 68

Figure 13. Total iron in treatment plant influent and effluent using ICP 69

Figure 14. Graph of total unfiltered iron influent, effluent, RAS and ML settled supernate 72

Figure 15. Graph of total iron (mg/L) / TSS (mg/L) for treatment plant influent and effluents 73

Figure 16. Amount of total S^{-2} present in the sampled digester sludge 74

Figure 17. Total iron, dissolved and suspended for control sample experiment A 76

Figure 18. Total iron, dissolved and suspended for reagent grade ferrous solution sample experiment A 76

Figure 19. Total iron, dissolved and suspended for industrial waste solution sample experiment A 77

Figure 20. Graph of total iron, total dissolved iron and total suspended iron for the control, ferrous solution and waste solution experiments 78

Figure 21. Total iron, dissolved and suspended for control sample experiment B. 80

Figure 22. Total iron, dissolved and suspended for ferrous solution sample experiment B 80

Figure 23. Total iron, dissolved and suspended for industrial waste solution sample experiment B 81

Figure 24. Graph of total iron, total dissolved iron and total suspended iron for the control, ferrous solution and waste solution samples experiment 82

Figure 25. Comparison of total iron filtered samples through 0.2 μm pore size and 0.45 μm pore size for control sample experiment B. 84

Figure 26. Graph of all pH data for control, ferrous solution and waste solution samples in experiment B: Activated sludge 86

Figure 27. All TSS data for trials 2 and 3 for control, ferrous and waste solutions in experiment B: Activated sludge 87

Figure 28. Iron / TSS ratio data for trials 2 and 3 for control, ferrous and waste solutions in experiment B: Activated sludge 87

Figure 29 Average iron for trials 2 and 3..... 88

Figure 30. Average TSS and iron / TSS ratio for trials 2 and 3..... 88

Figure 31. Graph of total iron for control sample for both experiment A and B. 90

Figure 32. Graph of total iron for ferrous sample for both experiment A and B. 90

Figure 33. Graph of total iron for waste sample for both experiment A and B... 91

Figure 34. Total iron analysis over experimental period for all experiments..... 94

Figure 35. TSS analysis over experimental period for all experiments..... 94

Figure 36. Iron/TSS ratio graph over experimental period for all experiments... 95

Figure 37. Transmittance data for all trials at 24 hours exposure..... 97

Figure 38. Transmittance data for all trials at 48 hours exposure..... 97

Figure 39. Particle 1 on 1.5 mg/L Experiment 1 at 48 hours..... 99

1.0 Introduction

Increasingly, concern over the use of chemicals for reducing microbial populations in wastewater has resulted in the implementation of alternative methods for wastewater disinfection. One of these alternatives is the use of ultraviolet light radiation. Ultraviolet light (UV) treatment is a physical process in which high intensity electromagnetic radiation is emitted from a mercury lamp which causes disruption of microbial cellular processes. UV radiation effectiveness is reduced by suspended particles in the wastewater or other materials which may absorb the UV light. One element in particular is iron. Iron is known to absorb UV light and therefore reduce the effectiveness against pathogenic organisms.

Anaerobic digesters are common to large wastewater treatment plants and are used to breakdown hard-to-degrade organic matter. The digester process produces by-products such as methane, carbon dioxide and offensive odorous gases such as hydrogen sulfide (H_2S). One method used to reduce emissions of these offensive gasses is the addition of iron. The iron will react with the hydrogen sulfide to produce a stable, non-odorous compound called pyrite (FeS). Sludge from these digesters is often disposed of at a lagoon for further degradation and settling. A portion of the lagoon supernatant is recycled to the headworks of the municipal wastewater treatment plant.

There is concern that if iron is used for the precipitation and removal of hydrogen sulfide gas, the pyrite produced in the reaction may resolubolize in the sludge lagoons and re-enter the treatment plant along with other dissolved iron added in excess amounts to anaerobic digesters, causing increased levels of iron and ultimately affecting the performance of the UV microorganism reduction.

1.1 Gold Bar Wastewater Treatment Plant Processes

Research samples for this thesis project were obtained from the Gold Bar Wastewater Treatment Plant (GBWWTP) located in Edmonton, Alberta, Canada. The Gold Bar WWTP uses a plug-flow activated sludge treatment process and treats approximately 95% of the domestic and industrial wastewater generated by the City of Edmonton. The remaining 5% are treated at the Capital Region Sewage Treatment Plant (CRSTP). Gold Bar WWTP discharges its treated effluent into the North Saskatchewan River, and is required to meet effluent standards established by Alberta Environmental Protection under the terms of the "Approval to Operate". The current requirements are a five-day carbonaceous biochemical oxygen demand ($cBOD_5$) of 25 mg/L and total suspended solids (TSS) of 25 mg/L. This is based on a daily average with neither $cBOD_5$ nor TSS to exceed 75 mg/L on more than one day during that same month. The current microbial reduction requirements are those established by Alberta Environmental Protection in June 1997. The effluent total coliform (TC) limit is 1000 CFU/ 100 mL in a grab sample, while fecal coliforms (FC) can not exceed 200 CFU/ 100 mL in a grab sample.

The main process stream of the Gold Bar wastewater treatment process consists of five main processes:

1. preliminary grit removal and screening;
2. primary settling of solids;
3. secondary treatment with air activated sludge and secondary clarification;
4. ultraviolet radiation of secondary clarifier effluent; and
5. anaerobic digestion for further degradation of settled organic matter.

A schematic of the wastewater treatment processes can be seen in Figure 1. The primary grit and screenings removed from the wastewater are collected and disposed of at the Clover Bar landfill located in the east end of the City of Edmonton. Biological gas production such as methane, which is produced during the anaerobic digestion of sludge, are used to fuel boilers, which heat the various buildings. The GBWWTP uses a Trojan UV 4000 unit as its sole means of microorganism reduction. The Trojan UV 4000 unit uses medium pressure mercury lamps that are unique in that they are self-cleaning in the removal of scale and biological film deposits. They can therefore maintain a more constant dose of ultraviolet radiation to the wastewater.

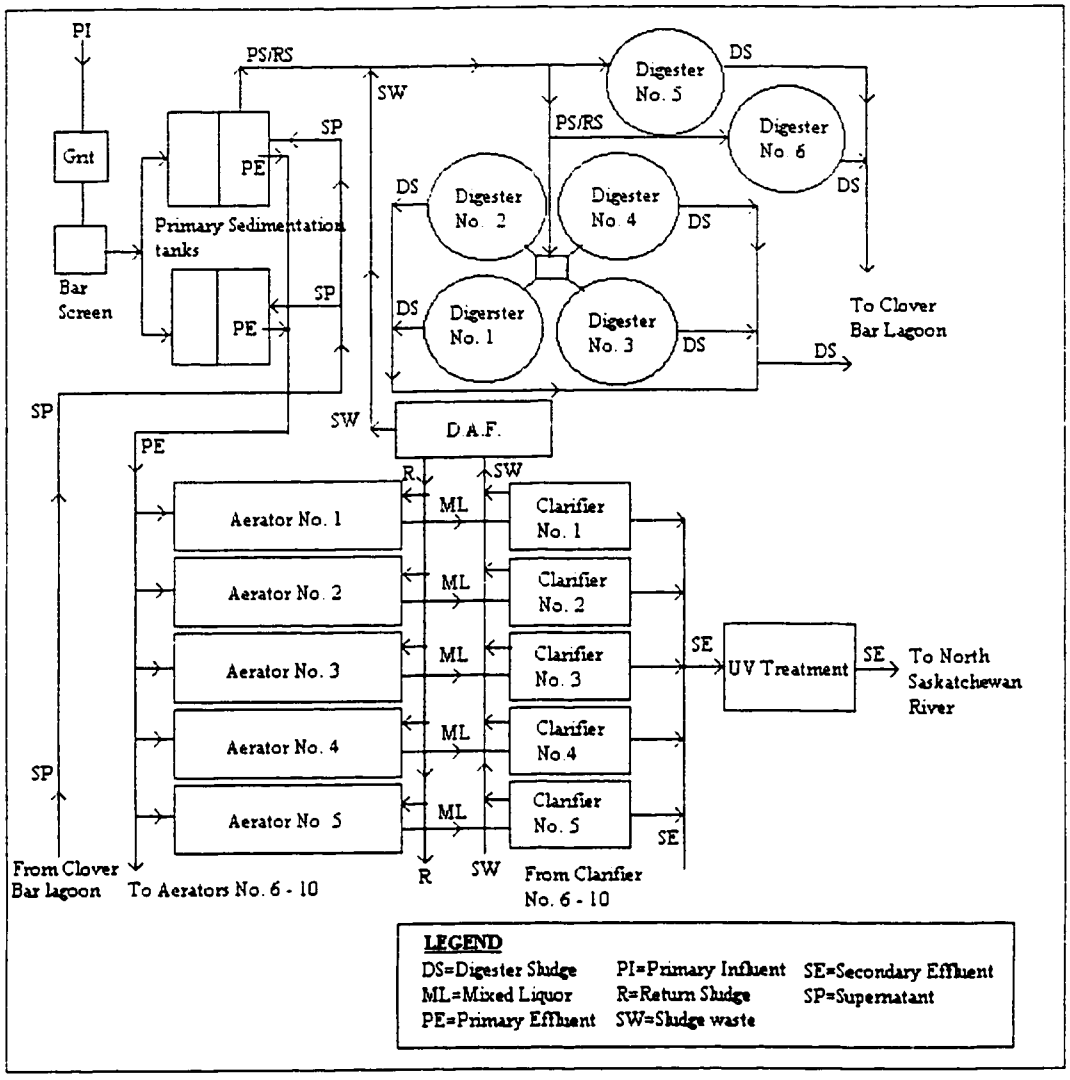

Figure 1. Flow schematic for Gold Bar Wastewater Treatment Plant

1.2 Previous anaerobic digester study

Graduate research was conducted at the University of Alberta into the removal of hydrogen sulfide gas from anaerobic digesters (Chiarella 1998). The research was performed at the GBWWTP owned and operated by the City of Edmonton, AB. Three different iron solutions were investigated in the removal of

H_2S gas. The first was a ferrous chloride solution ($FeCl_2 \bullet 4H_20$), with the reaction producing pyrite.

$$\mathbf{Fe^{2+} + HS^- \Leftrightarrow FeS + H^+} \qquad \mathbf{(1.1)}$$

The second was a ferric chloride solution ($FeCl_3 \bullet 6H_20$) which resulted in an ferric sulfide precipitate.

$$\mathbf{2Fe^{3+} + 3HS^- \Leftrightarrow Fe_2S_3 + 3H^+} \qquad \mathbf{(1.2)}$$

The third chemical added, was an industrial waste by-product with an extremely high ferrous iron content (153,000 mg/L), as well as other metals such as zinc at a concentration of (9,630 mg/L), which in-turn would react with H_2S and further precipitate sulfide. Concentrations of ferrous iron (Fe^{2+}) as high as 50 to 60 mg/L were found to precipitate 75% to 85% of the sulfide while much higher concentrations of ferric iron (Fe^{3+}), up to 330 mg/L, where necessary to achieve similar sulfide removal. The industrial waste by-product was found to give similar results to those obtained with the ferrous chloride solution. It was then concluded that only two of the three solutions were effective at reducing the sulfide gas (Chiarella 1998).

1.3 Cause for concern

In the H_2S reduction experiment, it was concluded that the addition of iron would result in the odor reduction due to the offensive hydrogen sulfide gas. Ferrous chloride solution and the industrial waste iron by-product solution were both determined to reduce effectively the amount of H_2S gas. If the GBWWTP

were to implement the addition of iron at the recommended concentrations to reduce the sulfide emissions, iron may eventually be re-cycled to the headworks of the treatment plant and be discharged with the final effluent. The sludge from the anaerobic digesters is discharged to the Clover Bar holding ponds. It is at the Clover Bar lagoons that the pyrite and insoluble sulfide precipitates generated in the anaerobic digester will settle out. Depending on the initial concentration of the pyrite and the pH of the lagoon, some of the iron may be re-solublolized. In 1997 Gold Bar WWTP had a daily flow of approximately 264 ML/day. Of this 264 ML/day, a maximum flow of 11 ML/day is recycled supernatant from the Clover Bar lagoons. Insoluble oxides such as FeO, Fe_3O_4 and Fe_2O_3 may be formed during aeration in the activated sludge process and iron may further precipitate out of solution. However, soluble and colloidal iron is present and may be carried over to the ultraviolet microorganism reduction stage. The concern was that the amount of iron reaching the UV process would increase as a result of the $FeCl_2$ odour reduction process.

2.0 Project objectives

The purpose of this study was to investigate the potential effect that the addition of iron to anaerobic digesters for odour control will have on the quartz lamp sleeve scale on the Trojan UV 4000 ultraviolet system. The major objectives of this study were as follows:

1. To quantify the amount of iron that will potentially be re-cycled into the WWTP from the Clover Bar sludge lagoons.
2. To estimate the amount of iron that would potentially reach the UV treatment system.
3. To experimentally determine the amount of iron scale that will form on the quartz lamp sleeves of the Trojan UV 4000 unit.
4. To assess the advisability of adding iron to the anaerobic digesters for the reduction of hydrogen sulfide gas.

3.0 Literature Review

3.1 Disinfection

Disinfection of wastewater is the removal of all pathogenic microorganisms. This is quite different from sterilization, which is the removal of all microorganisms (Metcalf and Eddy 1991). Pathogenic organisms (or particles in the case of viruses) are those which cause infection or disease and fall into three different categories. These include unicellular bacteria, virus particles and multi-cellular protozoa. Bacterial diseases include typhoid, cholera, paratyphoid and bacillary dysentery. Waterborne viral infections include enteroviruses, rotavirus and several different types of hepatitis virus. These viruses can cause gastroenteritis and infectious hepatitis. Two of the most important protozoan pathogens are *Cryptosporidium parvum*, which causes diarrhea, and *Giardia lamblia*, which will cause a mild to severe diarrhea, nausea and indigestion (Metcalf and Eddy 1991). Other organisms and the respective diseases they cause can be found in Table 1.

Disinfection indicator organisms are selected on the basis of their presence in high concentrations in wastewater. They must also have a similar sensitivity to a given disinfectant as the pathogens, and show a similar inactivation rate. The indicator must be easily quantifiable using reliable and reproducible methods. The most commonly used indicators are total and fecal coliforms, *Escherichia coli* and *fecal streptococci* (Sakamoto 1998).

Table 1. Infectious agents potentially present in raw domestic wastewater

(Adapted from Metcalf and Eddy (1991))

Organism	Disease	Remarks
Bacteria		
Escherichia coli	Gastroenteritis	Diarrhea
Legionella pneumophila	Legionellosis	Acute respiratory illness
Leptospira (150 spp.)	Leptospirosis	Jaundice, fever
Salmonella typhi	Typhoid fever	High fever, diarrhea
Vibrio cholerae	Cholera	Extremely heavy diarrhea
Viruses		
Adenovirus (31 types)	Respiratory disease	
Enteroviruses (67 types, e.g., polio, echo and Coxsackie)	Gastroenteritis, heart anomalies	
Hepatitis A	Infectious hepatitis	Jaundice, fever
Reovirus	Gastroenteritis	
Rotavirus	Gastroenteritis	
Protozoa		
Balantidium coli	Balantidiasis	Diarrhea, dysentery
Cryptosporidium	Cryptosporidiosis	Diarrhea
Entamoeba histolytica	Amebiasis	Prolonged diarrhea
Giardia lamblia	Giardiasis	Mild to sever diarrhea

3.2 Criteria needed for disinfection

When alternative disinfection systems are being considered, several factors must be taken into account. The disinfectant must be toxic to the intended organism and produce an effective kill at high dilutions or low concentrations of disinfectant. Regardless of the temperature or pH of the wastewater, the disinfectant should be highly soluble. Once the disinfectant is added to the wastewater, its potency should be stable for long periods of time.

Major concerns about some chemical disinfectants are that they will harm the aquatic environment to which they are eventually released. Therefore, the disinfectant chosen should be effective against the desired microorganism, yet disappear before reaching the receiving environment or are nontoxic to higher forms of life. The disinfectant should have a homogeneity in which the solution must be uniform in composition. Since we are dealing with disinfecting wastewater, we can assume that the solution is relatively high in organic matter. It is desirable that the disinfectant chosen should only interact with the intended microorganisms and not the other material present in the solution. Temperature fluctuations are common in many wastewater treatment plants and therefore the disinfectant must be able to maintain a sufficient potency throughout a wide range of temperatures. Several of the pathogenic organisms have protective coatings which may be difficult to penetrate. The disinfectant must be able to penetrate these surfaces and destroy or inactivate the organism. Wastewater treatment plants contain many components that may be susceptible to corrosion, therefore

the disinfectant that will minimize this effect should be chosen. In many instances the treated wastewater may still have some type of odor associated with it depending on the level of primary and secondary treatment. If this is the case, then a disinfectant that will reduce this odor may be considered. Finally the disinfection system should be relatively inexpensive to operate and maintain, and the disinfectant should be available in large quantities which are easily obtainable (Metcalf and Eddy 1991). Table 2 lists these mentioned parameters and the characteristics of some of the more commonly used disinfectants.

Table 2. Comparison of ideal and actual characteristics of commonly used disinfectants (after Metcalf and Eddy 1991)

Characteristic	Properties/ Response	Chlorine	Sodium hypochlorite	Calcium hypochlorite	Chlorine dioxide	Bromine chloride	Ozone	UV radiation
Toxicity to microorganisms	Should be highly toxic at high dilutions	High	High	High	High	High	High	High
Solubility	Must be soluble in water or cell tissue	Slight	High	High	High	Slight	High	N/A
Stability	Loss of germicidal action on standing should be low	Stable	Slightly unstable	Relatively stable	Unstable, must be generated as used	Slightly unstable	Unstable, must be generated as used	Must be generated as used
Nontoxic to higher forms of life	Should be toxic to microorganisms and nontoxic to man and other animals	Highly toxic to higher life forms	Toxic	Toxic	Toxic	Toxic	Toxic	Toxic
Homogeneity	Solution must be uniform in composition	Homogeneous	Homogeneous	Homogeneous	Homogeneous	Homogeneous	Homogeneous	N/A
Interaction with extraneous material	Should not be absorbed by organic material other than bacterial cells	High	High	High	High	High	High	High
Toxicity at ambient temperatures	Should be effective in ambient temperature range	High	High	High	High	High	High	Moderate
Penetration	Should have the capacity to penetrate through surfaces	High	High	High	High	High	High	Moderate
Noncorrosive and nonstaining	Should not disfigure metals or stain clothing	Highly corrosive	Corrosive	Corrosive	Highly corrosive	Corrosive	Highly corrosive	N/A
Availability	Should be available in large quantities and reasonably priced	Low cost	Moderate low cost	Moderately low cost	Moderately low cost	Moderately low cost	Moderately high cost	Moderately high cost

3.3 Mechanisms of disinfection

The ultimate goal of disinfection is the destruction of pathogens. But how exactly is this accomplished? Bacteria, viruses and protozoa each have structural components which protect them from their environments and provide structural support. Bacteria such as *Escherichia coli*, *Klebsiella* and *Salmonella* are classified as gram negative bacteria. Other bacteria such as *Streptococcus*, *Bacillus* and *Clostridium* are classified as gram positive bacteria (Prescott et al. 1990). Gram-positive or gram-negative refers to a characteristic of the outer membrane layer that the bacteria. This outer layer is known as peptidoglycan, and if altered, will compromise the integrity of the bacteria. Many antibiotics used in medicine today are designed to alter or disrupt this structural layer and destroy the bacteria (Levinson and Jawetz 1996). This too is the goal of a good disinfectant. It can alter the structure of enzymes which are crucial to the function of the microorganism, damage the outer peptidoglycan layer so that it can no longer protect the cell's inner contents and therefore cause cell death.

Viruses are quite unique and different from bacteria. Viruses do not have complex internal structures like bacteria and lack a peptidoglycan layer (Prescott et al. 1990). They are constructed strictly of protein and deoxyribonucleic acid (DNA) or ribonucleic acid (RNA), the building blocks of life. In some cases the virus may be encapsulated in a membrane, which is obtained from the host from which it is released during cell lysis (White and Fenner 1994). Alteration of

either the protein capsule or the generic material by any means will disrupt the ability of the virus to attach to and destroy its particular host cell.

3.4 Wastewater disinfection processes

There are several different ways in which disinfection can be carried out in a wastewater treatment plant. These include chemical agents, mechanical agents, and radiation.

3.4.1 Chemical agents

Of all the different disinfection agents available, the chemical agents are the most widely accepted and generally the most popular forms of disinfection. Chemical agents such as chlorine, bromine and iodine are known as strong oxidizing agents and are highly reactive. Chlorine is one of the most widely used chemical agents, while bromine and iodine are used on a more limited basis. Chlorine can be used as a disinfectant in several different ways. Chlorine gas when present with water will produce the following reaction:

$$\mathbf{Cl_2 + H_20 \Leftrightarrow HOCl + H^+ + Cl^-} \qquad \mathbf{(3.1)}$$

The hypochlorous acid (HOCl) will then further ionize to:

$$\mathbf{HOCl \Leftrightarrow H^+ + OCl^-} \qquad \mathbf{(3.2)}$$

The amount of HOCl and hypochlorite (OCl^-) that is found in solution is known as the free available chlorine. The reaction is dependent on temperature and the pH of the wastewater. These parameters are very important due to the

fact that the HOCl is about 40 to 80 times more effective as a disinfectant than is OCl^- (Metcalf and Eddy 1991).

Another strong oxidizing agent is the chemical ozone. Ozone is produced when air or pure oxygen are passed through an electrical field. The O_2 molecules are split and recombine to form as O_3. The ozone molecule is a highly reactive chemical and because of this must be generated on-site. Ozone's destructive nature is brought about by is decomposition (Metcalf and Eddy 1991). Ozone is an effective killing agent, however, its decomposition is such that it does not produce a long lasting residual in water. Chlorine is therefore chosen when residual effects are required since its decomposition rate is considerably less than that of ozone.

Chemicals which will change the pH of the wastewater may also be used as a disinfectant. Altering the pH of the water with either a highly acidic chemical or some type of alkaline agent will disrupt the chemical and biological nature of the pathogen. Generally, most bacteria can not survive in environments with a pH greater than 11 or less than 3. By changing the pH, the physical structure of essential biological proteins will be altered. This not only causes the functions of the biological process to be changed, but all inner and outer structures will change shape as well. The final result is the lysis of the cell and ultimate death (Metcalf and Eddy 1991).

3.4.2 Mechanical Agents

The mechanical agents of disinfection are essentially the entire wastewater treatment process. As the wastewater passes through the coarse and fine screens, particles are removed to which bacterial and other organisms may be attached. Grit chambers, sedimentation tanks and filters will also cause a reduction in the numbers of pathogens released to the receiving waters (Metcalf and Eddy 1991).

3.4.3 Radiation

Three types of radiation are commonly used for disinfection. These include electromagnetic, acoustic and particle. (EPA 1986). The high intensity of gamma rays which are emitted from radioisotopes such as cobalt 60 have been used to disinfect as well as sterilize both water and wastewater (EPA 1992). Electromagnetic radiation is produced by UV disinfection systems and is also found in natural sunlight. UV radiation is generated by mercury pressure lamps. These lamps are submerged into a wastewater flow to expose pathogenic organisms to high intensity electromagnetic radiation. Sunlight is also an effective disinfectant since ultraviolet radiation is a major component of the total amount of radiation that reaches the earth. Effluents that are clear and free of suspended solids are able to have sunlight provide some microbial reduction during daylight periods. If the effluent contains high amounts of particles, then these particles may absorb the UV radiation and essentially reduce the amount that will reach the intended microorganism. For better performance, the effluent must be stored outside in large shallow holding ponds for a specific length of time

before being discharged to any receiving waters. It is important that the ponds be shallow to allow for complete penetration of the effluent by the sunlight (Metcalf and Eddy 1991).

3.5 Ultraviolet light radiation

Disinfection by ultraviolet light is classified as a physical process relying on the propagation of electromagnetic energy from a source (lamp) to an organism's cellular material (specifically, the cell's genetic material) (EPA 1986). Disinfection of wastewater using ultraviolet light is somewhat of a misnomer. As mentioned previously, disinfection is the destruction of all pathogenic microorganisms, while sterilization is the complete destruction of all organisms present. When UV light is used for the destruction or inactivation of pathogenic microorganisms, it achieves bacterial reduction rather than disinfection. Alberta Environmental Protection has stated that a disinfection system must meet effluent requirements of 200 fecal coliform (FC) colony forming units (CFU) /100 mL sample, and 1000 total coliform (TC) CFU / 100 mL sample (AEP 1997). However, this is a working definition rather than the correct technical definition.

3.5.1 Mechanism of UV destruction

Lethal effects of solar radiation were first observed in the 1800s by Downes and Blount (EPA 1986). They described the lethal effects of solar radiation on a mixed microbial population and assigned the cause of these effects to short-wave UV radiation. In the earlier part of the twentieth century UV was

first considered for the disinfection of potable water, however, the technology was not reliable and other disinfection means were becoming more popular (i.e. chlorine). In many locations chlorine was adapted for the use in potable water since it was inexpensive and was able to maintain a residual throughout the distribution network. Therefore, research was focused on chemical rather than physical processes.

3.5.1.1 Electromagnetic radiation

To understand the mechanism of UV destruction, the basic premise behind radiation must first be understood. Radiation must be absorbed before it can have an effect. Light in the visible spectrum is absorbed by molecules called pigments in which color is observed by reflectance or transmittance (EPA 1986). Light is universally described by wavelength. The frequency and wavelength of radiation are related by equation 3.3:

$$c = \nu\lambda \qquad (3.3)$$

Where c = the velocity of light (3×10^8 m per second in free space)

ν = frequency of vibration (vibration per second)

λ = wavelength (m)

Several terms are used to describe the quantity of radiation. The most common are the erg, calorie and watt-second or joule. All are measurements of total quantity of energy or work. Intensity or energy density of the radiation is

expressed in terms of energy incident upon a unit area. In UV systems the most common units used are mWatt/cm^2 or μWatt/cm^2 (EPA 1986).

Quantum theory states that radiant energy occurs in discrete units or quanta. The energy of these fundamental units is related to its frequency.

$$\mathbf{E = h\nu = hc/\lambda} \qquad \textbf{(3.4)}$$

Where: E = energy of a single quantum (erg)

h = Planck's constant (6.62×10^{-27} erg-sec)

c = the velocity of light (3×10^{10} cm per second)

ν = frequency of vibration (vibration per second)

λ = wavelength (cm)

From this equation it is evident that the energy content of a quantum is identical for a given wavelength of light (EPA 1986).

3.5.1.2 Electromagnetic spectrum

From equation 3.4 it can be shown that the higher the wavelength, the lower the energy, and conversely, the shorter the wavelength the higher the energy. The visible light spectrum consists of wavelengths in the range of 400 nm to 750 nm. At this range, the quantum energy is such that it will result in chemical changes in living organisms. These would include processes such as photosynthesis, phototaxis, and vision. Wavelengths of radiation in the range of 750 nm to 10^5 nm are known as infrared. Wavelengths such as micro waves and radio waves, lie in the range 10^6 nm to 10^{13} nm. These wavelengths are such that

the amount of energy that they produce is low and could not result in any chemical change in living organisms (EPA 1992). As the wavelengths are decreased below the visible spectrum, the quantum energy is increased, causing more harm to molecules and eventually biological functions. Immediately below the visible spectrum is ultraviolet light, followed by X-rays and eventually gamma-rays and cosmic rays (Sakamoto 1998). The energy is so intense at these very short wavelengths that any molecule being struck by these rays is instantly ionized.

3.5.1.3 Ultraviolet light radiation spectrum

The UV light spectrum is in the range of 100 nm to 400 nm, which lies between X- rays and visible light. Within this range of UV light there are four divisions. These being vacuum UV from 100 to 200 nm, UV-C in the range of 200 nm to 280 nm, UV-B from 280 nm to 315 nm and finally UV-A from 315 nm to 400 nm (EPA 1992). The germicidal range which is found to be most harmful to the reproduction of microorganisms is found in the UV-C region. Within this region molecules with double bond structures absorb UV light to the greatest extent, disrupting their basic structure and, as a result, their function (Sakamoto 1998).

3.5.1.4 UV damage to DNA and RNA

Deoxyribonucleic acid (DNA) and ribonucleic acid (RNA) are the genetic material that direct the functions of each and every cell. Typically, DNA and RNA make up about 5 to 15 percent of a cell's dry weight (EPA 1986). DNA and RNA are comprised of 5 different molecules. There are two purines: adenine and guanine, and the three pyrimidines: cytosine, thymine and uracil. The differences in DNA and RNA are slight. DNA contains adenine, guanine, cytosine and thymine, while RNA contains adenine, guanine, cytosine and uracil (Prescott et al. 1990). As mentioned before, molecules with double bond structures such as long chain unsaturated fatty acids absorb UV light in the UV-C region. Purines and pyrimidines, particularly, absorb UV light at a wavelength of 260 nm. Absorption spectrums of UV irradiated nucleic acid indicate that the highest amount of UV light absorbed by the RNA molecules is at a wavelength of 260 nm. This can be seen in Figure 2. Additional work was conducted by Sakamoto on the effect that these wavelengths have on the kill of *E. coli*. The form of the two graphs contained in Figure 2 is almost identical, indicating that what is inactivating the bacteria is the disruption of the genetic code which controls reproduction.

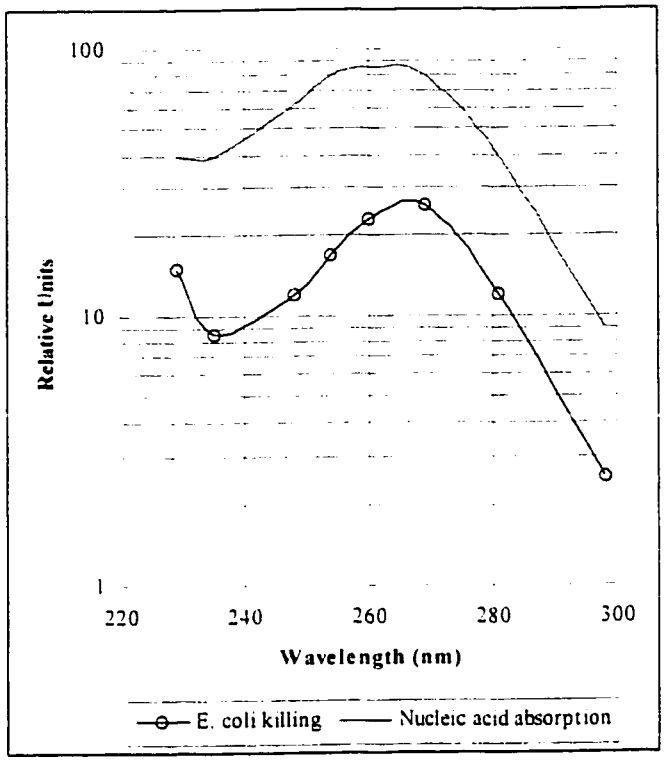

Figure 2. Absorption spectrum of Nucleic acids with comparison to *E. coli* killing (after Sakamoto 1998)

Damage to the genetic code occurs when UV light is absorbed by molecular bonds present in the genetic DNA. The purines and pyrimidines have molecular structures such that they are highly vulnerable to exposure to high energy UV light. The genetic code consists of alternating sequences of genetic base codes. Upon exposure to UV light, the genetic base code interaction is affected. When two thymine molecules are adjacent to one another, their double bonds absorb UV light and their original function is disrupted. Thymine bases normally interact with adenine, while guanine interact with cytosine. In RNA the only difference in the interactions is that thymine is not present, but is replaced by

uracil. The interaction is then between adenine and uracil. High intensity UV light disrupts these adjacent thymine molecules and results in the formation of a thymine dimer (Lehninger et al. 1993). This can be seen in Figure 3.

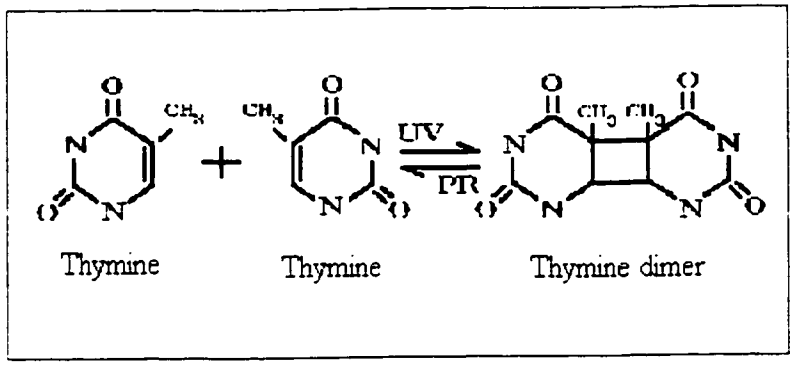

Figure 3. Thymine dimer

Due to the formation of these dimers, the genetic code is disrupted and function can be impaired. The genetic code is the building block from which all cell function is derived. Enzymes that normally would read these codes in a specific pattern are misguided by the formation of these dimers. If essential proteins are being produced, the disruption in the code will alter the position of certain amino acids and result in a possible inactive protein. Slight variations in the genetic code may be overlooked during replication and translation. However, if the UV energy is quite high and several sites on the strand have been disrupted, inactivation of the cell's function will result and ultimately cause death to the organism.

3.6 Microbial repair after exposure to UV

Bacteria have existed for millions of years and have adapted to extreme conditions. Upon exposure to UV damage, bacteria have evolved a repair process to reverse the destructive damage that is caused by this high intensity radiation. Provided that the damage is somewhat minimal, the organisms have several different repair processes. These include photo-reactivation, dark reactivation and in extreme cases, the SOS repair.

3.6.1 Photo-reactivation

Photo-reactivation is a process by which microorganisms have the ability to repair damage caused to DNA by exposure to high intensity electromagnetic radiation. Enzymes used for DNA replication are activated by longer wavelength light in the near UV and visible spectrum. This phenomenon, unique to UV, has been broadly termed photo-reactivation (EPA 1986). Photo-reactivation is not common to all microorganism and there is no classification as to which organisms have the ability to repair, and which do not. Some organisms which are known not to repair include *Haemophilus influenzae*, *Diplococcus pneumoniae*, *Bacillus subtilis*, and *Micrococcus radiodurnas*. Viruses generally do not have the ability to repair. However, when a virus is present within a cell, it too will be treated in the same way as the host DNA and will be repaired if its DNA is damaged (EPA 1986). Organisms which are known to undergo photoreactivation include *Streptomyces*, *Escherichia coli*, *Sacchaormyces*, *Aerobactor*, *Micrococcus*, *Erwinia*, *Proteus*, *Penicillium*, and *Nuerospora* (EPA 1986).

Several studies have been conducted (Baron 1997, Kashimada et al. 1996, Whitby et al. 1993), which indicate that, after exposure to UV radiation and subsequent exposure to light, bacterial counts increased as a result of some type of repair mechanism. Kashimada et al. (1996) investigated how visible light intensity relates to the photo-reactivation rate and the maximum survival in wastewater treatment processes. They investigated several different bacterial cultures including *E. coli* K12 A/λ(F+), *E. coli* B and indigenous heterotrophic bacteria, coliform groups and fecal coliforms in raw sewage influent. UV irradiation was accomplished by low pressure mercury lamp. After exposure to UV irradiation, the same organisms were exposed to fluorescent lamps, while others were exposed to sunlight. The bacterial cultures were then enumerated according to Standard Methods For Examination of Water and Wastewater (APHA 1992). *E. coli* cultures were exposed to a UV dose that ranged from 18.7 x 10^{-3} to 20.9 x 10^{-3} W sec/cm^2 while the effective dose at 360 nm wavelength of fluorescent light was kept constant at 0.15 x 10^{-3} W sec/cm^2 The results indicated that the cultures of *E. coli* did not photo-repair after 120 minutes of fluorescent light saturation. The heterotrophic and coliform bacteria were exposed to fluorescent light at a dose rates of 5.34 x 10^{-3} Wsec/cm^2 while the fecal coliforms were exposed to 3.85 x 10^{-3} W sec/cm^2. They were all then exposed to a light dose rate of 0.15 x 10^{-3} W sec/cm^2. These bacterial cultures did show some type of repair. Survival increased from 0.01 to 0.05 up to 0.3 to 0.5 log units after exposure time of 120 minutes. A possible explanation for why the *E. coli* bacteria

did not show some type of repair was that the exposure to these low doses of light was much less than that of ordinary sunlight and did not activate the required enzymes.

When the bacterial cultures were exposed to sunlight, photo-repair was observed with the *E. coli* cultures and repair was observed to be much more rapid than with fluorescent light. One interesting aspect with exposure to sunlight was that repair was observed to increase up to about 20 minutes of exposure, however after longer exposures to sunlight the survival was decreased. This decrease in survival can be explained by the disinfection due to sunlight. Sunlight can penetrate through the glass tubes that the cultures were stored in. Visible light within the range from wavelength 340 nm to 490 nm has some type of disinfection effect (Kashimada et al. 1996).

Seasonal variations are likely to affect the amount of photo-repair that will be experienced in the natural environment. This is due to light intensity and temperature, as well as overcast conditions. As would be expected, survival would be maximum during the summer months and least during the winter when the intensity of the effective light reaching the organism would be less. It is suggested that a mean repair level of 1.5 log should be anticipated as the maximum increase after UV exposure. Therefore, if a three log kill is required to meet microorganism reduction requirements, a 4.5 log reduction should be incorporated into the design of a UV system to account for possible photo-reactivation of the bacteria (EPA 1992).

3.6.2 Dark reactivation

Dark reactivation is a process by which repair of damaged DNA involves cleavage enzymes that clip out the thymine dimer (EPA 1992). The dark reaction, in which no light is required to activate the process is also known as excision repair. Specific enzymes nick the areas adjacent to the thymine dimer. An enzyme known as a exonuclease then releases the thymine dimer completely from the DNA strand and a replicating DNA enzyme then repairs the gap (EPA 1986).

3.6.3 SOS repair

When exposure to damaging high intensity radiation is quite severe, numerous sites on the DNA will be damaged. This normally would result in the death of the organism since the two repair mechanisms previously mentioned can not keep up the repair due to the increased number of damaged sites. This is when the microorganisms turn to what is known as the SOS repair mechanism. DNA damage is so great in these cases that the synthesis of the DNA stops completely, leaving many large gaps within the DNA strand. An enzyme known as recA will bind to the gaps and initiate strand exchange. Another protein known as lexA which is responsible for the regulation of proteins in DNA repair and synthesis is repressed by recA. Because of this repression of lexA, the replication and repair process is accelerated resulting in a repair system that can fix extensive damaged caused by UV radiation. This process is not without problems. Due to the fast repair of the DNA by recA, the replication is error prone and may produce

mutations in the DNA strand. However, to the survival of the organism, errors and mutations are better than no DNA replication at all (Prescott et al. 1990).

3.7 UV mercury quartz lamps

The high intensity electromagnetic radiation used in UV disinfection is generated by mercury vapor lamps, which are operated at either 10^{-3} to 10^{-2} torr (low-pressure lamps) or 10^{2} to 10^{4} torr (medium-pressure lamps) (Kwan et al. 1998).

3.7.1 Low pressure mercury lamps

Conventional low pressure mercury lamps are the most predominantly used lamp for the disinfection of wastewater. They produce a high output of germicidal UV radiation per watt of electrical energy consumed. However, they produce a low field of intensity (Havelaar et al. 1990). Low pressure lamps are often called monochromatic since they only produce a single energy intensity at 253.7 nm. When mercury vapor is maintained at a optimum pressure in the presence of a rare gas, it becomes an effective generator of high intensity light at a wavelength of 253.7 nm. The lower the vapor pressure inside the lamp, the greater the intensity of UV light at 253.7 nm. A low pressure mercury lamp has 35 to 40% of its input of energy converted to light, and approximately 85% of this light is generated at a 253.7 nm wavelength (EPA 1992).

Conventional low pressure mercury lamps may be installed in either closed chambers, teflon tubes or open channels. Open channel lamps may be placed either horizontally (parallel to the wastewater flow), or vertically (perpendicular to the flow).

High-intensity low pressure lamps are also available. These lamps operate at higher lamp discharge currents than the conventional low pressure mercury lamps. The low-pressure, high-intensity mercury lamps include special design features to maintain mercury pressure at an optimum level of 10^{-3} to 10^{-2} torr even at higher discharge currents. The energy efficiency from a high intensity lamp is the same as that of a conventional lamp and still produces a monochromic wave length at 253.7 nm. UV light is generated by an electrical discharge that generates light by transforming electrical energy into the kinetic energy of moving electrons (EPA 1992). This is then converted to radiation in a collision process.

3.7.2 Medium pressure lamps

Medium pressure mercury lamps operate at a higher pressure than do low pressure mercury lamps and have a higher field intensity of UV output. Because of this higher field intensity, they are somewhat less efficient because a substantial portion of the total energy is emitted in the visible spectrum (Havelaar et al. 1990). Medium pressure UV lamps are 254 mm in length and 25.4 mm in diameter. As mentioned previously they operate at higher vapor pressures, approximately 10^2 to 10^4 torr. The lamp wall temperature is substantially higher

than that of low pressure lamps and operate at temperatures from 600 to 800 °C. Medium pressure lamps are enclosed in a quartz sleeve which is 635 mm long and 89 mm in diameter. These quartz sleeves are cooled by the wastewater flowing past the disinfection modules and operate at a temperature of approximately 50 °C. (Murry 1998).

In medium pressure lamps all the mercury is evaporated and the pressure of the lamp is determined by the lamp manufacturer. This is quite different from low pressure mercury lamps which contain an excess amount of liquid mercury. The mercury pressure is controlled by the coolest part of the lamp wall. Medium pressure lamps generate more UV radiation than do the low pressure mercury lamps. The total amount of UV-C radiation that is produced by a medium pressure lamp is 9 to 14 W/cm arc length, which is about 50 to 80 times higher than that of the low pressure mercury lamp.

Medium pressure mercury lamps produce a very broad band spectrum of energy at several different germicidal wavelengths. However, medium pressure lamps are less efficient at producing radiation than are the low pressure mercury lamps. The energy output of a medium pressure lamps is 30 to 40% less than that of the low pressure systems. A large portion of the energy generated is converted to longer wavelength light and heat and only 25% of the radiation produced is in the UV-C germicidal region. In the low pressure mercury lamps, most if not all of the high intensity radiation is generated at the germicidal wavelength of 253.7

nm. In the medium pressure system, the UV-C light produced is not limited to 253.7 nm, but is distributed over the entire region (Kwan et al. 1998).

Medium pressure mercury lamps are often arranged in the same format as that of the low pressure mercury lamps, horizontal and parallel to the flow. Medium pressure lamps are often equipped with an automatic cleaning mechanism. This consists of a wiper that runs along the outside of the quartz lamp. To aid in cleaning, a chemical solution is used in conjunction with the wiper for the removal of scale. The most often used chemicals for the removal of quartz lamp sleeve scale are citric acid and Lime-A-Way®. Commercial detergents and dilute acids may also be used (EPA 1992). The cleaning mechanism is designed such that the lamps do not have to be removed or handled by an operator. The lamps may be cleaned while the UV system is in operation and therefore no down time in UV operation is required.

3.8 Effect of suspended solids on UV performance

Several factors can affect the transmission of UV light through a wastewater flow. Of the many criteria and design considerations that a wastewater treatment plant must operate under, suspended solids are of the utmost importance when considering the use of UV light for the disinfection of treated effluent. Suspended solids in treated effluent are regulated by provincial governments and vary from province to province. In Alberta, the Alberta Environmental Protection agency has set a 25 mg/L limit on the concentration of TSS that may be discharged to the environment. This is set on monthly average

of daily samples (AEP 1997). Suspended solids are composed of biological floc, oil and grease particles, clays and silts and numerous organic and inorganic compounds. All of these particulates present in the effluent being disinfected affect the ultimate performance of a UV facility. Particulate matter will absorb, scatter and hinder the effectiveness of UV treatment. As seen in Figure 4, UV light can be scattered by suspended solid and result in particle shading. Particles may not actually hinder the effectiveness of the UV and may just deflect it to other parts of the wastewater. Clay particles therefore, do little to inhibit UV disinfection because they tend to scatter UV light rather than absorb it (Qualls et al. 1983).

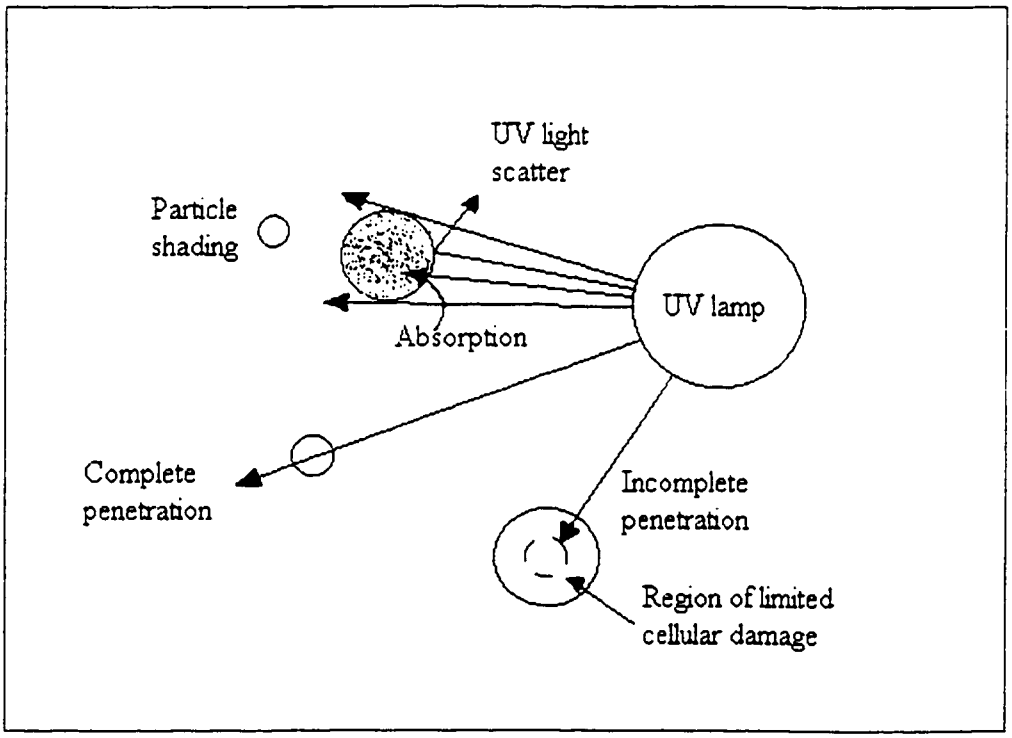

Figure 4. Particle shading and incomplete penetration (after Loge et al. 1996)

Without interference, UV light can generally penetrate bacteria completely. If there are compounds which absorb UV light then the result is incomplete penetration of the bacteria and only a limited number of sites on the DNA will be affected. Compounds that are known to absorb light are those with double bond structures such as nucleic acids and long chain fatty acids. Inorganic compounds such as iron are known to strongly absorb UV light and will result in loss of radiation reaching the intended organism (Sakamoto and Zimmer 1997).

3.8.1 The Lambert-Beer law

The fraction of light absorbed by a solution at a specific wavelength is related to the thickness of the absorbing layer and the concentration of the absorbing species. The following equation relates these factors:

$$\mathbf{\log (I_o/I) = \varepsilon c l = Absorbance} \qquad \mathbf{(3.5)}$$

Where: I_o = intensity of incident light

I = intensity of transmitted light

ε = molar absorption coefficient (L/mole-cm)

c = concentration (mole/L)

l = path length (cm)

This equation assumes that the incident light is monochromatic and that the solution is randomly oriented. Log (I_o/I) is called the absorbance, designated A. Therefore, $A = \varepsilon c l$. ε, the molar absorption coefficient varies with each absorbing compound, solvent and wavelength. Absorbance measurements are taken with a

set of standard solutions of known concentration at a specific wavelength. A sample of unknown concentration is then compared to this known set by a standard curve (Lehninger et al. 1993).

3.8.2 UV absorbance and transmittance

When designing a UV disinfection system, the absorbance and transmittance of the wastewater are two main criteria. Both of these parameters are determined by the composition of the waste being treated. Solutions with dissolved iron (and other dissolved materials) as well as high suspended solids will increase the absorbance of UV and decrease the transmittance. While conversely, solutions with low dissolved iron as well as low suspended solids will have a low absorbance and high transmittance. Absorbance and transmittance are related by equations 3.6 and 3.7.

$$\mathbf{A = -Log(T/100)} \qquad \mathbf{(3.6)}$$

Where:

A = Absorbance

T = Percent of light transmitted through a substance

$$\mathbf{\% T = 100 \times 10^{-(A)}} \qquad \mathbf{(3.7)}$$

Where:

A = Absorbance

T = Percent of light transmitted through a substance

Absorbance is measured by using a spectrophotometer and a quartz glass cuvette. A sample is placed in the cuvette and the absorbance reading is taken at a specific wavelength. The path length is determined by the size of the cuvette and is generally 1 cm in length. UV lamps are designed and spaced according to the absorbance and transmittance of the wastewater. As light is emitted from the lamp the intensity will attenuate with increasing distance from the lamp. This is due to the dissipation or dilution of the energy as the volume it occupies increases (EPA 1986). A second attenuation is caused by the absorbance of the UV energy by compounds present in the wastewater. This type of UV absorption is often referred to as UV demand. Table 3. lists the different amounts of absorbance that are experienced typically at three different stages of wastewater treatment.

Table 3. Absorbance and transmittance data for different levels of treatment (after EPA 1986)

	Percent Transmittance	Absorbance (a.u./cm)
Primary treatment	67 to 45	0.174 to 0.350
Secondary treatment	74 to 60	0.130 to 0.220
Tertiary treatment	82 to 67	0.087 to 0.174

3.9 Iron characteristics

Iron is known to be major factor in the performance of a UV microorganism reduction system. Large amounts of iron present in the wastewater, or a heavy build-up of iron scale on the quartz sleeve of the lamps will impede or absorb UV light. When UV light is absorbed, it reduces the dose which is available for microorganism reduction and therefore harmful pathogens may be released to the environment that may otherwise have been destroyed.

Iron is relatively abundant in the environment, and is only second to that of aluminum. It is a principle constituent of many igneous rocks, especially those containing basic silicate minerals. The divalent iron (Fe^{+2}) links the chains of silicon-oxygen tetrahedra in minerals of pyroxenes and amphiboles and links individual tetrahedra in the structure of fayalite (Hem and Cropper 1959). The trivalent iron (Fe^{+3}) sometimes replaces aluminum in a few silicate minerals. Iron is very commonly found in the form of oxide and sulfide, with ferric oxides being the most common. Iron is found in aqueous solutions as either ferric (Fe^{+3}) or ferrous (Fe^{+2}) ions and is subject to hydrolysis. Ferric hydroxide has a very low solubility in water. The pH of a body of water is a determining factor in the solubility of iron compounds. Most natural bodies of water do not often have pH values that are low enough to prevent hydroxides from forming. Under oxidizing conditions, practically all iron present in solution is precipitated as ferric hydroxides. Iron also has a tendency to form chemical complexes with organic

and inorganic compounds which become very stable and often do not remain in solution (Hem and Cropper 1959).

Of the forms of iron found in nature, ferric hydroxide is the most abundant. The structural formula $Fe(OH)_3$ is also depicted as $Fe_2O_3 \bullet 3H_2O$. At equilibrium ferric hydroxide in the pH range of 5 to 8 has a very low solubility. It is considered to be a weak base and ionizes to form the following cations:

- $Fe(OH)_2^+$
- FeO^+
- $FeOH^+$
- Fe^{+3}

Anions of ferric hydroxide are formed at very high pH's. These include ferrite, FeO_2^- and FeO_2^{-2}. Ferric iron forms complexes with many different types of inorganic and organic compounds. Of the inorganic compounds, complexes with chloride, fluoride, phosphate, sulfate and carbonate ions are the most common.

Ferrous iron has an oxidation state that is considerably less strong than that of ferric iron in forming complexes. Ferrous hydroxide $Fe(OH)_2$ is a much stronger base than is ferric hydroxide and ionizes to:

- $FeOH^+$
- Fe^{++}

In strong alkaline conditions, ferrous hydroxide forms hypoferrite, FeO_2^{--}. In natural waters the most frequent form of ferrous iron is the cation Fe^{+2}. Iron has the capability of forming many different complexes, however, under conditions found in natural waters they form a much smaller group (Hem and Cropper 1959). These complexes can be seen in Table 4.

Table 4. Iron complexes found in natural water conditions at equilibrium (Hem and Cropper 1959).

Chemical reactions at equilibrium	Equilibrium constants
$Fe(OH)_2(aq) \Leftrightarrow FeOH^+ + OH^-$	2.0×10^{-5}
$FeOH^+ \Leftrightarrow Fe^{++} + OH^-$	4.5×10^{-6}
$Fe(OH)_2(s) \Leftrightarrow Fe^{++} + 2OH^-$	1.8×10^{-15}
$Fe(OH)_2(s) \Leftrightarrow FeOH^+ + OH^-$	4.0×10^{-10}
$Fe(OH)_2(s) \Leftrightarrow FeO_2H^+ + H^+$	5.0×10^{-19}
$Fe(OH)_3(aq) \Leftrightarrow Fe(OH)_2^+ + OH^-$	2.5×10^{-8}
$Fe(OH)_2^+ \Leftrightarrow FeOH^{++} + OH^-$	4.5×10^{-10}
$FeOH^{++} \Leftrightarrow Fe^{+++} + OH^-$	2.7×10^{-12}
$Fe(OH)_3(s) \Leftrightarrow Fe^{+++} + 3OH^-$	6.0×10^{-38}
$Fe(OH)_3(s) \Leftrightarrow Fe(OH)_2^+ + OH^-$	5.3×10^{-17}
$Fe(OH)_3(aq) \Leftrightarrow Fe^{+++} + 3OH^-$	4.0×10^{-29}
$Fe^{+++} + Cl^- \Leftrightarrow FeCl^{++}$	33.0
$FeCl_2^+ + Cl^- \Leftrightarrow FeCl_3(aq)$	0.1

aq = dissolved species
s = solid phase

3.10 Quartz lamp fouling

Deposition of undesirable materials or surface fouling on the UV quartz lamp sleeves is of particular concern for the proper operation of a UV disinfection unit. Fouling will block and absorb UV light from penetrating the treated effluent and will potentially reduce the disinfection capabilities of the disinfection unit. Fouling occurs in numerous instances in natural, domestic and industrial processes. Fouling may occur with or without a temperature gradient, however higher temperatures may complicate the process, although it is not essential to the phenomenon. Fouling is of concern when cost factors are involved (Suitor et al. 1977). Often it results in a loss of productivity. Increased fouling will decrease final effluent quality by increasing microbial counts. Fouling may also

necessitate higher UV doses which increase energy costs, and may increase the cleaning costs. Finally, the unit may need to be oversized to overcome the effect that scaling has on the mechanical and physical process involved (Epstein 1983).

3.10.1 Classification of Fouling

Fouling can be divided into six different categories (Epstein 1983):

1. precipitation fouling;
2. particulate fouling;
3. chemical reaction fouling;
4. corrosion fouling;
5. biological fouling; and
6. freezing or solidification fouling

Precipitation fouling:

Is the process in which dissolved substances in the liquid (i.e. calcium, magnesium and iron) crystallize from solution and are deposited onto a substrate (quartz). This process is sometimes referred to as scaling.

Particle fouling:

Is the deposit of fine particles present in solution onto the surface of a substrate. If the velocity of the liquid is low, then settling is governed by gravity and is known as sedimentation fouling. This is often not the case in UV systems since velocities across the lamps is generally too great.

Chemical reaction fouling:

Fouling is a result of a chemical reaction which is a result of the heated substrate surface. The surface material is not considered to be a reactant, but a catalyst for the reaction.

Corrosion fouling:

Particles deposited on the substrate surface which are a result of corrosion within the system.

Biological fouling:

Is the accumulation of biological material on the substrate surface. With the accumulation of biological growth, an extra slime layer is often generated causing further fouling.

Freezing or solidification fouling:

Fouling due to the freezing of the process fluid itself on the surface of the substrate (Melo et al. 1988). This type of fouling is not of concern when dealing with wastewater since operating temperatures are never below freezing.

Of the six classifications of fouling, none operate on an individual basis. It may be difficult to determine what particular process is being conducted at what time. For example, during crystallization, the fouling may be occurring directly on the heated surface of the quartz, in which case the fouling would be precipitation fouling, or may be a result of reactions in the bulk solution followed by particle fouling. It may be a case of both interactions at the same time. Chemical precipitation may also be hard to distinguish from that of particulate fouling. Chemical precipitation may be a reaction in solution followed by settling

out on the substrate surface. These interactions can therefore be classified as synergistic or mutually reinforcing (Epstein 1983).

3.10.2 Fouling events

Of the previously mentioned fouling classifications, the events that most likely occur during fouling are as follows (Garret-Price et al. 1985):

1. initiation;
2. transport;
3. attachment;
4. transformation; and
5. removal;

Initiation:

Initiation refers to the establishment of certain conditions that promote fouling. Several gradients such as temperature, concentration and velocity, as well as an oxygen-depletion zone are required. Crystal nucleation sites and the formation of a sticky film on the heat transfer surface are also required.

Transport:

Of the five events that occur during fouling, transport has been the most widely studied. Several transport mechanisms have been identified and are as follows:

a) *Diffusiophoresis*: A concentration gradient is established in which diffusion occurs from high concentrations in the liquid to lower concentrations at the substrate surface.

b) *Turbulent diffusion*: Eddies are present at the surface of the heat transfer layer which draw particles in toward the surface.

c) *Reaction-Rate controlled*: Accumulation of substrate at the surface is dependent upon the chemical reactions at the surface.

d) *Inertial Impaction*: The inertia of a particle with respect to the solution velocity will cause the particle to deviate from the solution streamlines and onto the surface. This is enhanced when the bulk liquid experiences direction changes with bends or turns in the liquid path.

e) *Thermophoresis*: This is a transport process in which particles will move to a cold surface under the influence of a temperature gradient. This is significant for particles < 5 microns and dominates at 0.1 microns.

f) *Brownian diffusion*: Particles are randomly associated with the bulk solution and collide into one another. They may then be propelled to the substrate surface. The process is negligible for particles over 0.1 micron.

g) *Electrophoresis*: Any particle that has a net charge opposite to that of the substrate surface will be transported to the surface. This process is particularly evident with particles below 0.1 micron. Anything larger would require a very strong electrical field to be drawn in.

h) *Gravity*: Particles that are larger then 1.0 microns may settle out of solution.

Attachment:

Very little is known about the attachment of particles to the heat transfer surface. Some attachment processes which are thought to aid in particle fouling include

van der Waals force, electrostatic forces, surface tensions, and external force fields.

Transformation:

Transformation may involve changes in the crystal or chemical structure of the scale (Epstein 1983). This may arise from dehydration. Any changes that may occur after particles are deposited are often referred to as aging of the scale.

Removal:

Removal of scale may start as early as initiation. Removal may be a result of erosion, dissolution and spalling. Erosion is usually the removal of small particulates, while dissolution is the removal of scale in ionic form. Spalling is the removal of large masses of scale.

3.10.3 Mineral scales

Calcium is the most abundant metal ion present in water. Calcium exists in almost all natural bodies of water. It is most prominent in ground and surface waters, from dolomitic areas and often occurs in effluents from domestic and industrial sources (Najibi et al. 1997). The presence of bicarbonate (CO_3^{-2}) in these types of waters may cause the formation of solid calcium carbonate ($CaCO_3$). Calcium carbonate has an inverse solubility in water (i.e., is less soluble at higher temperatures), and will crystallize on heat transfer surfaces (Najibi et al. 1997). Calcium carbonate is the main constituent of hard and tenacious scale. This scale is found not only in heat transfer systems, but also in potable waters (Andritsos et al. 1996). As mentioned, scale will deposit

regardless of temperature, therefore, not only heat transfer systems experience scale deposits, but common pipes and water faucets in the home will also experience scale.

3.10.4 Iron and possible scale formation

Much research has been conducted as to the effects that minerals such as calcium and magnesium have on the formation and deposit of unwanted scale. In UV systems, calcium and magnesium do not pose a great threat to the performance and operation of the disinfection unit. The presence of iron in wastewater on the other hand is of somewhat greater concern. Iron is known to absorb UV light and therefore is responsible for the reduction of transmittance and ultimately the increase in microbial counts due to the loss of UV radiation reaching the intended organism. (Gehr and Wright 1998) investigated the effect of using $FeCl_3$ in primary wastewater treatment at the La Piniere wastewater treatment plant on the island of Laval (Quebec, Canada). There was concern that the levels of iron reaching the UV treatment system were adversely affecting its performance. Levels above 3 mg/L total iron were often observed in the influent to the UV system, as well, the levels of suspended solids (SS) were high at 30 mg/L and UV_{254} transmission was low at 32%. Disinfection limits of 2,500 colony-forming units (CFU)/100 mL, were imposed prior to photoreactivation. Three different types of UV disinfection units were tested. A low pressure mercury lamp system which consisted of 3 banks of lamps in series, another low pressure mercury lamp system with 2 banks of lamps, and a medium pressure

disinfection unit. It was observed that at these effluent qualities the disinfection limit was not met by the low pressure systems and that fouling of the lamps occurred almost immediately. The medium pressure system did meet the required limits, yet effluent conditions at the time of testing of the medium pressure system seemed to be somewhat better than had been experienced by the low pressure systems. It was concluded, then, that the use of ferric chloride as a coagulant hindered the performance of the disinfection systems, and that fouling occurred rapidly and was a serious problem. The medium pressure system did, however, have an advantage over the low pressure system in that automated lamp cleaning was available.

The GBWWTP was one of the first large scale treatment plants to install a medium pressure UV disinfection unit. This unit is equipped with an automatic cleaning mechanism in which a squeegee type system is drawn over the quartz lamp and scale is dissolved with the aid of Lime-A-Way®. In 1995, prior to the installation of the UV system at GBWWTP, CH_2M Hill Engineering conducted a study on the future performance of the UV system (CH2M-Hill 1995). They were to investigate the dose response relationship, fouling potential, headloss, and possible disinfection by-product formation that may result from treated wastewater being disinfected by UV radiation. Cleaning of the UV lamps was designed for once every 4 hours. After 4 hours of operation the degree of fouling was found to be 2.6 %. After 8 hours operation it was estimated to be approximately 5 %. Fouling was determined by using an intensity meter as well

as the solution's percent transmission at 254 nm. This can be seen in Figure 5. It was found that by cleaning the lamps every four hours, the fouling rate would not be a problem to the performance of the UV system.

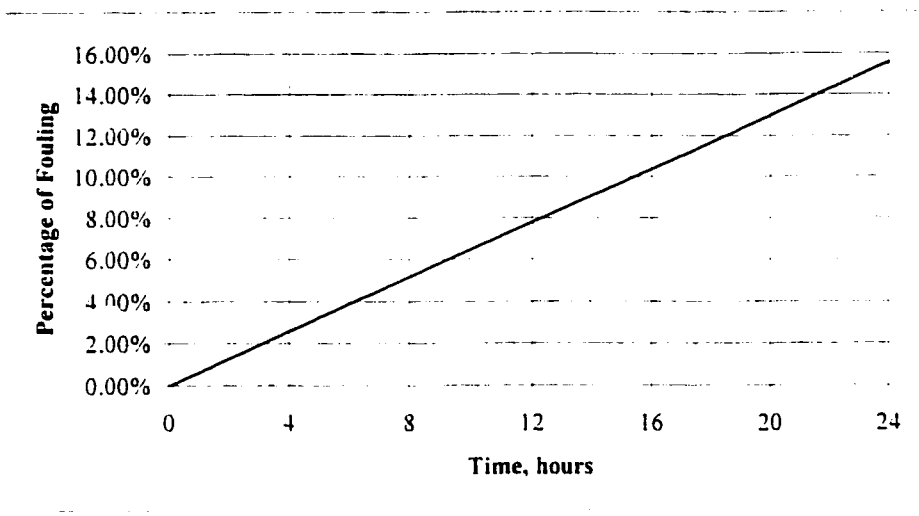

Figure 5. Estimated lamp sleeve fouling rate (after CH2M-Hill 1995)

4.0 Methods and Materials

4.1 Materials

The following table lists the material used in all experiments.

Table 5. Materials for all experiments conducted

Material	Product identification and supplier
1,10-phenanthroline	P-70, Fisher Scientific
Acetic Acid trace metal grade	A507SK-212, Fisher Scientific
Ammonium Acetate ACS grade	A639-500, Fisher Scientific
Ferrous chloride	J.T. Backer chemical Co.
Ferrous ammonium sulfate	Fisher Scientific
HCl	A508SK-212 trace metal grade, Fisher Scientific
Helium	Praxair
Hydroxylamine HCl	H330-100, Fisher Scientific
Industrial waste product	Daam Galvanizing Inc.
NaOH	SS255B-1 10 N, Fisher Scientific
Potassium Permanganate	P279-500, Fisher Scientific
Sodium Phosphate Monobasic	S369-1, Fisher Scientific
Sodium Phosphate	S393-3, Fisher Scientific
Aerator	Portable air compressor, Evans Electroselenium Ltd.
Automatic Titrater	Mettler Toledo DL53
Heating coil	Electrothermal heating tape
Heating plate	PC-35, Corning
Heating regulator	Variable auto transformer, Staco Energy Products Co.
Magnetic stirrer	Mag-mix, CGA Precision Scientific
Peristaltic pump	Pump drive, Cole Parmer Instruments Co.
Pump controller	Master flex high capacity, Cole Parmer Instruments Co.
UV/visible spectrophotometer	Ultraspec 2000, Pharmacia Biotech.
Closed loop reactor	Acrylic plate and pipe
Aerobic mixed liquor	Aeration tank four, GBWWTP
Anaerobic digester sludge	Digester three, GBWWTP
Return activated sludge	GBWWTP
Filter paper	0.2 μm, Gelman Sciences

Table 5. Materials for all experiments conducted (continued)

Filter paper	0.45 μm, Gelman Sciences
Glass beads	3 mm 11-312A, Fisher Scientific
Glass curettes	OS 1.000, Fisher Scientific
Glass cylinder	U of A technical services
Graduated cylinder	1 L, Fisher Scientific
Nalgene tank	60 L, Nalge Company
Plastic pails	Fisher Scientific
pH meter	Accumet 915, Fisher Scientific
TSS filter papers	Whatman
Quartz glass coupons	Trojan Technologies Inc.
Sample flask 1 L	Wheaton

4.2 Analytical techniques

4.2.1 Total sulfide measurement

In order to estimate the maximum amount of iron required to precipitate sulfide in the digester sludge, total sulfide in the anaerobic digester sludge was measured according to the analytical procedure described in Chiarella (1998). 500 mL of anaerobic digester sludge was collected from digester 3, at the 7.9 m level. The sample was placed in a Wheaton 1 L flask, to which 120 mL of phosphate buffer was added. The addition of phosphate buffer was to minimize pH change in the solution during the release of CO_2. The solution was placed on a magnetic stir plate and mixed for one hour while helium (He) was bubbled through the flask. Gases that were released due to the helium sparging were bubbled through 10 mL of 2 N NaOH, where all forms of sulfide (H_2S and HS^-) gas were converted to the bisulfide form (S^{-2}). The NaOH solution containing

bisulfide was analyzed using a Mettler Automatic Titrater by titrating with 0.05 M silver nitrate ($AgNO_3$). Results were reported in mg/L based on a volume of 0.5 L anaerobic digester sludge.

4.2.2 Ferrous and Ferric iron determination

Soluble iron will absorb UV light at the germicidal wavelength of 254 nm, and thereby reduce the amount of radiation that can reach the targeted microorganisms. The insoluble iron will either be precipitated during the aeration stage of treatment or pass by the UV lamps in the form of particulate matter. The iron may also be bound to other particles present in solution Many methods of determining soluble iron in solution are available. One in particular is the atomic absorption spectroscopy method. This method determines total iron present at the atomic level. However, this will only analyze the total amount of iron present in the sample. Additional methods include the inductive coupled plasma or (ICP). This technique too will only detect total iron. This thesis project was to investigate the different forms that iron may exist as ferrous (Fe^{2+}) and ferric (Fe^{3+}) ions. Therefore, a method was required that distinguished between the ferrous and ferric ions. The method that was chosen is know as the 1,10 phenanthroline iron detection method 3500-Fe D (APHA 1992) The orange-red complex that is produced from this experiment follows the Lambert-Beer law and absorbs light at 510 nm. A standard curve was prepared for the range of 0 mg/L to 3.6 mg/L total iron. The standard curve can be seen in Figure 6.

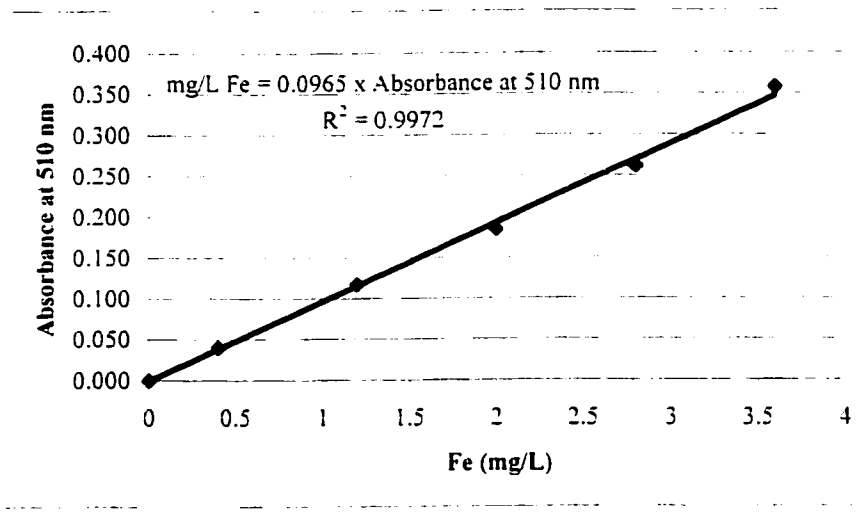

Figure 6. Calibration line for iron analysis

The samples of wastewater that were tested were low in organic material, yet contained some suspended solids that may absorb light at the 510 nm wavelength. To overcome this interference a sample was carried thought out the entire experiment without the addition of 1,10-phenanthroline. This blank was then used as reference. The difference between the blank and the actual sample was then taken as the amount of iron present in the sample being analyzed.

The detection limit of this procedure is 10 μg/L using a spectrophotometer and cell path lengths of 5 cm or longer. In this experiment a 1 cm path length was used for which the detection limit is 0.1 mg/L.

4.2.3 TSS analysis

Total suspended solids (TSS) analysis was conducted using the procedure found in Standard Methods (2450D) (APHA 1992)

4.3 Experimental protocol

4.3.1 Digester sludge experiment protocol

The anaerobic digester sludge was sampled from anaerobic digester 3 and was drawn off from mid-depth (the 7.9 m level). Additional samples were taken to perform the total sulfide measurements. A measured quantity of either reagent grade ferrous chloride solution or industrial waste ferrous chloride solution was added to 15 L of digester sludge and rapidly mixed for 30 seconds to simulate iron additions to an anaerobic digester. To simulate conditions at the Clover Bar sludge lagoon, the 15 L of digester sludge was allowed to settle for seven days with no additional mixing. Seven days of settling was intended to allow settling of particles, and the iron-hydrogen sulfide reaction in the sludge to reach equilibrium. After 7 days, a thick grease and fat layer that had developed was removed, and a portion of the supernatant was carefully decanted so as to not to agitate the settled particles. The supernatant was drawn off to represent the recycle of Clover Bar sludge lagoon supernatant to the Gold Bar wastewater treatment plant. This supernatant was then used in subsequent experiments.

4.3.1.1 Experiment A: Digester sludge

The purpose of this anaerobic digester sludge experiment was to simulate Gold Bar treatment plant conditions in accordance with that suggested by Chiarella (1998) to reduce the offensive odour associated with the release of hydrogen sulfide gas. 15 liters of digester sludge were obtained from digester 3 at

the 7.9 m level and placed in 20 L plastic containers. Twelve digester sludge samples were drawn off, one per day. Either ferrous chloride, industrial waste solution or no iron (control) was added to each sludge sample. 5.125 g/L of ferrous chloride solution ($FeCl_2.H_2O$) was added to 15 L of digester sludge to provide a final ferrous ion concentration of 95.9 mg/L as Fe^{2+}. The industrial iron waste solution containing 153,000 mg/L as Fe^{2+} was diluted 100 fold. From this dilution 750 mL was added to the 15 L sludge sample to give a concentration of 72.9 mg/L as Fe^{2+}. This concentration of industrial waste solution iron was selected based on results reported in Chiarella (1998). Each test was repeated three times for a total of twelve tests.

4.3.1.2 Experiment B: Digester sludge

The purpose of this experiment was the same as that in section 4.3.1.1. Statistical analysis is essential to validate data, therefore a second set of similar anaerobic digester experiments was conducted. In experiment B three trials were conducted in triplicate for a total of nine tests. In each test either ferrous chloride, industrial waste solution or no iron (control) was added to a 15 L sludge sample. Reagent grade ferrous chloride solution or industrial waste solution was added to each 15 L sludge sample to give 95.9 mg Fe^{2+}/L sludge or 76.2 mg Fe^{2+}/L sludge, respectively. These iron concentrations were selected to yield maximum sulfide precipitation as reported in Chiarella (1998).

4.3.2 Activated sludge experimental protocol

The purpose of the activated sludge experiment was to simulate the conditions in the activated sludge aeration tanks which would receive raw wastewater containing high iron concentrations resulting from the sulfide precipitation program. The wastewater treatment plant had an average flow of 264 ML/d in 1997, of which recycled supernatant from the Clover Bar sludge lagoons accounted for a maximum of 11 ML/d. This ratio (1:24) was used when simulating the effect of the activated sludge process on influent iron.

4.3.2.1 Experiment A: Activated sludge

In experiment A, tests were conducted on a bench scale in which 0.6 L of supernatant from settled anaerobic digester sludge (see section 4.3.1.1) was added to 14.4 L of settled activated sludge collected from the sludge return line to an aeration tank. Upon addition of the 0.6 L of sludge supernatant, the mixture was flash mixed for 30 seconds and aerated well. 1 L of this mixture was removed after the initial flash mix and placed into a 1000 mL graduated cylinder and allowed to settle for 30 minutes. After 30 minutes of settling, the supernatant from the 1000 mL graduated cylinder was removed and analyzed for total and ferrous iron using the 1,10-phenanthroline iron detection method. Total and ferrous iron tests were conducted on unfiltered samples as well as samples filtered through a 0.45 μm pore microfilter membrane. The mixture of settled sludge supernatant and return activated sludge (RAS) was aerated for a period of 6 hours

with an external aeration compressor. The compressor provided sufficient pressure, to both aerate and mix the sample completely, as shown in Figure 7. Samples were withdrawn at 0, 2, 4 and 6 hours, placed in 1000 mL graduated cylinders and settled for 30 minutes. The supernatant was then analyzed for total and ferrous iron.

Figure 7. Aeration of mixed liquor

4.3.2.2 Experimental arrangement for experiment A

The following tables show the experimental arrangement for iron experiments A.

Table 6. Experimental arrangement for experiment A: Digester sludge, Control sample.

Trial	Digester Sludge (L)	Settling time (days)	Iron Addition (mg Fe^{2+}/L)
1	15	7	None
2	15	7	None
3	15	7	None
4	15	7	None

Table 7. Experimental arrangement for experiment A: Activated sludge, Control sample

Trial	Digester sludge settled supernatant (L)	RAS (L)	Sample Port	Aeration Time (hr)
1	0.6	14.4	RSP-4	6
2	0.6	14.4	RSP-4	6
3	0.6	14.5	RSP-4	6
4	0.6	14.4	RSP-4	6

Table 8. Experimental arrangement for experiment A: Digester sludge, Ferrous sample.

Trial	Digester Sludge (L)	Settling time (days)	Fe^{2+} (mg/L)
1	15	7	95.6
2	15	7	95.6
3	15	7	95.6
4	15	7	95.6

Table 9. Experimental arrangement for experiment A: Activated sludge, Ferrous solution sample

Trial	Digester Sludge settled supernatant (L)	RAS (L)	Sample Port	Aeration Time (hr)
1	0.6	14.4	RSP-4	6
2	0.6	14.4	RSP-4	6
3	0.6	14.4	RSP-4	6
4	0.6	14.4	RSP-4	6

Table 10. Experimental arrangement for experiment A: Digester sludge, Waste solution sample.

Trial	Digester Sludge (L)	Settling time (days)	Fe^{2+} (mg/L)
1	15	7	72.9
2	15	7	72.9
3	15	7	72.9
4	15	7	72.9

Table 11. Experimental arrangement for experiment A: Activated sludge, Waste solution sample

Trial	Digester Sludge settled supernatant (L)	RAS (L)	Sample Port	Aeration Time (hr)
1	0.6	14.4	RSP-4	6
2	0.6	14.4	RSP-4	6
3	0.6	14.4	RSP-4	6
4	0.6	14.4	RSP-4	6

4.3.2.3 Experiment B: Activated sludge

For this set of tests, 0.6 L of the settled digester sludge supernatant described in section 4.3.2.1 was added to 14.4 L of activated sludge mixed liquor taken from an activated sludge aeration tank. Experimental procedures are as indicated in section 4.3.2.1, however, sampling times and measured parameters differed. In the first trial, samples were collected at time zero and 6 hours, while in the second and third trials samples were withdrawn at time zero, three hours and four hours. The pH of the activated sludge mixture was measured during the aeration period for trials two and three. Total suspended solids (TSS) analyses were also conducted on all samples to investigate the possible connection between mg/L Fe and mg/L TSS.

4.3.2.4 Experimental arrangement for experiment B

The following tables show the experimental arrangement for iron experiments B.

Table 12. Experimental arrangement for experiment B: Digester sludge, Control sample.

Trial	Digester Sludge (L)	Settling time (days)	Iron Addition (mg Fe^{2+}/L)
1	15	7	None
2	15	7	None
3	15	7	None

Table 13. Experimental arrangement for experiment B: Activated sludge, Control sample

Trial	Digester Sludge settled supernatant (L)	Mixed Liquor (L)	Sample Port	Aeration Time (hr)
1	0.6	14.4	4P-4	6
2	0.6	14.4	4P-4	4
3	0.6	14.4	4P-4	4

Table 14. Experimental arrangement for experiment B: Digester sludge, Ferrous sample.

Trial	Digester Sludge (L)	Settling time (days)	Fe^{2+} (mg/L)
1	15	7	95.9
2	15	7	95.9
3	15	7	95.9

Table 15. Experimental arrangement for experiment B: Activated sludge, Ferrous solution sample

Trial	Digester Sludge (L)	Mixed Liquor (L)	Sample Port	Aeration Time (hr)
1	0.6	14.4	4P-4	6
2	0.6	14.4	4P-4	4
3	0.6	14.4	4P-4	4

Table 16. Experimental arrangement for experiment B: Digester sludge, Waste solution sample.

Trial	Digester Sludge (L)	Settling time (days)	Fe^{2+} (mg/L)
1	15	7	76.2
2	15	7	76.2
3	15	7	76.2

Table 17. Experimental arrangement for experiment B: Activated sludge, Waste solution sample

Trial	Digester Sludge (L)	Mixed Liquor (L)	Sample Port	Aeration Time (hr)
1	0.6	14.4	4P-4	6
2	0.6	14.4	4P-4	4
3	0.6	14.4	4P-4	4

4.3.3 Wastewater Treatment plant influent and effluent analysis

Prior to the digester and activated sludge iron experimental work, total, ferrous, and ferric iron was analyzed in influent raw wastewater, final treated effluent, settled return activated sludge (RAS), and settled mixed liquor (ML). Total suspended solids (TSS) was also measured. A ratio of total iron mg/L to TSS (mg/L) was established to investigate the amount of iron that was associated with the suspended solids. It has been suggested that an iron/TSS ratio of less than 0.05 would be suitable for UV disinfection (Sakamoto and Zimmer 1997)

4.3.4 Iron quartz sleeve scaling experiment

An experimental protocol was developed to determine the amount of iron scale that may be deposited on the surface of the quartz lamp sleeves. Under normal conditions the ultraviolet light lamps operate at extremely high temperatures, approximately 600 °C to 800 °C. This temperature range refers to the core or internal temperature of the lamp. At the surface of the lamp sleeve, the temperatures are considerably lower. This is due to the cooling effect of the large volumes of effluent passing over the surface of the sleeve. Several experiments have been conducted to calculate the exact surface temperature of the quartz lamps. Temperatures have been found to be as low as 35 °C and as high as 50°C (Sakamoto 1998). Since full-scale online experiments at the Gold Bar Wastewater Treatment Plant involving the quartz lamps and addition of iron to the wastewater were impossible, a bench scale experiment was developed.

4.3.4.1 Quartz scale experimental procedure

The purpose of this experimental procedure was to investigate the possible iron scale formation that will result on the quartz lamp sleeves with the addition of increased iron concentrations in the raw effluent. A quartz lamp sleeve was obtained from the wastewater treatment plant and cut into 10 mm by 10 mm pieces. These small quartz glass pieces were attached to a heating column with water-insoluble clear silicone (see Figure 8). 30 L of mixed liquor obtained from aeration tank four, sample port 4P-4 was spiked with a solution of ferrous chloride

to give an initial iron concentration in the mixed liquor of 1.5 mg/L total iron. This experiment was run twice more using initial iron concentrations of 1.5 mg/L total iron and of 3.0 mg/L total iron. The mixed liquor spiked with the iron solution was aerated for 6 hours. Figure 7 indicates the intensity of the aeration, while Figure 9 gives an indication of the amount of mixed liquor being aerated. Upon the completion of aeration the mixed liquor was allowed to settle for 30 minutes. In Figure 10 it can be seen that the volume of biomass present in the mixed liquor has settled to just over $1/6^{th}$ of the initial volume of 30 L. At the completion of the 30 minute settling period, the supernatant was decanted so as not to disturb the settled biomass. The supernatant was placed in the closed loop flow system seen in Figure 11. The effluent was pumped using a peristaltic pump which kept the effluent flowing through the closed loop flow system at a constant rate. The experiment was conducted for a total of 48 hours. An additional test was conducted, in which treated effluent was taken directly from the clarifier, just before entering the UV chamber. No iron was added during this test. This was to investigate actual plant conditions and to compare these to experimental results.

4.3.4.2 Iron scale determination

Three of the 10 mm by 10 mm quartz glass pieces that were attached to the heating column were removed at 24 hours and another three at 48 hours. They were then analyzed by two different methods to determine the type and amount of scale that was deposited on them. In order to determine the composition of the scale that was formed on the quartz glass coupons, a scanning electron

microscope (SEM) was used. Using the process of x-ray defraction specific elements can be quantified. Quartz glass coupons from all experiments were examined using the SEM in which a picture was taken of an overview area on each quartz coupon. Pictures were also taken of three specific areas within each overview to provide a representation of the sample. The overview and three areas were analyzed using x-ray defraction to detect the presence of specific elements. This detected the presence of mainly calcium, magnesium, iron, silica, aluminum, gold, potassium, chloride, phosphorus and oxygen. Since the quartz glass coupon is composed of silica dioxide (SiO_2) a large portion of the analysis is Si and O. In most instances the Si and O were ignored. However, in some analyses the Si was associated with Al from clay particles and was therefore included in the quantitative analysis. This type of analysis does not provide quantitative data as to the amount, but rather a qualitative assessment of the composition of the scale and the relative amount of each element present. In the second method, the scale on the quartz coupons was analyzed using ICP by Enviro-Test Laboratories and 26 different elements were quantified. The method used was the US EPA method No. 200.8.

4.3.4.3 Experimental arrangement for quartz sleeve experiments

The following tables show the experimental arrangement for the quartz sleeve scale experiments.

Table 18 Experimental arrangement for 1.5 mg/L trials

Trial	Mixed Liquor (L)	Settling time (minutes)
1	30	30
2	30	30
3	30	30

Table 19 Experimental arrangement for 3.0 mg/L trial

Trial	Mixed Liquor (L)	Settling time (minutes)
1	30	30

Table 20 Experimental arrangement for treated effluent

Trial	Treated effluent (L)	Settling time (minutes)
1	30	0

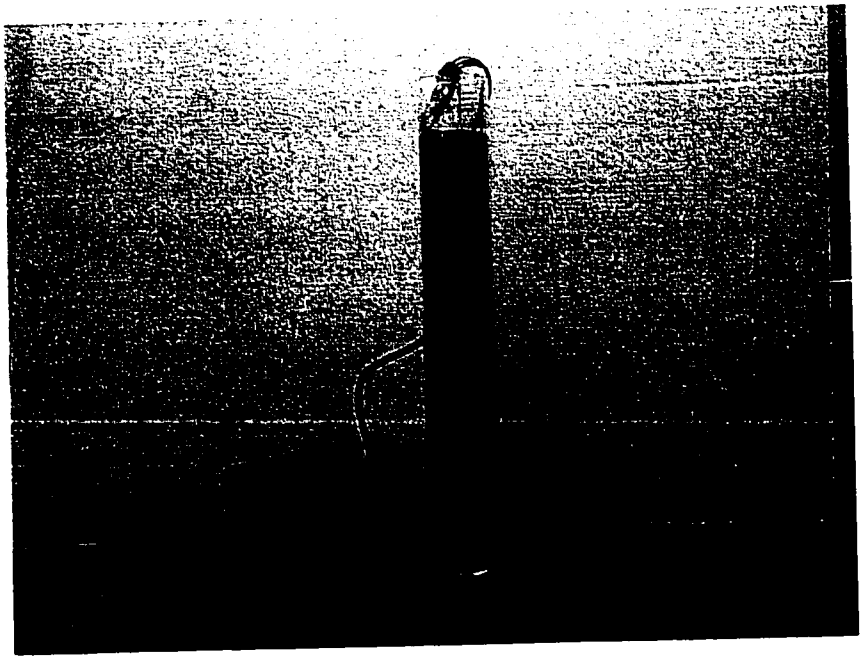

Figure 8. Heating column used to heat quartz glass pieces to 50 °C.

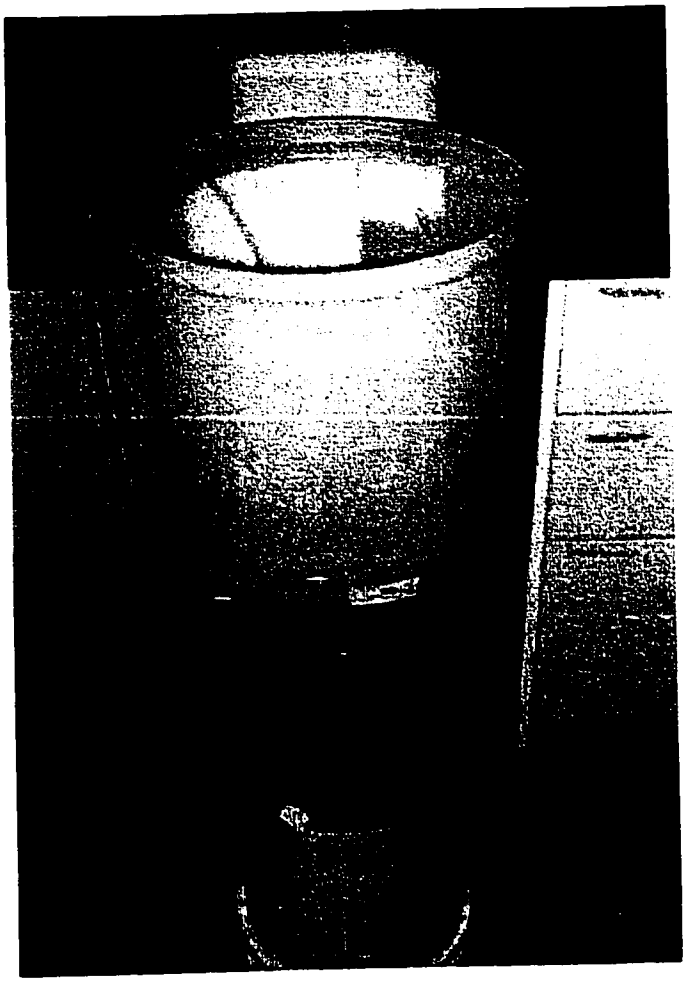

Figure 9. Tank used to hold mixed liquor during aeration

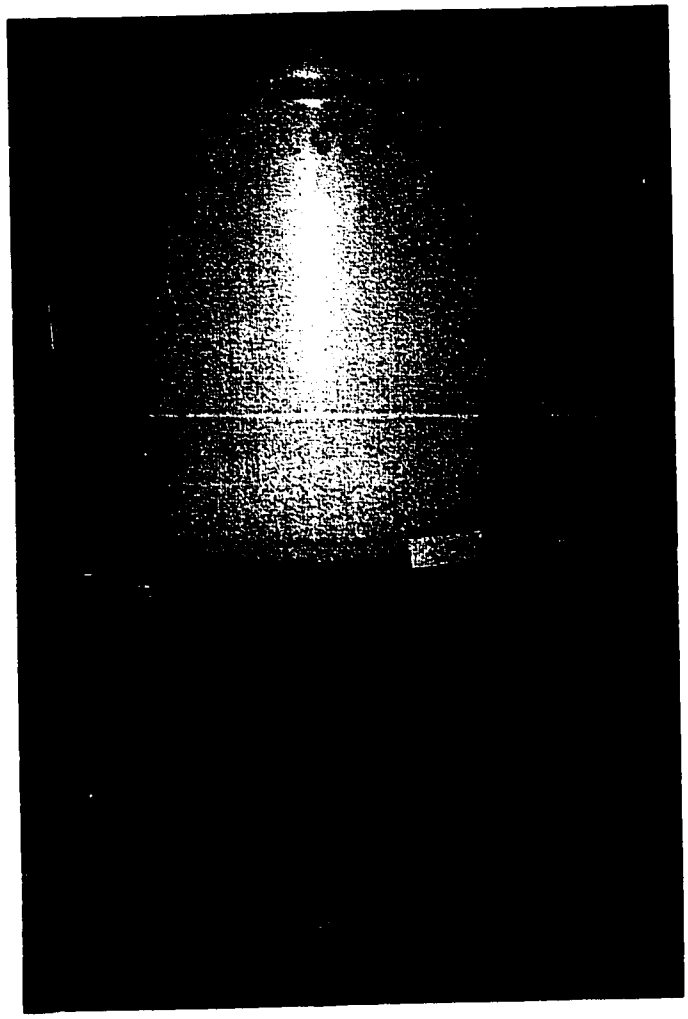

Figure 10. Volume of mixed liquor at the completion of settling

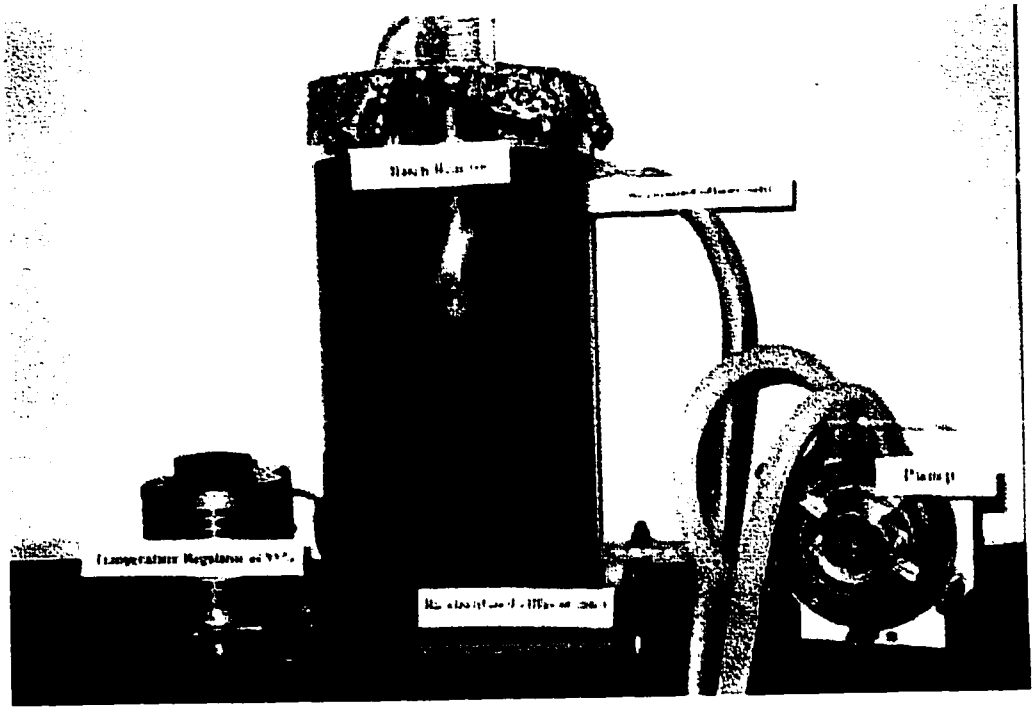

Figure 11. Batch Reactor set up used in scale experiment

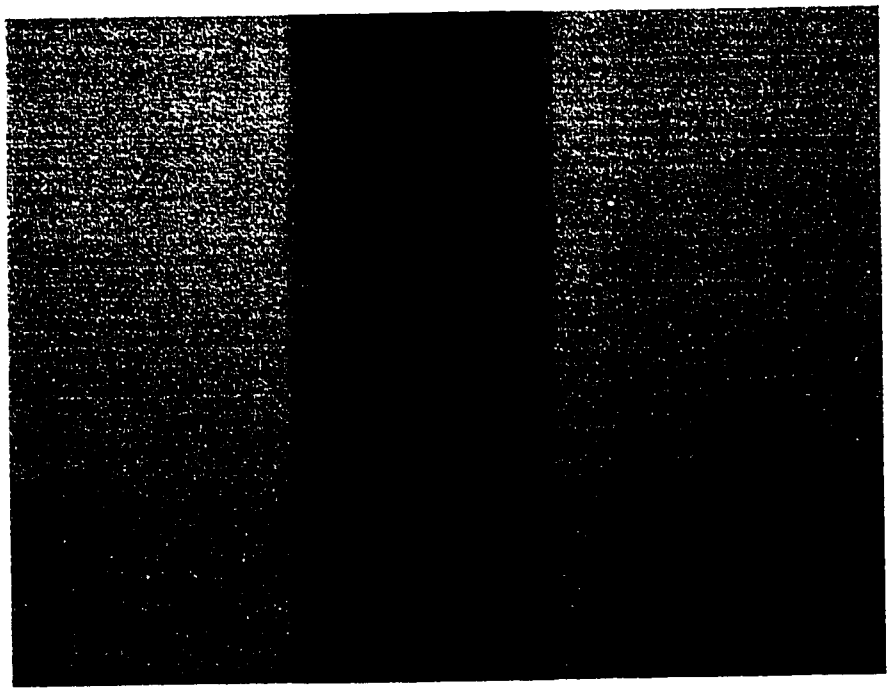

Figure 12 Close up of quartz glass coupons

5.0 Results and Discussion

5.1 Current treatment plant iron concentrations

Gold Bar wastewater treatment plant conducts total iron analysis using the inductive couple plasma (ICP) technique at the onsite laboratory approximately once per month on influent raw wastewater and final treated effluent. Total iron data for the period from January 9, 1997 to August 5, 1998 can be seen in Figure 13 and Table 21.

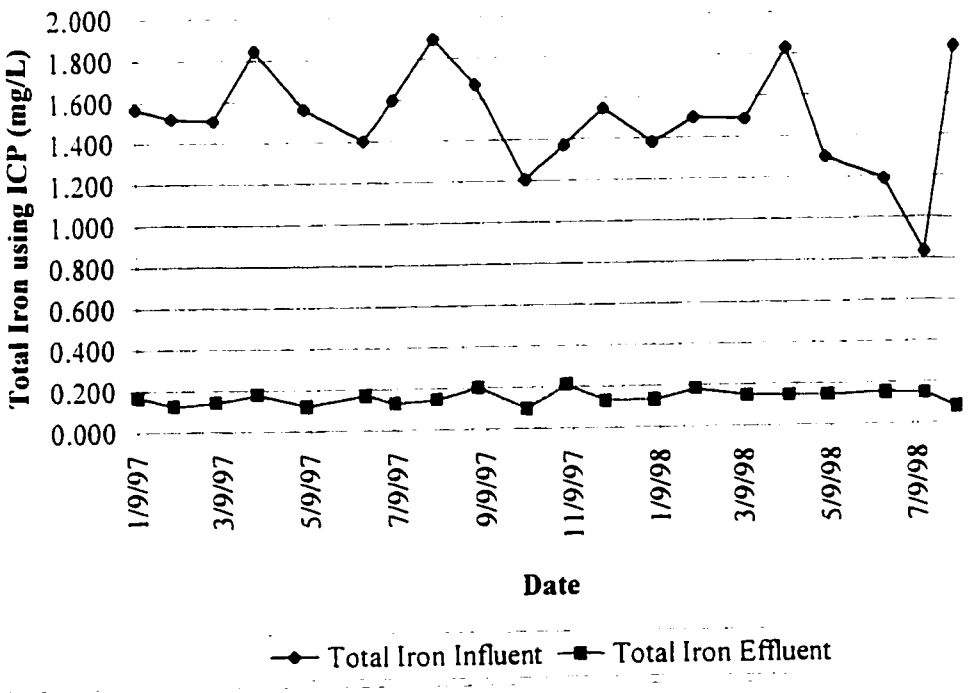

Figure 13. Total iron in treatment plant influent and effluent using ICP

Table 21. Data for total iron in plant influent and effluent

Date	Total Iron Influent (mg/L)	Total Iron Effluent (mg/L)
09-Jan-97	1.568	0.1729
03-Feb-97	1.520	0.1256
04-Mar-97	1.508	0.1420
02-Apr-97	1.846	0.1799
06-May-97	1.563	0.1218
16-Jun-97	1.404	0.1714
07-Jul-97	1.602	0.1331
05-Aug-97	1.894	0.1463
03-Sep-97	1.671	0.2047
07-Oct-97	1.205	0.0974
04-Nov-97	1.373	0.2124
02-Dec-97	1.550	0.1331
05-Jan-98	1.380	0.1350
03-Feb-98	1.500	0.1820
11-Mar-98	1.490	0.1490
09-Apr-98	1.830	0.1470
06-May-98	1.300	0.1450
16-Jun-98	1.190	0.1550
14-Jul-98	0.833	0.1480
05-Aug-98	1.830	0.0840
Average	**1.503**	**0.1493**

Total iron in the raw influent is seen to vary considerably from month to month. This may be explained by variations in weather patterns and discharges from industrial processes into the collection system. The average influent iron concentration over the 20 month period shown in Table 21 and Figure 13 is 1.503 mg/L of total iron. The total iron measured in the treated effluent was found to be very constant and averages 0.149 mg/L. This indicates that the treatment process can handle variations in total iron influent and still produce consistently low total iron in the final treated effluent.

5.2 Iron determination on treatment plant influent and effluents

All data and graphs for iron determination on treatment plant influent and effluent can be found in Appendix F. A typical total iron analysis for treatment plant influent and effluent can be seen in Figure 14. These graphs represent the measured amounts of iron at each stage of treatment. Total iron values for the influent and effluents can be seen in Table 22. TSS analyses of all samples can be seen in Table 23. Table 24 contains the Iron / TSS ratios calculated from data in Table 22 and Table 23. The graph of total iron / TSS can be seen in Figure 15.

Table 22. Total iron data for treatment plant influent and effluents

	Raw influent (mg/L)	Treated effluent (mg/L)	RAS (mg/L)	ML (mg/L)
Trial 1	1.839	0.228	0.212	0.104
Trial 2	1.244	0.093	0.373	0.202
Trial 3	1.943	0.114	N/A	0.161

Table 23. TSS data for supernatant treatment plant influent and effluents

	Raw influent (mg/L)	Treated effluent (mg/L)	RAS (mg/L)	ML (mg/L)
Trial 1	377	70	53	13
Trial 2	263	47	67	32
Trial 3	300	37	87	23

Table 24. Ratio data for treatment plant influent and effluents

	Raw influent Iron /TSS	Treated effluent Iron /TSS	RAS Iron /TSS	ML Iron /TSS
Trial 1	0.00488	0.00326	0.00400	0.00800
Trial 2	0.00473	0.00198	0.00429	0.00631
Trial 3	0.00648	0.00308	N/A	0.00700

RAS = recycled activated sludge
ML = mixed liquor

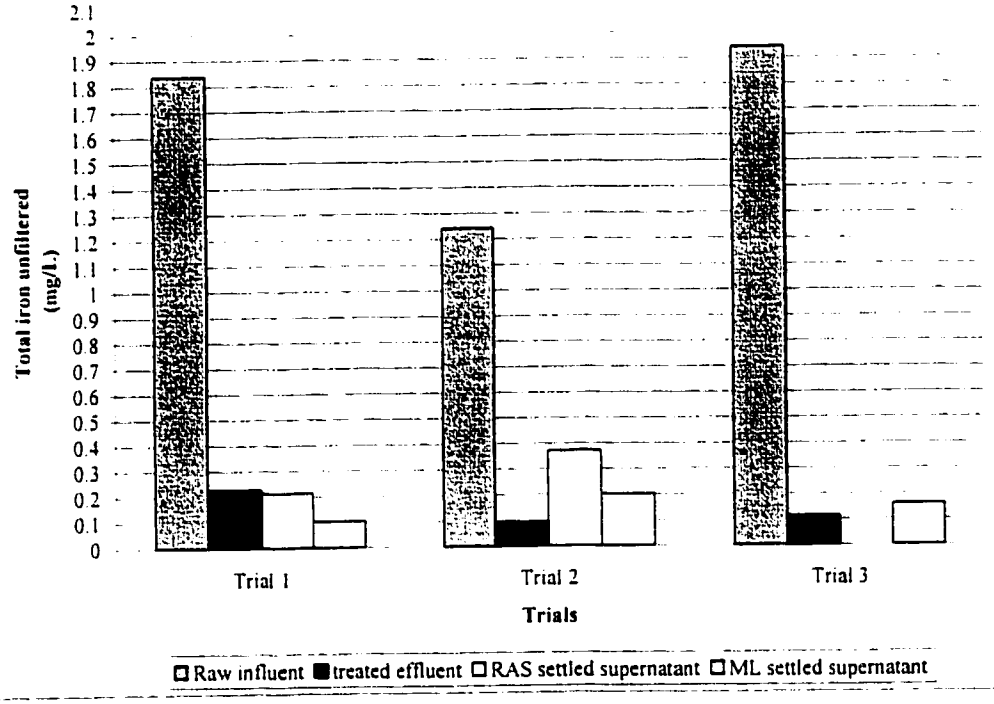

Figure 14. Graph of total unfiltered iron influent, effluent, RAS and ML settled supernate

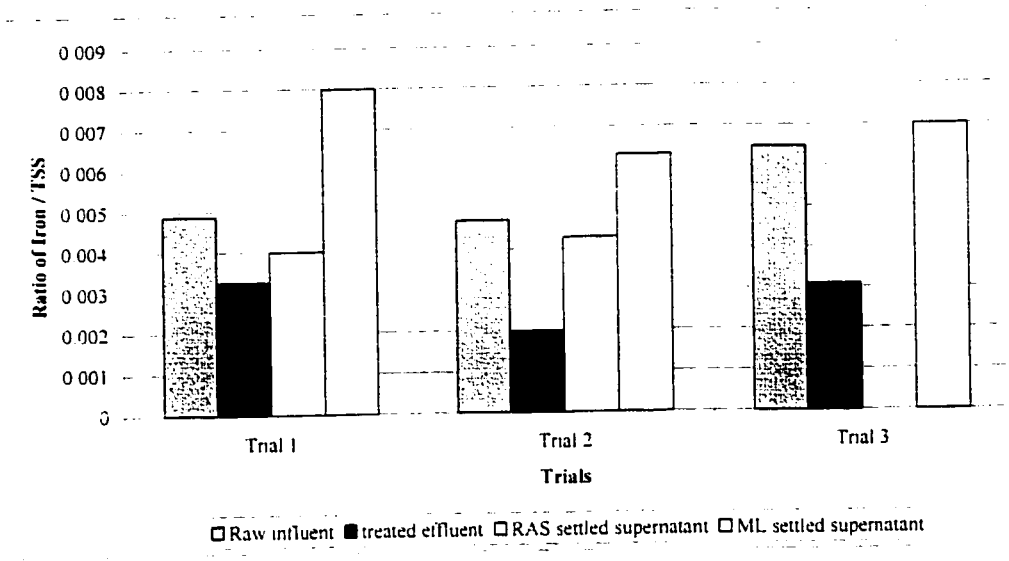

Figure 15. Graph of total iron (mg/L) / TSS (mg/L) for treatment plant influent and effluents

As seen in Figure 14 the average total iron in the raw influent was approximately 1.657 mg/L. This is consistent with values reported in Table 21. The treated effluent, RAS and ML contain average total iron concentrations of 0.145 mg/L, 0.292 mg/L, and 0.155 mg/L respectively. These are consistent with that reported by Gold Bar staff with the exception of the RAS which was somewhat higher. The ratio of total iron / TSS is consistent for each sample and is generally below 0.05.

5.3 Sulfide analysis

Experimental tests outlined in section 4.3.2.1 were conducted to determine the amount of total sulfide that was present in each sample of digester sludge. This procedure was reported in Chiarella (1998). By following this experimental

procedure. the average total sulfide concentration in the digester sludge sampled was found to be 18.7 mg/L. This can be seen in Figure 16. Data used to prepare Figure 16 can be found in Table 25. All the sulfide experimental data can be found in Appendix A.

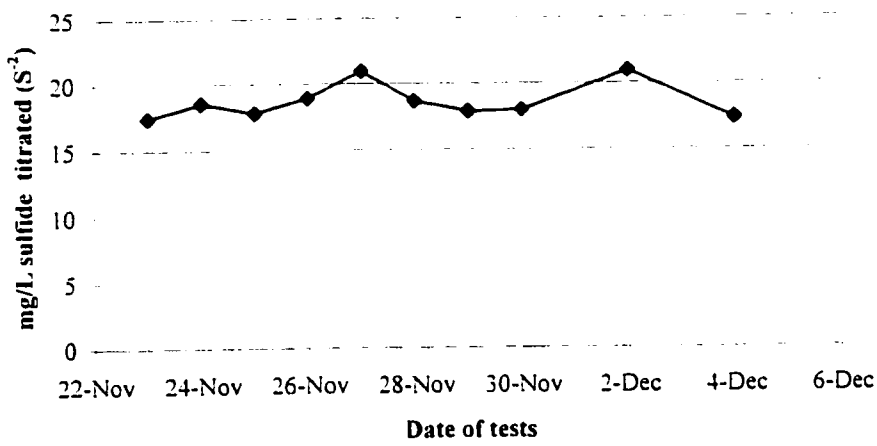

Figure 16. Amount of total S^{-2} present in the sampled digester sludge

Table 25. Total S^{-2} data for the duration of the sulfide experiment

Date	Total S^{-2} (mg/L)
23-Nov	17.5
24-Nov	18.6
25-Nov	17.8
26-Nov	18.9
27-Nov	21.0
28-Nov	18.7
29-Nov	17.9
30-Nov	18.0
2-Dec	20.9
4-Dec	17.4
Average	**18.7**

As reported in Chiarella (1998), the highest amount of sulfide found was 18.3 mg/L, while that found in these experiments was 21.0 mg/L. Variations in season and wastewater composition may be responsible for these slight differences in total sulfide concentrations. Ferrous and industrial waste solution concentrations were chosen to be in excess of those reported in Chiarella (1998). Concentrations of iron solutions used in Chiarella (1998) were 69.7 mg Fe^{2+}/L and 61.2 mg Fe^{2+}/L, respectively. The excess amounts of iron solutions used in this work had concentrations of 95.9 mg Fe^{2+}/L for the ferrous reagent grade solution and 76.2 mg Fe^{2+}/L for the industrial waste solution. These values were to represent a worst case condition. If sulfide concentrations were low, then an excess of iron will remain and be discharged to the Clover Bar sludge lagoons, and may be recycled back to the headworks of the wastewater treatment plant.

5.4 Aerated return activated sludge (RAS) iron analysis experiment A

As described in section 4.3.2.1, return activated sludge (RAS) was obtained from an aeration tank. Total, ferrous, and ferric iron determination was conducted using the 1,10-phenanthroline iron determination method. All data and graphs may be found in Appendix B. Typical total iron, total dissolved iron, and total suspended iron graphs for the control sample, ferrous solution sample and industrial waste solution sample can be see in Figure 17 to Figure 19. Figure 20 is a typical graph of all three trials combined.

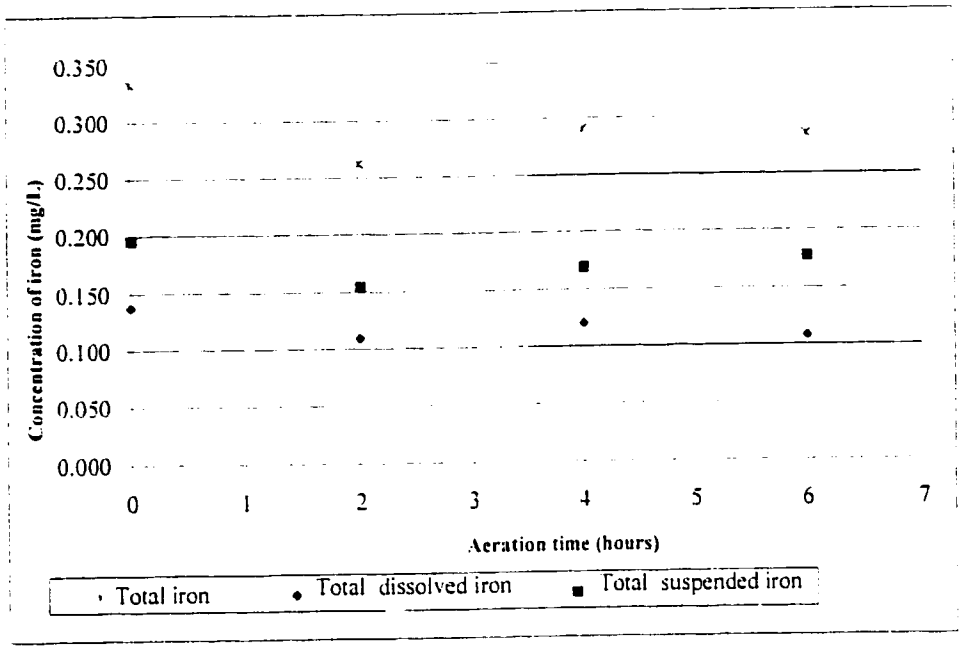

Figure 17. Total iron, dissolved and suspended for control sample experiment A

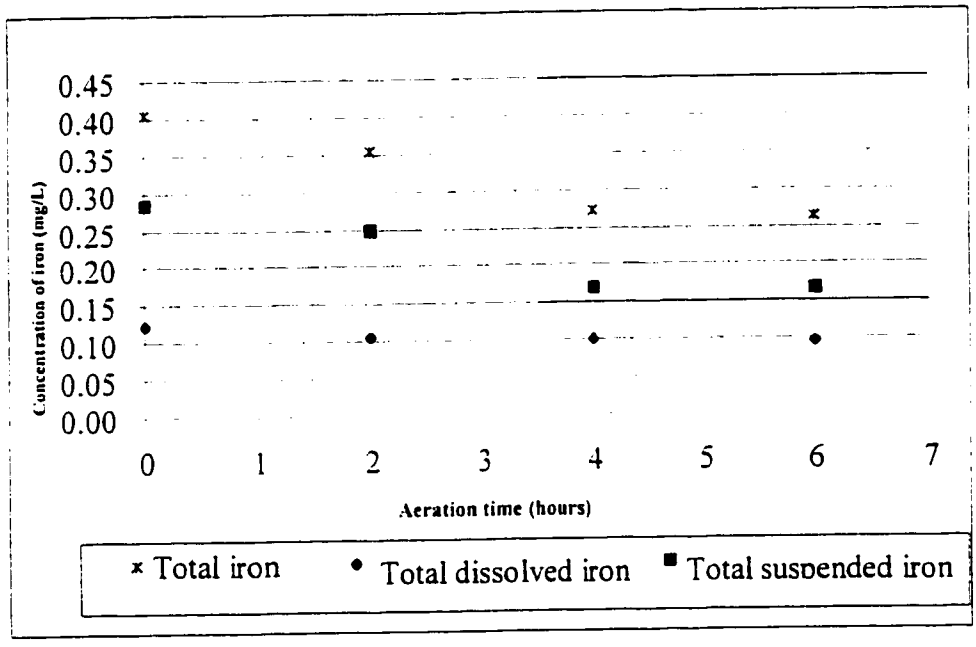

Figure 18. Total iron, dissolved and suspended for reagent grade ferrous solution sample experiment A

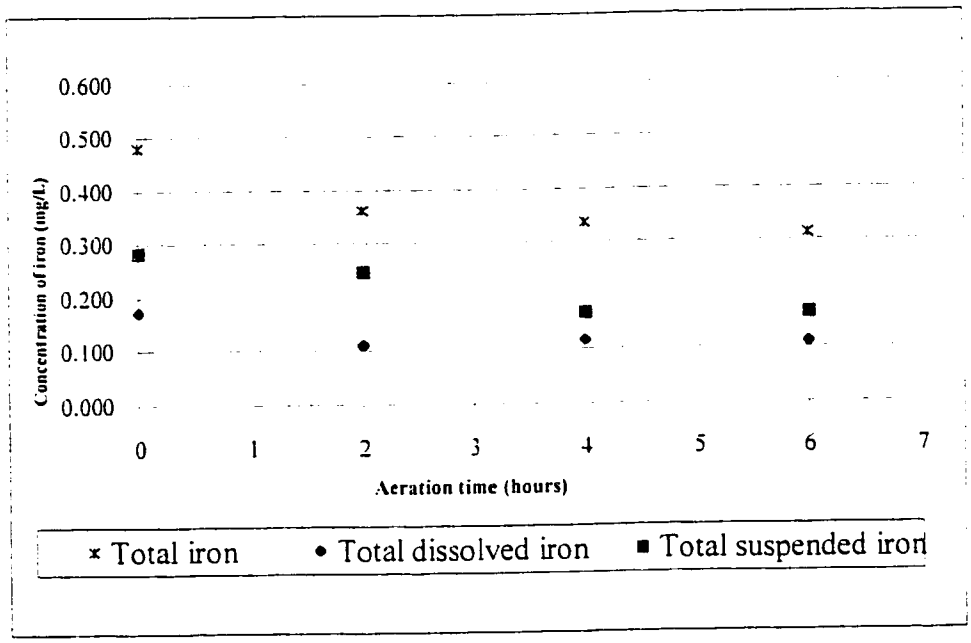

Figure 19. Total iron, dissolved and suspended for industrial waste solution sample experiment A

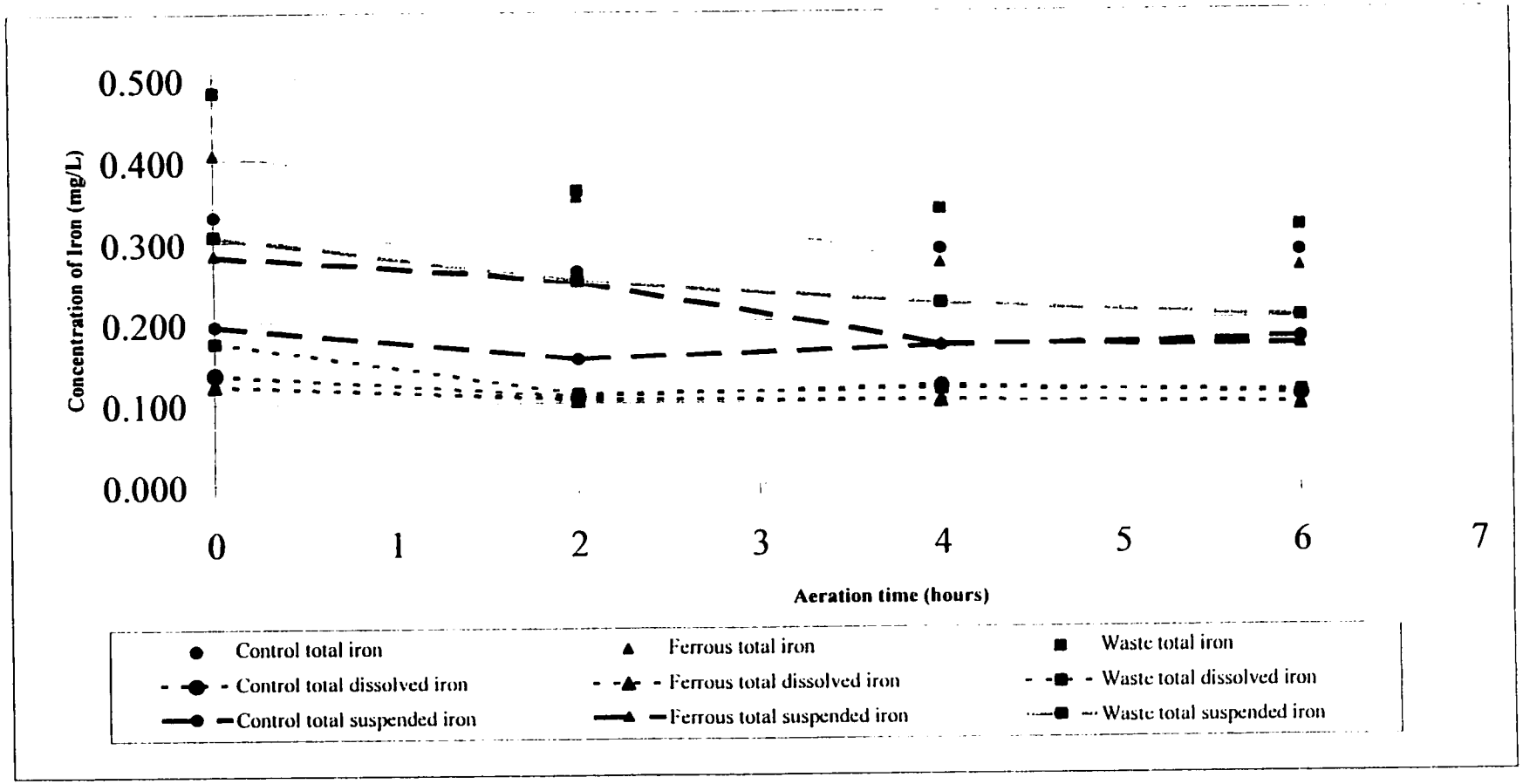

Figure 20. Graph of total iron, total dissolved iron and total suspended iron for the control, ferrous solution and waste solution experiments

As seen in Figure 20, the ferrous, waste and control sample total iron concentration were all reduced to approximately 0.30 mg/L at the end of the aeration time. The total dissolved iron stayed relatively constant throughout the aeration time and was approximately 0.10 mg/L. The total suspended iron calculated from the difference between total and dissolved iron was approximately 0.20 mg/L. These data provide evidence that variations in influent iron concentrations will be reduced over the six hour aeration period and be lowered to levels already experienced at the wastewater treatment plant.

5.5 Aerated mixed liquor iron analysis experiment B.

For the first set of trials, samples were only taken at time zero and hour 6. These were tested for unfiltered and filtered total iron and ferrous iron. TSS and pH were not measured. It was determined that this did not yield sufficient information and that more frequent sampling and additional measurements were needed. Therefore, for trials two and three, sampling was conducted at time zero, hour three and hour four. It was during these trials that the pH of the mixed liquor was measured whenever possible. The TSS was analyzed at each sample time. TSS is in Appendix D and pH is in Appendix E. All data and graphs may be found in Appendix C. Typical total iron, total dissolved iron, and total suspended iron graphs for the control sample, ferrous solution sample and industrial waste solution sample can be see in Figure 21 to Figure 23. Figure 24 is a typical graph of all three trials combined.

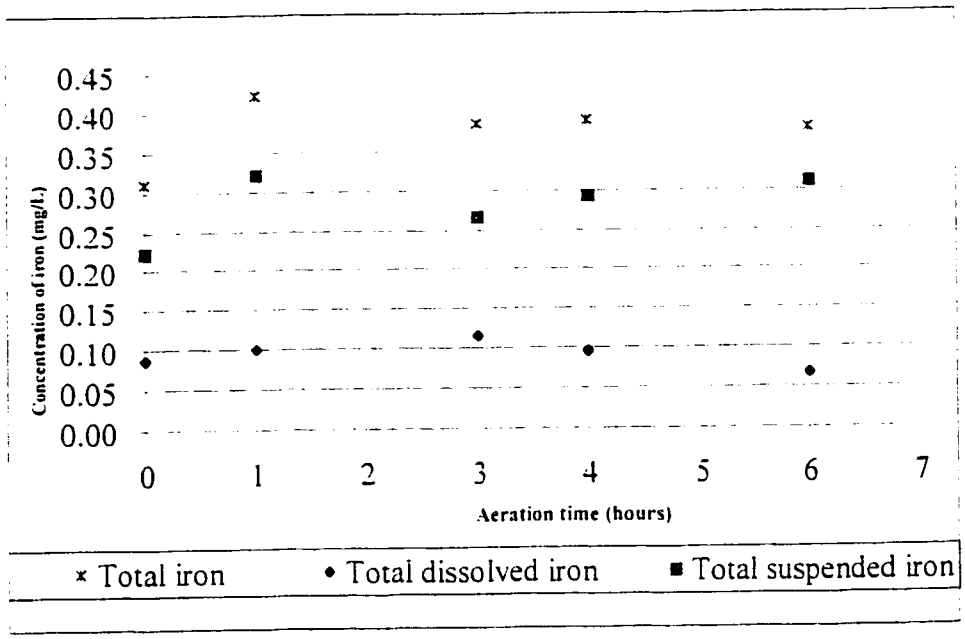

Figure 21. Total iron, dissolved and suspended for control sample experiment B.

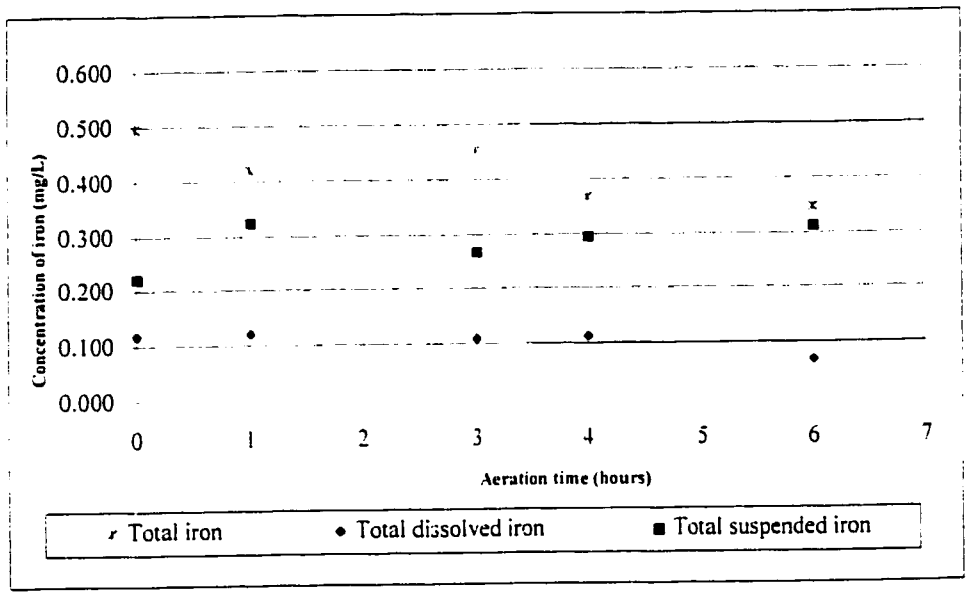

Figure 22. Total iron, dissolved and suspended for ferrous solution sample experiment B

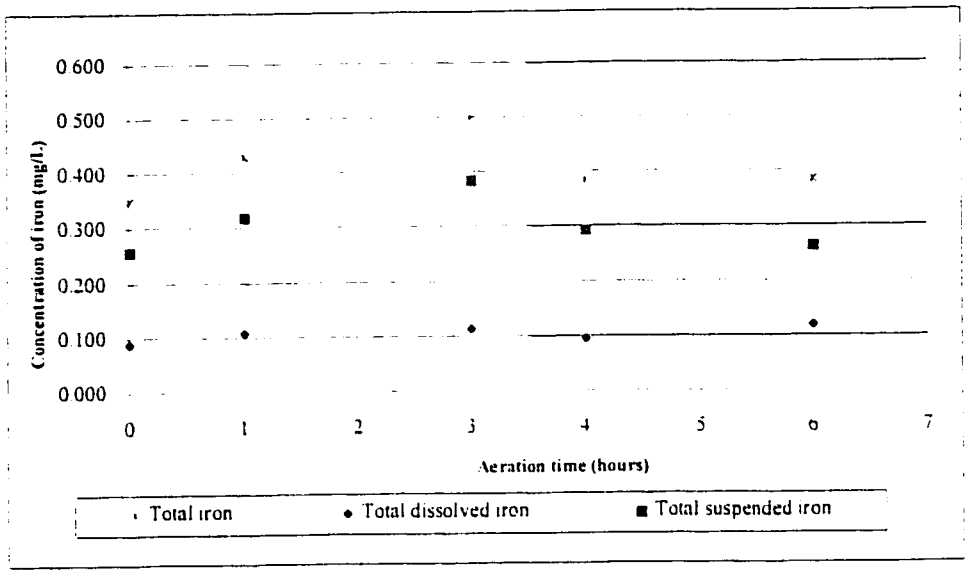

Figure 23. Total iron, dissolved and suspended for industrial waste solution sample experiment B

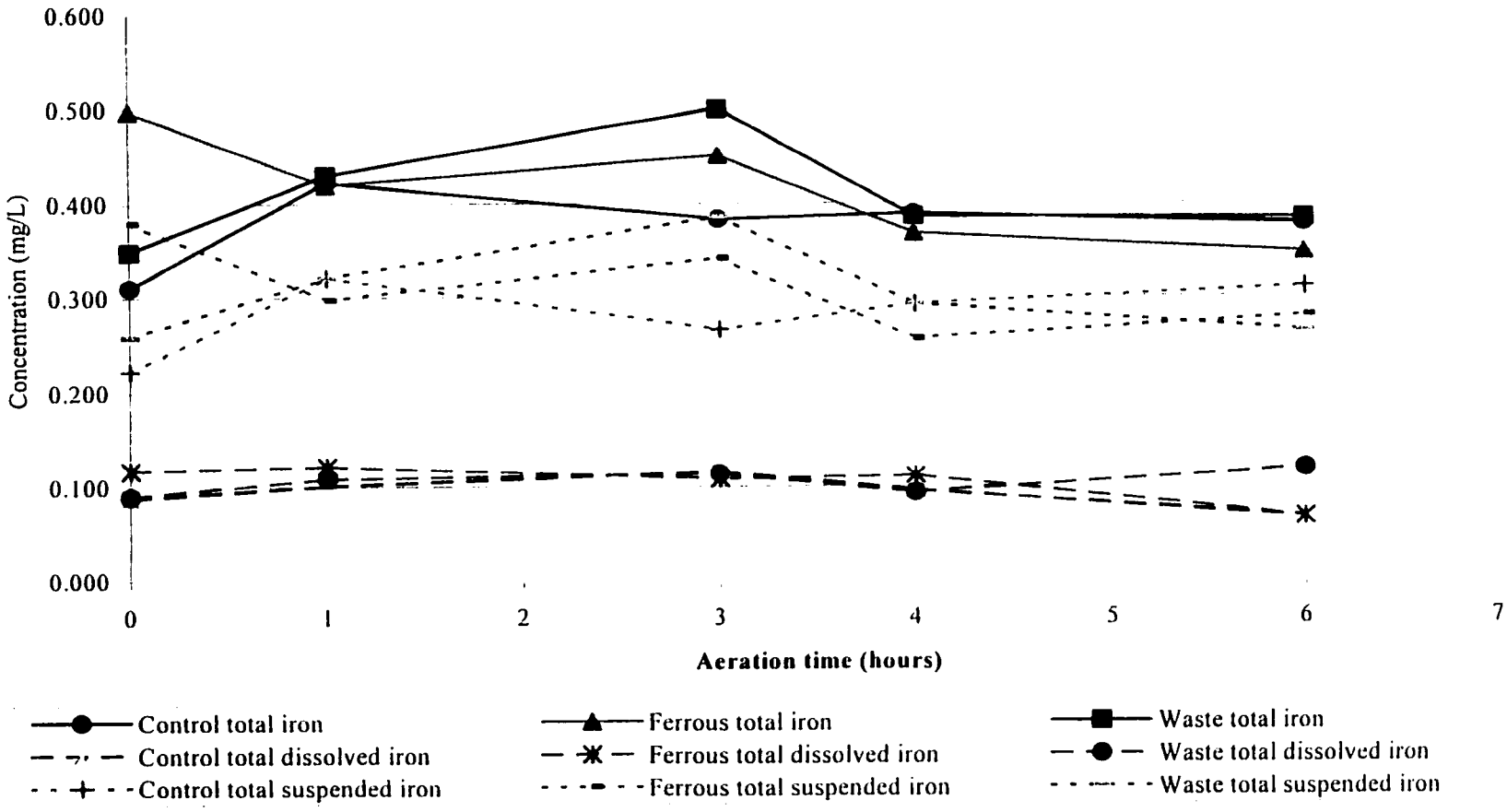

Figure 24. Graph of total iron, total dissolved iron and total suspended iron for the control, ferrous solution and waste solution samples experiment

As seen in Figure 24, the ferrous, waste and control sample total iron concentration were all reduced to approximately 0.375 mg/L at the end of the aeration period. This is similar to that found in experiment A. The total dissolved iron concentration stayed relatively constant throughout the aeration period as it did in experiment A and was approximately 0.100 mg/L. The total suspended iron concentration was a bit higher than that in experiment A and was approximately 0.300 mg/L. These data provide evidence that the use of mixed liquor will provide the same iron removal as that of the return activated sludge used in experiment A. These two experiments will be compared in section 5.9.

5.6 Comparison of 0.45 μm filtered and 0.2 μm filtered effluents in experiment B

In experiment B, samples were filtered with a 0.45 μm pore membrane filter. Additional filtration was conducted using a smaller membrane filter size of 0.2 μm. The purpose of this extra filtration was to investigate the possibility of iron associated with smaller particle sizes. Only total iron was analyzed on the filtered samples that were run through the 0.2 μm membrane. These were then compared to the total dissolved iron samples that were run through the 0.45 μm membrane. The control sample results are shown in Figure 25. The comparison graph for the ferrous and waste solutions can be found in Appendix C.

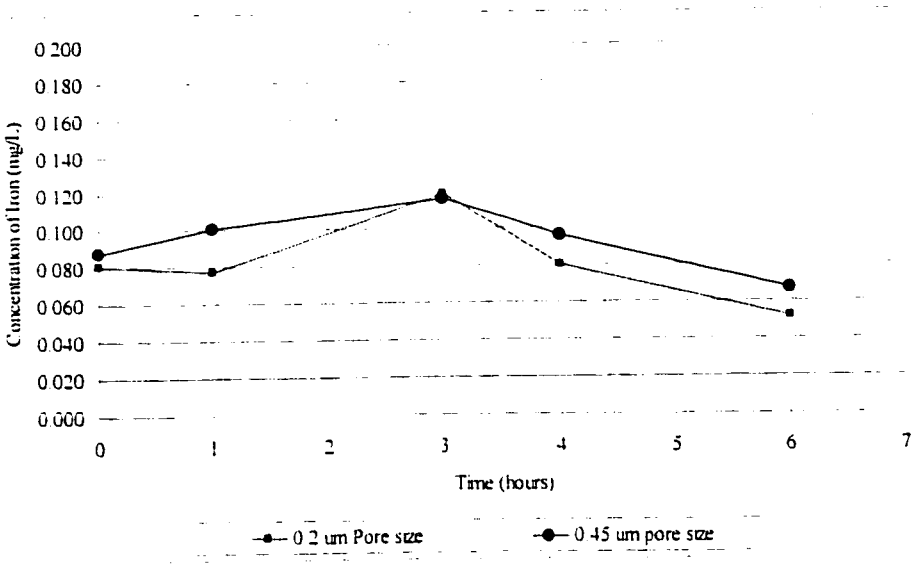

Figure 25. Comparison of total iron filtered samples through 0.2 μm pore size and 0.45 μm pore size for control sample experiment B.

A comparison of the two sets of data shows that there were no statistically significant difference in the amount of iron associated with filtrate which passed through the 0.45 μm membrane filter or the 0.2 μm filter. This is shown in Table 26 to Table 28. We can therefore conclude that a negligible amount of iron is associated with particles in the size range of 0.2 to 0.45 μm.

Table 26. Statistical analysis of 0.45 μm and 0.2 μm samples, (control)

Time	Paired t-test	Degrees of freedom	Critical t for $\alpha = 0.05$
0	0.382	4	2.776
1	0.190	2	4.303
3	0.415	2	4.303
4	0.146	2	4.303

Paired t-test, one-tail, equal variance

Table 27. Statistical analysis of 0.45 μm and 0.2 μm samples, (ferrous solution)

Time	Paired t-test	Degrees of freedom	Critical t for $\alpha = 0.05$
0	0.248	4	2.776
1	0.238	2	4.303
3	0.249	2	4.303
4	0.102	2	4.303

Paired t-test, one-tail, equal variance

Table 28. Statistical analysis of 0.45 μm and 0.2 μm samples, (waste solution)

Time	Paired t-test	Degrees of freedom	Critical t for $\alpha = 0.05$
0	0.341	4	2.776
1	0.026	2	4.303
3	0.012	2	4.303
4	0.000	2	4.303

Paired t-test, one-tail, equal variance

5.7 pH analysis of experiment B

The pH of the mixture of 0.6 L of digester sludge settled supernatant and 14.4 L of activated sludge was measured to see if continual aeration was resulting in a pH shift in the solution and whether this was affecting iron removal. Normally, the activated sludge process produces CO_2 as a by-product of the degradation of organic matter. The activated sludge that was used in this experiment was already low in $cBOD_5$. The pH was found to increase due to the loss of CO_2 which would cause a shift in the carbonate-bicarbonate system. A graph of all trials and samples can be seen in Figure 26. All other data and graphs can be found in Appendix E.

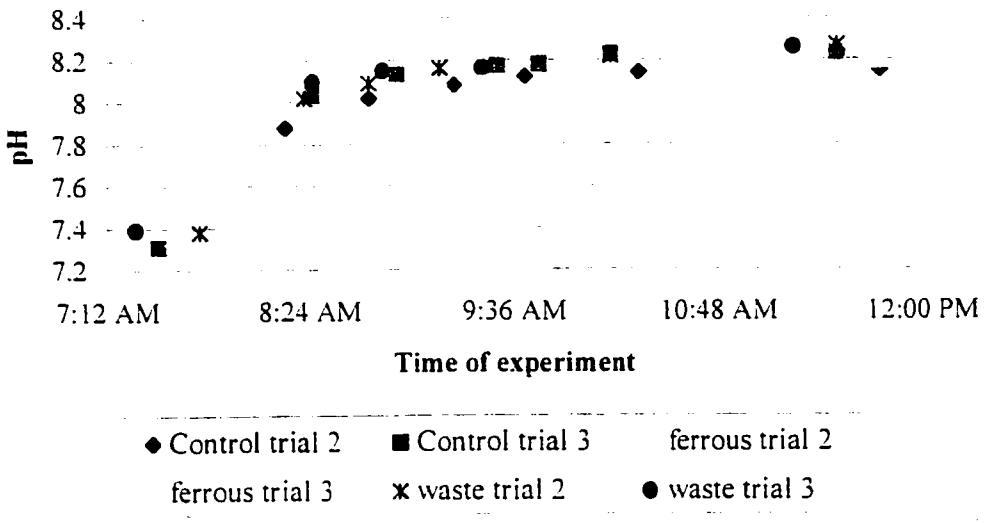

Figure 26. Graph of all pH data for control, ferrous solution and waste solution samples in experiment B: Activated sludge.

It can be seen in Figure 26 that in all three samples, the pH of the solution levels off to a pH value of approximately 8.2. With an increase in the pH, the total, ferrous and ferric iron concentrations were observed to decline over the 6 hours of aeration. At these pH ranges most of the ferrous and ferric iron will generally be found in the insoluble form and be precipitated out during the oxidation of the activated sludge.

5.8 TSS and iron / TSS ratio analysis of Experiment B

All TSS data can be found in Appendix D. Typical TSS, iron / TSS ratio and average TSS and iron/TSS graphs can be seen in Figure 27 to Figure 30.

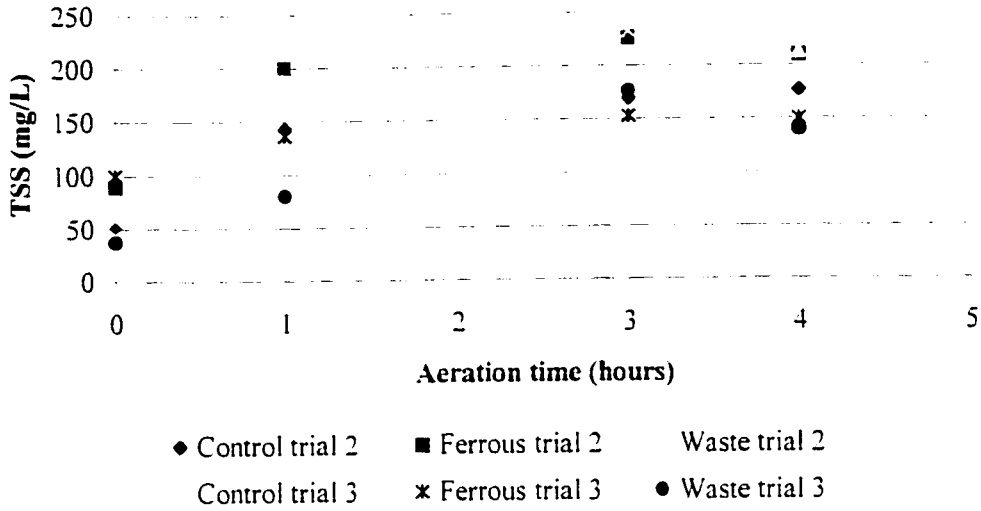

Figure 27. All TSS data for trials 2 and 3 for control, ferrous and waste solutions in experiment B: Activated sludge.

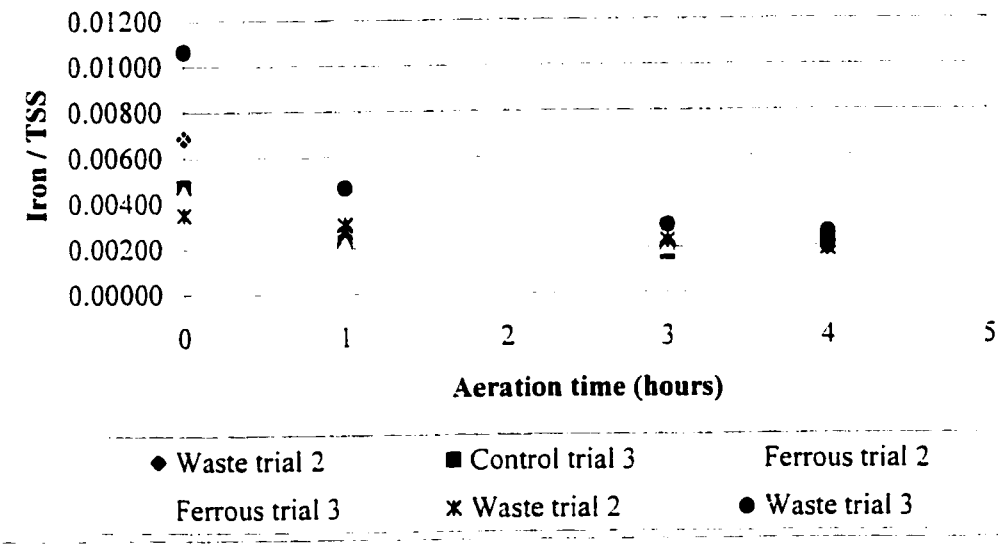

Note: This is in liquid after settling

Figure 28. Iron / TSS ratio data for trials 2 and 3 for control, ferrous and waste solutions in experiment B: Activated sludge

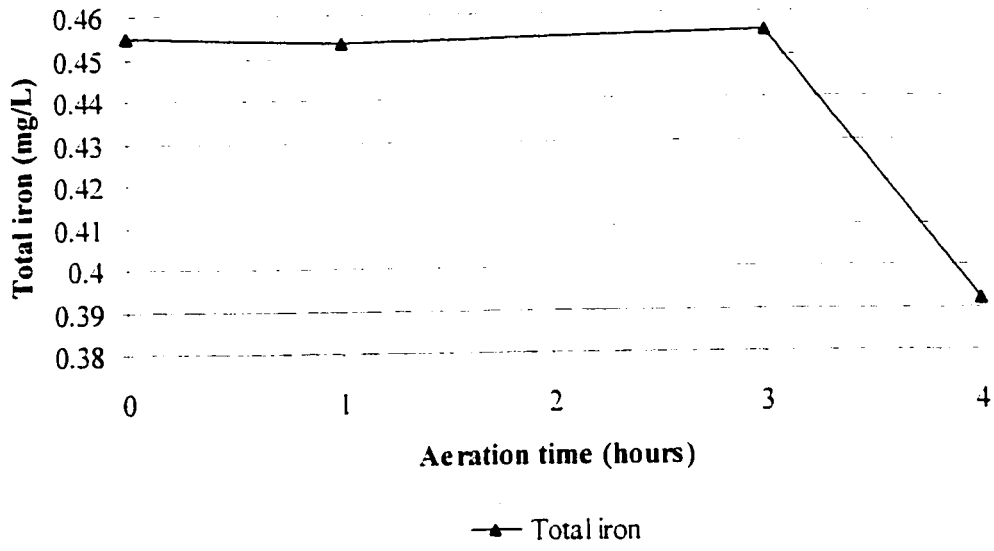

Figure 29 Average iron for trials 2 and 3.

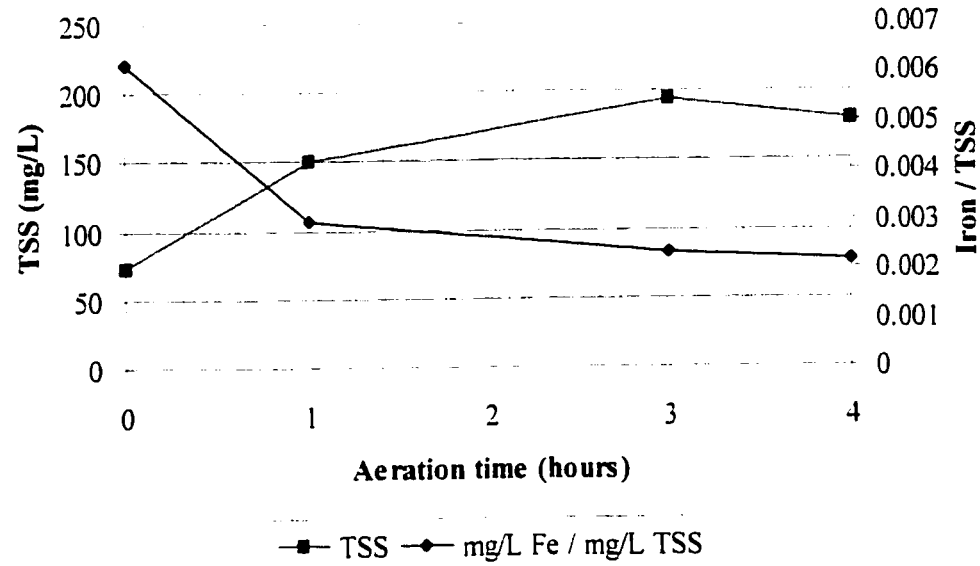

Note: This is in liquid after settling

Figure 30. Average TSS and iron / TSS ratio for trials 2 and 3

Figure 27 indicates that the TSS of the settled supernatant was increasing over the 4-hour aeration period. This may have been due to over-aeration of the activated sludge which may cause the biomass to settle slower than normal. However, when we look at Figure 28, the iron to TSS ratio declined over the same period, indicating that the iron in solution is associated with the TSS. These graphs therefore provide evidence that when the TSS is abnormally high, the ratio of iron / TSS is still below 0.05. Therefore there is no concern with the amounts of iron added to the mixed liquor.

5.9 Combined experiments A and B.

Return activated sludge from the clarifier was used in experiment A, whereas aerated mixed liquor from the aeration tank was used in experiment B.

Figure 31 to Figure 33 are typical results of the comparison of these two experiments. All graphs can be found in Appendix G. In general, all graphs indicate that the results from two trials were similar.

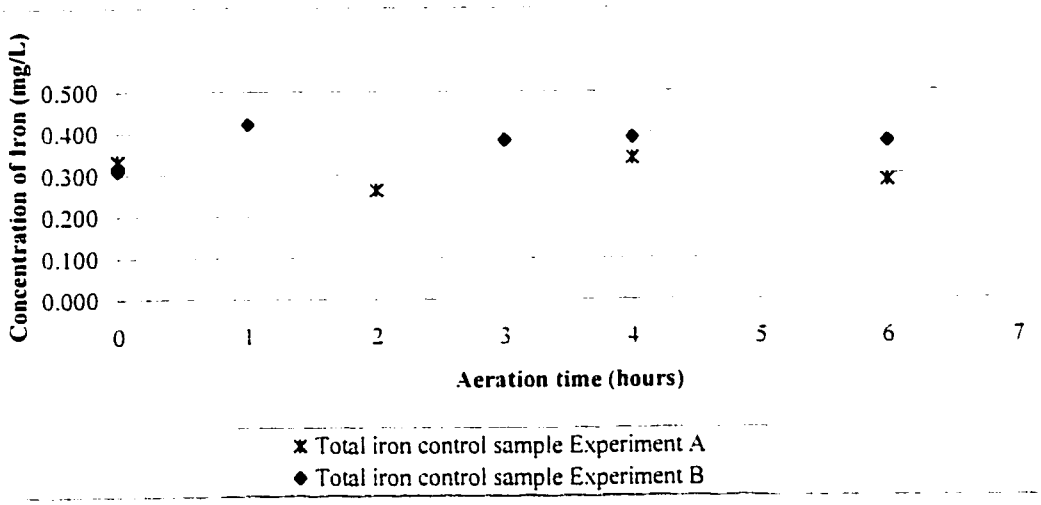

Figure 31. Graph of total iron for control sample for both experiment A and B

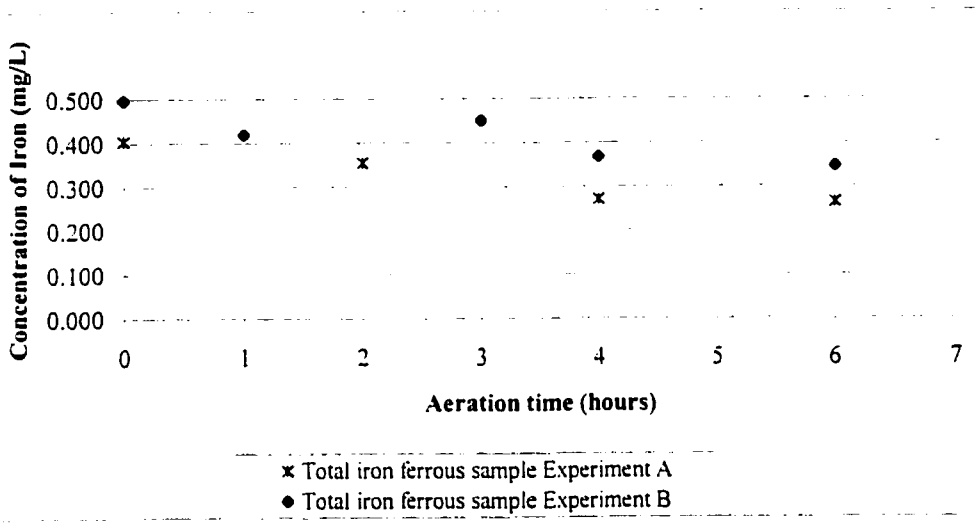

Figure 32. Graph of total iron for ferrous sample for both experiment A and B

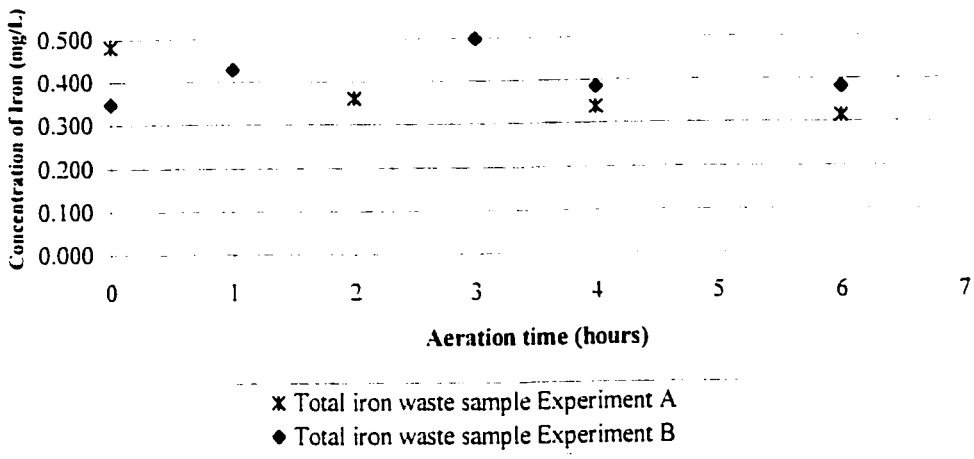

Figure 33. Graph of total iron for waste sample for both experiment A and B

5.9.1 Statistical comparison of experiments A and B for all samples of total and ferrous irons

Statistical analysis was conducted using the pooled two sample t-statistic (Moore et. al. 1993) where:

$$t = \frac{x_1 - x_2}{S_p\sqrt{\frac{1}{n_1} + \frac{1}{n_2}}} \qquad S_p = \sqrt{\frac{(n_1 - 1)\cdot S_1^2 + (n_2 - 1)\cdot S_2^2}{n_1 + n_2 - 2}}$$

t = Pooled two sample t statistic

S_p = Pooled estimator of variance

x_1 and x_2 = samples

n_1 and n_2 = sample trial numbers

S_1 and S_2 = sample standard deviation

Table 29 to 31 indicate whether to reject, or accept the null (H_o) and alternative (H_a) hypotheses. These being H_o: $\mu_1 = \mu_2$ or H_a: $\mu_1 \neq \mu_2$.

Table 29 Statistics of experiment A and B control sample

Type	Time	Calculated t	Degrees of freedom	Critical t for α= 0.05	Decision
Total iron	0 hr	0.337	4	2.776	Accept
Total iron	4 hr	0.724	3	3.182	Accept
Ferrous iron	0 hr	2.505	4	2.776	Accept
Ferrous iron	4 hr	0.049	2	4.303	Accept
Total dissolved iron	0 hr	2.586	5	2.571	Reject H_o
Total dissolved iron	4 hr	2.172	4	2.776	Accept
Ferrous dissolved iron	0 hr	3.333	5	2.571	Reject H_o
Ferrous dissolved iron	4 hr	0.032	4	2.776	Accept

Table 30 Statistics of experiment A and B ferrous sample

Type	Time	Calculated t	Degrees of freedom	Critical t for α= 0.05	Decision
Total iron	0 hr	0.789	5	2.571	Accept
Total iron	4 hr	1.085	4	2.776	Accept
Ferrous iron	0 hr	3.53	5	2.571	Reject H_o
Ferrous iron	4 hr	N/A	N/A	N/A	N/A
Total dissolved iron	0 hr	0.303	5	2.571	Accept
Total dissolved iron	4 hr	0.660	4	2.776	Accept
Ferrous dissolved iron	0 hr	0.528	5	2.571	Accept
Ferrous dissolved iron	4 hr	0.397	4	2.776	Accept

Table 31 Statistics of experiment A and B waste sample

Type	Time	Calculated t	Degrees of freedom	Critical t for $\alpha = 0.05$	Decision
Total iron	0 hr	1.918	5	2.571	Accept
Total iron	4 hr	0.882	4	2.776	Accept
Ferrous iron	0 hr	9.930	5	2.571	Reject H_o
Ferrous iron	4 hr	N/A	N/A	N/A	N/A
Total dissolved iron	0 hr	2.760	5	2.571	Reject H_o
Total dissolved iron	4 hr	3.161	4	2.776	Reject H_o
Ferrous dissolved iron	0 hr	2.481	5	2.571	Accept
Ferrous dissolved iron	4 hr	1.998	4	2.776	Accept

5.10 Quartz scale analysis

Quartz glass coupons (10 mm by 10 mm) were attached to a heating column and exposed to effluent obtained from settled aerated mixed liquor that was spiked with ferrous chloride to give a final concentration of 1.5 mg/L Fe^{2+}. The quartz coupons were removed at 24 hours and 48 hours of exposure. The effluent was analyzed for total iron, ferrous iron and TSS at time zero, 24 and 48 hours. The graphs of effluent total iron, TSS and iron/TSS concentrations and ratio over the experimental period can be seen in Figure 34 to 36. All data can be found in Appendix H.

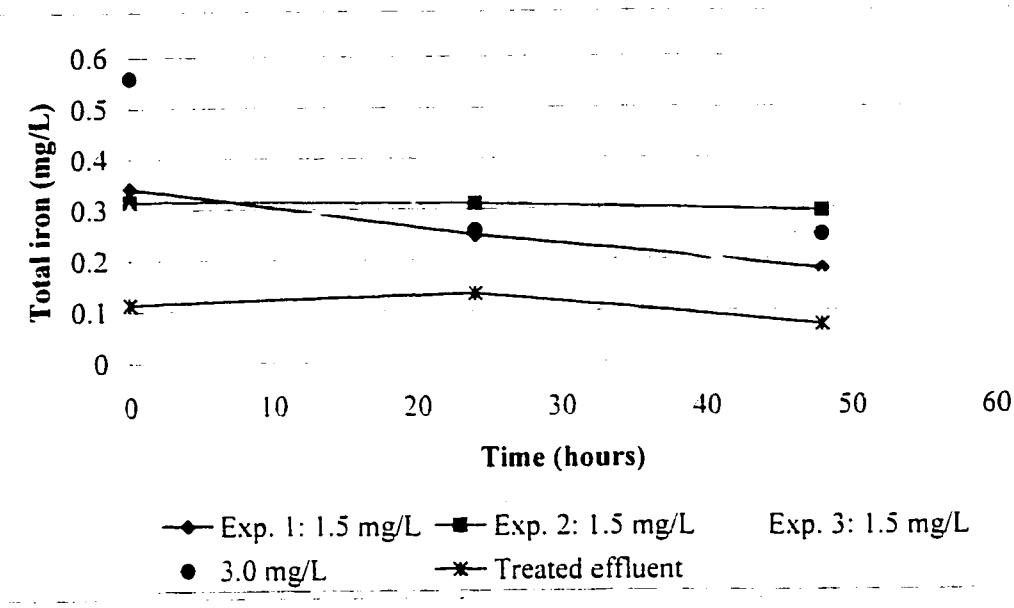

Figure 34. Total iron analysis over experimental period for all experiments

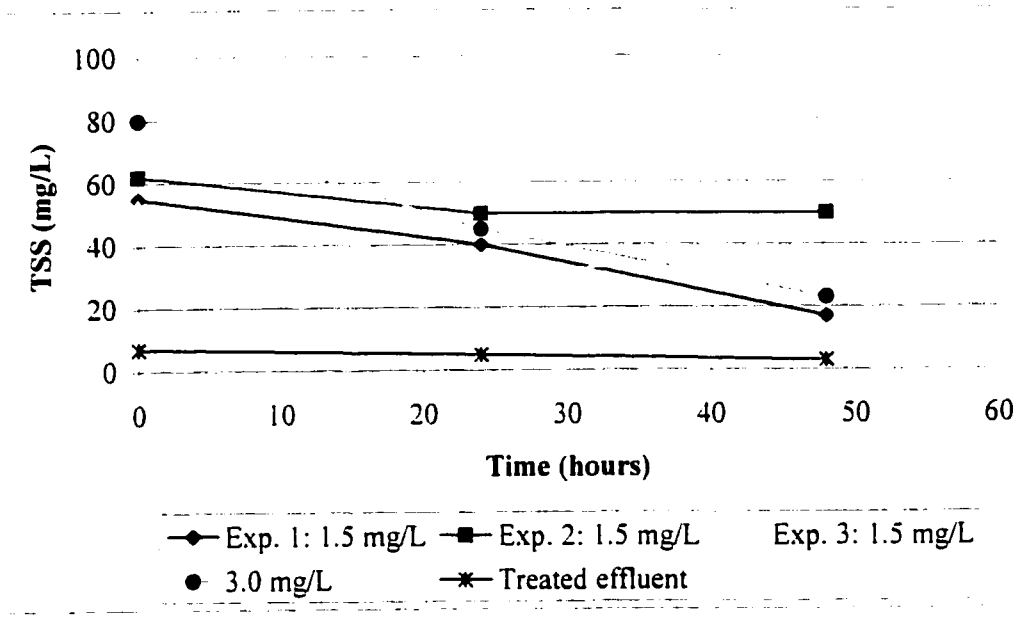

Figure 35. TSS analysis over experimental period for all experiments.

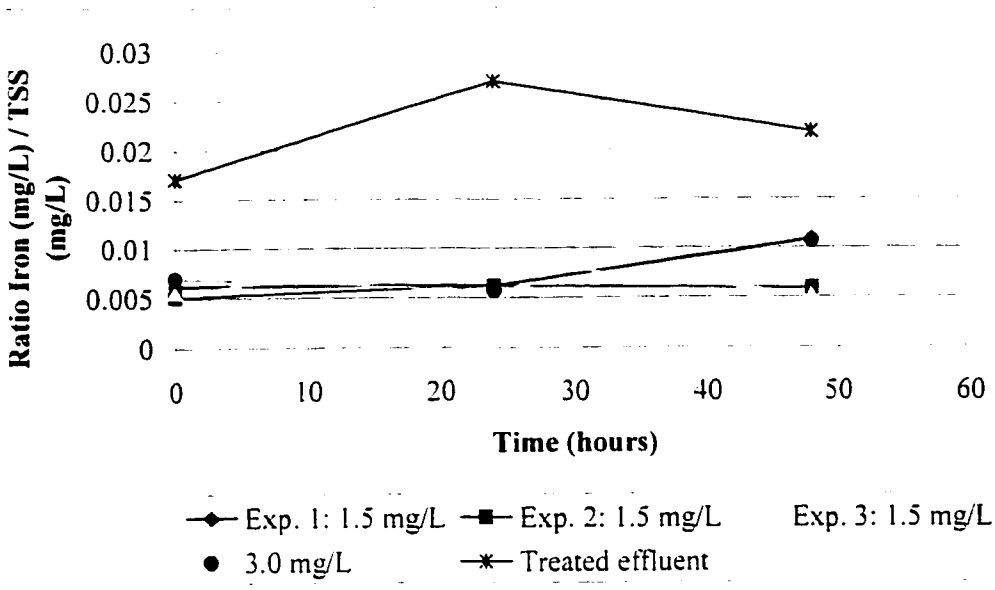

Figure 36. Iron/TSS ratio graph over experimental period for all experiments

Figure 34 indicates that as the experiment was conducted over the 48 hour time period, the level of iron in the effluent decreased. This may be due to several factors. Some of the suspended solids would have attached to the reactor and heating column and therefore would not have been drawn off during sampling. A portion of the suspended solids settled out of solution as a result of low velocity of the effluent being recycled in the closed loop reactor. Because of the decrease in suspended solids in the effluent, the total iron in the effluent was decreased.

5.10.1 Transmittance data for quartz glass pieces

Once the quartz glass pieces were removed from the heating column, they were placed in the UV spectrophotometer and analyzed for absorbance and transmittance at 254 nm. A clean quartz glass piece was used as reference to which all other quartz glass pieces were compared. This transmittance experiment was conducted to investigate how the scale present on the surface of the quartz will affect the output of available UV radiation. All data can be found in Appendix J. Table 32 contains typical data for absorbance and transmittance for the quartz glass coupons. Figure 37 and Figure 38 are graphical representations of the data.

Table 32. Transmittance data 1.5 mg/L sample at 24 hours exposure, experiment 1.

	1.5 mg/L at 24 hours Experiment 1	
Trial	Absorbance (254 nm)	%T
1	0.126	74.6
2	0.126	74.6
3	0.118	76.1
4	0.126	74.6
5	0.120	75.9
6	0.119	76.0
Average	**0.123**	**75.3**

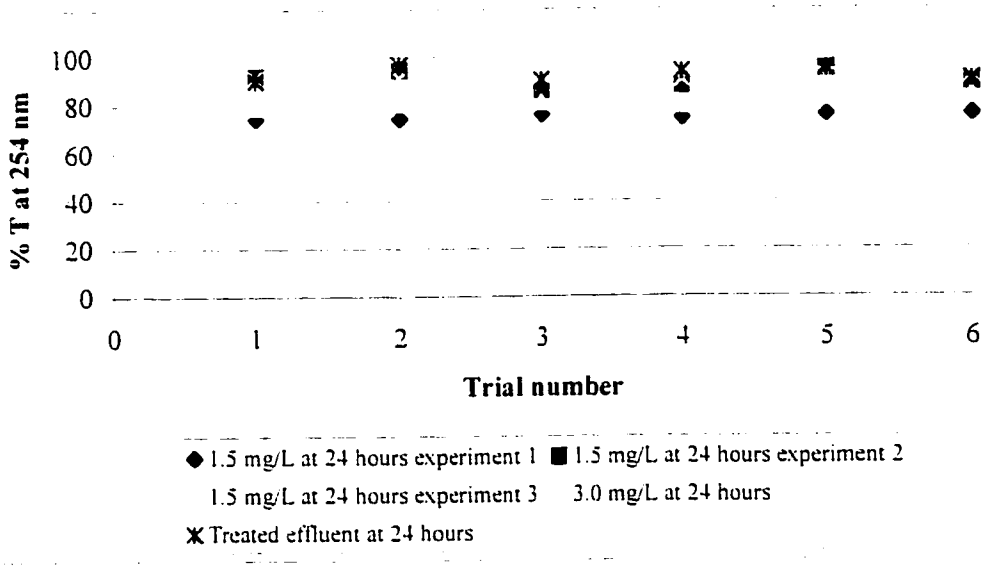

Figure 37. Transmittance data for all trials at 24 hours exposure

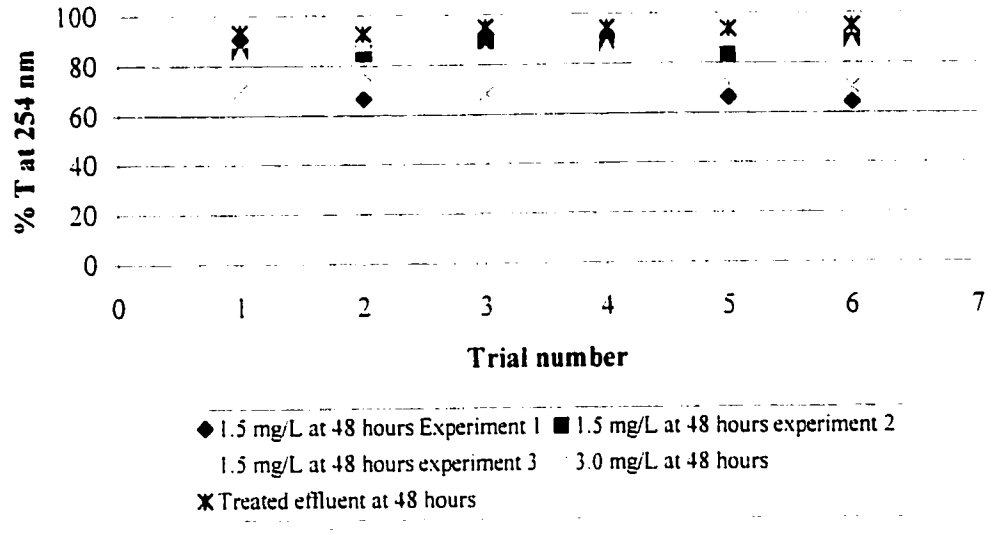

Figure 38. Transmittance data for all trials at 48 hours exposure

5.10.2 Scanning electron microscope x-ray defraction

All data and pictures may be found in Appendix I. A typical picture of the surface of the quartz can be seen in Figure 39. Table 33 shows relative amounts of elements on the particle pictured in Figure 39. The majority of this particle is composed of calcium, magnesium, silica and aluminum as well as a very small portion of iron. The atomic percent values in Table 33 are values relative to the sample as a whole and are not compared to a control value. Therefore some trial and error is involved in this type of procedure to determine what the compound is actually composed of. Depending on how thick the sample is, the quartz glass will be incorporated into the atomic percent skewing the results.

Figure 39. Particle 1 on 1.5 mg/L Experiment 1 at 48 hours

Table 33. Quantitative analysis data of particle 1 on 1.5 mg/L Experiment 1 at 48 hours

Date of Experiment: April 19 1998

Element	Relative Atomic Number	Normal wt %	Atomic %
Na	0.0010	0.21	0.31
Mg	0.0865	13.13	18.30
P	0.0000	0.00	0.00
Cl	0.0069	0.78	0.75
Ca	0.5369	56.21	47.54
K	0.0094	0.92	0.80
Fe	0.0387	4.45	2.70
Al	0.0399	5.98	7.52
Si	0.1381	18.32	22.09
Total		**100.00**	**100.01**

5.10.3 Inductive coupled plasma analysis on quartz scale

The quartz glass pieces that were exposed to the effluent from the aerated mixed liquor supernatant were sent to an independent laboratory to be analyzed for a total of 26 different elements using inductive couple plasma technique (ICP). Three quartz pieces were analyzed at the same time to provide a larger surface area from which to draw data from. This would provide a surface area of 300 mm^2. Table 34 shows typical results of the 26 different elements on the quartz glass coupon. All other data can be found in Appendix K. Since there was only one sample number per test, statistical analysis of the data does not provide evidence that there is any significant difference between samples analyzed at 24 and 48 hours. This is also true for comparison of 1.5 mg/L samples and the treated effluent sample. If we assume that the combined area on the quartz glass pieces is approximately 300 mm^2, neglecting some curvature, we can calculate the mass of element per area. The

quartz lamp sleeve was approximately 530 mm in length and had a circumference of 240 mm. By neglecting the rounded end of the lamp which is not cleaned by the automatic cleaning mechanism, the total surface area of the lamp is approximately 127,000 mm^2. From these measurements the total element scale per lamp can be calculated. This is shown in Table 34.

Table 34. 1.5 mg/L sample, experiment 2 at 24 hours

Metals, Dissolved	Results (μg)	Detection limit (μg)	Mass per area (μg/mm^2)	Lamp scale (μg/lamp)
Aluminum (Al)	4.5	0.2	0.01500	1908
Barium (Ba)	0.071	0.002	0.00024	30.104
Beryllium (Be)	0.00	0.01	0.00000	0
Bismuth (Bi)	0.004	0.001	0.00001	1.696
Boron (B)	0.38	0.04	0.00127	161.12
Cadmium (Cd)	0.022	0.002	0.00007	9.328
Calcium (Ca)	11	1	0.03667	4664
Chromium (Cr)	0.481	0.008	0.00160	203.944
Cobalt (Co)	0.004	0.002	0.00001	1.696
Copper (Cu)	0.08	0.24	0.00027	33.92
Iron (Fe)	3.2	0.2	0.01067	1356.8
Lead (Pb)	0.137	0.002	0.00046	58.088
Magnesium (Mg)	1.8	0.2	0.00600	763.2
Manganese (Mn)	0.056	0.002	0.00019	23.744
Molybdenum (Mo)	0.003	0.002	0.00001	1.272
Nickel (Ni)	0.042	0.002	0.00014	17.808
Phosphorus (P)	2.5	0.2	0.00833	1060
Potassium (K)	3.0	0.2	0.01000	1272
Silver (Ag)	0.004	0.004	0.00001	1.696
Sodium (Na)	9	2	0.03000	3816
Strontium (Sr)	0.070	0.002	0.00023	29.68
Thallium (Ti)	0.000	0.001	0.00000	0
Tin (Sn)	0.067	0.004	0.00022	28.408
Uranium (U)	<0.002	0.002	0.00001	0.848
Vanadium (V)	0.009	0.002	0.00003	3.816
Zinc (Zn)	0.43	0.04	0.00143	182.32

Iron was found to be present in varying percentages in practically all x-ray defraction and ICP analyses. As seen in Table 35, total iron lamp scale is presented as a percent of all element scale found on the surface of the quartz lamp sleeve. All iron percentages found using x-ray defraction SEM analyses were combined and presented in Table 36.

Table 35. Percent of iron associated with quartz lamp sleeve scale using ICP analyses.

Trial	Time (hr)	Total 26-element lamp scale (μg/lamp)	Iron scale (μg/lamp)	Iron scale (%)
1.5 mg/L exp. 2	24	15604.9	1354.7	8.7
1.5 mg/L exp. 3	24	25669.2	3894.7	15.2
Clarifier 4 effluent	24	26298.3	5926.7	22.5
1.5 mg/L exp. 2	48	23218.1	3217.3	13.9
1.5 mg/L exp. 3	48	13920.5	1100.7	7.9
Clarifier 4 effluent	48	26912.6	4487.3	16.7

Table 36. Percent of iron found in all x-ray defraction analyses.

Experimental Test	Iron scale relative to other elements tested shown as percent (%)
Overview of 1.5 mg/L Experiment 1 at 24 hours	3.94
Area 1	2.58
Area 2	6.16
Area 3	2.84
Overview of 1.5 mg/L Experiment 1 at 48 hours	9.08
Area 1	2.70
Area 2	7.39
Area 3	6.29
Overview of 1.5 mg/L Experiment 2 at 24 hours	Not Calculated
Area 1	7.37
Area 2	0.54
Area 3	41.10
Overview of 1.5 mg/L Experiment 2 at 48 hours	Not Calculated
Area 1	2.69
Area 2	1.88
Area 3	1.89
Overview of 1.5 mg/L Experiment 3 at 24 hours	Not Calculated
Area 1	7.11
Area 2	4.42
Area 3	6.45
Overview of 1.5 mg/L Experiment 3 at 48 hours	Not Calculated
Area 1	2.02
Area 2	4.66
Area 3	2.65
Overview 3.0 mg/L Experiment 1 at 24 hours	5.67
Area 1	20.35
Area 2	2.43
Area 3	9.91
Overview 3.0 mg/L Experiment 1 at 48 hours	12.29
Area 1	13.50
Area 2	7.07
Area 3	2.26
Overview of clarifier 4 effluent at 24 hours	Not Calculated
Area 1	1.29
Area 2	0.00
Area 3	2.16
Overview of clarifier 4 effluent at 48 hours	Not Calculated
Area 1	4.53
Area 2	10.34
Area 3	0.00

As can be seen in Table 35 and Table 36 the percentages of iron vary considerably from sample to sample and are found as low as zero percent and as much as 41.1 % of the sample mass. Results contained in these tables, and those contained in Appendix K, do not reveal the trend of scale deposition increasing with time (that is shown in Figure 5) as average scale deposits build up on an entire quartz sleeve. Because the coupons represent discrete samples of scale deposition, the results illustrate the spatially random nature of scale deposition. This indicates that testing using a larger quartz surface or even full-scale testing is required to yield data needed to evaluate adequately the effect of increased iron concentrations on average deposition rates. Table 35 and Table 36 provide meager information as to the amounts of iron scales deposited, however, they do indicate that iron deposits may be problematic if iron concentrations are not kept in check. Some of the highest amounts of iron deposits were found to be in the 3.0 mg/L experiments. The activated sludge spiked with 3.0 mg/L total iron was an extreme experimental condition which is double the average iron concentration currently entering the wastewater treatment plant. The UV treatment unit at the WWTP is equipped with an automatic sleeve cleaning device that is currently set to clean sleeves daily. The frequency of cleaning can be increased if needed. Because the effect of the automatic cleaning process could not be duplicated adequately in the laboratory, the ability of the process to remove the deposits and maintain process efficiency can not be speculated upon.

6.0 Conclusion

Based on the experimental results the following conclusions can be made:

1. The total iron concentrations in experiments A and B were found to be lowered to levels that are already experienced at the wastewater treatment plant. The results from iron experiments, A and B, were found to be statistically similar, indicating repeatability of the experimental protocol and validity of the results.
2. Final total iron concentrations resulting from tests using various concentrations of ferrous iron (either as reagent grade or waste ferrous) were not different from those of control tests in which no iron was added. Therefore iron added to raw wastewater will be oxidized and precipitated in the aeration tanks, or removed in the clarifier and will have little or no effect on the overall iron concentrations in the final effluent.
3. Analysis of deposits on samples of quartz sleeve scale indicates that scale will form on the sleeves as a result of suspended particles present in the effluent. After aeration of the mixed liquor spiked with a ferrous chloride solution the concentration of total iron was found to be similar to that already experienced at the wastewater treatment plant. The scale was found to be mostly calcium and magnesium deposits, as well as some clay particles. Iron was found to be present on all quartz glass coupons in varying percentages. Because the UV disinfection system is equipped with an automatic cleaning mechanism which wipes the quartz lamp sleeves with a solution of Lime-A-Way once per day, the amount of

iron scale that may be present is unlikely to hinder the disinfection ability of the WWTP provided that the cleaning mechanism removes all residue and iron scale deposits.

7.0 Recommendations

In order to understand and improve the procedures involved in the formation of iron scale on the UV quartz lamp sleeves the following recommendations were made for further study:

1. Determination of the effective UV radiation that is passing through the quartz sleeve before and after scaling has occurred.
2. Determination of the attenuation of the UV radiation as the distance away from the quartz lamp sleeve increases.
3. Perform microbial tests on effluents that have been exposed to UV radiation from lamps with and without scale.
4. In addition to the standard total and fecal coliform test, conduct microbial tests on harder to disinfect organisms and specific pathogens.
5. Establish a pilot project in which an iron solution is added to the anaerobic digesters. The iron could then be tracked from the anaerobic digesters to Clover Bar lagoon and back through the wastewater treatment plant.

8.0 References

AEP. June 1997. Standards and Guidelines for municipal waterworks, wastewater and storm drainage systems. *Alberta Environment Protection* , Edmonton, Alberta.

Andritsos, N., M. Kontopoulou, and A. J. Karabelas. 1996. Calcium carbonate deposit formation under isothermal conditions. *Canadian journal of chemical engineering,* **74**: 911-919.

APHA. 1992. *Standard Methods for the Examination of Water and Wastewater.* 18th Edition. Washington, DC.

Baron, J. 1997. Repair of wastewater microorganisms after ultraviolet disinfection under seminatural conditions. *Water Environment Research,* **69**: 992-998.

CH2M-Hill. 1995. Gold Bar WWTP UV disinfection upgrade analyses of confirmatory pilot testing results, Technical Memorandum No. 13. CH2M HILL Engineering, Edmonton, Alberta.

Chiarella, R. 1998. M.Sc. Thesis, H_2S Reduction in Anaerobic Digester Sludge. *Department of Civil and Environmental Engineering.* University of Alberta, Edmonton. Pages 213

EPA. Design manual municipal wastewater disinfection. EPA/625/1-86/021 U. S. Environmental Protection Agency, Office of Research and Development, Water Engineering Research Laboratory, Center for Environmental Research Information, Cincinnati, Ohio. Oct. 1986.

EPA. *Ultraviolet Disinfection Technology Assessment*. EPA 832-R-92-004. U.S. Environmental Protection Agency Office of Wastewater Enforcement and Compliance. Washington, D.C. Sept. 1992.

Epstein, N. 1983. Fouling of heat exchangers. *Heat Exchangers Theory and Practice*. McGraw Hill., 979 p.

Garret-Price, B. A., S. A. Smith, R. L. Watts, J. G. Knudsen, W. J. Marner, and J. W. Suitor. 1985. *Fouling of Heat Exchangers Characteristics, Costs, Prevention, Control, and removal*. Noyes Publications. Park Ridge, NJ., 415 p.

Gehr, R., and H. Wright. 1998. UV Disinfection of Wastewater coagulated with ferric chloride: Recalcitrance and fouling problems. *IAWQ 19th Biennial International Conference*, Vol. 4., page 22-29., Vancouver, B.C.

Havelaar, A. H., C. C. E. Meulemans, W. M. Pot Hogeboom, and J. Koster. 1990. Inactivation of bacteriophage MS2 in wastewater effluent with monochromatic and polychromatic ultraviolet light. *Water Res.*, **24**., 1387-1393.

Hem, J. D., and W. H. Cropper. 1959. *Chemistry of Iron in Natural Water: Survey of Ferrous-Ferric Chemical Equilibria and Redox Potentials*. U.S. Government Printing Office, Washington, DC., 30 p.

Kashimada, K., N. Kamiko, K. Yamamoto, and S. Ohgaki. 1996. Assessment of photoreactivation following ultraviolet light disinfection. *Water Science and Technology*, **33**, 261-269.

Kwan. A., J. Archer. F. Soroushian. A. Mohammed, and G. Tchobanoglous. 1998. Evaluation of UV Disinfection alternatives for a large-scale application. *Water Quality International 1998.* Trojan Technologies Inc., Vancouver, Canada.

Lehninger, A. L., D. L. Nelson, and M. M. Cox. 1993. *Principles of Biochemistry* 2nd edition. Worth Publishers, New York, NY. 1013 p.

Levinson, W., and E. Jawetz. 1996. *Medical Microbiology and Immunology Examination and board review.* Appleton and Lange, Stamford, CT., 523 p.

Loge, F. J., R. W. Emerick, M. Heath, J. Jacangelo, G. Tchobanoglous, and J. L. Darby. 1996. Ultraviolet disinfection of secondary wastewater effluents: Prediction of performance and design. *Water Environment Research,* **68**, 900-916.

Melo, L. F., T. R. Bott, and C. A. Bernardo. 1988. *Fouling science and technology.* Kluwer Academic Publishers, Dordrecht / Boston / London, 744 p.

Metcalf and Eddy. 1991. *Wastewater Engineering Treatment, Disposal and Reuse.* McGraw-Hill, New York, NY. 1334 p.

Murray, D. S. 1998. Operating Costs of Medium Pressure Ultraviolet Disinfection Systems. *Disinfection'98 The latest Trends in Wastewater Disinfection: Chlorination vs. UV Disinfection*, April 19-22. Baltimore, Maryland.

Moore, D.S., McCabe G. P. 1993. Introduction to the Practice of Statistics. Second edition. W.H. Freeman and Company. New York, NY. 854 p.

Najibi, S. H., H. Muller-Steinhagen, and M. Jamialahmadi. 1997. Calcium Carbonate Scale formation during subcooled flow boiling. *Journal of heat transfer transaction of the ASME*, **119**, 767-775.

Prescott, L. M., J. P. Harley, and D. A. Klein. 1990. *Microbiology second edition*. Wm. C. Brown Publishers, Oxford, England. 912 p.

Qualls, R. G., M. P. Flynn, and J. D. Johnson. 1983. The role of suspended particles in ultraviolet disinfection. *Journ., Water Pollution Control Federation*, **55**, 1280-1285.

Sakamoto, G. 1998. Overview of Wastewater disinfection. *Water Quality International 1998*. Trojan Technologies Inc., Vancouver, Canada.

Sakamoto, G., and C. Zimmer. 1997. UV Disinfection for wastewater reclamation: The effect of particle size and suspended solids. *1997 PNPCA annual conference*, Seattle, Washington.

Suitor, J. W., W. J. Marner, and R. B. Ritter. 1977. The history and status of research in fouling of heat exchangers in cooling water service. *Can. Journ. of Chem. Eng.*, **55**, 374-380.

Whitby, G. E., G. Palmateer, R. W. Morris, W. O. K. Grabow, and A. P. Dufour. 1993. The effect of UV transmission, suspended solids and photoreactivation on microorganisms in wastewater treated with UV light. *Water Science and Technology*, **27**, 379-386.

White, D. O., and F. J. Fenner. 1994. *Medical Virology*. Academic Press, San Diego CA. 603 p.

Appendix A. Data for Sulfide Analysis

Table A 1. 2 L of digester sludge from digester 3 at the 7.9 m level

Date of Experiment: November 23 1998

Run	Sample (mL)	0.4 M Phosphate Buffer (mL)	Stripping time (hr)	Sulfide (S^{-2}) (mg)	mg/L
Trial 1	500	120	1	8.872	17.744
Trial 2	500	120	1	8.396	16.792
Trial 3	500	120	1	8.583	17.166
Trial 4	500	120	1	9.089	18.178
				Average	17.470

Table A 2. 2 L of digester sludge from digester 3 at the 7.9 m level

Date of Experiment: November 24 1998

Run	Sample (mL)	0.4 M Phosphate Buffer (mL)	Stripping time (hr)	Sulfide (S^{-2}) (mg)	Mg/L
Trial 1	500	120	1	9.285	18.570
Trial 2	500	120	1	9.253	18.506
Trial 3	500	120	1	9.360	18.720
Trial 4	500	120	1	9.290	18.580
				Average	18.594

Table A 3. 2 L of digester sludge from digester 3 at the 7.9 m level

Date of Experiment: November 25 1998

Run	Sample (mL)	0.4 M Phosphate Buffer (mL)	Stripping time (hr)	Sulfide (S^{-2}) (mg)	Mg/L
Trial 1	500	120	1	9.128	18.256
Trial 2	500	120	1	8.763	17.526
Trial 3	500	120	1	8.776	17.552
Trial 4	500	120	1	9.005	18.010
				Average	17.836

Table A 4. 2 L of digester sludge from digester 3 at the 7.9 m level

Date of Experiment: November 26 1998

Run	Sample (mL)	0.4 M Phosphate Buffer (mL)	Stripping time (hr)	Sulfide (S^{-2}) (mg)	mg/L
Trial 1	500	120	1	9.572	19.144
Trial 2	500	120	1	9.334	18.668
Trial 3	500	120	1	9.514	19.028
Trial 4	500	120	1	10.430	20.860
				Average	18.947

Note: Trial 4 was omitted

Table A 5. 2 L of digester sludge from digester 3 at the 7.9 m level

Date of Experiment: November 27 1998

Run	Sample (mL)	0.4 M Phosphate Buffer (mL)	Stripping time (hr)	Sulfide (S^{-2}) (mg)	mg/L
Trial 1	500	120	1	10.106	20.212
Trial 2	500	120	1	10.885	21.77
Trial 3	500	120	1	9.514	19.028
Trial 4	500	120	1	10.430	20.860
				Average	20.991

Note: Trial 3 and 4 were omitted

Table A 6. 2 L of digester sludge from digester 3 at the 7.9 m level

Date of Experiment: November 28 1998

Run	Sample (mL)	0.4 M Phosphate Buffer (mL)	Stripping time (hr)	Sulfide (S^{-2}) (mg)	mg/L
Trial 1	500	120	1	9.115	18.230
Trial 3	500	120	1	9.601	19.202
Trial 2	500	120	1	8.847	17.694
Trial 4	500	120	1	14.187	28.374
				Average	18.716

Note: trial 4 was omitted

Table A 7. 2 L of digester sludge from digester 3 at the 7.9 m level

Date of Experiment: November 29 1998

Run	Sample (mL)	0.4 M Phosphate Buffer (mL)	Stripping time (hr)	Sulfide (S^{-2}) (mg)	mg/L
Trial 1	500	120	1	8.73	17.460
Trial 2	500	120	1	9.173	18.346
Trial 3	500	120	1	12.463	24.926
Trial 4	500	120	1	12.768	25.536
				Average	17.903

Note: Trial 3 and 4 were omitted

Table A 8. 2 L of digester sludge from digester 3 at the 7.9 m level

Date of Experiment: November 30 1998

Run	Sample (mL)	0.4 M Phosphate Buffer (mL)	Stripping time (hr)	Sulfide (S^{-2}) (mg)	mg/L
Trial 1	500	120	1	9.015	18.030
Trial 2	500	120	1	8.941	17.882
Trial 3	500	120	1	8.860	17.720
Trial 4	500	120	1	9.218	18.436
				Average	18.017

Table A 9. 2 L of digester sludge from digester 3 at the 7.9 m level

Date of Experiment: December 1 1998

Run	Sample (mL)	0.4 M Phosphate Buffer (mL)	Stripping time (hr)	Sulfide (S^{-2}) (mg)	mg/L
Trial 1	500	120	1	8.951	17.902
Trial 2	500	120	1	9.621	19.242
Trial 3	500	120	1	10.537	21.074
Trial 4	500	120	1	11.295	22.590
				Average	20.202

Note: Titrater leaked and caused higher sulfide values, therefore omitted

Table A 10. 2 L of digester sludge from digester 3 at the 7.9 m level

Date of Experiment: December 2 1998

Run	Sample (mL)	0.4 M Phosphate Buffer (mL)	Stripping time (hr)	Sulfide (S^{-2}) (mg)	mg/L
Trial 1	500	120	1	10.282	20.564
Trial 2	500	120	1	10.063	20.126
Trial 3	500	120	1	10.637	21.274
Trial 4	500	120	1	10.945	21.890
				Average	20.964

Table A 11. 2 L of digester sludge from digester 3 at the 7.9 m level

Date of Experiment: December 3 1998

Run	Sample (mL)	0.4 M Phosphate Buffer (mL)	Stripping time (hr)	Sulfide (S^{-2}) (mg)	mg/L
Trial 1	500	120	1	9.994	19.988
Trial 2	500	120	1	10.916	21.832
Trial 3	500	120	1	11.825	23.650
Trial 4	500	120	1	12.926	25.852
				Average	22.831

Note: Titrater leaked and caused higher sulfide values, therefore omitted

Table A 12. 2 L of digester sludge from digester 3 at the 7.9 m level

Date of Experiment: December 4 1998

Run	Sample (mL)	0.4 M Phosphate Buffer (mL)	Stripping time (hr)	Sulfide (S^{-2}) (mg)	mg/L
Trial 1	500	120	1	8.604	17.208
Trial 2	500	120	1	8.72	17.44
Trial 3	500	120	1	8.691	17.382
Trial 4	500	120	1	8.728	17.456
				Average	17.372

Appendix B. Iron Experiment A. Data and Graphs

Table B 1. Iron Analysis for Experiment A, Control sample 1.

Date of Experiment: December 1 1998

Run Time (hour)	**Unfiltered sample**				**Filtered sample 0.45 μm pore size**			
	Total iron		*Ferrous iron*		*Total iron*		*Ferrous iron*	
	Absorbance 510 nm	mg/L	Absorbance 510 nm	mg/L	Absorbance 510 nm	mg/L	Absorbance 510 nm	mg/L
Zero	0.0520	0.539	0.0410	0.425	0.0130	0.135	0.0080	0.083
2	0.0150	0.155	0.0140	0.145	0.0115	0.119	0.0060	0.062
4	0.0510	0.528	0.0355	0.368	0.0125	0.130	0.0060	0.062
6	0.0155	0.161	0.0035	0.036	0.0120	0.124	0.0070	0.073

Table B 2. Iron Analysis for Experiment A, Control sample 2.

Date of Experiment: December 4 1998

Run Time (hour)	**Unfiltered sample**				**Filtered sample 0.45 μm pore size**			
	Total iron		*Ferrous iron*		*Total iron*		*Ferrous iron*	
	Absorbance 510 nm	mg/L	Absorbance 510 nm	mg/L	Absorbance 510 nm	mg/L	Absorbance 510 nm	mg/L
Zero	0.0230	0.238	0.0260	0.269	0.0155	0.161	0.0070	0.073
2	0.0255	0.264	0.0135	0.140	0.0105	0.109	0.0070	0.073
4	0.0255	0.264	0.0165	0.171	0.0105	0.109	0.0040	0.041
6	0.0280	0.290	0.0145	0.150	0.0120	0.124	0.0050	0.052

Table B 3. Iron Analysis for Experiment A, Control sample 3.

Date of Experiment: December 9 1998

Run Time (hour)	**Unfiltered sample**				**Filtered sample 0.45 μm pore size**			
	Total iron		*Ferrous iron*		*Total iron*		*Ferrous iron*	
	Absorbance 510 nm	mg/L	Absorbance 510 nm	mg/L	Absorbance 510 nm	mg/L	Absorbance 510 nm	mg/L
Zero	0.0430	0.446	0.0210	0.218	0.0155	0.161	0.0075	0.078
2	0.0330	0.342	0.0115	0.119	0.0115	0.119	0.0045	0.047
4	0.0305	0.316	0.0110	0.114	0.0130	0.135	0.0055	0.057
6	0.0250	0.259	0.0065	0.067	0.0095	0.098	0.0040	0.041

Table B 4. Iron Analysis for Experiment A, Control sample 4.

Date of Experiment: December 14 1998

Run Time (hour)	**Unfiltered sample**				**Filtered sample 0.45 μm pore size**			
	Total iron		*Ferrous iron*		*Total iron*		*Ferrous iron*	
	Absorbance 510 nm	mg/L	Absorbance 510 nm	mg/L	Absorbance 510 nm	mg/L	Absorbance 510 nm	mg/L
Zero	0.0305	0.316	0.0140	0.145	0.0090	0.093	0.0055	0.057
2	0.0280	0.290	0.0135	0.140	0.0085	0.088	0.0050	0.052
4	0.0425	0.440	0.0050	0.052	0.0105	0.109	0.0045	0.047
6	0.0415	0.430	0.0165	0.171	0.0080	0.083	0.0055	0.057

Table B 5. Iron Analysis for Experiment A, Ferrous iron sample 1.

Date of Experiment: December 2 1998

Run Time (hour)	**Unfiltered sample**				**Filtered sample 0.45 μm pore size**			
	Total iron		*Ferrous iron*		*Total iron*		*Ferrous iron*	
	Absorbance 510 nm	mg/L	Absorbance 510 nm	mg/L	Absorbance 510 nm	mg/L	Absorbance 510 nm	mg/L
Zero	0.0270	0.280	0.0310	0.321	0.0110	0.114	0.0070	0.073
2	0.0125	0.130	0.0085	0.088	0.0115	0.119	0.0050	0.052
4	0.0135	0.140	0.0015	0.016	0.0080	0.083	0.0065	0.067
6	0.0130	0.135	0.0075	0.078	0.0065	0.067	0.0040	0.041

Table B 6. Iron Analysis for Experiment A, Ferrous iron sample 2.

Date of Experiment: December 7 1998

Run Time (hour)	**Unfiltered sample**				**Filtered sample 0.45 μm pore size**			
	Total iron		*Ferrous iron*		*Total iron*		*Ferrous iron*	
	Absorbance 510 nm	mg/L	Absorbance 510 nm	mg/L	Absorbance 510 nm	mg/L	Absorbance 510 nm	mg/L
Zero	0.0340	0.352	0.0255	0.264	0.0090	0.093	0.005	0.052
2	0.0370	0.383	0.0220	0.228	0.0065	0.067	0.005	0.052
4	0.0235	0.244	0.0110	0.114	0.0095	0.098	0.005	0.052
6	0.0205	0.212	0.0090	0.093	0.0090	0.093	0.004	0.041

Table B 7. Iron Analysis for Experiment A, Ferrous iron sample 3.

Date of Experiment: December 10 1998

Run Time (hour)	**Unfiltered sample**				**Filtered sample 0.45 μm pore size**			
	Total iron		*Ferrous iron*		*Total iron*		*Ferrous iron*	
	Absorbance 510 nm	mg/L	Absorbance 510 nm	mg/L	Absorbance 510 nm	mg/L	Absorbance 510 nm	mg/L
Zero	0.0520	0.539	0.0325	0.337	0.0135	0.140	0.007	0.073
2	0.0465	0.482	0.0125	0.130	0.0115	0.119	0.004	0.041
4	0.0375	0.389	0.0110	0.114	0.0115	0.119	0.005	0.052
6	0.0360	0.373	0.0110	0.114	0.0120	0.124	0.004	0.041

Table B 8. Iron Analysis for Experiment A, Ferrous iron sample 4.

Date of Experiment: December 15 1998

Run Time (hour)	**Unfiltered sample**				**Filtered sample 0.45 μm pore size**			
	Total iron		*Ferrous iron*		*Total iron*		*Ferrous iron*	
	Absorbance 510 nm	mg/L	Absorbance 510 nm	mg/L	Absorbance 510 nm	mg/L	Absorbance 510 nm	mg/L
Zero	0.0435	0.451	0.0255	0.264	0.0135	0.140	0.0090	0.093
2	0.0410	0.425	0.0190	0.197	0.0110	0.114	0.0055	0.057
4	0.0305	0.316	0.0120	0.124	0.0100	0.104	0.0040	0.041
6	0.0325	0.337	0.0125	0.130	0.0095	0.098	0.0050	0.052

Table B 9. Iron Analysis for Experiment A, Waste solution iron sample 1.

Date of Experiment: December 3 1998

Run Time (hour)	Unfiltered sample				Filtered sample 0.45 μm pore size			
	Total iron		*Ferrous iron*		*Total iron*		*Ferrous iron*	
	Absorbance 510 nm	mg/L	Absorbance 510 nm	mg/L	Absorbance 510 nm	mg/L	Absorbance 510 nm	mg/L
Zero	0.0545	0.565	0.0335	0.347	0.0220	0.228	0.0115	0.119
2	0.0285	0.295	0.0060	0.062	0.0105	0.109	0.0055	0.057
4	0.0335	0.347	0.0105	0.109	0.0105	0.109	0.0055	0.057
6	0.0280	0.290	0.0065	0.067	0.0095	0.098	0.0050	0.052

Table B 10. Iron Analysis for Experiment A, Waste solution iron sample 2.

Date of Experiment: December 8 1998

Run Time (hour)	Unfiltered sample				Filtered sample 0.45 μm pore size			
	Total iron		*Ferrous iron*		*Total iron*		*Ferrous iron*	
	Absorbance 510 nm	mg/L	Absorbance 510 nm	mg/L	Absorbance 510 nm	mg/L	Absorbance 510 nm	mg/L
Zero	0.0380	0.394	0.0265	0.275	0.0140	0.145	0.0080	0.083
2	0.0290	0.301	0.0140	0.145	0.0105	0.109	0.0050	0.052
4	0.0270	0.280	0.0095	0.098	0.0105	0.109	0.0055	0.057
6	0.0230	0.238	0.0095	0.098	0.0105	0.109	0.0040	0.041

Table B 11. Iron Analysis for Experiment A, Waste solution iron sample 3.

Date of Experiment: December 11 1998

Run Time (hour)	Unfiltered sample				Filtered sample 0.45 μm pore size			
	Total iron		*Ferrous iron*		*Total iron*		*Ferrous iron*	
	Absorbance 510 nm	mg/L	Absorbance 510 nm	mg/L	Absorbance 510 nm	mg/L	Absorbance 510 nm	mg/L
Zero	0.0570	0.591	0.0335	0.347	0.0185	0.192	0.0070	0.073
2	0.0545	0.565	0.0215	0.223	0.0140	0.145	0.0060	0.062
4	0.0420	0.435	0.0180	0.187	0.0125	0.130	0.0050	0.052
6	0.0405	0.420	0.0115	0.119	0.0115	0.119	0.0045	0.047

Table B 12. Iron Analysis for Experiment A, Waste solution iron sample 4.

Date of Experiment: December 16 1998

Run Time (hour)	Unfiltered sample				Filtered sample 0.45 μm pore size			
	Total iron		*Ferrous iron*		*Total iron*		*Ferrous iron*	
	Absorbance 510 nm	mg/L	Absorbance 510 nm	mg/L	Absorbance 510 nm	mg/L	Absorbance 510 nm	mg/L
Zero	0.0370	0.383	0.0285	0.295	0.0130	0.135	0.0070	0.073
2	0.0280	0.290	0.0135	0.140	0.0085	0.088	0.0050	0.052
4	0.0280	0.290	0.0135	0.140	0.0115	0.119	0.0050	0.052
6	0.0305	0.316	0.0075	0.078	0.0120	0.124	0.0030	0.031

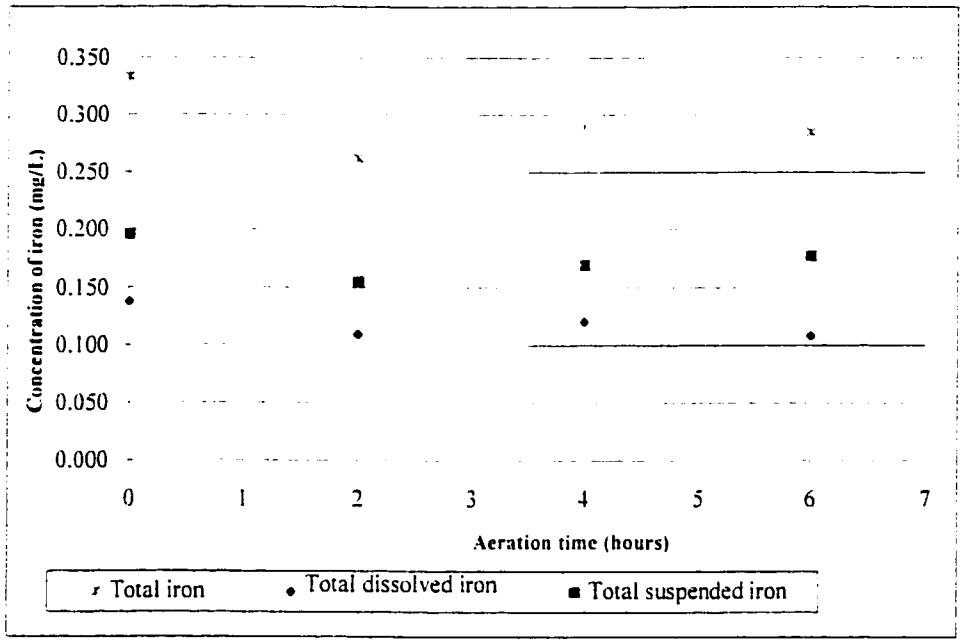

Figure B 1. Total iron, dissolved and suspended for control sample experiment A.

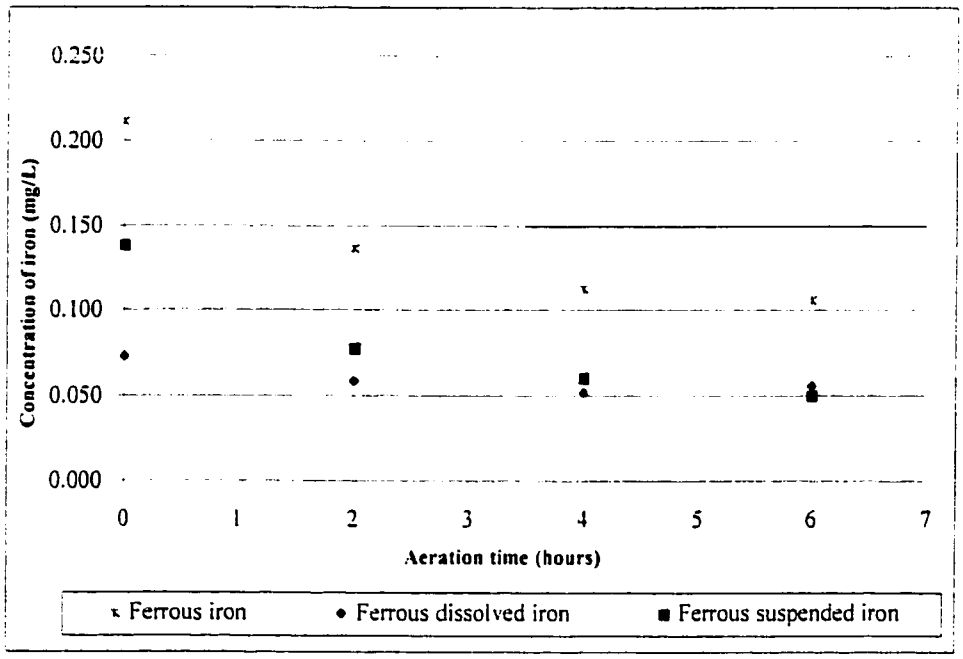

Figure B 2. Ferrous iron, dissolved and suspended for control sample experiment A

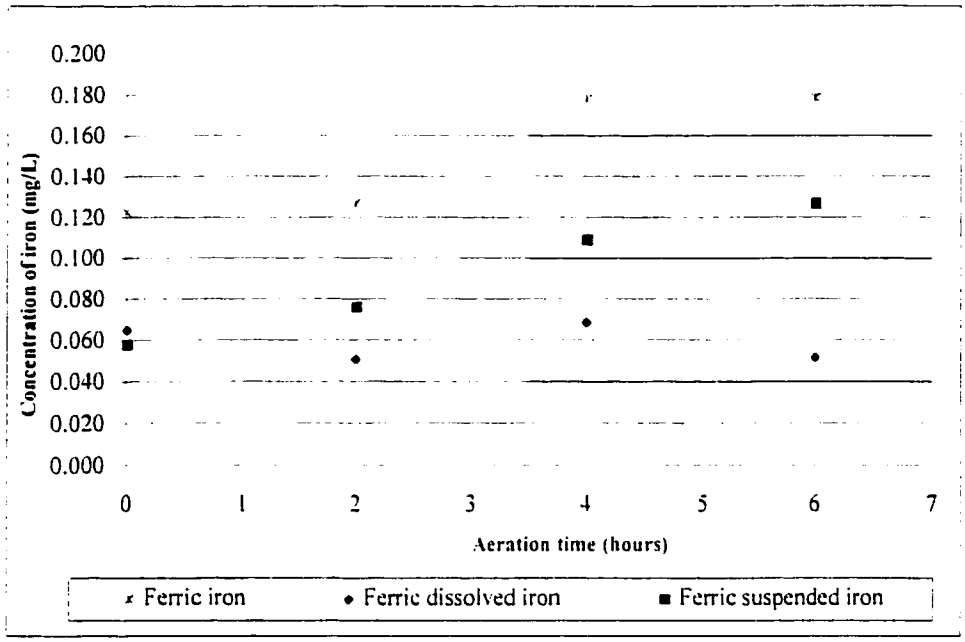

Figure B 3. Ferric iron, dissolved and suspended for control sample experiment A

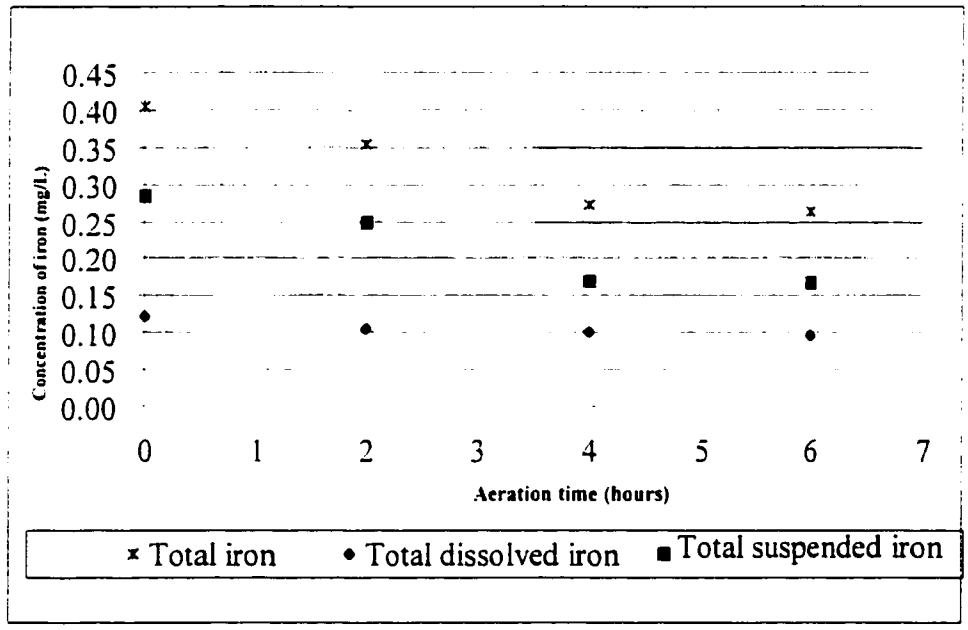

Figure B 4. Total iron, dissolved and suspended for ferrous solution sample experiment A

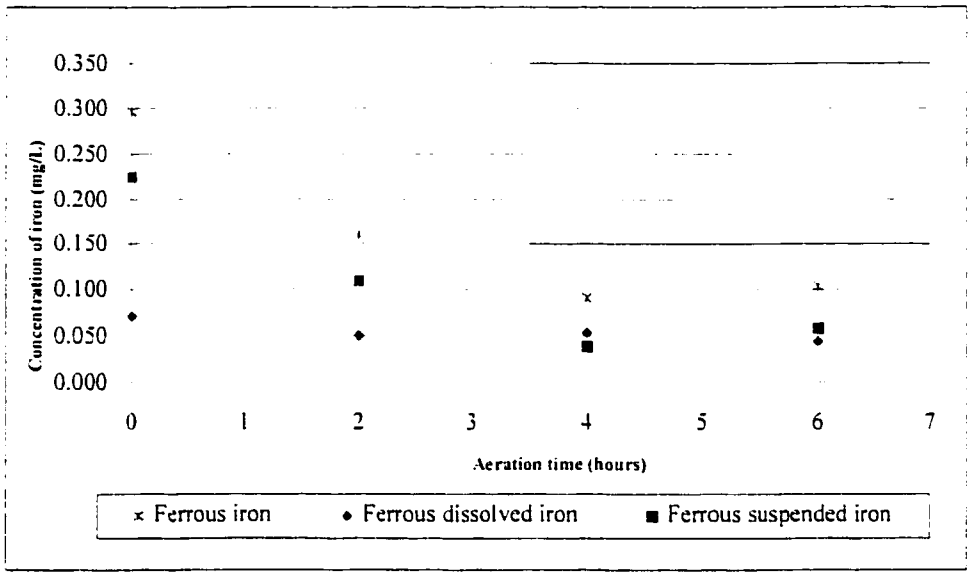

Figure B 5. Ferrous iron, dissolved and suspended for ferrous solution sample experiment A

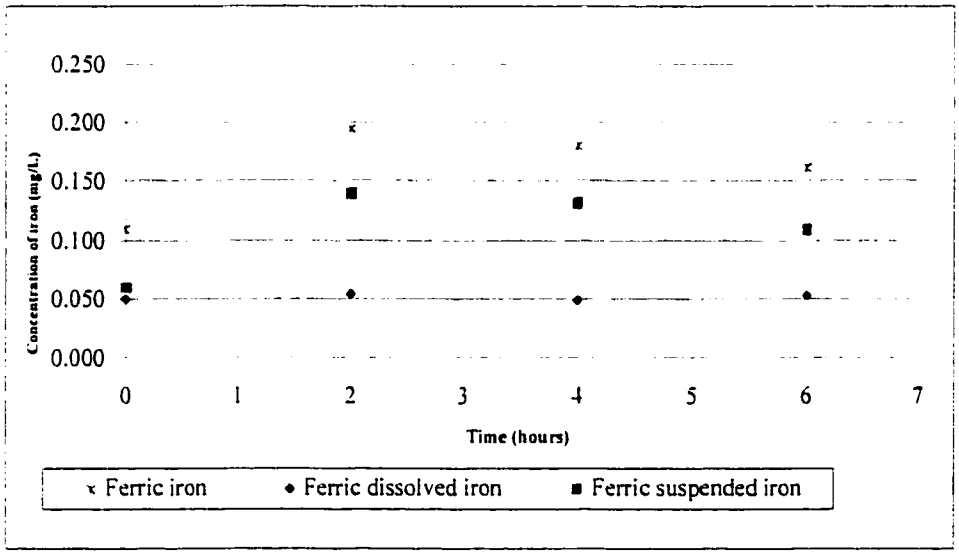

Figure B 6. Ferric iron, dissolved and suspended for ferrous solution sample experiment A

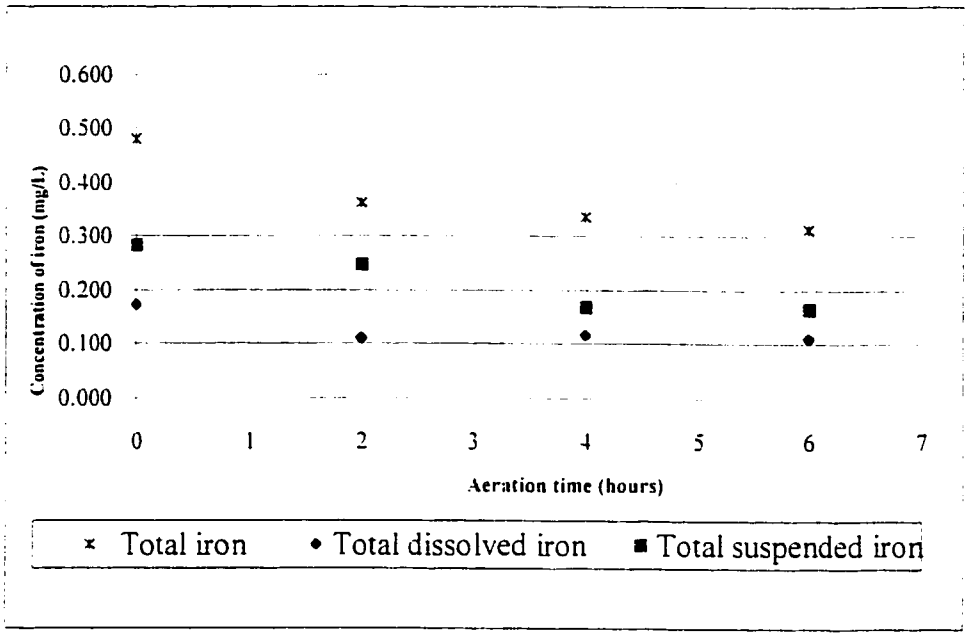

Figure B 7. Total iron, dissolved and suspended for industrial waste solution sample experiment A.

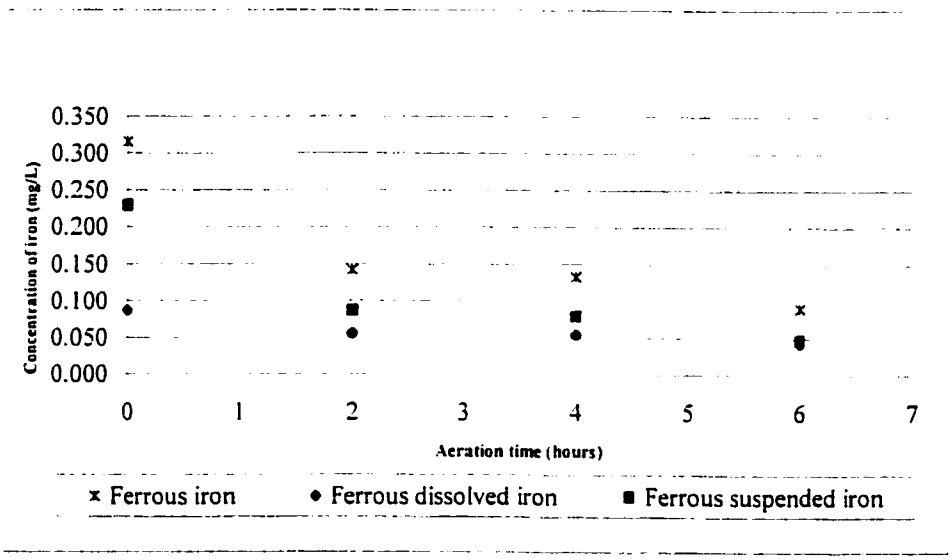

Figure B 8. Ferrous iron, dissolved and suspended for industrial waste solution sample experiment A.

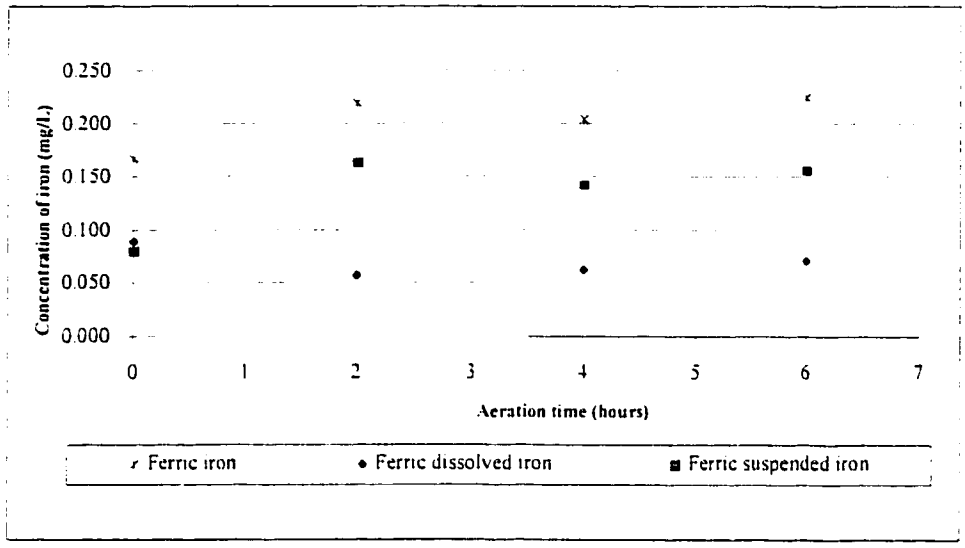

Figure B 9. Ferric iron, dissolved and suspended for industrial waste solution sample experiment A.

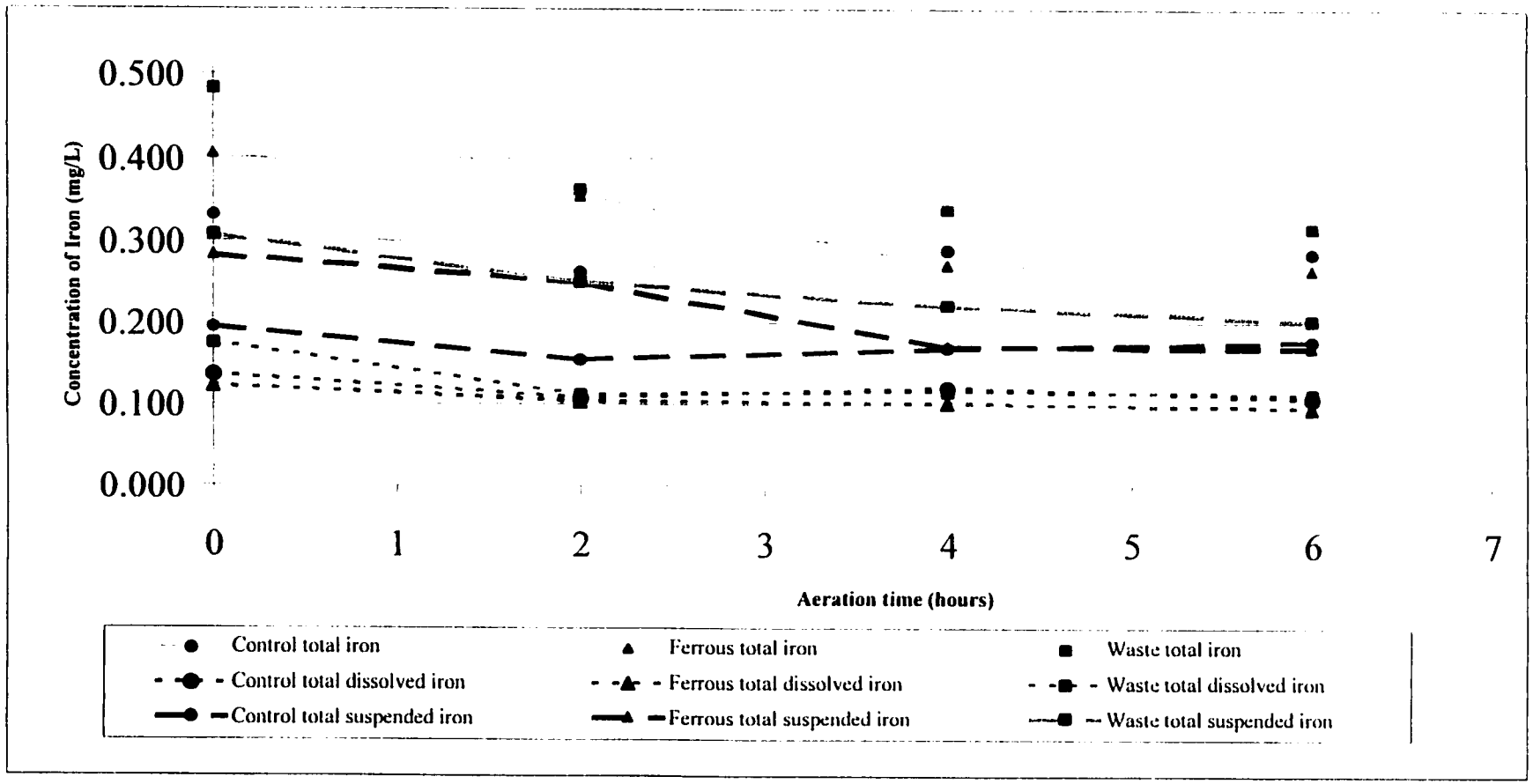

Figure B 10. Graph of total iron, total dissolved iron and total suspended iron for the control, ferrous solution and waste solution samples experiment A

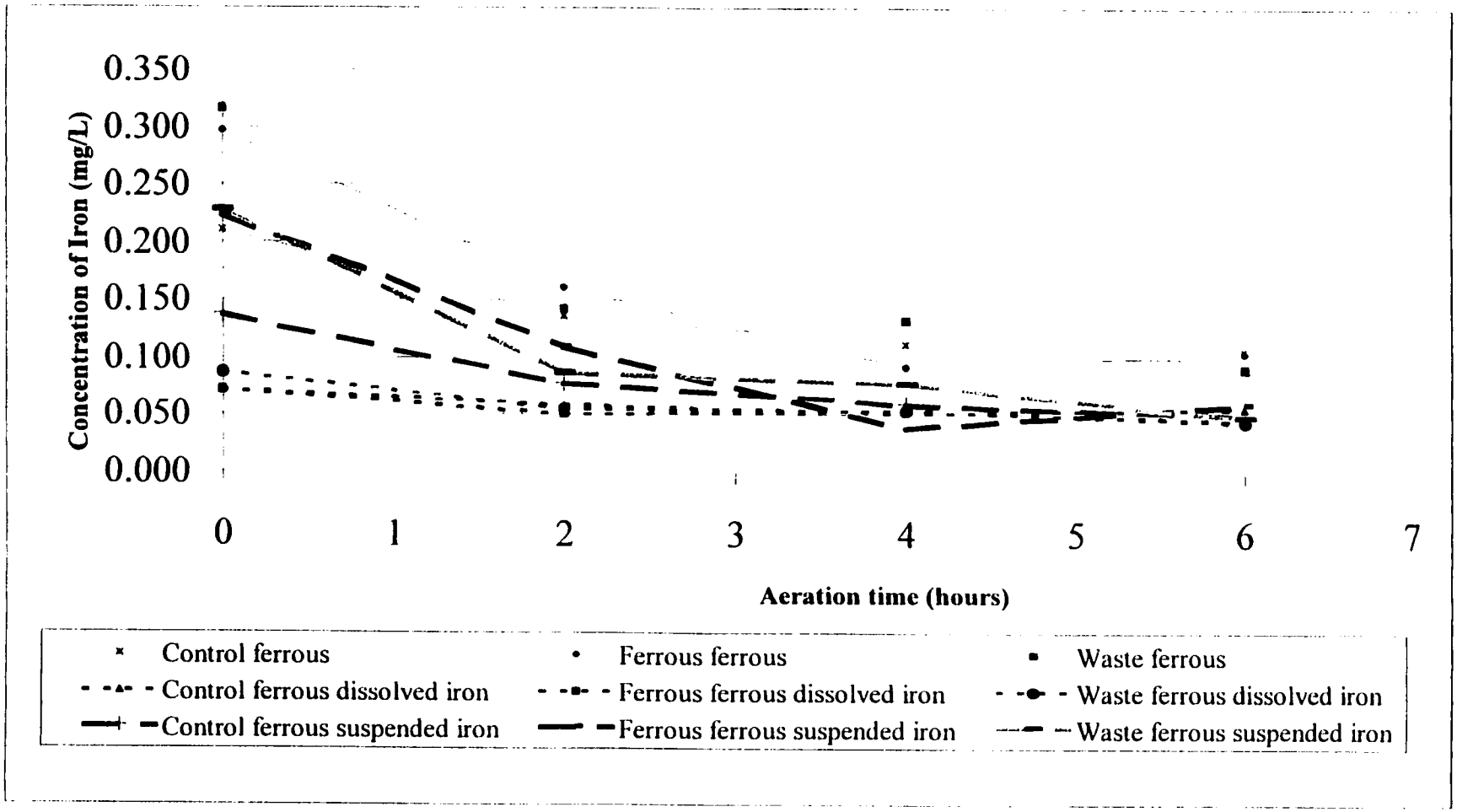

Figure B 11. Graph of ferrous iron, ferrous dissolved iron and ferrous suspended iron for the control, ferrous solution and waste solution samples experiment A

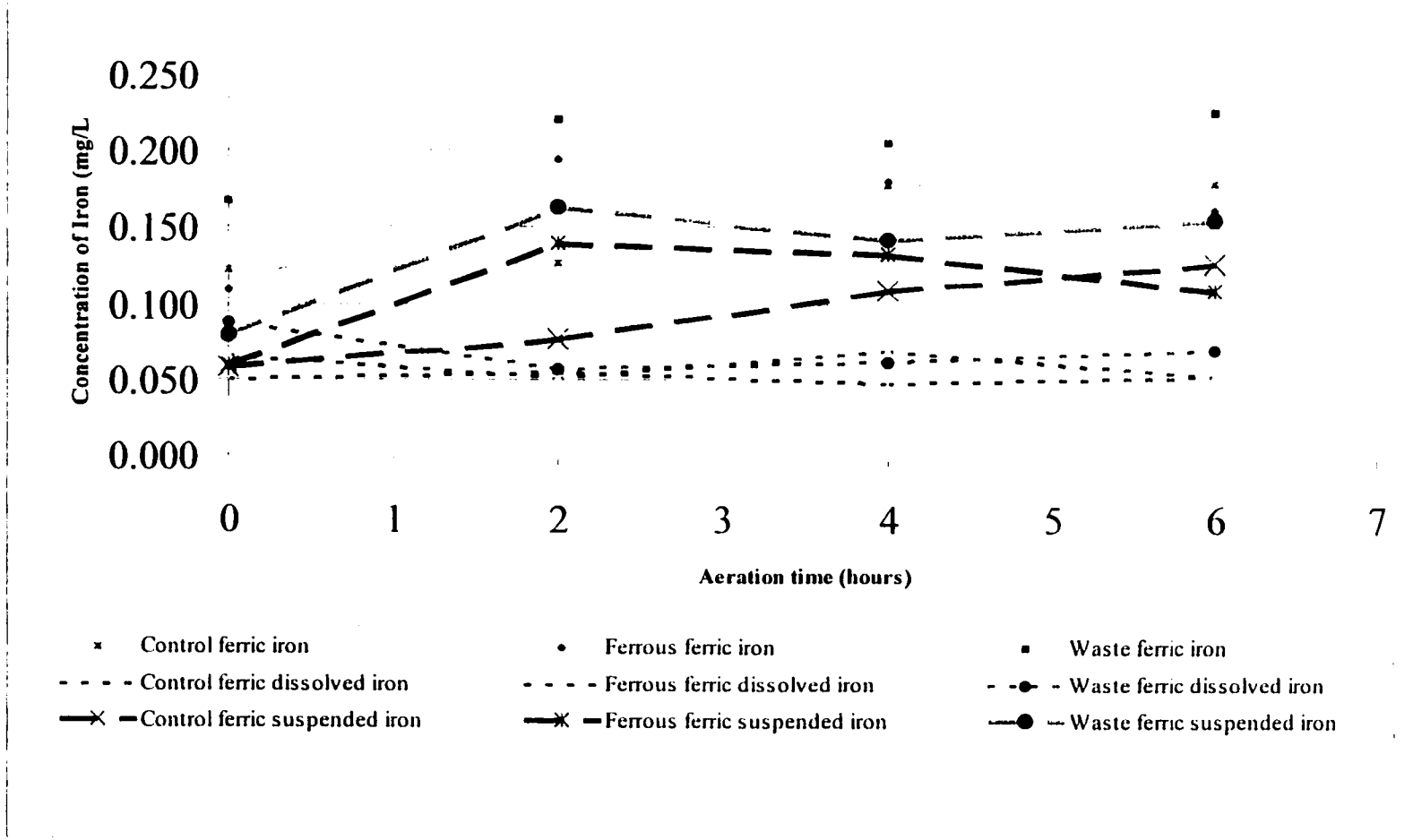

Figure B 12. Graph of ferric iron, ferric dissolved iron and ferric suspended iron for the control, ferrous solution and waste solution samples experiment A

Appendix C. Iron Experiment B. Data and Graphs

Table C 1. Iron Analysis for Experiment B, Control sample 1.

Date of Experiment: February 1 1998

	Digester supernate				Mixed liquor supernate			
	Total iron		*Ferrous iron*		*Total iron*		*Ferrous iron*	
	Absorbance 510 nm	mg/L	Absorbance 510 nm	mg/L	Absorbance 510 nm	mg/L	Absorbance 510 nm	mg/L
Initial	0.1435	1.487	0.1210	1.254	N/A	N/A	N/A	N/A

Run Time (hour)	Unfiltered sample				Filtered sample 0.45 μm pore size			
	Total iron		*Ferrous iron*		*Total iron*		*Ferrous iron*	
	Absorbance 510 nm	mg/L	Absorbance 510 nm	mg/L	Absorbance 510 nm	mg/L	Absorbance 510 nm	mg/L
Zero	0.0285	0.295	0.0055	0.057	0.0085	0.088	0.0030	0.031
6	0.0365	0.378	0.0100	0.104	0.0065	0.067	0.0060	0.062

Run Time (hour)	Filtered sample 0.20 μm pore size	
	Total iron	
	Absorbance 510 nm	mg/L
Zero	0.0085	0.088
6	0.0050	0.052

Table C 2. Iron Analysis for Experiment B, Control sample 2.

Date of Experiment: February 4 1998

	Digester supernate				Mixed liquor supernate			
	Total iron		*Ferrous iron*		*Total iron*		*Ferrous iron*	
	Absorbance 510 nm	mg/L	Absorbance 510 nm	mg/L	Absorbance 510 nm	mg/L	Absorbance 510 nm	mg/L
Initial	0.1825	1.891	0.079	0.819	0.0205	0.212	0.005	0.052

Run Time (hour)	Unfiltered sample				Filtered sample 0.45 μm pore size			
	Total iron		*Ferrous iron*		*Total iron*		*Ferrous iron*	
	Absorbance 510 nm	mg/L	Absorbance 510 nm	mg/L	Absorbance 510 nm	mg/L	Absorbance 510 nm	mg/L
Zero	0.0350	0.363	0.0135	0.140	0.0080	0.083	0.0035	0.036
1	0.0390	0.404	0.0140	0.145	0.0115	0.119	0.0060	0.062
3	0.0350	0.363	0.0225	0.233	0.0115	0.119	0.0060	0.062
4	0.0325	0.337	0.0105	0.109	0.0100	0.104	0.0045	0.047

Run Time (hour)	Filtered sample 0.20 μm pore size	
	Total iron	
	Absorbance 510 nm	mg/L
Zero	0.0110	0.114
1	0.0650	0.067
3	0.0125	0.130
4	0.0070	0.073

Table C 3. Iron Analysis for Experiment B, Control sample 3.

Date of Experiment: February 9 1998

	Digester supernate				Mixed liquor supernate			
	Total iron		*Ferrous iron*		*Total iron*		*Ferrous iron*	
	Absorbance 510 nm	mg/L	Absorbance 510 nm	mg/L	Absorbance 510 nm	mg/L	Absorbance 510 nm	mg/L
Initial	0.5575	5.777	0.1495	1.549	0.0155	0.161	0.0120	0.124

Run Time (hour)	Unfiltered sample				Filtered sample 0.45 μm pore size			
	Total iron		*Ferrous iron*		*Total iron*		*Ferrous iron*	
	Absorbance 510 nm	mg/L	Absorbance 510 nm	mg/L	Absorbance 510 nm	mg/L	Absorbance 510 nm	mg/L
Zero	0.0265	0.275	0.0105	0.109	0.0090	0.093	0.0055	0.057
1	0.0425	0.440	0.0155	0.161	0.0080	0.083	0.0095	0.098
3	0.0390	0.404	0.0090	0.093	0.0110	0.114	0.0060	0.062
4	0.0425	0.440	0.0175	0.181	0.0085	0.088	0.0055	0.057

Run Time (hour)	Filtered sample 0.20 μm pore size	
	Total iron	
	Absorbance 510 nm	mg/L
Zero	0.0040	0.041
1	0.0085	0.088
3	0.0105	0.109
4	0.0085	0.088

Table C 4. Iron Analysis for Experiment B, Ferrous solution sample 1.

Date of Experiment: February 2 1998

	Digester supernate				Mixed liquor supernate			
	Total iron		*Ferrous iron*		*Total iron*		*Ferrous iron*	
	Absorbance 510 nm	mg/L	Absorbance 510 nm	mg/L	Absorbance 510 nm	mg/L	Absorbance 510 nm	mg/L
Initial	0.4415	4.575	0.2450	2.539	0.0150	0.155	0.0030	0.031

Run Time (hour)	Unfiltered sample				Filtered sample 0.45 μm pore size			
	Total iron		*Ferrous iron*		*Total iron*		*Ferrous iron*	
	Absorbance 510 nm	mg/L	Absorbance 510 nm	mg/L	Absorbance 510 nm	mg/L	Absorbance 510 nm	mg/L
Zero	0.0385	0.399	0.0115	0.119	0.0120	0.124	0.007	0.073
6	0.0335	0.347	0.0040	0.041	0.0065	0.067	0.005	0.052

Run Time (hour)	Filtered sample 0.20 μm pore size	
	Total iron	
	Absorbance 510 nm	mg/L
Zero	0.0125	0.130
6	0.0120	0.124

Table C 5. Iron Analysis for Experiment B, Ferrous solution sample 2.

Date of Experiment: February 5 1998

	Digester supernate				Mixed liquor supernate			
	Total iron		*Ferrous iron*		*Total iron*		*Ferrous iron*	
	Absorbance 510 nm	mg/L	Absorbance 510 nm	mg/L	Absorbance 510 nm	mg/L	Absorbance 510 nm	mg/L
Initial	0.5940	6.155	0.3135	3.249	0.0330	0.342	0.0065	0.067

Run Time (hour)	Unfiltered sample				Filtered sample 0.45 μm pore size			
	Total iron		*Ferrous iron*		*Total iron*		*Ferrous iron*	
	Absorbance 510 nm	mg/L	Absorbance 510 nm	mg/L	Absorbance 510 nm	mg/L	Absorbance 510 nm	mg/L
Zero	0.0390	0.404	0.0180	0.187	0.0120	0.124	0.0065	0.067
1	0.0420	0.435	0.0160	0.166	0.0115	0.119	0.0085	0.080
3	0.0435	0.451	0.0165	0.171	0.0090	0.093	0.0065	0.067
4	0.0295	0.306	0.0150	0.155	0.0090	0.093	0.0065	0.047

Run Time (hour)	Filtered sample 0.20 μm pore size	
	Total iron	
	Absorbance 510 nm	mg/L
Zero	0.0250	0.259
1	0.0120	0.124
3	0.0095	0.098
4	0.0075	0.078

Table C 6. Iron Analysis for Experiment B, Ferrous solution sample 3.

Date of Experiment: February 10 1998

	Digester supernate				Mixed liquor supernate			
	Total iron		*Ferrous iron*		*Total iron*		*Ferrous iron*	
	Absorbance 510 nm	mg/L	Absorbance 510 nm	mg/L	Absorbance 510 nm	mg/L	Absorbance 510 nm	mg/L
Initial	0.651	6.746	0.327	3.389	0.0210	0.218	0.0060	0.062

Run Time (hour)	Unfiltered sample				Filtered sample 0.45 μm pore size			
	Total iron		*Ferrous iron*		*Total iron*		*Ferrous iron*	
	Absorbance 510 nm	mg/L	Absorbance 510 nm	mg/L	Absorbance 510 nm	mg/L	Absorbance 510 nm	mg/L
Zero	0.0665	0.689	0.0215	0.223	0.0100	0.104	0.0060	0.062
1	0.0390	0.404	0.0180	0.187	0.0120	0.124	0.0070	0.073
3	0.0435	0.451	0.0120	0.124	0.0120	0.124	0.0055	0.057
4	0.0415	0.430	0.0130	0.135	0.0125	0.130	0.0065	0.067

Run Time (hour)	Filtered sample 0.20 μm pore size	
	Total iron	
	Absorbance 510 nm	mg/L
Zero	0.0080	0.083
1	0.0080	0.083
3	0.0090	0.093
4	0.0075	0.078

Table C 7. Iron Analysis for Experiment B, Waste solution sample 1.

Date of Experiment: February 3 1998

	Digester supernate				Mixed liquor supernate			
	Total iron		*Ferrous iron*		*Total iron*		*Ferrous iron*	
	Absorbance 510 nm	mg/L	Absorbance 510 nm	mg/L	Absorbance 510 nm	mg/L	Absorbance 510 nm	mg/L
Initial	0.3505	3.632	0.1675	1.736	0.0230	0.238	0.0090	0.093

Run Time (hour)	Unfiltered sample				Filtered sample 0.45 μm pore size			
	Total iron		*Ferrous iron*		*Total iron*		*Ferrous iron*	
	Absorbance 510 nm	mg/L	Absorbance 510 nm	mg/L	Absorbance 510 nm	mg/L	Absorbance 510 nm	mg/L
Zero	0.0280	0.290	0.0095	0.098	0.0050	0.052	0.0055	0.057
6	0.0370	0.383	0.0085	0.088	0.0115	0.119	0.0060	0.062

Run Time (hour)	Filtered sample 0.20 μm pore size	
	Total iron	
	Absorbance 510 nm	mg/L
Zero	0.0110	0.114
6	0.0090	0.093

Table C 8. Iron Analysis for Experiment B, Waste solution sample 2.

Date of Experiment: February 8 1998

	Digester supernate				Mixed liquor supernate			
	Total iron		*Ferrous iron*		*Total iron*		*Ferrous iron*	
	Absorbance 510 nm	mg/L	Absorbance 510 nm	mg/L	Absorbance 510 nm	mg/L	Absorbance 510 nm	mg/L
Initial	0.4435	4.596	0.1575	1.632	0.0030	0.031	0.0065	0.067

Run Time (hour)	Unfiltered sample				Filtered sample 0.45 μm pore size			
	Total iron		*Ferrous iron*		*Total iron*		*Ferrous iron*	
	Absorbance 510 nm	mg/L	Absorbance 510 nm	mg/L	Absorbance 510 nm	mg/L	Absorbance 510 nm	mg/L
Zero	0.0350	0.363	0.0090	0.093	0.0090	0.093	0.0010	0.010
1	0.0470	0.487	0.0115	0.119	0.0100	0.104	0.0050	0.052
3	0.0455	0.472	0.0055	0.057	0.0110	0.114	0.0055	0.057
4	0.0390	0.404	0.0160	0.166	0.0090	0.093	0.0060	0.041

Run Time (hour)	Filtered sample 0.20 μm pore size	
	Total iron	
	Absorbance 510 nm	mg/L
Zero	0.0120	0.124
1	0.0070	0.073
3	0.0055	0.057
4	0.0085	0.088

Table C 9. Iron Analysis for Experiment B, Waste solution sample 3.

Date of Experiment: February 11 1998

	Digester supernate				Mixed liquor supernate			
	Total iron		*Ferrous iron*		*Total iron*		*Ferrous iron*	
	Absorbance 510 nm	mg/L	Absorbance 510 nm	mg/L	Absorbance 510 nm	mg/L	Absorbance 510 nm	mg/L
Initial	0.2805	2.907	0.1525	1.580	0.0185	0.192	0.011	0.114

Run Time (hour)	Unfiltered sample				Filtered sample 0.45 μm pore size			
	Total iron		*Ferrous iron*		*Total iron*		*Ferrous iron*	
	Absorbance 510 nm	mg/L	Absorbance 510 nm	mg/L	Absorbance 510 nm	mg/L	Absorbance 510 nm	mg/L
Zero	0.0380	0.394	0.0065	0.067	0.0120	0.124	0.0055	0.057
1	0.0360	0.373	0.0110	0.114	0.0110	0.114	0.0075	0.078
3	0.0510	0.528	0.0085	0.088	0.0110	0.114	0.0060	0.062
4	0.0355	0.368	0.0100	0.104	0.0090	0.093	0.0050	0.052

Run Time (hour)	Filtered sample 0.20 μm pore size	
	Total iron	
	Absorbance 510 nm	mg/L
Zero	0.0065	0.067
1	0.0080	0.083
3	0.0070	0.073
4	0.0085	0.088

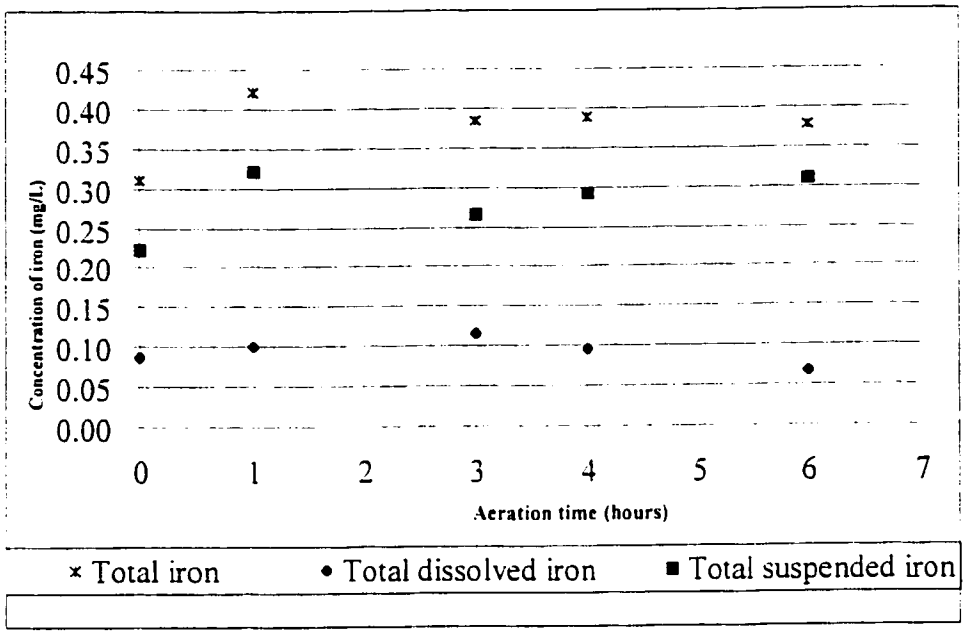

Figure C 1. Total iron, dissolved and suspended for control sample experiment B.

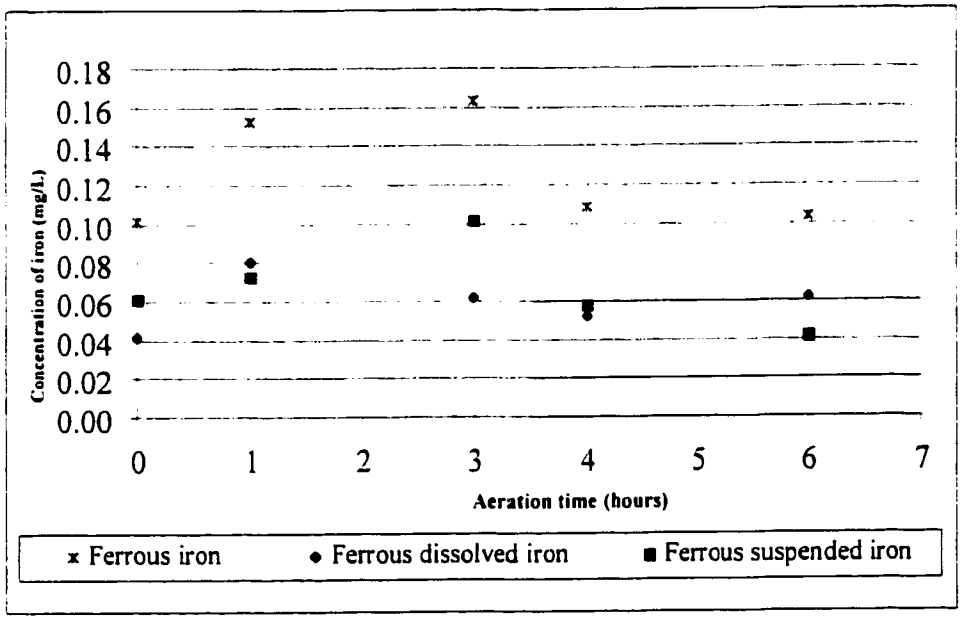

Figure C 2. Ferrous iron, dissolved and suspended for control sample experiment B

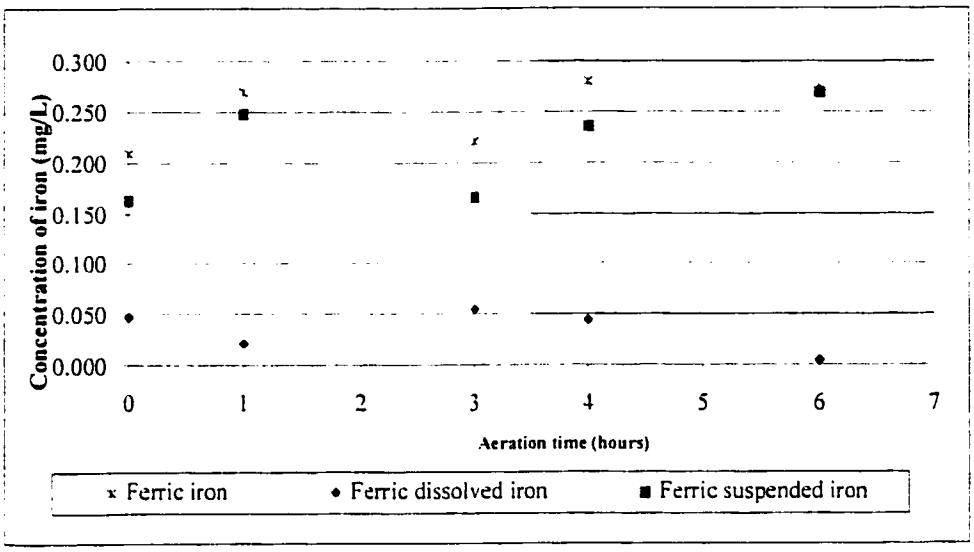

Figure C 3. Ferric iron, dissolved and suspended for control sample experiment B.

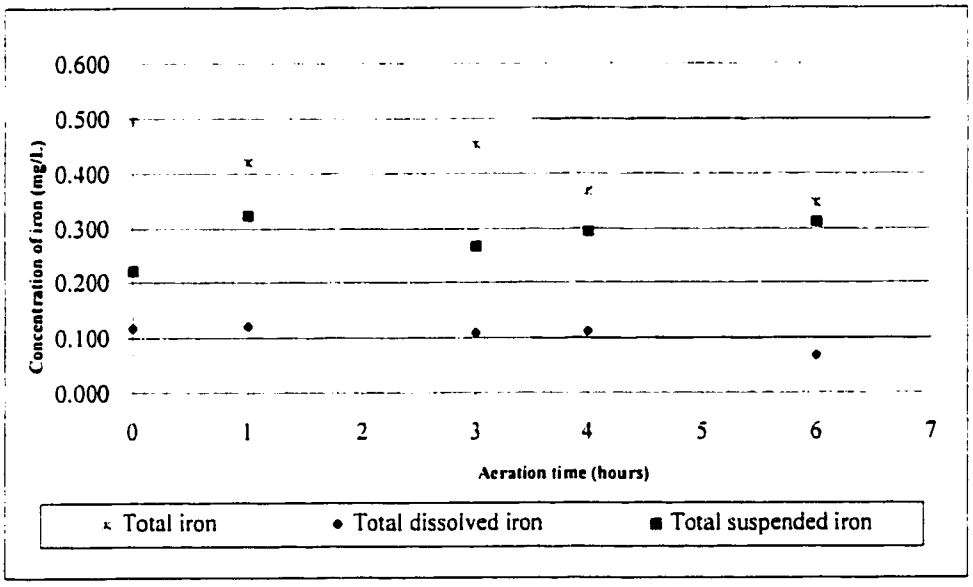

Figure C 4. Total iron, dissolved and suspended for ferrous solution sample experiment B.

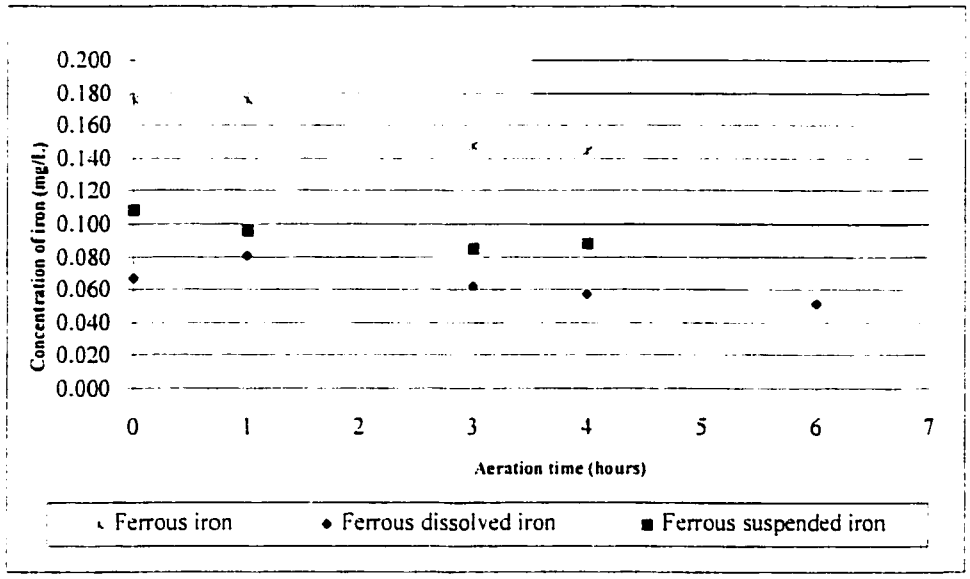

note:Ferrous iron and ferrous suspended iron from hour 6 are omited

Figure C 5. Ferrous iron, dissolved and suspended for ferrous solution sample experiment B

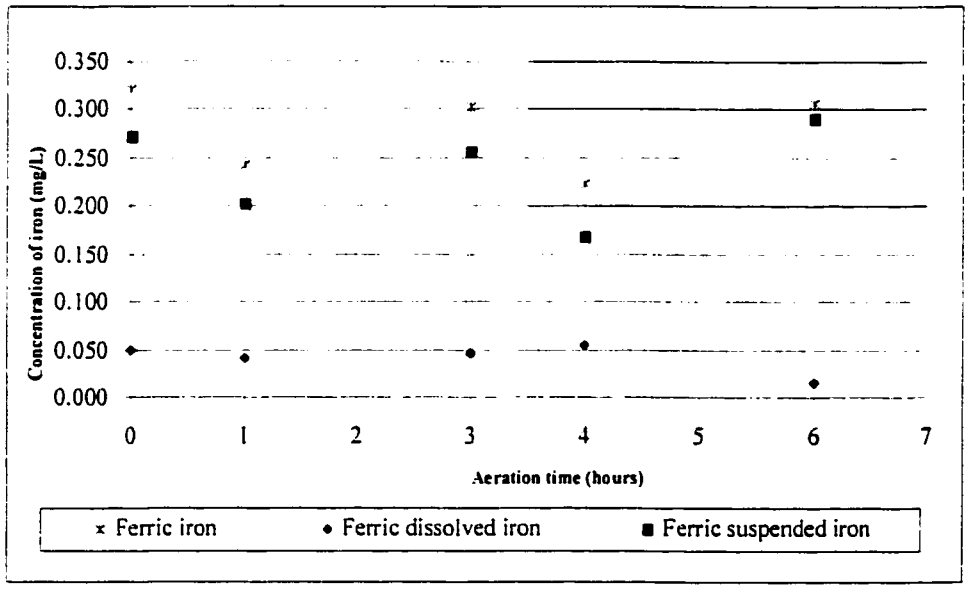

Figure C 6. Ferric iron, dissolved and suspended for ferrous solution sample experiment B

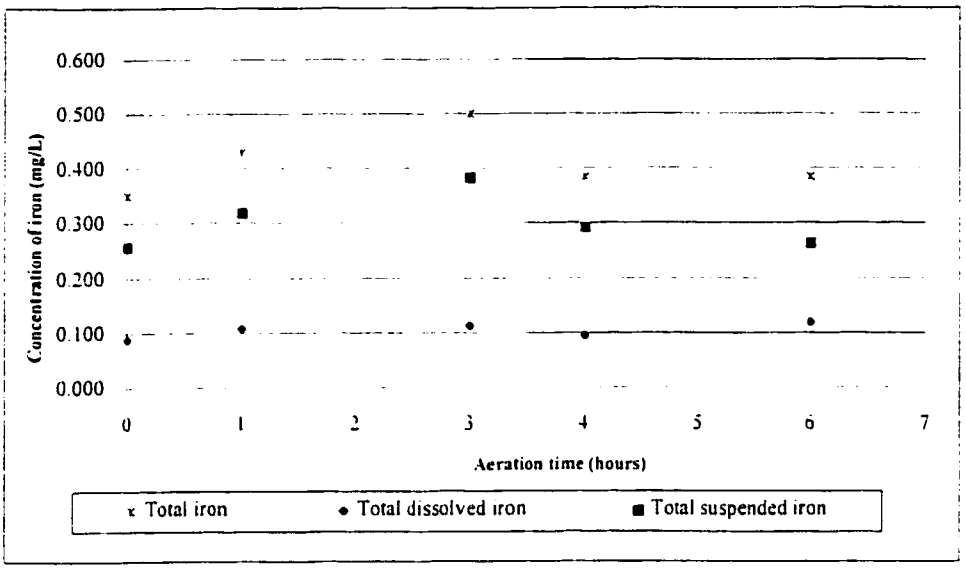

Figure C 7. Total iron, dissolved and suspended for industrial waste solution sample experiment B

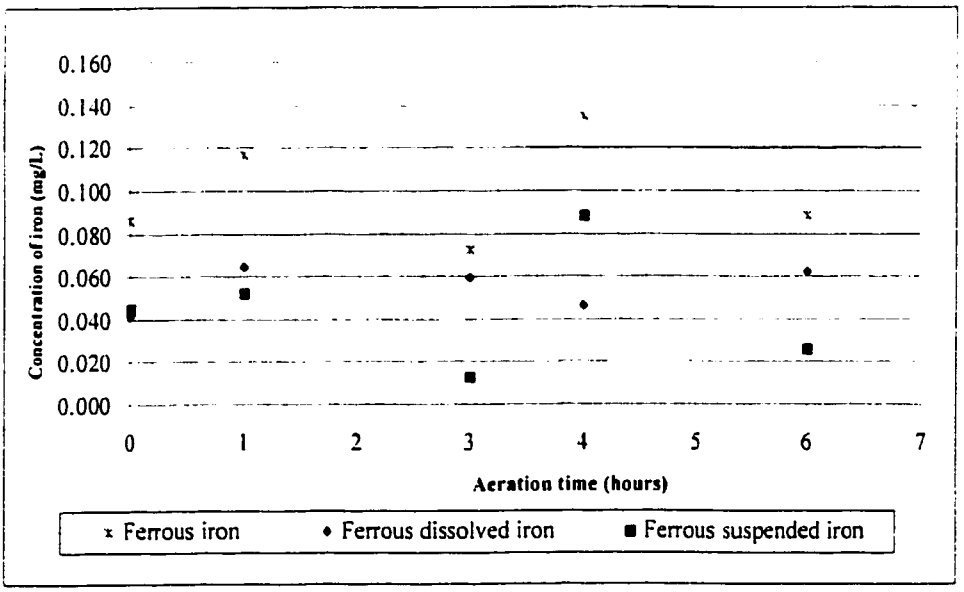

Figure C 8. Ferrous iron, dissolved and suspended for industrial waste solution sample experiment B

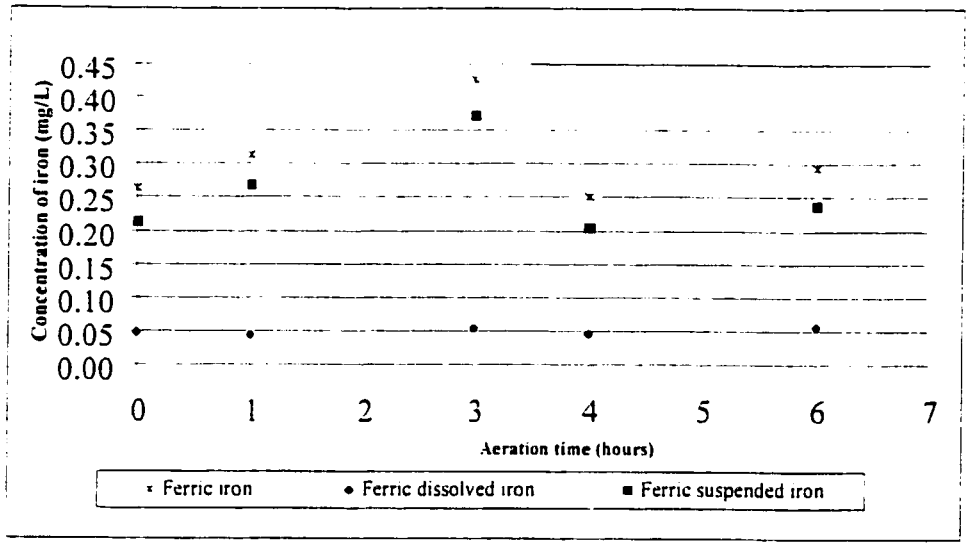

Figure C 9. Ferric iron, dissolved and suspended for industrial waste solution sample experiment B

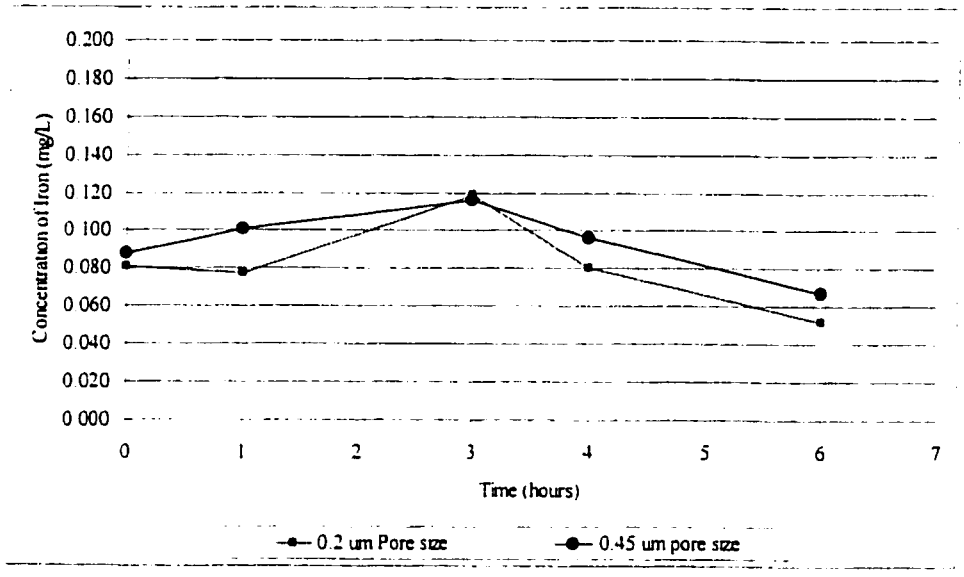

Figure C 10. Comparison of total iron filtered samples through 0.2 μm pore size and 0.45 μm pore size for control sample experiment B.

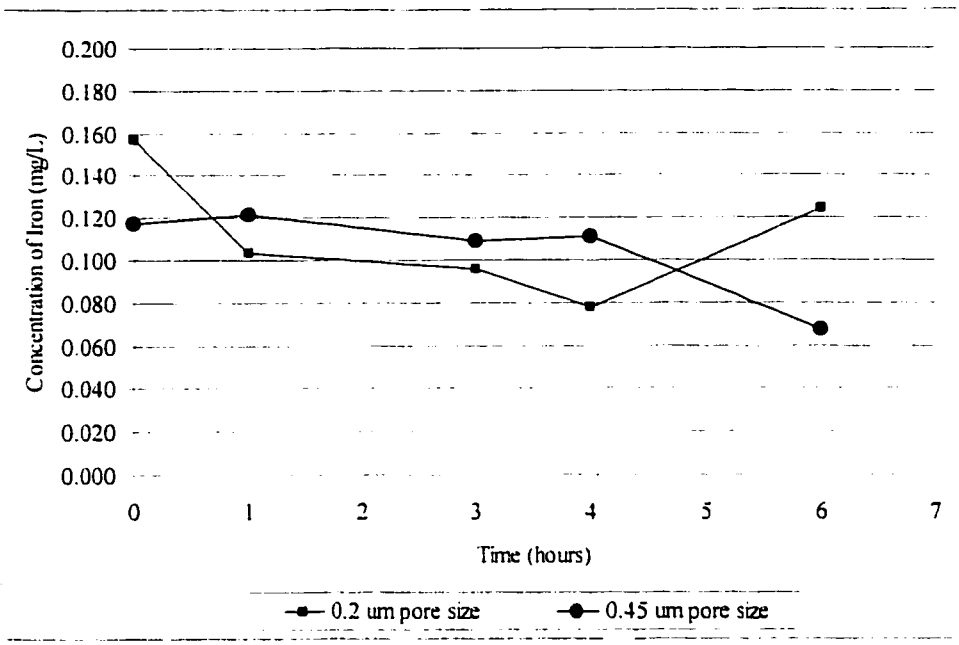

Figure C 11. Comparison of total iron filtered samples through 0.2 μm pore size and 0.45 μm pore size for ferrous solution sample experiment B.

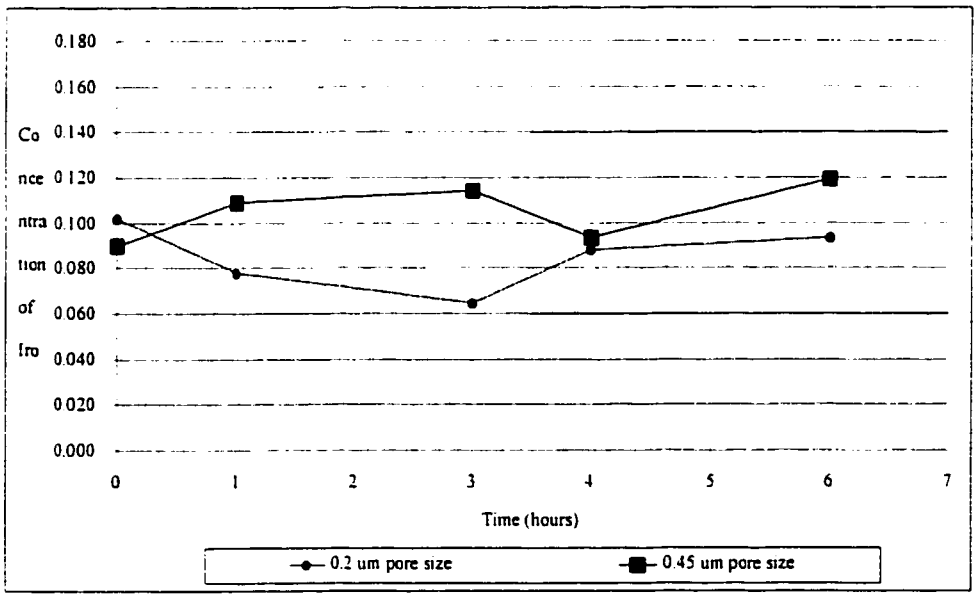

Figure C 12. Comparison of total iron filtered samples through 0.2 μm pore size and 0.45 μm pore size for industrial waste solution sample experiment B.

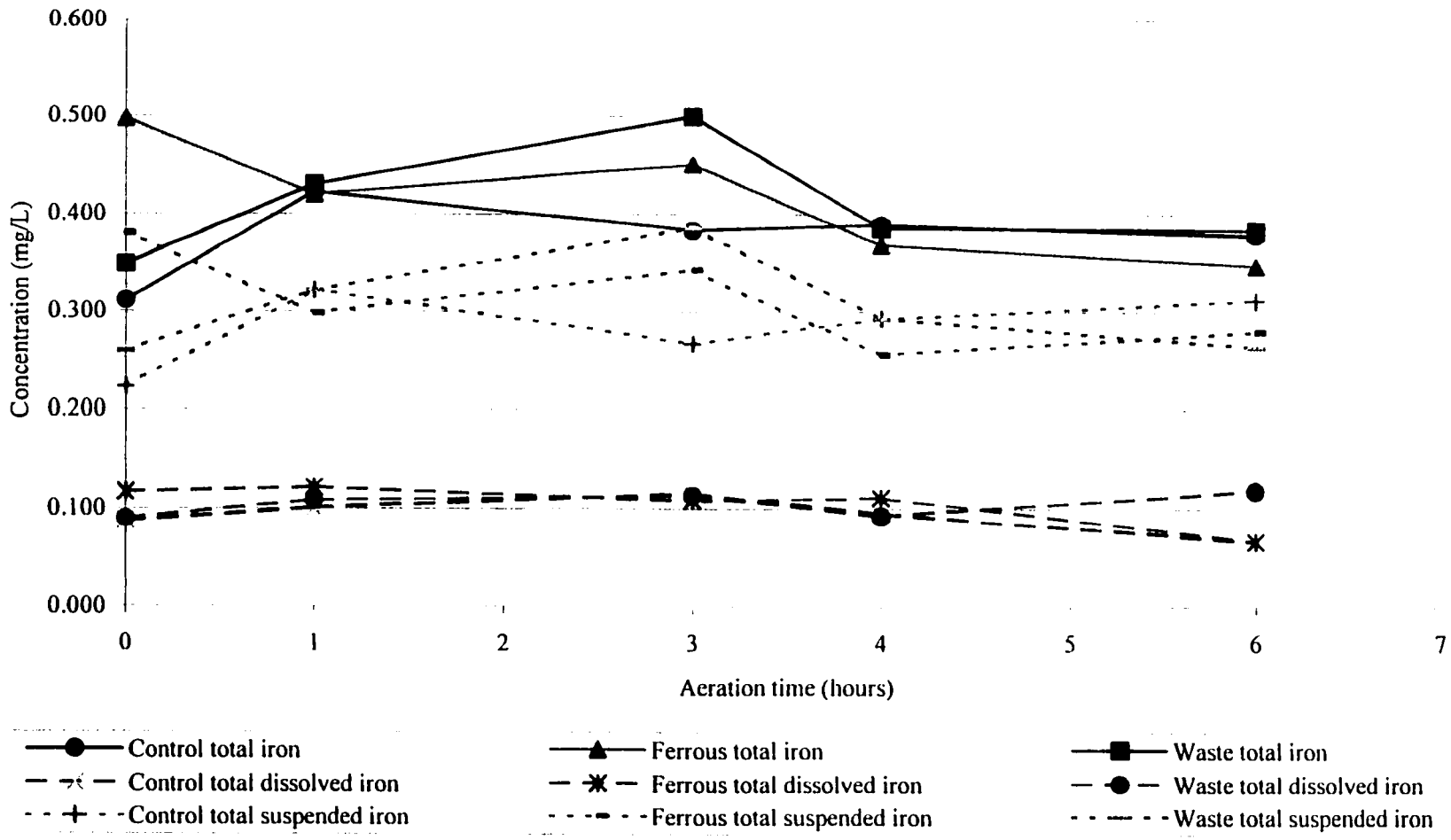

Figure C 13. Graph of total iron, total dissolved iron and total suspended iron for the control, ferrous solution and waste solution samples experiment B.

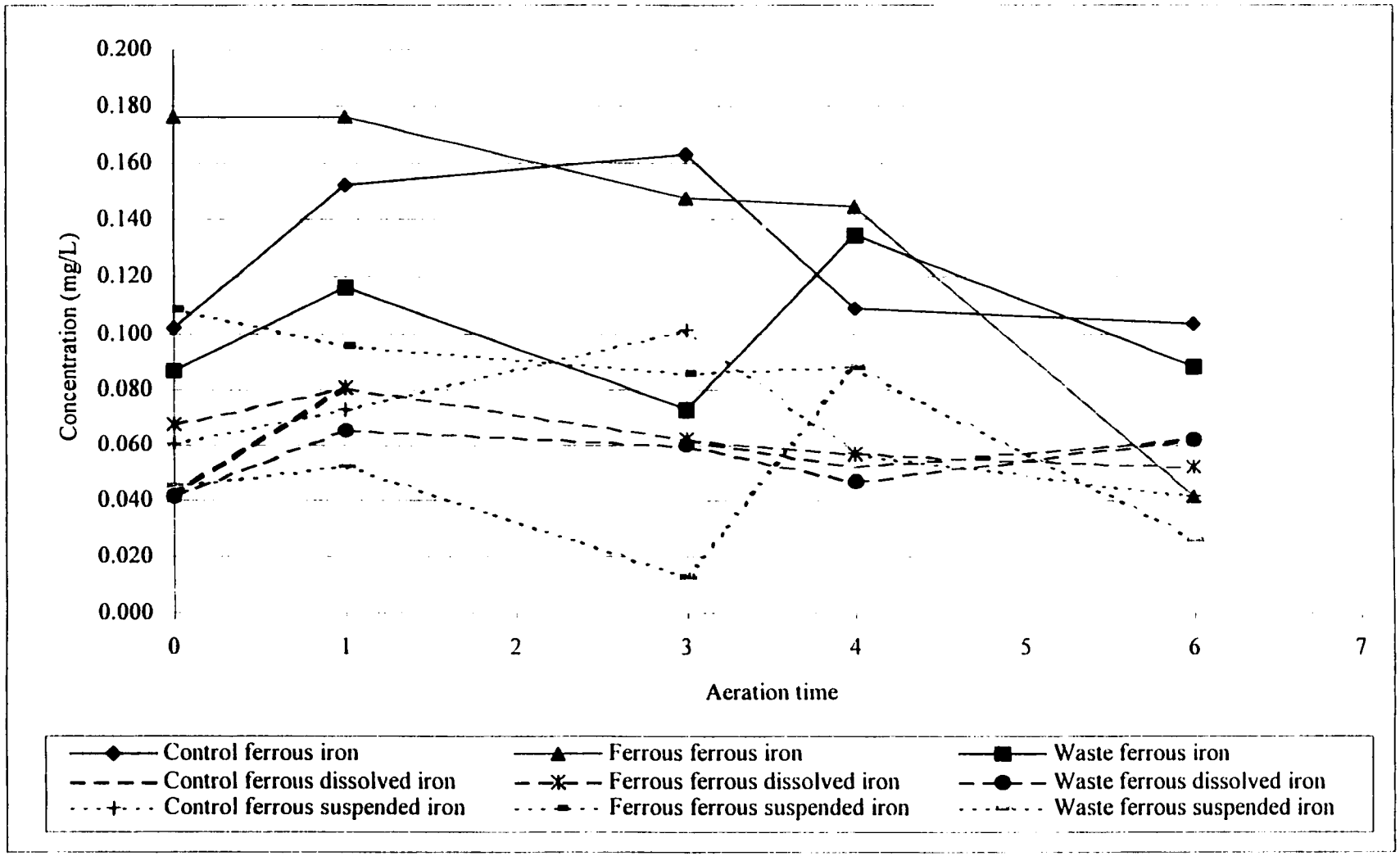

Figure C 14. Graph of ferrous iron, ferrous dissolved iron and ferrous suspended iron for the control, ferrous solution and waste solution samples experiment B

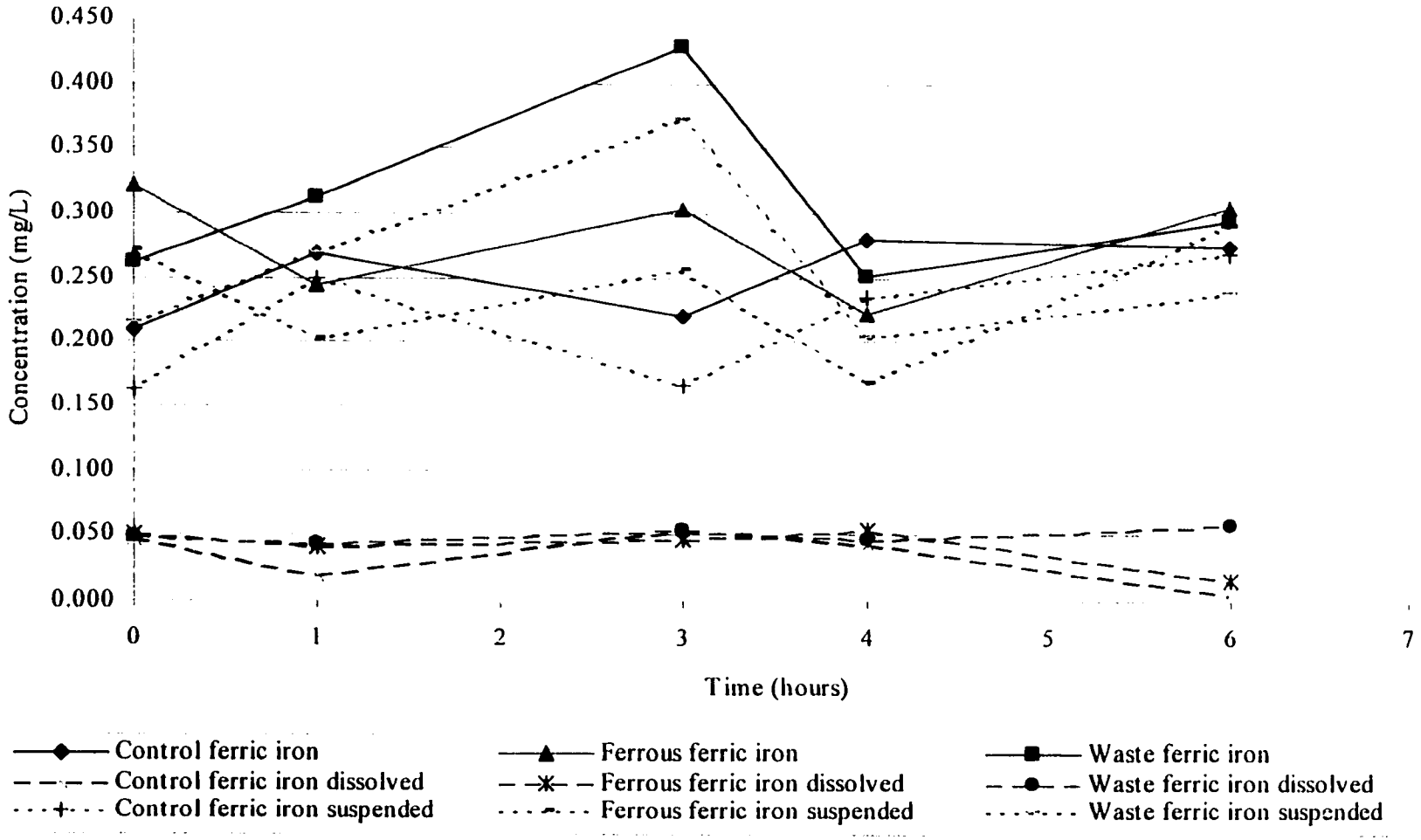

Figure C 15. Graph of ferric iron, ferric dissolved iron and ferric suspended iron for the control, ferrous solution and waste solution samples experiment B

Appendix D. TSS Data for Experiment B

Table D 1. Experiment B: Activated sludge: TSS mg/L data for Trial 2 and Trial 3

	Trial 2 Data			Trial 3 Data			
Time	Control Sample	Ferrous Sample	Waste Sample	Control Sample	Ferrous Sample	Waste Sample	Average TSS
Zero	53	90	103	58	100	37	73.5
1	143	200	160	187	137	80	151.2
3	170	227	207	233	153	177	194.5
4	177	210	213	190	150	140	180.0

Table D 2. Experiment B: Activated sludge: Ratio of mg/L Fe / mg/L TSS for Trial 2 and Trial 3

	Trial 2 Data			Trial 3 Data			
Time	Control Sample	Ferrous Sample	Waste Sample	Control Sample	Ferrous Sample	Waste Sample	Average Ratio
Zero	0.00685	0.00449	0.00352	0.00474	0.00689	0.01065	0.00619
1	0.00283	0.00218	0.00304	0.00235	0.00295	0.00466	0.00300
3	0.00214	0.00199	0.00228	0.00173	0.00295	0.00298	0.00234
4	0.00190	0.00146	0.00190	0.00232	0.00287	0.00263	0.00218

Table D 3. Experiment B: Activated sludge: Iron mg/L data for Trial 2 and Trial 3

	Trial 2 Data			Trial 3 Data			
Time	Control Sample	Ferrous Sample	Waste Sample	Control Sample	Ferrous Sample	Waste Sample	Average total iron
Zero	0.363	0.404	0.363	0.275	0.689	0.394	0.415
1	0.404	0.435	0.487	0.44	0.404	0.373	0.424
3	0.363	0.451	0.472	0.404	0.451	0.528	0.445
4	0.337	0.306	0.404	0.44	0.43	0.368	0.381

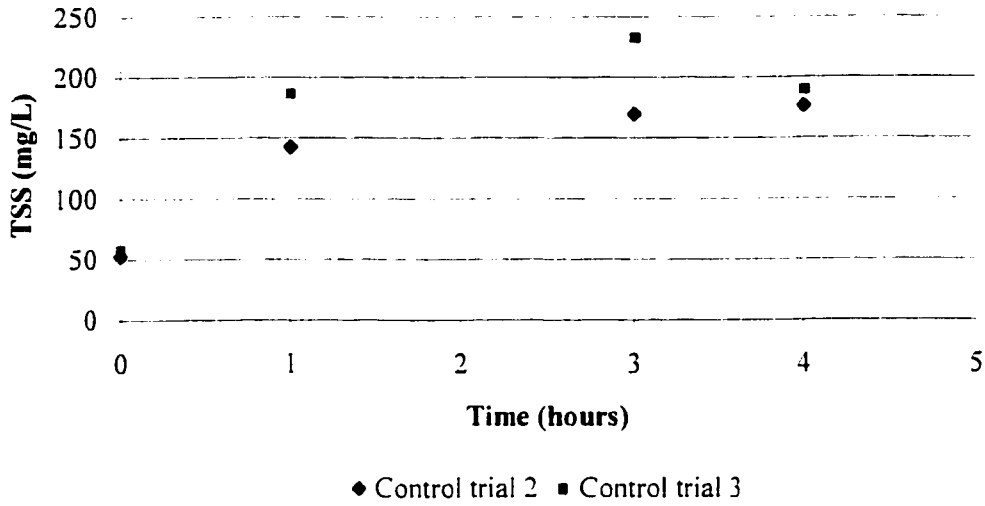

Figure D 1. TSS graph for control trials 2 and 3 for experiment B

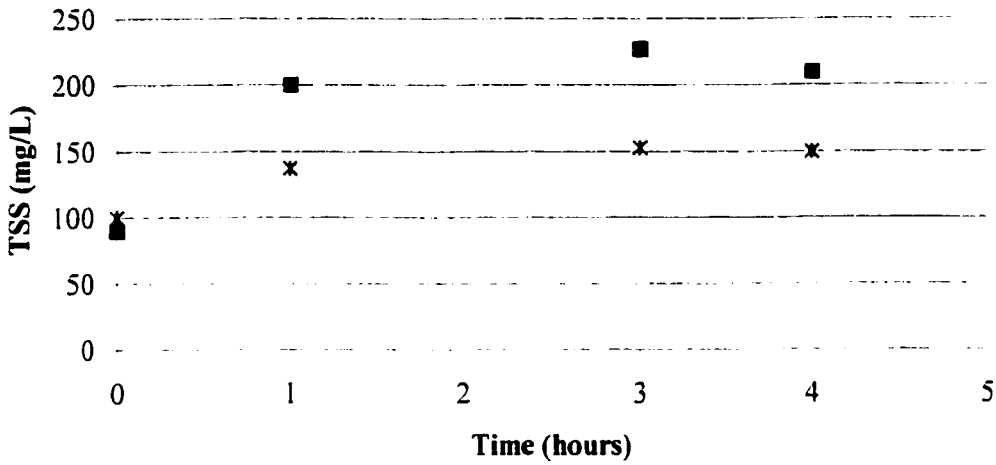

Figure D 2. TSS graph for ferrous solution trials 2 and 3 for experiment B

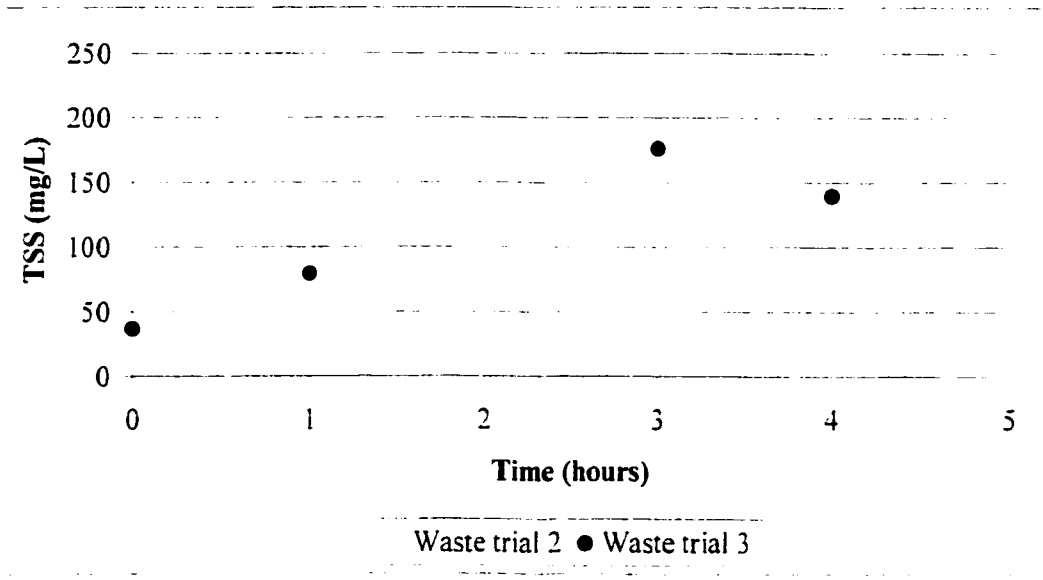

Figure D 3. TSS graph for waste solution trials 2 and 3 for experiment B

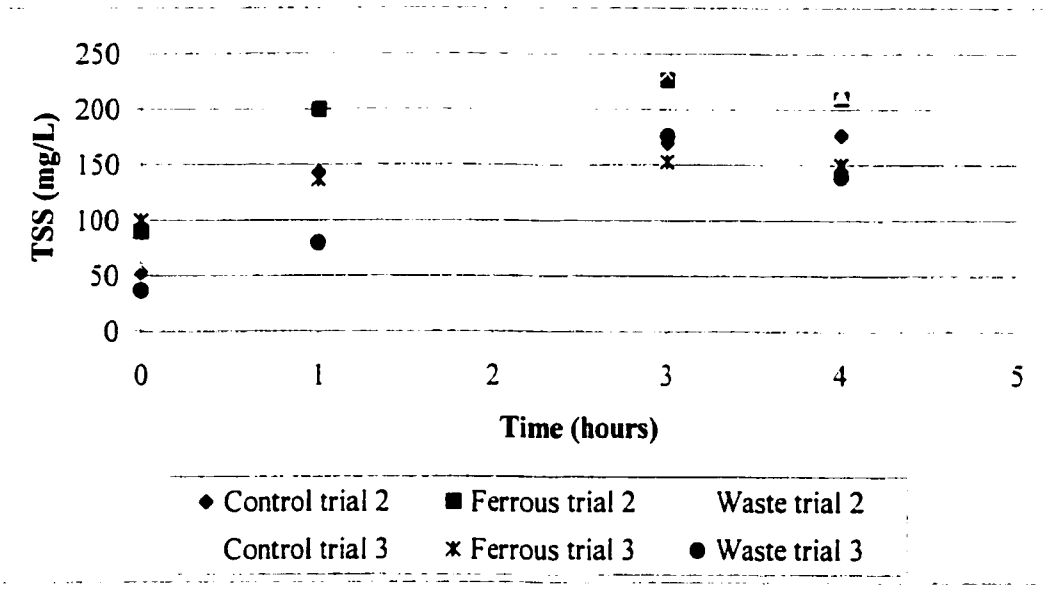

Figure D 4. Combined TSS graph for control, ferrous and waste solutions for experiment B

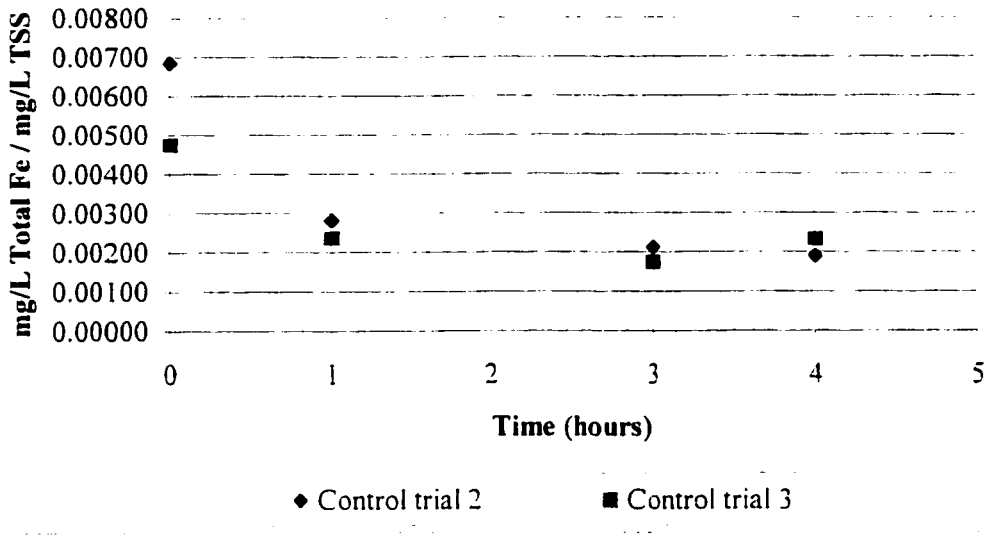

Figure D 5. Iron / TSS ratio for control trial 2 and 3 for experiment B

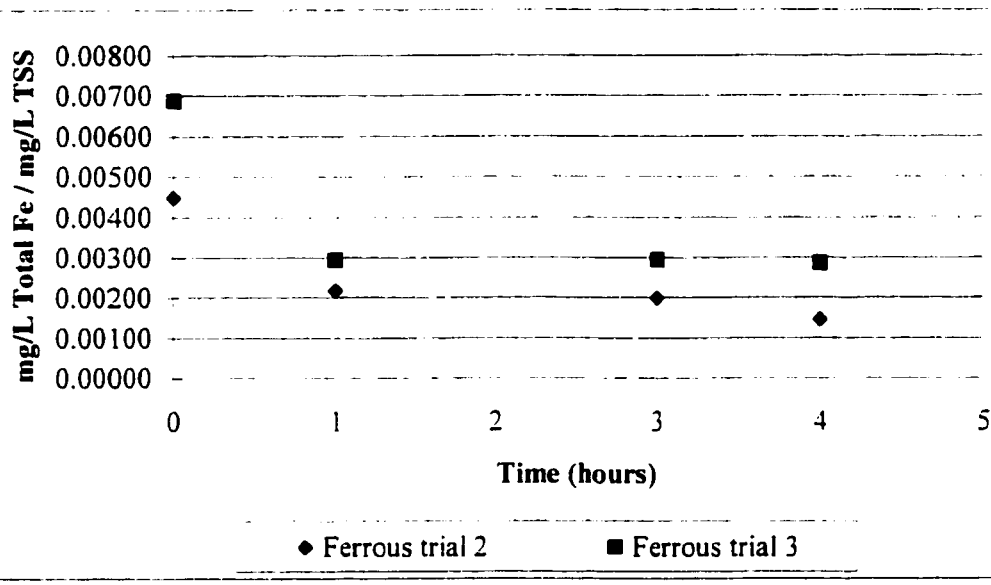

Figure D 6. Iron / TSS ratio for ferrous sample for trial 2 and 3 for experiment B

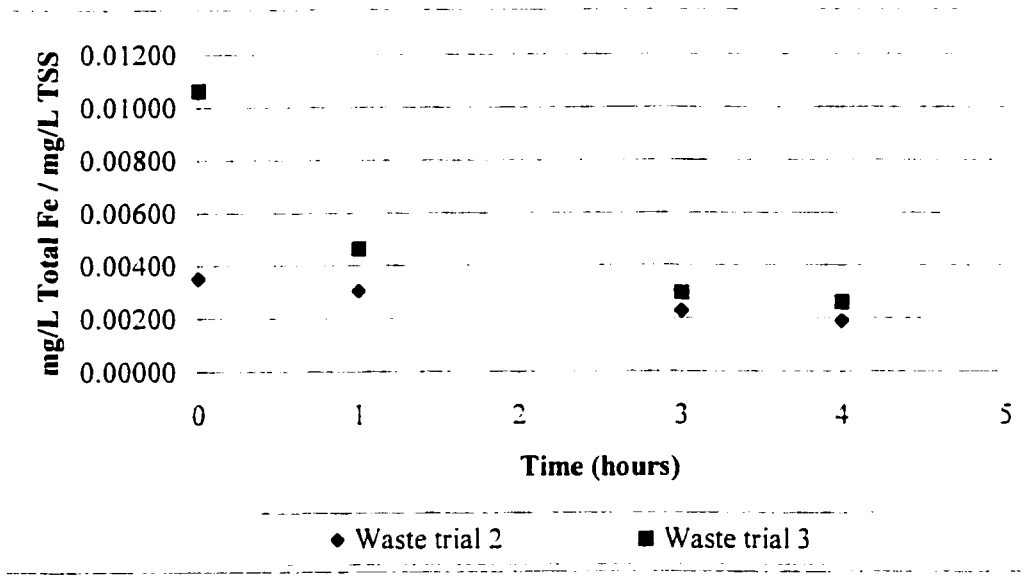

Figure D 7. Iron / TSS ratio for waste sample for trial 2 and 3 for experiment B

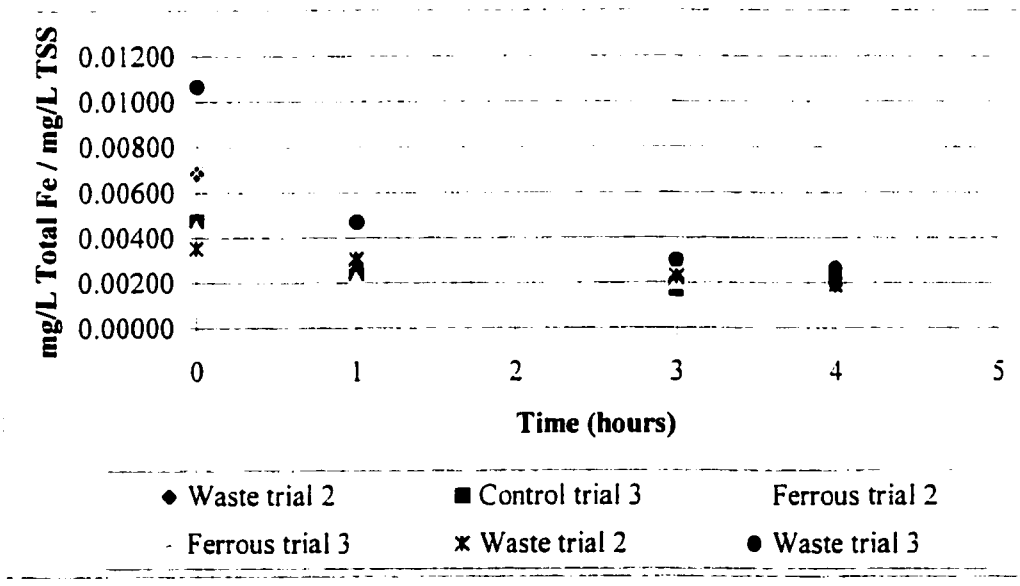

Figure D 8. Combined iron /TSS ratio graph for control, ferrous and waste solutions for experiment B

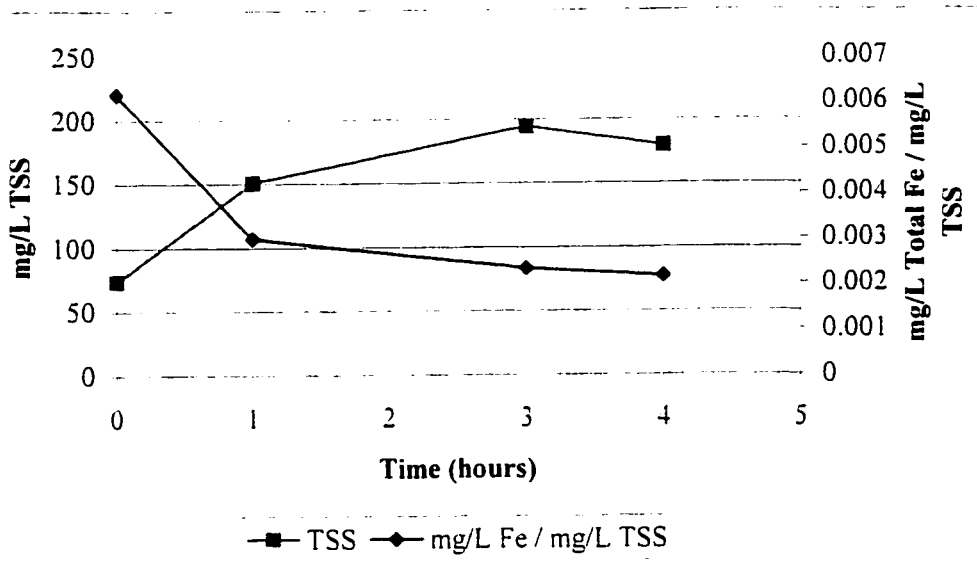

Figure D 9. combined TSS and iron / TSS ratio graph for control, ferrous and waste solutions for experiment B

Appendix E. Iron Experiment B, pH Data

Table E 1. Experiment B: Activated sludge: pH of Control sample Trial 2

Date of Experiment: February 4 1998

Sample	Initial pH of Sample
Raw	8.24
Mixed Liquor	7.00

Time of reading	pH of sample during aeration
8:15 AM	7.88
8:45 AM	8.02
9:15 AM	8.08
9:40 AM	8.12
10:20 AM	8.14
11:45 AM	8.15

Table E 2. Experiment B: Activated sludge: pH of Control sample Trial 3

Date of Experiment: February 9 1998

Sample	Initial pH of Sample
Raw	8.25
Mixed Liquor	7.03

Time of reading	pH of sample during aeration
7:30 AM	7.31
8:25 AM	8.04
8:55 AM	8.13
9:30 AM	8.17
9:45 AM	8.18
10:10 AM	8.23
11:30 AM	8.23

Table E 3. Experiment B: Activated sludge: pH of Ferrous sample Trial 2

Date of Experiment: February 5 1998

Sample	Initial pH of Sample
Raw	8.12
Mixed Liquor	6.93

Time of reading	pH of sample during aeration
7:45 AM	7.30
8:40 AM	8.00
9:00 AM	8.06
9:50 AM	8.13
11:45 AM	8.19

Table E 4 Experiment B: Activated sludge: pH of Ferrous sample Trial 3

Date of Experiment: February 10 1998

Sample	Initial pH of Sample
Raw	8.09
Mixed Liquor	7.08

Time of reading	pH of sample during aeration
7:35 AM	7.29
8:15 AM	7.99
8:35 AM	8.05
9:10 AM	8.11
9:55 AM	8.13
10:30 AM	8.19
11:35 AM	8.23

Table E 5. Experiment B: Activated sludge: pH of Waste sample Trial 2

Date of Experiment: February 8 1998

Sample	Initial pH of Sample
Raw	8.31
Mixed Liquor	6.99

Time of reading	pH of sample during aeration
7:45 AM	7.38
8:22 AM	8.02
8:45 AM	8.09
9:10 AM	8.16
10:10 AM	8.22
11:30 AM	8.27

Table E 6. Experiment B: Activated sludge: pH of Waste sample Trial 3

Date of Experiment: February 11 1998

Sample	Initial pH of Sample
Raw	8.10
Mixed Liquor	7.10

Time of reading	pH of sample during aeration
7:22 AM	7.39
8:25 AM	8.10
8:50 AM	8.15
9:25 AM	8.16
11:15 AM	8.26

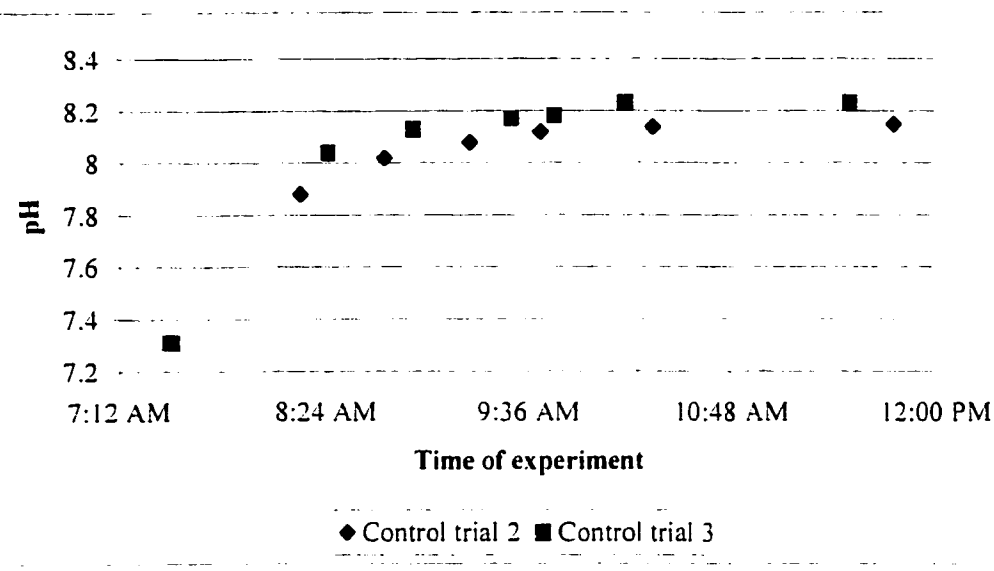

Figure E 1. Graph of pH data for trials 2 and 3 for control sample in experiment B: Activated sludge.

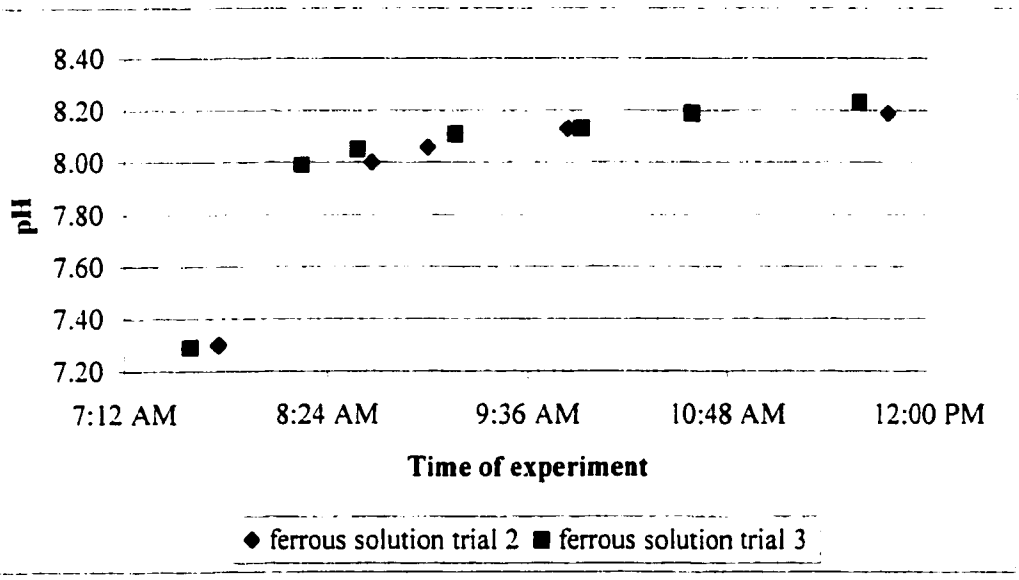

Figure E 2. Graph of pH data for trials 2 and 3 for ferrous solution sample in experiment B: Activated sludge.

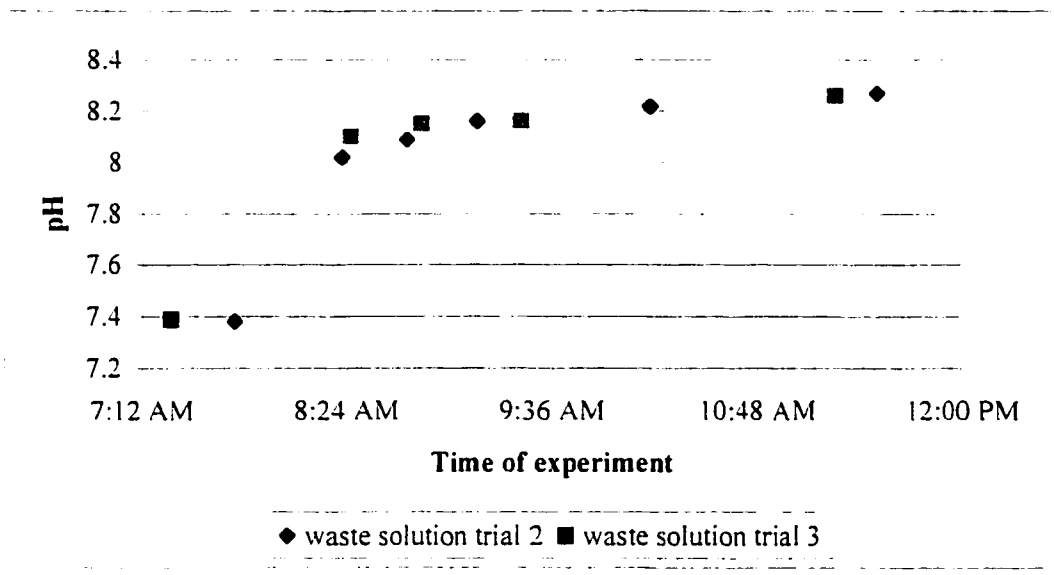

Figure E 3. Graph of pH data for trials 2 and 3 for waste solution sample in experiment B: Activated sludge.

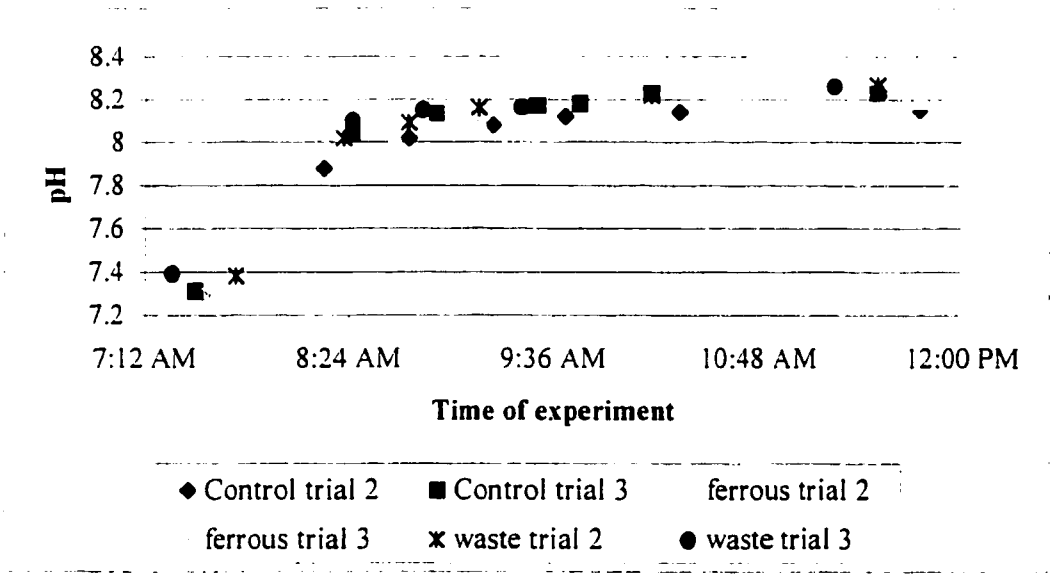

Figure E 4. Graph of all pH data for control, ferrous solution and waste solution samples in experiment B: Activated sludge.

Appendix F. Data for Raw Influent, Treated Effluent, RAS and Mixed Liquor

Table F 1. Iron tests for treatment plant raw influent

Date of Experiment: January 22,25,27 1999

Run Time (hour)	**Unfiltered sample**				**Filtered sample 0.45 μm pore size**			
	Total iron		*Ferrous iron*		*Total iron*		*Ferrous iron*	
	Absorbance 510 nm	mg/L	Absorbance 510 nm	mg/L	Absorbance 510 nm	mg/L	Absorbance 510 nm	mg/L
Influent 1	0.1775	1.839	0.0905	0.938	0.0410	0.425	0.0560	0.580
Influent 2	0.1200	1.244	0.0525	0.544	0.0210	0.218	0.0300	0.311
Influent 3	0.1875	1.943	0.0770	0.798	0.0420	0.435	0.0760	0.788

Run Time (hour)	**Filtered sample 0.20 μm pore size**	
	Total iron	
	Absorbance 510 nm	mg/L
Influent 1	0.0355	0.368
Influent 2	0.0175	0.181
Influent 3	0.0450	0.466

Table F 2. Iron tests for treatment plant treated effluent

Date of Experiment: January 22,25,27 1999

Run Time (hour)	**Unfiltered sample**				**Filtered sample 0.45 μm pore size**			
	Total iron		*Ferrous iron*		*Total iron*		*Ferrous iron*	
	Absorbance 510 nm	mg/L	Absorbance 510 nm	mg/L	Absorbance 510 nm	mg/L	Absorbance 510 nm	mg/L
Effluent 1	0.0220	0.228	0.0175	0.181	0.0115	0.119	0.0105	0.109
Effluent 2	0.0090	0.093	0.0035	0.036	0.0050	0.052	0.0020	0.021
Effluent 3	0.0110	0.114	0.0030	0.031	0.0045	0.047	0.0020	0.021

Run Time (hour)	**Filtered sample 0.20 μm pore size**	
	Total iron	
	Absorbance 510 nm	mg/L
Effluent 1	0.0100	0.104
Effluent 2	0.0025	0.026
Effluent 3	0.0050	0.052

Table F 3. Iron tests for treatment plant RAS

Date of Experiment: January 24,26,28 1999

Run Time (hour)	**Unfiltered sample**				**Filtered sample 0.45 μm pore size**			
	Total iron		*Ferrous iron*		*Total iron*		*Ferrous iron*	
	Absorbance 510 nm	mg/L	Absorbance 510 nm	mg/L	Absorbance 510 nm	mg/L	Absorbance 510 nm	mg/L
RAS 1	0.0205	0.212	0.0195	0.202	0.0105	0.019	0.0140	0.145
RAS 2	0.0360	0.373	0.0200	0.207	0.0110	0.114	0.0015	0.016
RAS 3	N/A	N/A	N/A	N/A	N/A	N/A	N/A	N/A

Run Time (hour)	**Filtered sample 0.20 μm pore size**	
	Total iron	
	Absorbance 510 nm	mg/L
RAS 1	0.0100	0.104
RAS 2	0.0115	0.119
RAS 3	N/A	N/A

Table F 4. Iron tests for treatment plant mixed liquor settled supernate

Date of Experiment: January 24,26,28 1999

Run Time (hour)	**Unfiltered sample**				**Filtered sample 0.45 μm pore size**			
	Total iron		*Ferrous iron*		*Total iron*		*Ferrous iron*	
	Absorbance 510 nm	mg/L	Absorbance 510 nm	mg/L	Absorbance 510 nm	mg/L	Absorbance 510 nm	mg/L
ML 1	0.0100	0.104	0.0045	0.047	0.0025	0.026	0.0010	0.010
ML 2	0.0195	0.202	0.0110	0.114	0.0030	0.031	0.0020	0.021
ML 3	0.0155	0.161	0.0040	0.041	0.0035	0.036	0.0010	0.010

Run Time (hour)	**Filtered sample 0.20 μm pore size**	
	Total iron	
	Absorbance 510 nm	mg/L
ML 1	0.0015	0.016
ML 2	0.0030	0.031
ML 3	0.0030	0.031

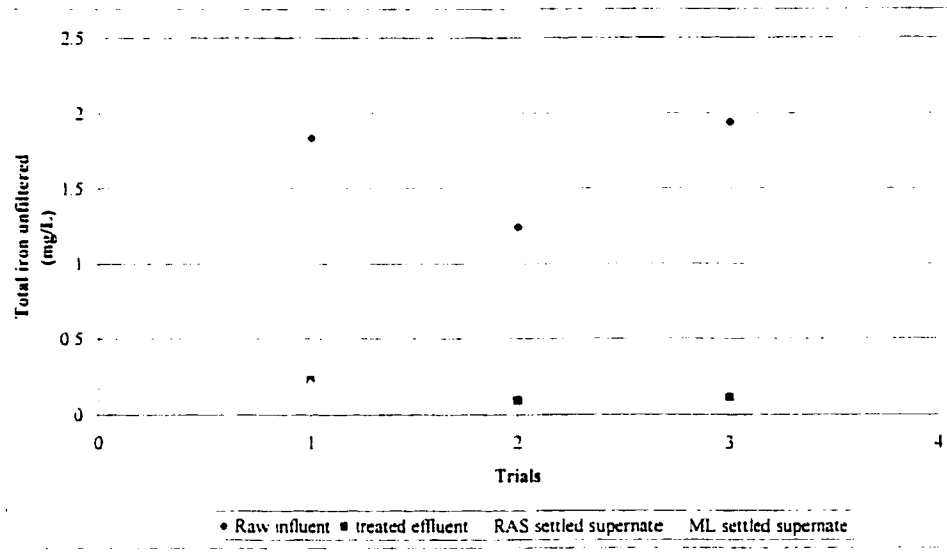

Figure F 1. Graph of total unfiltered iron in the raw influent, treated effluent, RAS and ML settled supernate

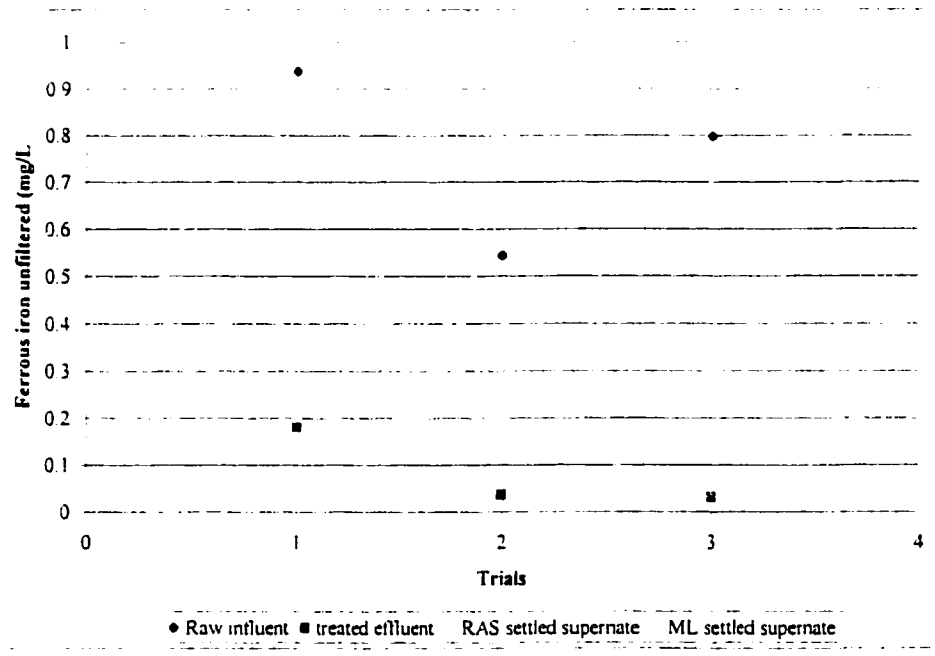

Figure F 2. Graph of ferrous iron unfiltered in the raw influent, treated effluent, RAS and ML settled supernate

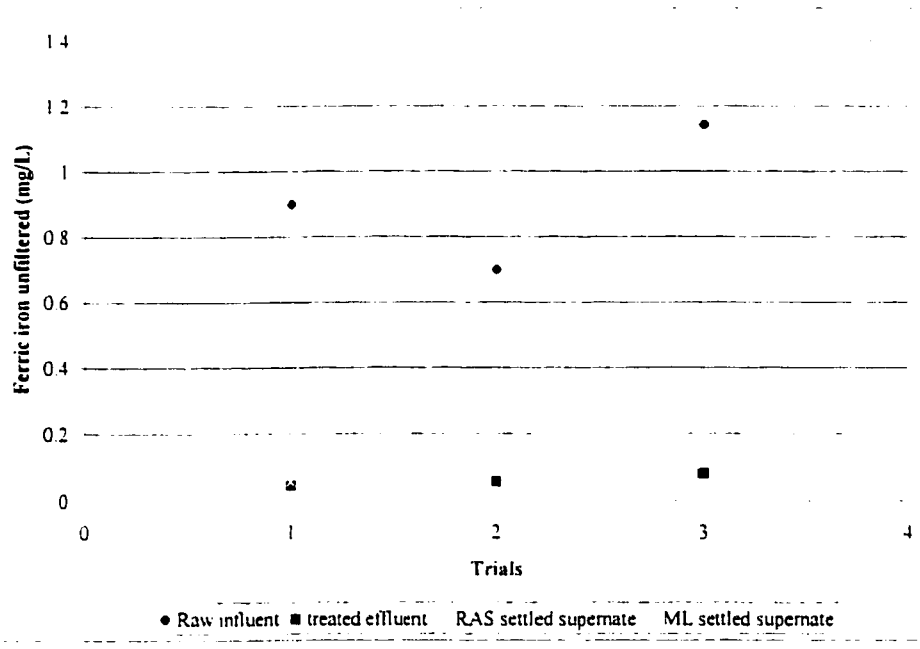

Figure F 3. Graph of ferric iron unfiltered in the raw influent, treated effluent, RAS and ML settled supernate

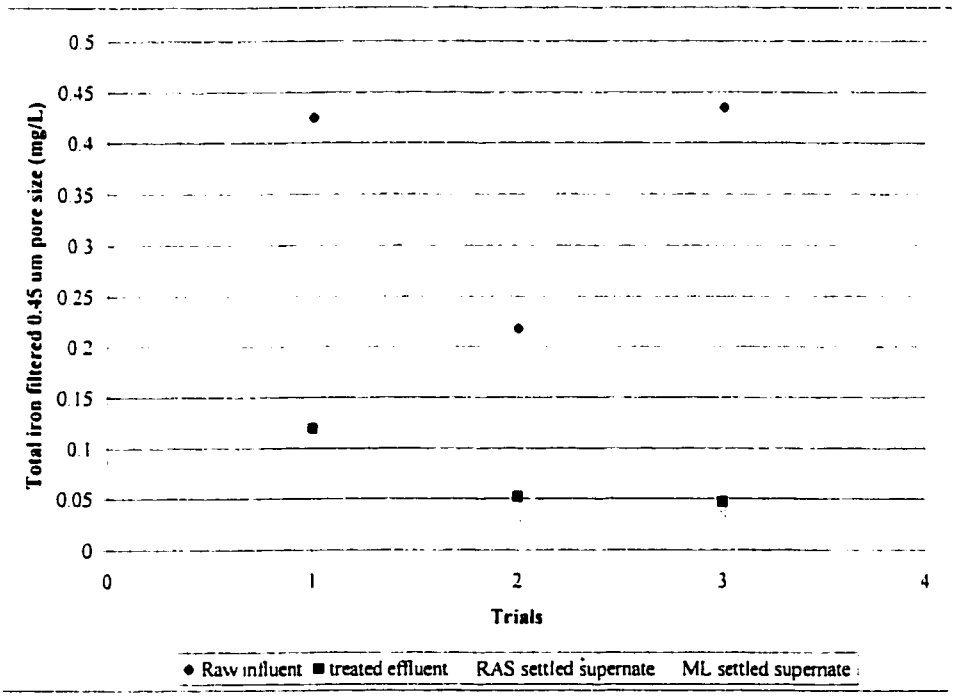

Figure F 4. Graph of total dissolved iron for raw influent, treated effluent, RAS and ML settled supernate

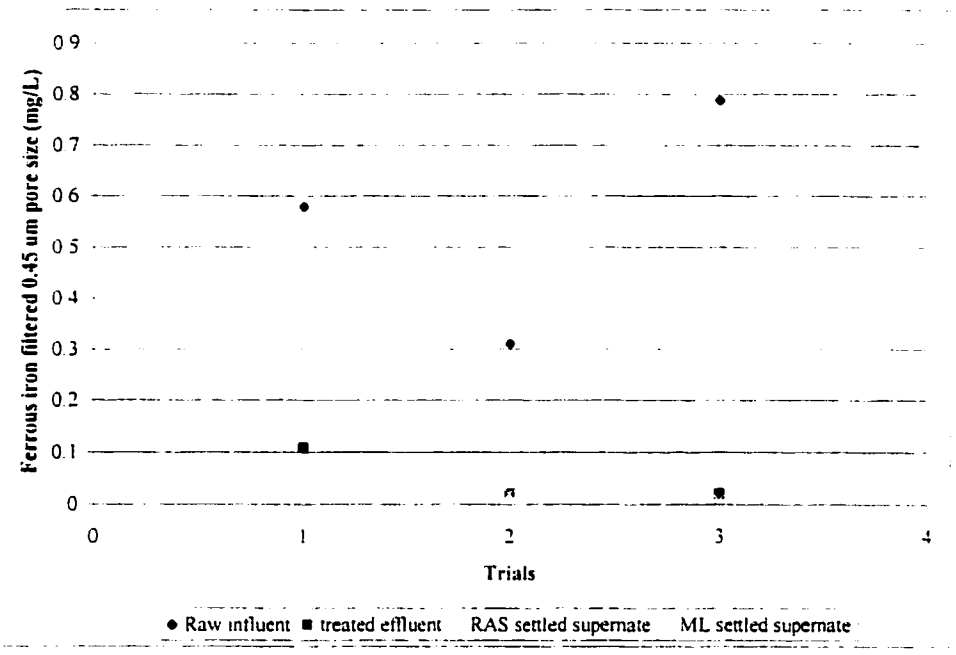

Figure F 5. Graph of ferrous dissolved iron for the raw influent, treated effluent, RAS and ML settled supernate

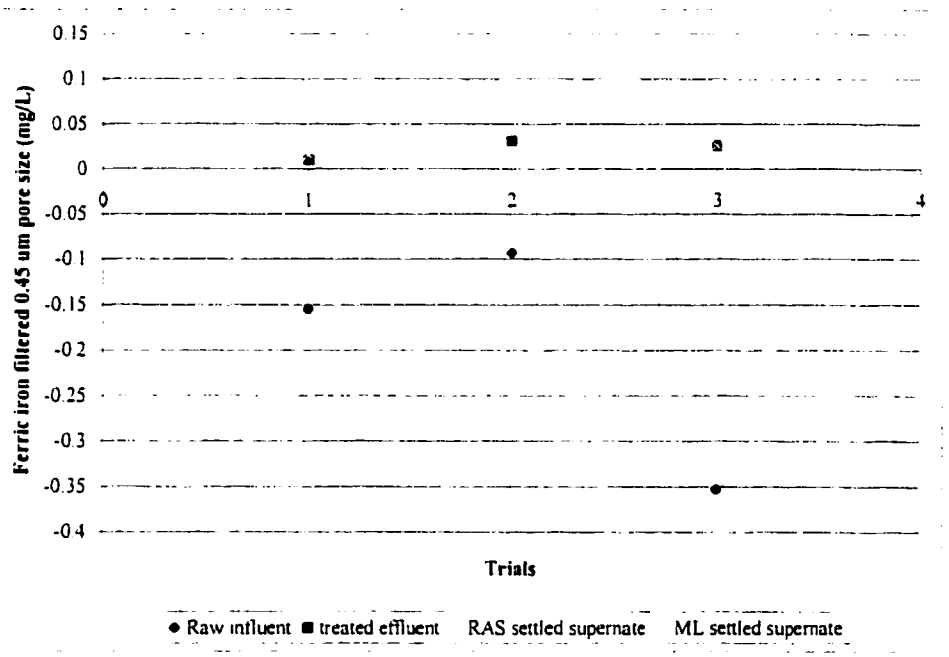

Figure F 6. Graph of ferric dissolved iron for raw influent, treated effluent, RAS and ML settled supernate

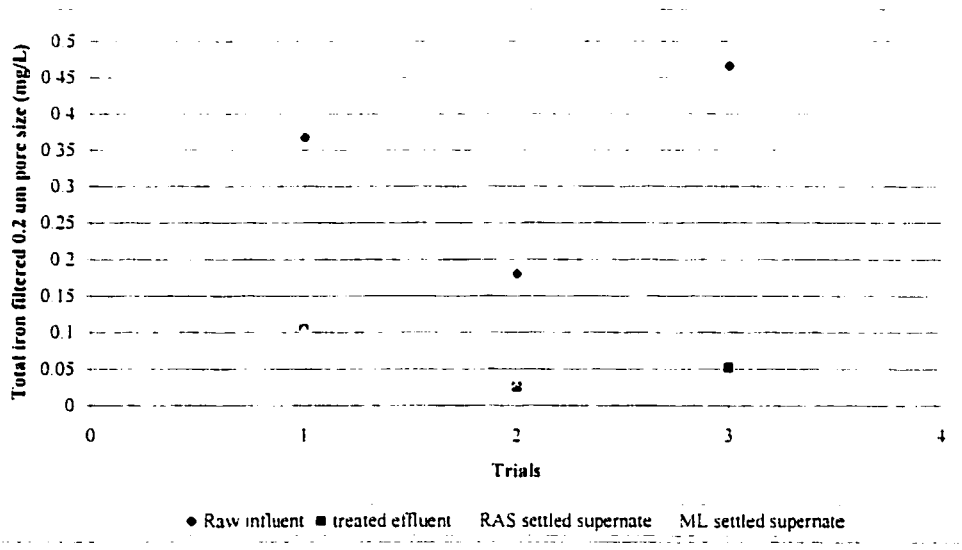

Figure F 7. Graph of total dissolved iron filtered through a 0.2 μm pore size for raw influent, treated effluent, RAS and ML settled supernate

Appendix G. Iron Experiment A and B Combined Graphs

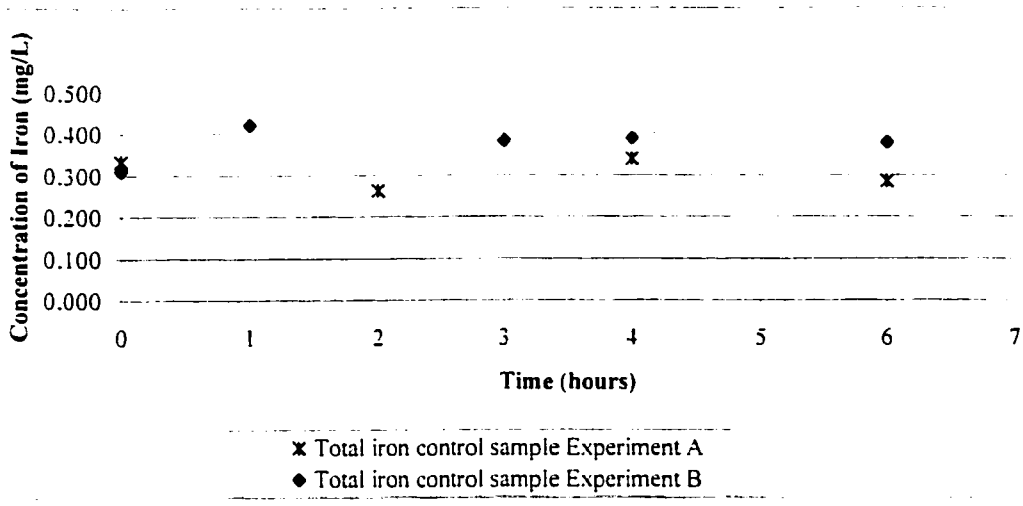

Figure G 1. Graph of total iron for control sample for both experiment A and B

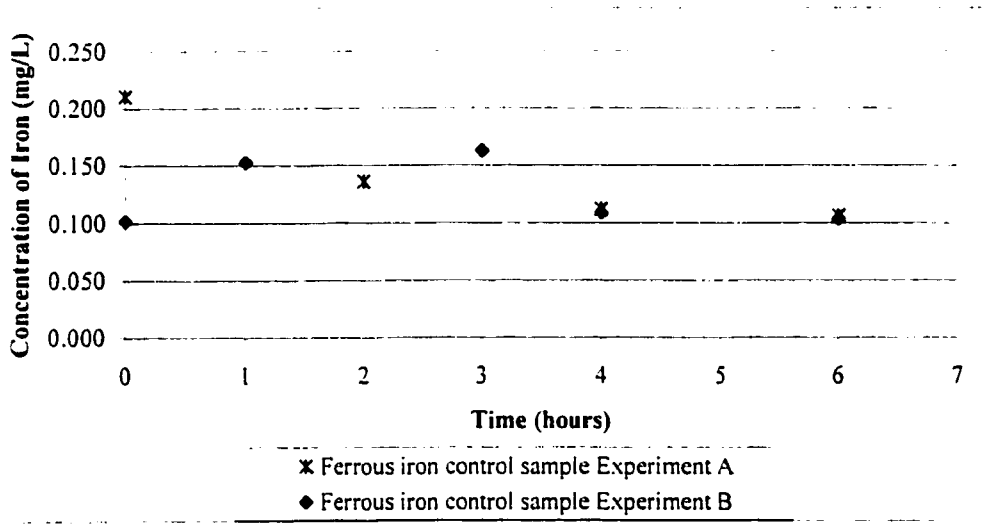

Figure G 2. Graph of ferrous iron for control sample for both experiment A and B

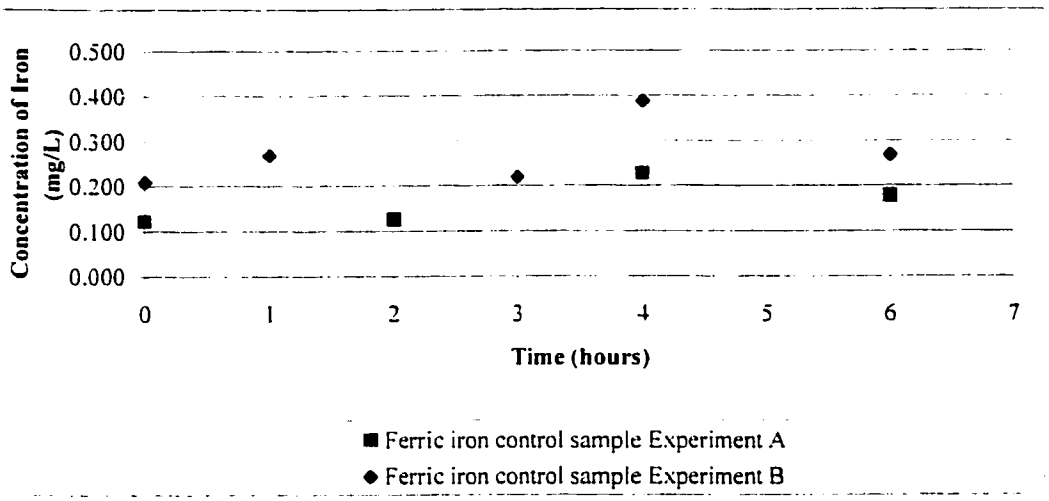

Figure G 3. Graph of ferric iron for control sample for both experiment A and B

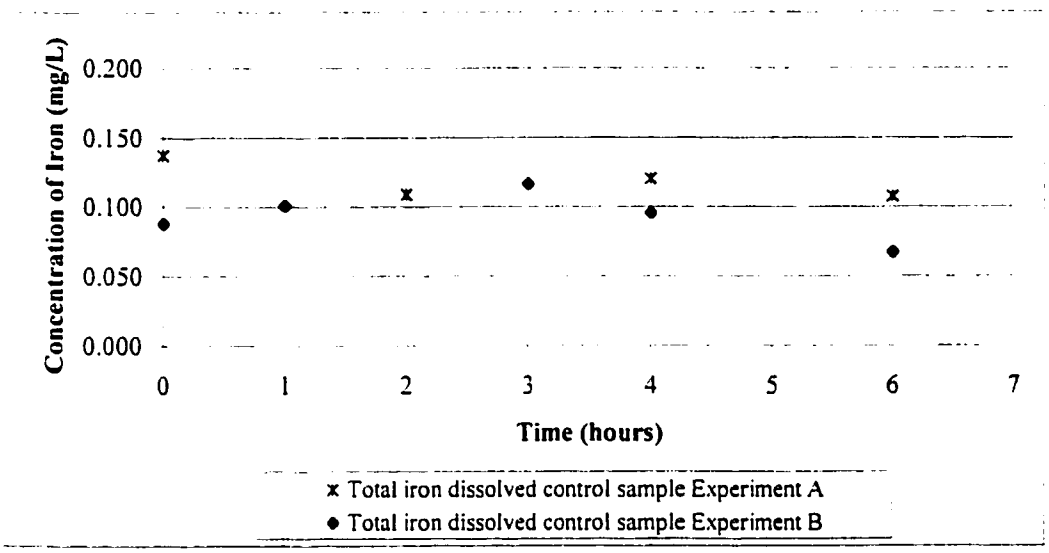

Figure G 4. Graph of total dissolved iron for control sample for both experiment A and B

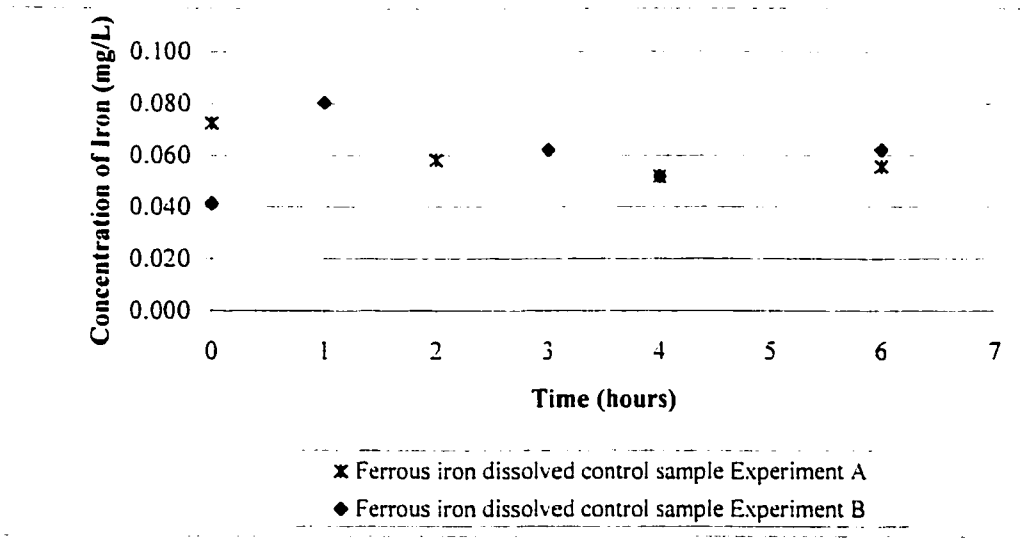

Figure G 5. Graph of ferrous dissolved iron for control sample for both experiment A and B

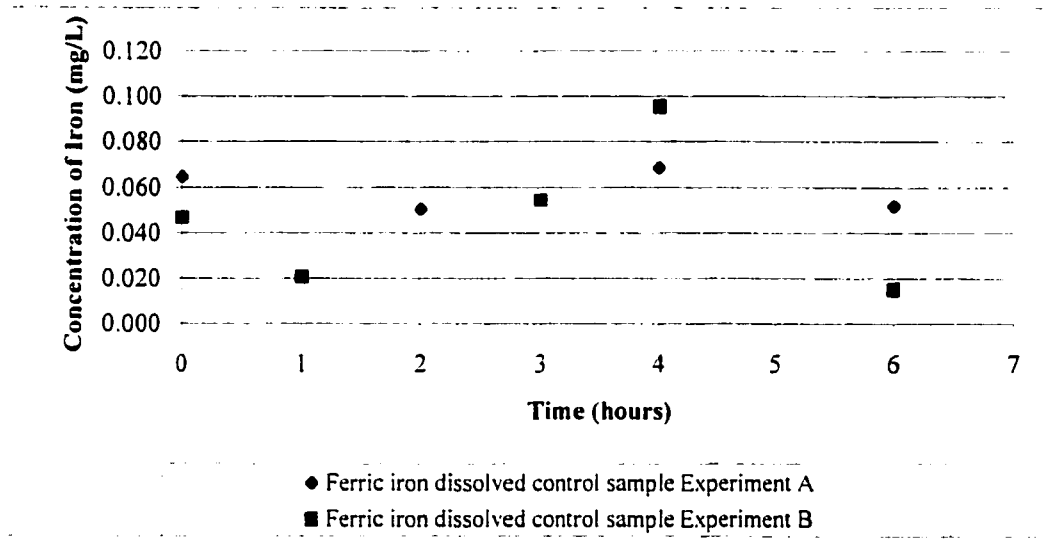

Figure G 6. Graph of ferric dissolved iron for control sample for both experiment A and B

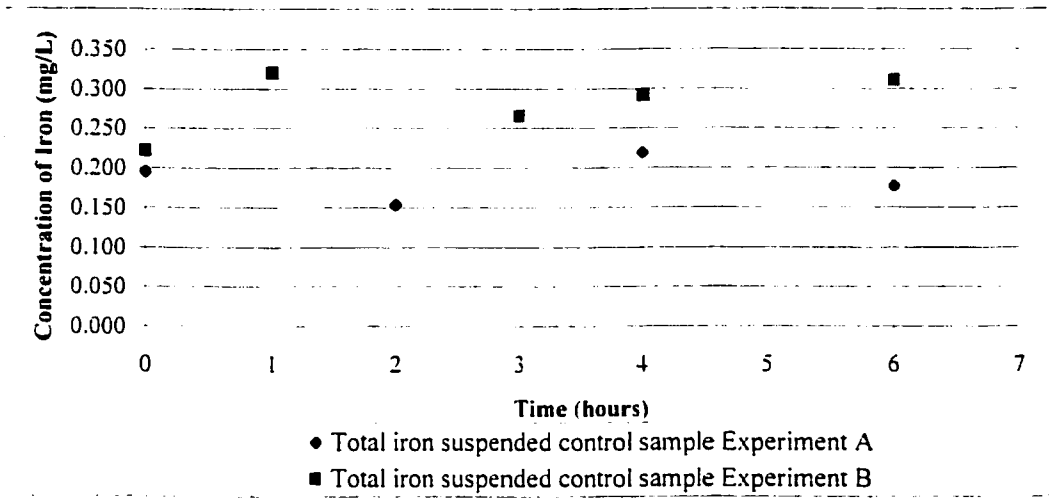

Figure G 7. Graph of total suspended iron for control sample for both experiment A and B

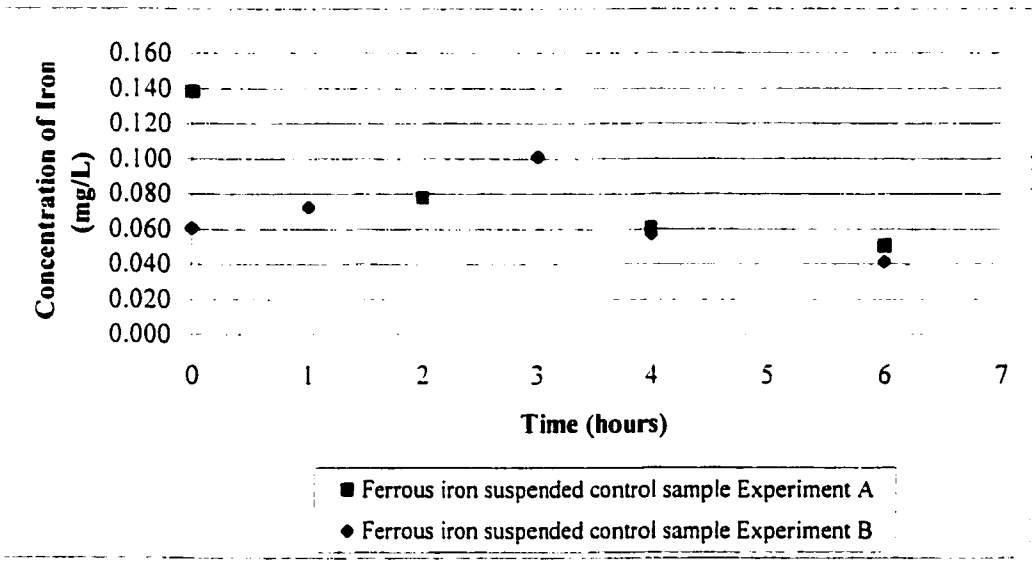

Figure G 8. Graph of ferrous suspended iron for control sample for both experiment A and B

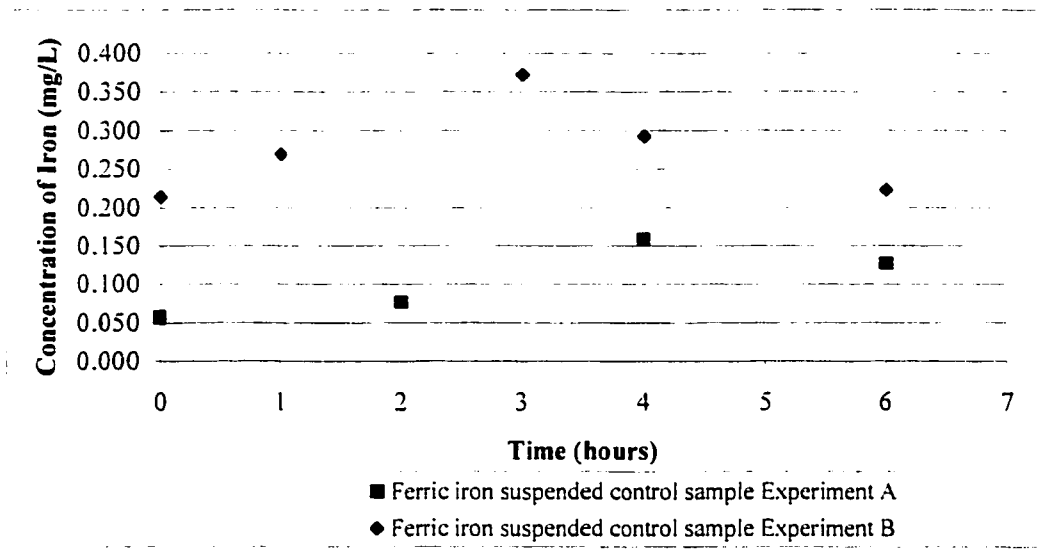

Figure G 9. Graph of ferric suspended iron for control sample for both experiment A and B

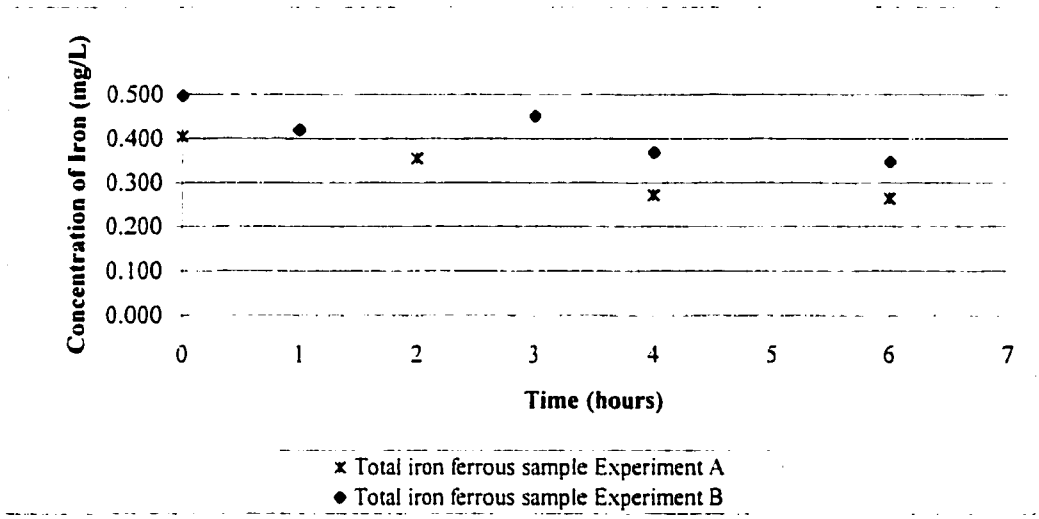

Figure G 10. Graph of total iron for ferrous sample for both experiment A and B

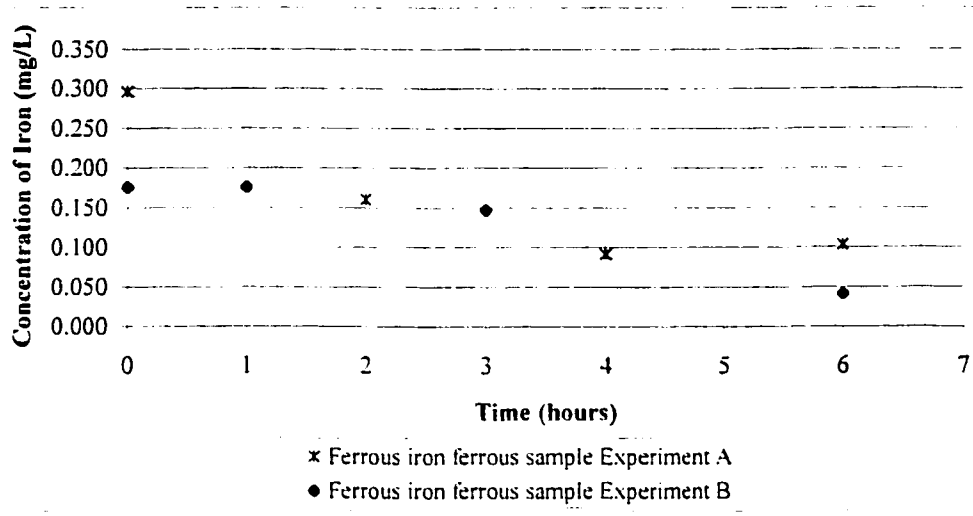

Figure G 11. Graph of ferrous iron for ferrous sample for both experiment A and B

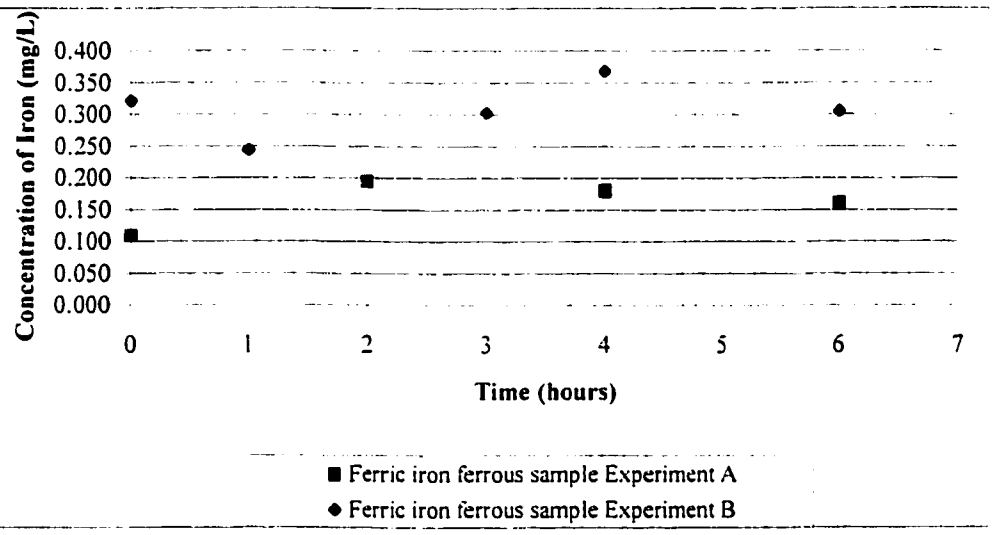

Figure G 12. Graph of ferric iron for ferrous sample for both experiment A and B

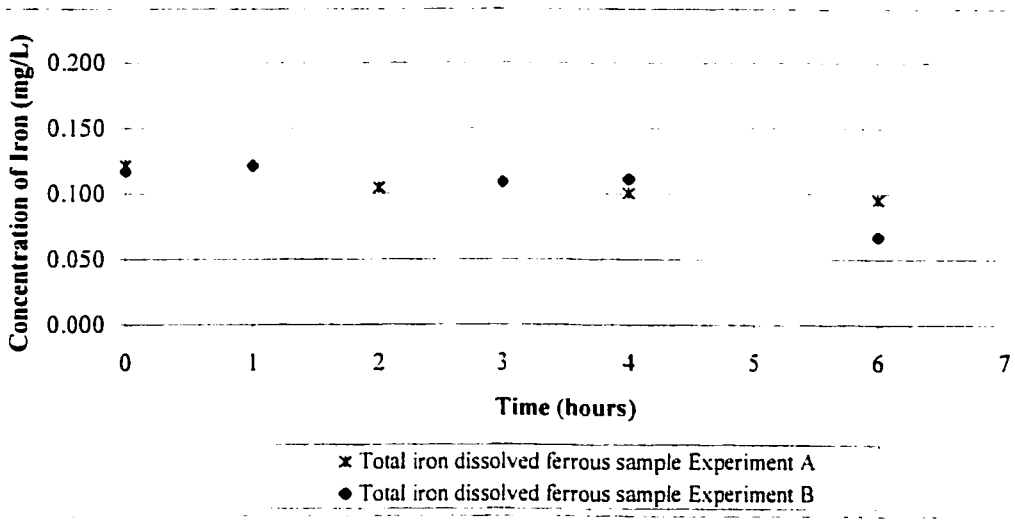

Figure G 13. Graph of total dissolved iron for ferrous sample for both experiment A and B

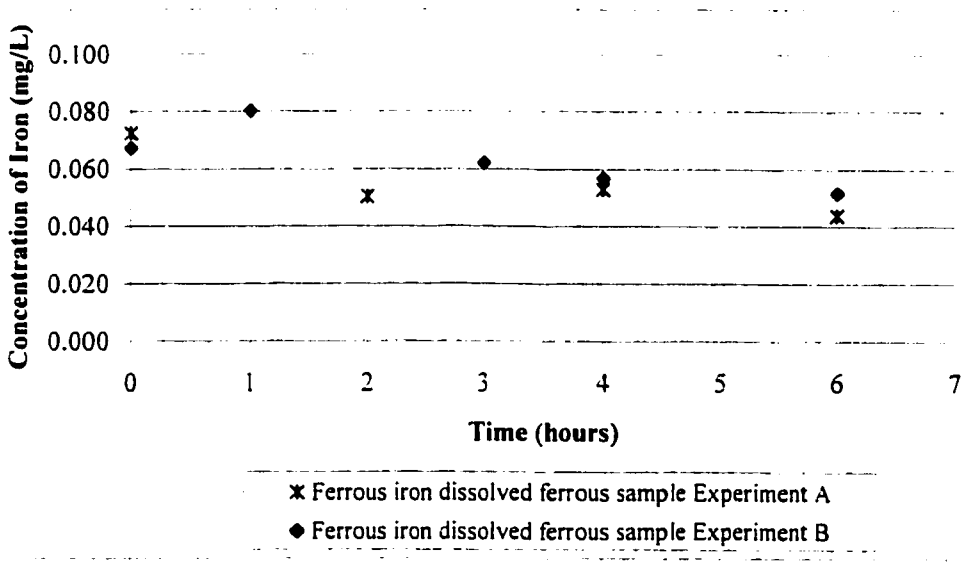

Figure G 14. Graph of ferrous dissolved iron for ferrous sample for both experiment A and B

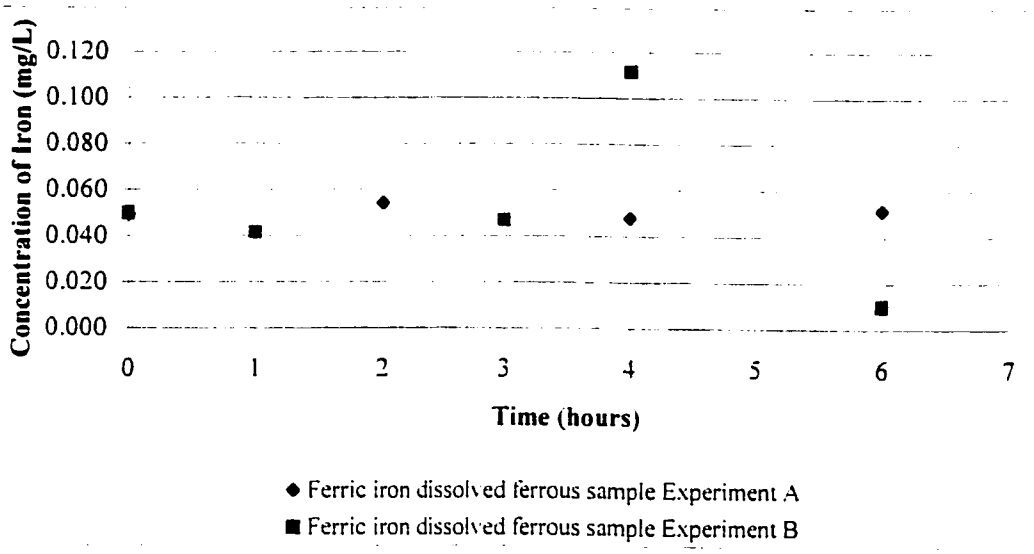

Figure G 15. Graph of ferric dissolved iron for ferrous sample for both experiment A and B

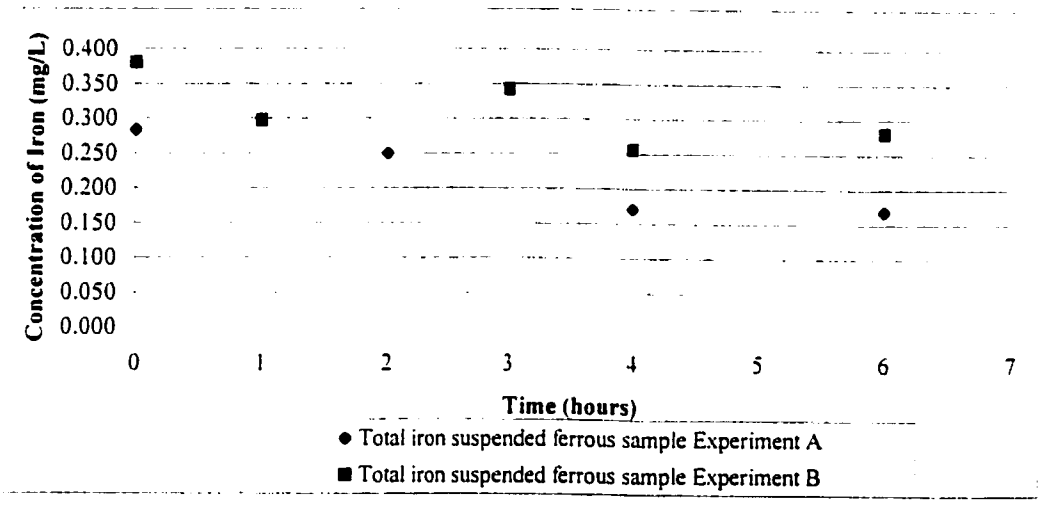

Figure G 16. Graph of total suspended iron for ferrous sample for both experiment A and B

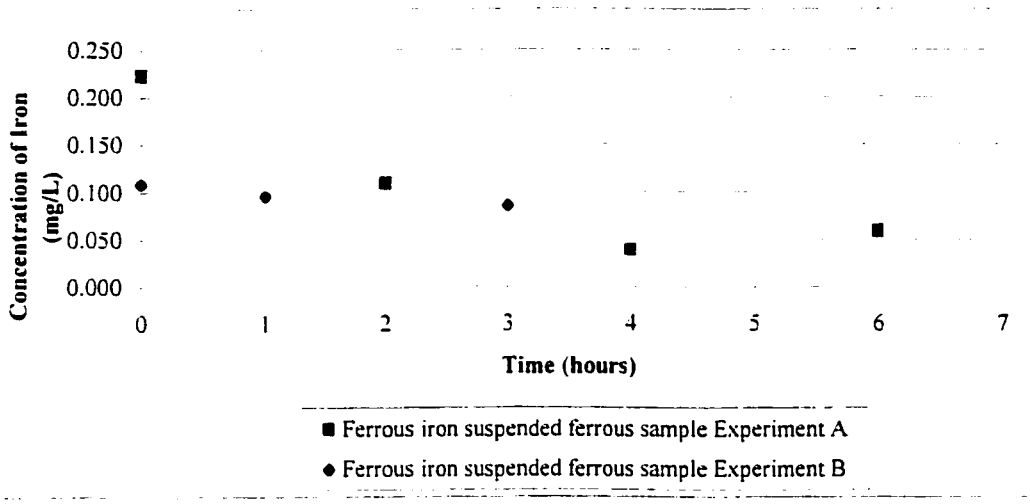

Figure G 17. Graph of ferrous suspended iron for ferrous sample for both experiment A and B

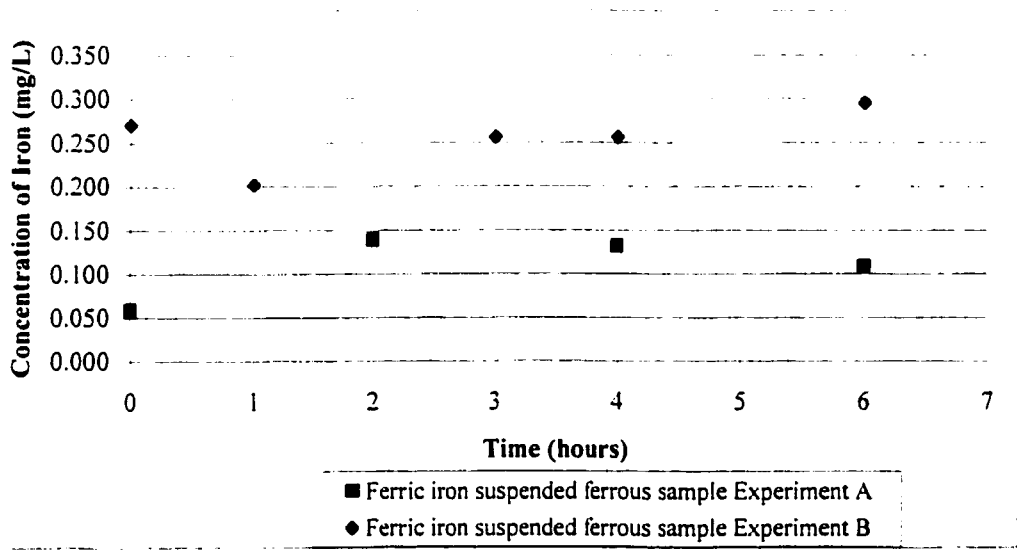

Figure G 18. Graph of ferric suspended iron for ferrous sample for both experiment A and B

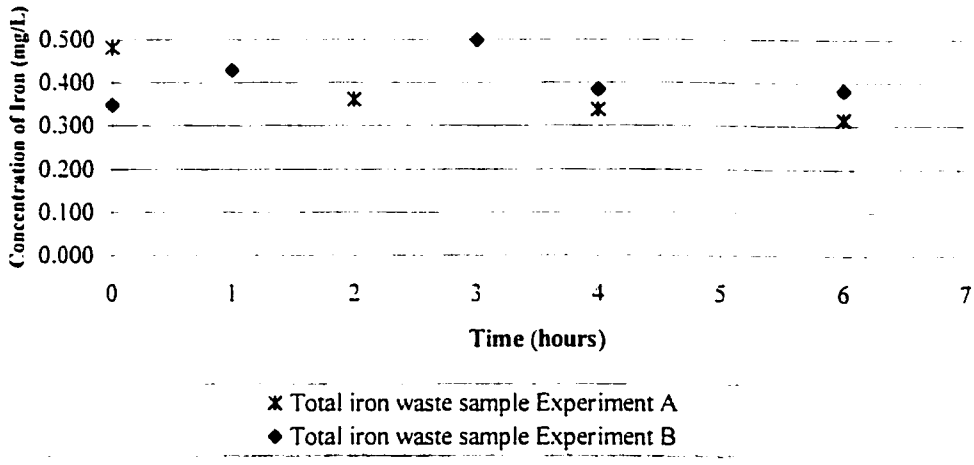

Figure G 19. Graph of total iron for waste sample for both experiment A and B

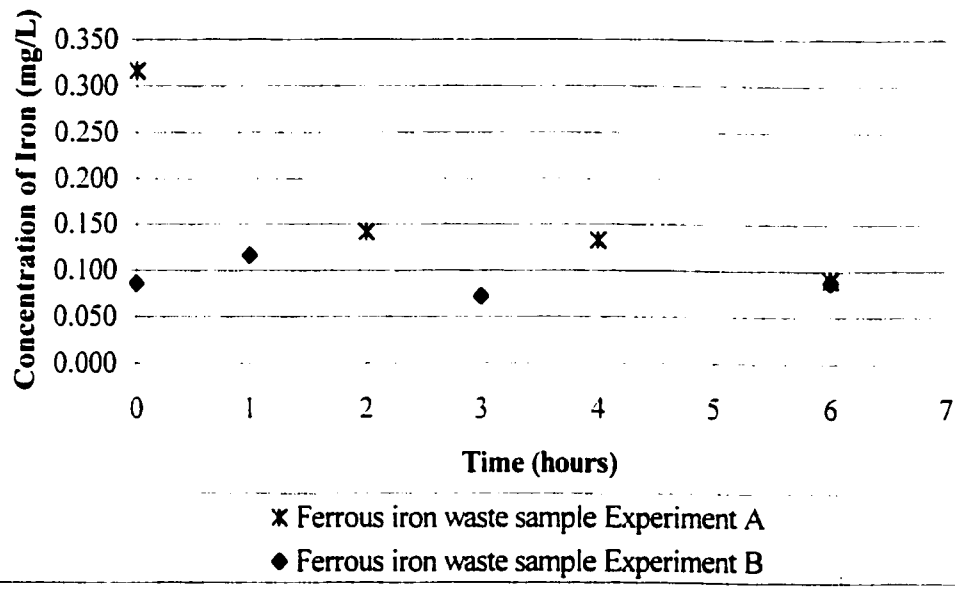

Figure G 20. Graph of ferrous iron for waste sample for both experiment A and B

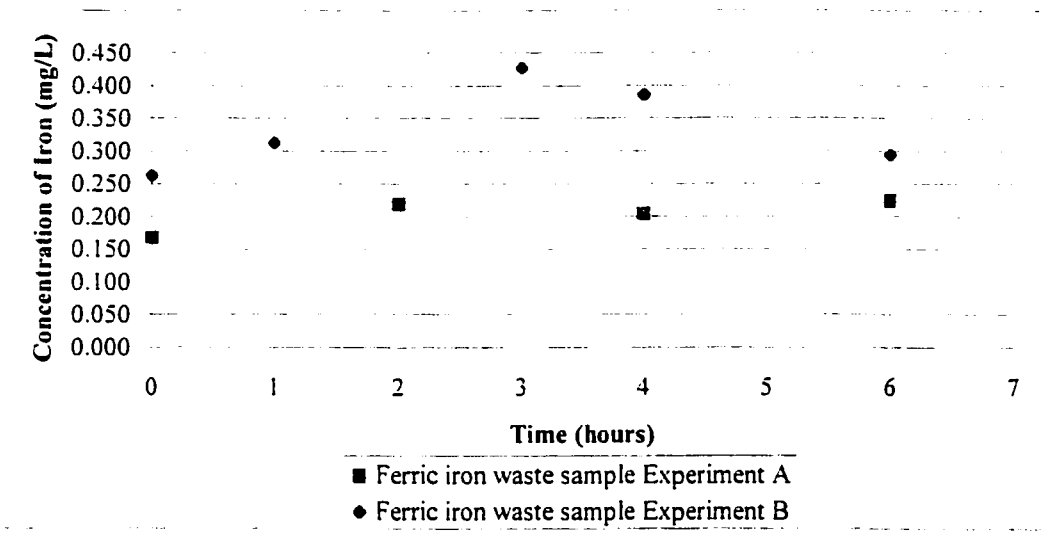

Figure G 21. Graph of ferric iron for waste sample for both experiment A and B

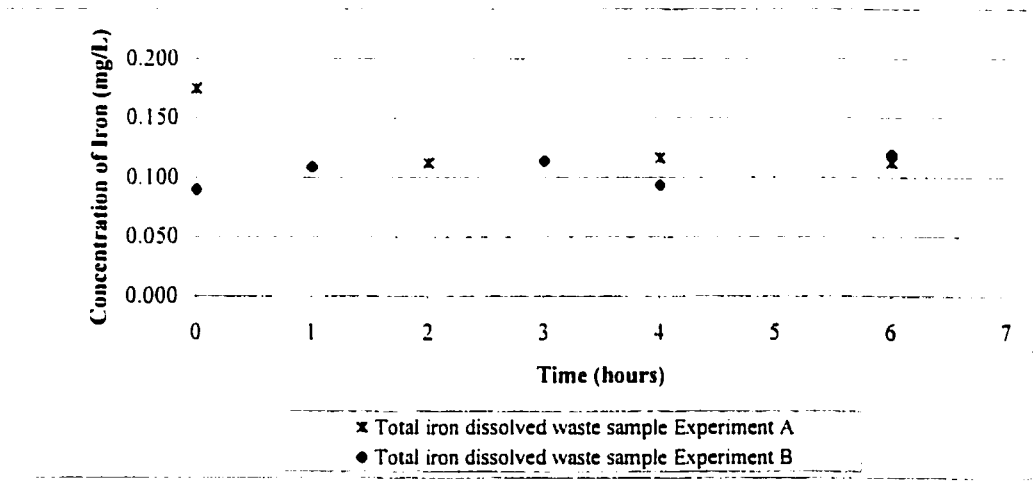

Figure G 22. Graph of total dissolved iron for waste sample for both experiment A and B

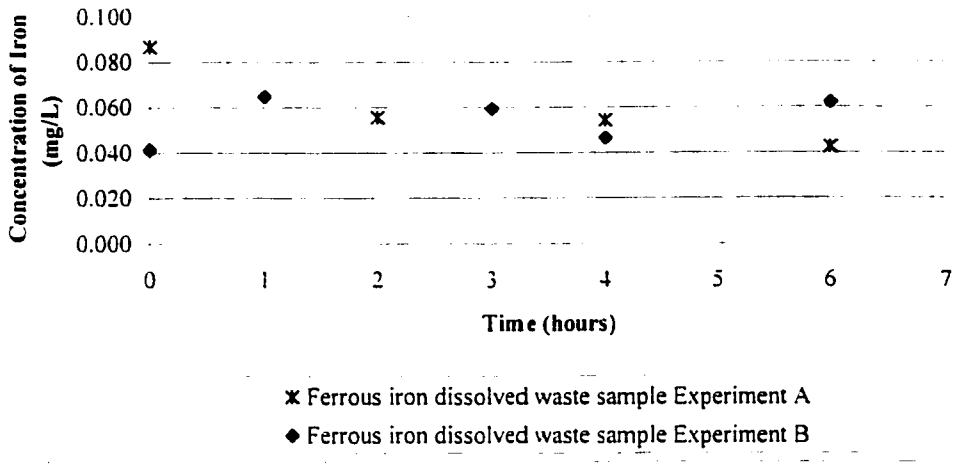

Figure G 23. Graph of ferrous dissolved iron for waste sample for both experiment A and B

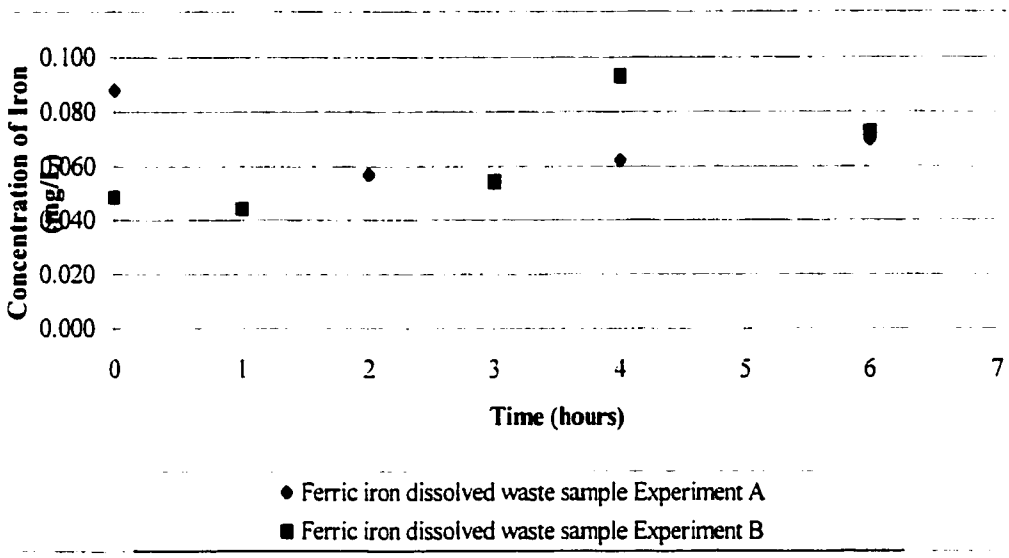

Figure G 24. Graph of ferric dissolved iron for waste sample for both experiment A and B

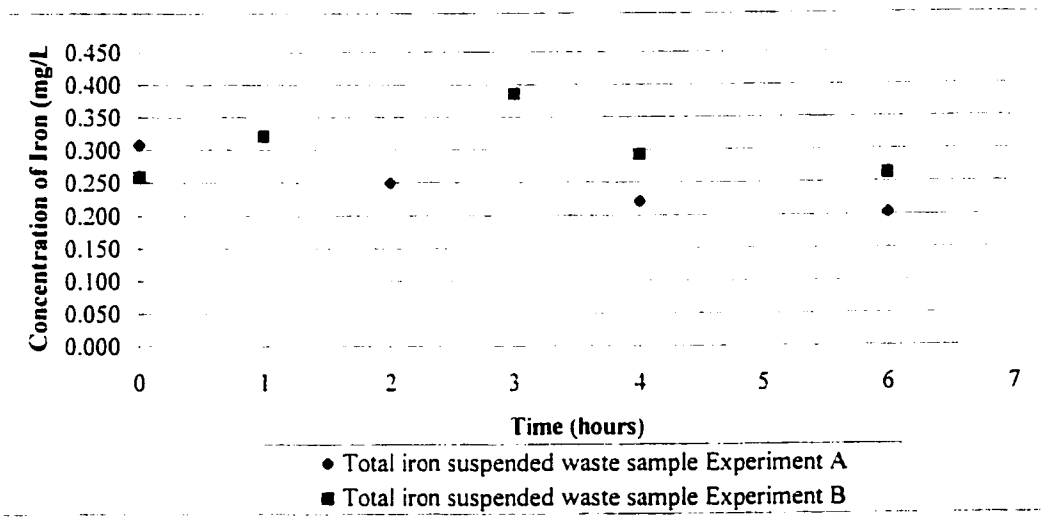

Figure G 25. Graph of total suspended iron for waste sample for both experiment A and B

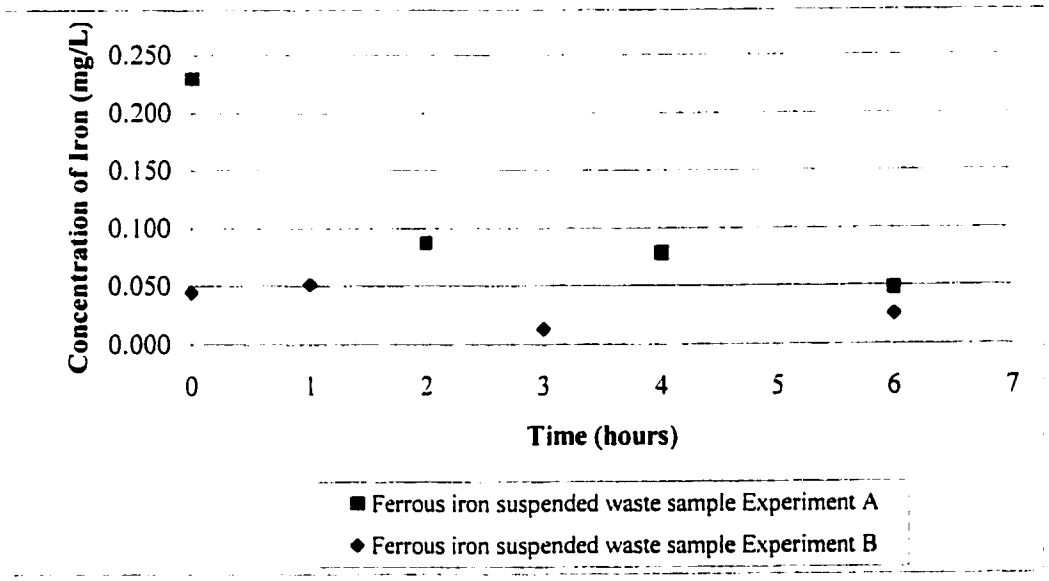

Figure G 26. Graph of ferrous suspended iron for waste sample for both experiment A and B

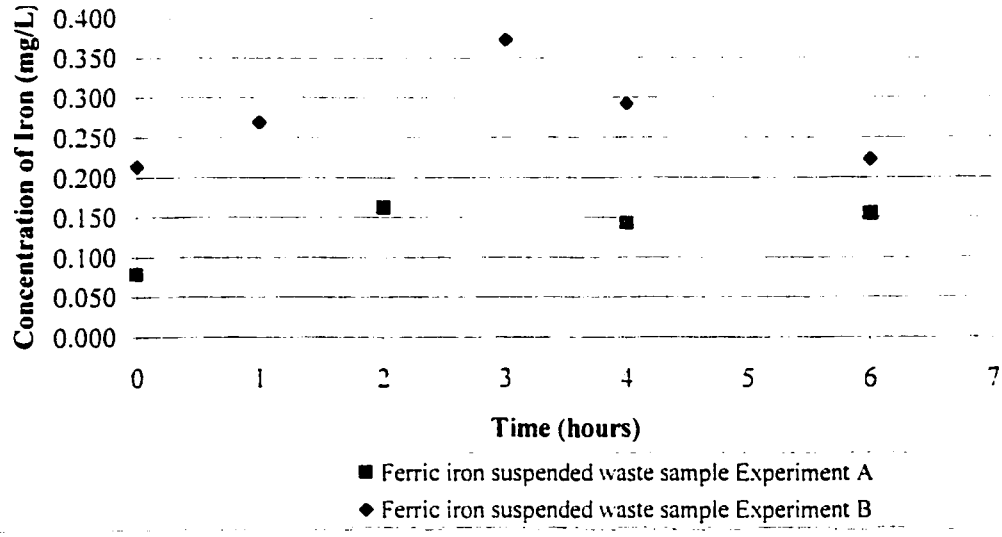

Figure G 27. Graph of ferric suspended iron for waste sample for both experiment A and B

Appendix H. Iron Scale Data

Table H 1. Iron Analysis for scale experiment 1, 1.5 mg/L initial iron concentration.

Date of Experiment: March 8 - 10 1998

Run Time (hours)	**Unfiltered sample**				**Filtered sample 0.45 μm pore size**			
	Total iron		*Ferrous iron*		*Total iron*		*Ferrous iron*	
	Absorbance 510 nm	mg/L	Absorbance 510 nm	mg/L	Absorbance 510 nm	mg/L	Absorbance 510 nm	mg/L
Zero	0.0330	0.342	0.0110	0.114	0.0135	0.140	0.0050	0.052
24	0.0240	0.249	0.0055	0.057	0.0040	0.041	0.0020	0.021
48	0.0175	0.181	0.0070	0.073	0.0050	0.052	0.0010	0.010

Table H 2. Iron Analysis for scale Experiment 2, 1.5 mg/L initial iron concentration.

Date of Experiment: May 6 - 8 1998

Run Time (hours)	**Unfiltered sample**				**Filtered sample 0.45 μm pore size**			
	Total iron		*Ferrous iron*		*Total iron*		*Ferrous iron*	
	Absorbance 510 nm	mg/L	Absorbance 510 nm	mg/L	Absorbance 510 nm	mg/L	Absorbance 510 nm	mg/L
Zero	0.0305	0.316	0.0105	0.109	0.0140	0.145	0.0055	0.057
24	0.0300	0.311	0.0070	0.073	0.0090	0.093	0.0022	0.021
48	0.0285	0.295	0.0030	0.031	0.0055	0.057	0.0010	0.010

Table H 3. Iron Analysis for scale experiment 3, 1.5 mg/L initial iron concentration.

Date of Experiment: May 10 - 12 1998

Run Time (hour)	**Unfiltered sample**				**Filtered sample 0.45 μm pore size**			
	Total iron		*Ferrous iron*		*Total iron*		*Ferrous iron*	
	Absorbance 510 nm	mg/L	Absorbance 510 nm	mg/L	Absorbance 510 nm	mg/L	Absorbance 510 nm	mg/L
Zero	0.0290	0.301	0.0090	0.093	0.0130	0.135	0.0050	0.052
24	0.0275	0.285	0.0060	0.062	0.0065	0.067	0.0020	0.021
48	0.0160	0.166	0.0025	0.026	0.0100	0.104	0.0040	0.041

Table H 4. Iron Analysis for scale experiment, 3.0 mg/L initial iron concentration.

Date of Experiment: March 24 - 26 1998

Run Time (hour)	**Unfiltered sample**				**Filtered sample 0.45 μm pore size**			
	Total iron		*Ferrous iron*		*Total iron*		*Ferrous iron*	
	Absorbance 510 nm	mg/L	Absorbance 510 nm	mg/L	Absorbance 510 nm	mg/L	Absorbance 510 nm	mg/L
Zero	0.0540	0.560	0.0120	0.124	0.0115	0.119	0.0050	0.052
24	0.0250	0.259	0.0065	0.067	0.0070	0.073	0.0025	0.026
48	0.0240	0.249	0.0025	0.026	0.0065	0.067	0.0065	0.067

Table H 5. Iron Analysis for scale experiment, WWTP treated effluent

Date of Experiment: May 13 - 15 1998

Run Time (hour)	**Unfiltered sample**				**Filtered sample 0.45 μm pore size**			
	Total iron		*Ferrous iron*		*Total iron*		*Ferrous iron*	
	Absorbance 510 nm	mg/L	Absorbance 510 nm	mg/L	Absorbance 510 nm	mg/L	Absorbance 510 nm	mg/L
Zero	0.0110	0.114	0.0090	0.093	0.0055	0.057	0.0040	0.041
24	0.0130	0.135	0.0030	0.031	0.0080	0.083	0.0030	0.031
48	0.0070	0.073	0.0020	0.021	0.0050	0.052	0.0025	0.026

Table H 6. Scaling Experiment 1, with 1.5 mg/L iron

Date of Experiment: March 8 –10 1999

Time (hours)	Total iron (mg/L)	TSS (mg/L)	Ratio mg/L Fe / mg/L TSS
0	0.342	55	0.006218
24	0.249	40	0.006218
48	0.181	17	0.010881

Table H 7. Scaling Experiment 2, with 1.5 mg/L iron

Date of Experiment: May 6–8 1999

Time (hours)	Total iron (mg/L)	TSS (mg/L)	Ratio mg/L Fe / mg/L TSS
0	0.316	62	0.005125
24	0.311	50	0.006217
48	0.295	50	0.005907

Table H 8. Scaling Experiment 3, with 1.5 mg/L iron

Date of Experiment: May 10 –12 1999

Time (hours)	Total iron (mg/L)	TSS (mg/L)	Ratio mg/L Fe / mg/L TSS
0	0.300	53	0.00563
24	0.284	33	0.00876
48	0.165	32	0.00523

Table H 9. Scaling Experiment with 3.0 mg/L iron

Date of Experiment: March 24 - 26 1999

Time (hours)	Total iron (mg/L)	TSS (mg/L)	Ratio mg/L Fe / mg/L TSS
0	0.560	80	0.00699
24	0.259	45	0.00576
48	0.249	23	0.01066

Table H 10. Iron scaling Experiment, WWTP treated effluent

Date of Experiment: March 13 –15 1999

Time (hours)	Total iron (mg/L)	TSS (mg/L)	Ratio mg/L Fe / mg/L TSS
0	0.114	7	0.01709
24	0.135	5	0.02694
48	0.073	3	0.02176

Appendix I. Quantitative Analysis Data for Quartz Glass Piece

Table I 1. Quantitative analysis data of clean area on blank sample

Date of Experiment: April 19 1998

Element	Relative Atomic Number	Normal wt %	Atomic %
Na	0.0000	0.00	0.00
Mg	0.0003	0.05	0.04
P	0.0000	0.00	0.00
Cl	0.0000	0.00	0.00
Ca	0.0000	0.00	0.00
K	0.0001	0.01	0.00
Fe	0.0000	0.00	0.00
Al	0.0020	0.25	0.19
Si	0.4042	46.48	33.15
O	0.0000	53.21	66.62
Total		**100.00**	**100.00**

Table I 2. Quantitative analysis data of surface debris on blank sample

Date of Experiment: April 19 1998

Element	Relative Atomic Number	Normal wt %	Atomic %
Na	0.0000	0.00	0.00
Mg	0.0006	0.09	0.07
P	0.0000	0.00	0.00
Cl	0.0004	0.05	0.03
Ca	0.0000	0.00	0.00
K	0.0000	0.00	0.00
Fe	0.0000	0.00	0.00
Al	0.0017	0.21	0.16
Si	0.4041	46.46	33.14
O	0.0000	53.19	66.60
Total		**100.00**	**100.00**

Table I 3. Quantitative analysis data of scratch area (fish) on blank sample

Date of Experiment: April 19 1998

Element	Relative Atomic Number	Normal wt %	Atomic %
Na	0.0002	0.04	0.03
Mg	0.0006	0.08	0.06
P	0.0000	0.00	0.00
Cl	0.0003	0.04	0.02
Ca	0.0000	0.00	0.00
K	0.0000	0.00	0.00
Fe	0.0000	0.00	0.00
Al	0.0018	0.23	0.17
Si	0.4038	46.43	33.12
O	0.0000	53.18	66.59
Total		**100.00**	**99.99**

Table I 4. Quantitative analysis data of overview on 1.5 mg/L sample; Experiment 1 at 24 hours

Date of Experiment: April 19 1998

Element	Relative Atomic Number	Normal wt %	Atomic %
Na	0.0562	12.42	19.77
Mg	0.0000	0.00	0.00
P	0.0000	0.00	0.00
Cl	0.2671	27.52	28.12
Ca	0.5021	53.29	47.92
K	0.0078	0.80	0.75
Fe	0.0527	5.97	3.94
Total		**100.00**	**100.50**

Table I 5. Quantitative analysis data of area 1 on 1.5 mg/L sample; Experiment 1 at 24 hours

Date of Experiment: April 19 1998

Element	Relative Atomic Number	Normal wt %	Atomic %
Na	0.0202	4.59	7.29
Mg	0.0403	6.95	10.46
P	0.0662	7.66	9.02
Cl	0.0499	5.28	5.44
Ca	0.6814	70.31	64.06
K	0.0136	1.26	1.18
Fe	0.0344	3.95	2.58
Total		**100.00**	**100.03**

Table I 6. Quantitative analysis of particle 2 on 1.5 mg/L sample; Experiment 1 at 24 hours

Date of Experiment: April 19 1998

Element	Relative Atomic Number	Normal wt %	Atomic %
Na	0.0252	6.21	10.60
Mg	0.0036	0.67	1.18
P	0.0000	0.00	0.00
Cl	0.1681	17.10	18.60
Ca	0.6328	65.63	62.58
K	0.0148	1.42	1.47
Fe	0.0789	8.97	6.16
Total		**100.00**	**100.59**

Table I 7. Quantitative analysis of particle 3 on 1.5 mg/L sample; Experiment 1 at 24 hours

Date of Experiment: April 19 1998

Element	Relative Atomic Number	Normal wt %	Atomic %
Na	0.0181	3.83	5.84
Mg	0.0337	5.48	7.94
P	0.1017	12.18	13.83
Cl	0.0649	7.24	7.19
Ca	0.5447	57.05	50.05
K	0.0079	0.78	0.71
Fe	0.0397	4.52	2.84
Al	0.0618	8.92	11.61
Total		**100.00**	**100.01**

Table I 8. Quantitative analysis of overview on 1.5 mg/L sample; Experiment 1 at 48 hours

Date of Experiment: April 19 1998

Element	Relative Atomic Number	Normal wt %	Atomic %
Na	0.0744	15.24	21.30
Mg	0.0364	6.61	8.63
P	0.0000	0.00	0.00
Cl	0.1267	14.66	13.32
Ca	0.2077	22.01	17.46
K	0.0049	0.53	0.45
Fe	0.1422	15.77	9.08
Al	0.1590	25.18	29.82
Total		**100.00**	**100.06**

Table I 9. Quantitative analysis data of area 1 on 1.5 mg/L sample; Experiment 1 at 48 hours

Date of Experiment: April 19 1998

Element	Relative Atomic Number	Normal wt %	Atomic %
Na	0.0010	0.21	0.31
Mg	0.0865	13.13	18.30
P	0.0000	0.00	0.00
Cl	0.0069	0.78	0.75
Ca	0.5369	56.21	47.54
K	0.0094	0.92	0.80
Fe	0.0387	4.45	2.70
Al	0.0399	5.98	7.52
Si	0.1381	18.32	22.09
Total		**100.00**	**100.01**

Table I 10. Quantitative analysis of Particle 2 on 1.5 mg/L sample; Experiment 1 at 48 hours

Date of Experiment: April 19 1998

Element	Relative Atomic Number	Normal wt %	Atomic %
Na	0.0105	1.84	2.44
Mg	0.0127	1.75	2.20
P	0.0000	0.00	0.00
Cl	0.0186	2.55	2.19
Ca	0.0350	3.90	2.96
K	0.0091	1.07	0.84
Fe	0.1204	13.56	7.39
Al	0.0579	7.02	7.91
Si	0.5719	68.31	74.06
Total		**100.00**	**99.99**

Table I 11. Quantitative analysis of Particle 3 on 1.5 mg/L sample; Experiment 1 at 48 hours

Date of Experiment: April 19, 1998

Element	Relative Atomic Number	Normal wt %	Atomic %
Na	0.0414	8.44	9.90
Mg	0.0240	4.02	4.51
P	0.0000	0.00	0.00
Cl	0.2286	25.50	19.34
Ca	0.1683	18.22	12.25
K	0.0057	0.64	0.42
Fe	0.1163	13.06	6.29
Al	0.1116	16.25	16.27
C	0.0000	13.87	31.06
Total		**100.00**	**100.04**

Table I 12. Quantitative analysis of particle 1 on 1.5 mg/L sample; Experiment 2 at 24 hours

Date of Experiment: May 17, 1999

Element	Relative Atomic Number	Normal wt %	Atomic %
S	0.1412	17.92	28.45
Fe	0.0916	8.08	7.37
Zn	0.0946	9.90	7.70
Cu	0.5572	58.52	46.86
Ca	0.0242	2.47	3.13
Mg	0.0086	3.11	6.49
Total		**100.00**	**100.00**

Table I 13. Quantitative analysis of particle 2 on 1.5 mg/L sample; Experiment 2 at 24 hours

Date of Experiment: May 17, 1999

Element	Relative Atomic Number	Normal wt %	Atomic %
S	0.0000	0.00	0.00
Fe	0.0089	1.02	0.54
Zn	0.0032	0.37	0.17
Cu	0.0000	0.00	0.00
Ca	0.1543	7.16	12.65
Mg	0.0063	0.74	0.89
Al	0.1964	21.54	23.56
Si	0.4616	59.17	62.18
Total		**100.00**	**99.99**

Table I 14. Quantitative analysis of particle 3 on 1.5 mg/L sample; Experiment 2 at 24 hours

Date of Experiment: May 17, 1999

Element	Relative Atomic Number	Normal wt %	Atomic %
Fe	0.5335	56.12	41.10
Ca	0.0963	9.41	9.62
Mg	0.0122	2.97	5.01
Al	0.1129	21.06	31.92
K	0.0143	1.46	1.53
Ti	0.0377	3.82	3.27
S	0.0000	0.00	0.00
Na	0.0098	3.62	6.42
Mn	0.0143	1.54	1.15
Total		**100.00**	**100.02**

Table I 15. Quantitative analysis of Particle 1 on 1.5 mg/L sample; Experiment 2 at 48 hours

Date of Experiment: May 17, 1999

Element	Relative Atomic Number	Normal wt %	Atomic %
Fe	0.0453	5.13	2.69
Ca	0.0135	1.53	1.12
Mg	0.0162	1.92	2.32
K	0.0626	7.38	5.52
Ti	0.0060	0.70	0.43
Na	0.0019	0.28	0.35
Mn	0.0002	0.02	0.01
Cl	0.0052	0.71	0.59
Al	0.2340	26.29	28.54
Si	0.4137	56.04	58.44
Total		**100.00**	**100.01**

Table I 16. Quantitative analysis of Particle 2 on 1.5 mg/L sample; Experiment 2 at 48 hours

Date of Experiment: May 17, 1999

Element	Relative Atomic Number	Normal wt %	Atomic %
Fe	0.0306	3.49	1.88
Ca	0.0784	8.71	6.52
Mg	0.0087	1.07	1.31
K	0.0018	0.21	0.16
Ti	0.0470	5.54	3.47
Na	0.0010	0.16	0.20
Cl	0.0030	0.41	0.34
Al	0.0392	4.33	4.81
Si	0.6860	76.08	81.27
Total		**100.00**	**99.96**

Table I 17. Quantitative analysis of Particle 3 on 1.5 mg/L sample; Experiment 2 at 48 hours

Date of Experiment: May 17, 1999

Element	Relative Atomic Number	Normal wt %	Atomic %
Fe	0.0303	3.46	1.89
Ca	0.1732	19.19	4.55
Mg	0.0110	1.40	1.76
K	0.0020	0.23	0.18
Ti	0.0070	0.84	0.54
Na	0.0055	0.88	1.16
Mn	0.0009	0.11	0.06
P	0.0077	1.35	1.32
Cl	0.0093	1.25	1.07
S	0.0000	0.00	0.00
Al	0.0680	7.79	8.77
Au	0.0000	0.00	0.00
Si	0.5464	63.50	68.71
Total		**100.00**	**100.01**

Table I 18. Quantitative analysis of particle 1 on 1.5 mg/L sample; Experiment 3 at 24 hours

Date of Experiment: May 17, 1999

Element	Relative Atomic Number	Normal wt %	Atomic %
Fe	0.0979	11.03	7.11
Ca	0.4825	49.49	44.49
Mg	0.0492	9.25	13.73
K	0.0054	0.53	0.49
Ti	0.0394	4.73	3.56
Na	0.0352	8.45	13.26
Mn	0.0108	1.25	0.83
P	0.0589	7.09	8.25
Cl	0.0751	8.18	8.33
S	0.0000	0.00	0.00
Total		**100.00**	**100.05**

Table I 19. Quantitative analysis of particle 2 on 1.5 mg/L sample; Experiment 3 at 24 hours

Date of Experiment: May 17, 1999

Element	Relative Atomic Number	Normal wt %	Atomic %
Fe	0.0735	8.29	4.42
Ca	0.0082	0.93	0.69
Mg	0.0098	1.22	1.50
K	0.0561	6.61	5.04
Ti	0.0107	1.24	0.77
Na	0.0032	0.51	0.66
Mn	0.0000	0.00	0.00
P	0.0000	0.00	0.00
Cl	0.0064	0.87	0.73
S	0.0000	0.00	0.00
Al	0.1986	22.76	25.12
Si	0.4340	57.57	61.07
Total		**100.00**	**100.00**

Table I 20. Quantitative analysis of particle 3 on 1.5 mg/L sample; Experiment 3 at 24 hours

Date of Experiment: May 17, 1999

Element	Relative Atomic Number	Normal wt %	Atomic %
Fe	0.0867	9.85	6.45
Ca	0.5631	58.55	53.53
Mg	0.0565	9.44	14.26
K	0.0176	1.71	1.61
P	0.0458	5.53	6.54
Cl	0.0648	7.08	7.30
S	0.0160	1.79	2.04
Al	0.0393	6.05	8.26
Total		**100.00**	**99.99**

Table I 21. Quantitative analysis of Particle 1 on 1.5 mg/L sample; Experiment 3 at 48 hours

Date of Experiment: May 17, 1999

Element	Relative Atomic Number	Normal wt %	Atomic %
Fe	0.0328	3.73	2.02
Ca	0.1077	12.13	9.13
Mg	0.0182	2.28	2.83
K	0.0573	6.62	5.11
Ti	0.0059	0.70	0.44
Na	0.0051	0.80	1.04
Mn	0.0000	0.00	0.00
P	0.0000	0.00	0.00
Cl	0.0160	2.13	1.82
S	0.0000	0.00	0.00
Al	0.1276	14.76	16.51
Si	0.4580	56.85	61.09
Total		**100.00**	**99.99**

Table I 22. Quantitative analysis of Particle 2 on 1.5 mg/L sample; Experiment 3 at 48 hours

Date of Experiment: May 17, 1999

Element	Relative Atomic Number	Normal wt %	Atomic %
Fe	0.0777	8.77	4.66
Ca	0.0382	4.25	3.15
Mg	0.0288	3.70	4.52
K	0.0163	1.91	1.45
Ti	0.0099	1.15	0.71
Na	0.0111	1.77	2.28
Mn	0.0016	0.18	0.10
P	0.0000	0.00	0.00
Cl	0.0137	1.87	1.56
S	0.0000	0.00	0.00
Al	0.1641	19.77	21.75
Si	0.4256	56.63	59.82
Total		**100.00**	**100.00**

Table I 23. Quantitative analysis of Particle 3 on 1.5 mg/L sample; Experiment 3 at 48 hours

Date of Experiment: May 17, 1999

Element	Relative Atomic Number	Normal wt %	Atomic %
Fe	0.0435	4.96	2.65
Ca	0.0802	8.99	6.69
Mg	0.0293	3.69	4.54
K	0.0047	0.56	0.42
Ti	0.0128	1.51	0.95
Na	0.0117	1.80	2.32
Mn	0.0000	0.00	0.00
P	0.0000	0.00	0.00
Cl	0.0346	4.71	3.96
S	0.0000	0.00	0.00
Al	0.0366	4.27	4.72
Au	0.0000	0.00	0.00
Si	0.6089	69.51	73.76
Total		**100.00**	**100.01**

Table I 24. Quantitative analysis of overview on 3.0 mg/L sample at 24 hours

Date of Experiment: April 19 1998

Element	Relative Atomic Number	Normal wt %	Atomic %
Na	0.0565	9.69	12.52
Mg	0.0845	12.77	15.39
P	0.0000	0.00	0.00
Cl	0.0000	0.00	0.00
Ca	0.1833	19.33	14.37
K	0.0000	0.00	0.00
Fe	0.0961	10.73	5.67
Al	0.3136	47.48	52.28
Total		**100.00**	**100.23**

Table I 25. Quantitative analysis of particle 1 on 3.0 mg/L sample at 24 hours

Date of Experiment: April 19 1998

Element	Relative Atomic Number	Normal wt %	Atomic %
Na	0.0033	0.86	1.38
Mg	0.0344	6.26	8.98
P	0.0000	0.00	0.00
Cl	0.0185	2.21	2.18
Ca	0.1899	19.47	17.01
K	0.0071	0.74	0.70
Fe	0.2976	32.39	20.35
Al	0.2409	38.07	49.54
Total		**100.00**	**100.14**

Table I 26. Quantitative analysis of particle 2 on 3.0 mg/L sample at 24 hours

Date of Experiment: April 19 1998

Element	Relative Atomic Number	Normal wt %	Atomic %
Na	0.0082	1.95	3.27
Mg	0.0056	0.97	1.55
P	0.0008	0.09	0.12
Cl	0.1931	19.59	21.33
Ca	0.6078	62.76	60.44
K	0.0047	0.46	0.46
Fe	0.0308	3.51	2.43
Al	0.0206	2.93	4.18
Ti	0.0623	7.74	6.24
Total		**100.00**	**100.02**

Table I 27. Quantitative analysis of particle 3 on 3.0 mg/L sample at 24 hours

Date of Experiment: April 19 1998

Element	Relative Atomic Number	Normal wt %	Atomic %
Na	0.0177	3.77	4.11
Mg	0.0184	3.00	3.15
P	0.0000	0.00	0.00
Cl	0.0173	2.09	1.40
Ca	0.0866	9.07	5.61
K	0.0072	0.78	0.46
Fe	0.2015	22.44	9.91
Al	0.2810	40.19	36.87
C	0.0000	18.66	38.60
Total		**100.00**	**100.11**

Table I 28. Quantitative analysis of overview on 3.0 mg/L sample at 48 hours

Date of Experiment: April 19 1998

Element	Relative Atomic Number	Normal wt %	Atomic %
Na	0.0083	2.01	2.34
Mg	0.0256	4.45	4.88
P	0.0000	0.00	0.00
Cl	0.0255	2.98	2.23
Ca	0.1659	17.23	11.43
K	0.0166	1.75	1.19
Fe	0.2321	25.81	12.29
Al	0.1914	28.99	28.56
C	0.0000	16.78	37.09
Total		**100.00**	**100.01**

Table I 29. Quantitative analysis of particle 1 on 3.0 mg/L sample at 48 hours

Date of Experiment: April 19 1998

Element	Relative Atomic Number	Normal wt %	Atomic %
Na	0.0000	0.00	0.00
Mg	0.0092	1.61	1.70
P	0.0000	0.00	0.00
Cl	0.0722	8.37	6.48
Ca	0.1373	14.35	9.70
K	0.0177	1.90	1.36
Fe	0.2503	27.69	13.50
Al	0.2034	29.76	30.13
C	0.0000	16.32	37.28
Total		**100.00**	**100.15**

Table I 30. Quantitative analysis of particle 2 on 3.0 mg/L sample at 48 hours

Date of Experiment: April 19 1998

Element	Relative Atomic Number	Normal wt %	Atomic %
Na	0.0000	0.00	0.00
Mg	0.0163	2.39	2.27
P	0.0000	0.00	0.00
Cl	0.0075	0.95	0.67
Ca	0.0533	5.77	3.33
K	0.0106	1.20	0.71
Fe	0.1502	17.07	7.07
Al	0.0848	11.03	9.45
Si	0.2957	38.14	31.39
C	0.0000	23.45	45.15
Total		**100.00**	**99.99**

Table I 31. Quantitative analysis of particle 3 on 3.0 mg/L sample at 48 hours

Date of Experiment: April 19 1998

Element	Relative Atomic Number	Normal wt %	Atomic %
Na	0.0013	0.21	0.19
Mg	0.0070	0.88	0.77
P	0.0000	0.00	0.00
Cl	0.0025	0.33	0.20
Ca	0.0397	4.41	2.36
K	0.0053	0.62	0.34
Fe	0.0606	7.01	2.26
Al	0.0457	5.22	4.14
Si	0.4777	54.53	41.55
C	0.0000	26.79	47.75
Total		**100.00**	**99.99**

Table I 32. Quantitative analysis of particle 1 on clarifier 4 effluent sample at 24 hours

Date of Experiment: May 17, 1999

Element	Relative Atomic Number	Normal wt %	Atomic %
Fe	0.0215	2.46	1.29
Ca	0.0735	8.32	6.07
Mg	0.0074	0.86	1.04
K	0.0045	0.54	0.40
Ti	0.0032	0.38	0.23
Na	0.0019	0.27	0.34
Mn	0.0000	0.00	0.00
P	0.0050	0.95	0.09
Cl	0.0037	0.52	0.44
S	0.0000	0.00	0.00
Al	0.0503	5.31	5.74
Au	0.0000	0.00	0.00
Si	0.7332	80.39	83.57
Total		**100.00**	**100.02**

Table I 33. Quantitative analysis of particle 2 clarifier 4 effluent sample at 24 hours

Date of Experiment: May 17, 1999

Element	Relative Atomic Number	Normal wt %	Atomic %
Fe	0.0000	0.00	0.00
Ca	0.1062	11.97	8.64
Mg	0.0060	0.68	0.81
K	0.0022	0.26	0.19
Ti	0.0000	0.00	0.00
Na	0.0054	0.73	0.93
Mn	0.0005	0.06	0.03
P	0.0000	0.00	0.00
Cl	0.0028	0.39	0.32
S	0.0000	0.00	0.00
Al	0.1309	13.84	14.84
Au	0.0000	0.00	0.00
Si	0.6111	72.07	74.24
Total		**100.00**	**100.00**

Table I 34. Quantitative analysis of particle 3 clarifier 4 effluent sample at 24 hours

Date of Experiment: May 17, 1999

Element	Relative Atomic Number	Normal wt %	Atomic %
Fe	0.0353	4.03	2.16
Ca	0.1025	11.52	8.62
Mg	0.0122	1.52	1.86
K	0.0066	0.78	0.60
Ti	0.0064	0.76	0.48
Na	0.0073	1.12	1.45
P	0.0082	1.47	1.43
Cl	0.0300	4.09	3.46
S	0.0000	0.00	0.00
Al	0.0344	3.86	4.28
Au	0.0000	0.00	0.00
Si	0.6379	70.85	75.64
Total		**100.00**	**99.98**

Table I 35. Quantitative analysis of particle 1 clarifier 4 effluent sample at 48 hours

Date of Experiment: May 17, 1999

Element	Relative Atomic Number	Normal wt %	Atomic %
Fe	0.0690	7.78	4.53
Ca	0.3935	41.34	33.80
Mg	0.0250	4.34	5.94
K	0.0000	0.00	0.00
Ti	0.0000	0.00	0.00
Na	0.0643	12.80	18.33
P	0.0888	11.37	12.05
Cl	0.0532	6.17	5.77
S	0.0000	0.00	0.00
Al	0.1085	16.20	19.64
Total		**100.00**	**100.06**

Table I 36. Quantitative analysis of particle 2 clarifier 4 effluent sample at 48 hours

Date of Experiment: May 17, 1999

Element	Relative Atomic Number	Normal wt %	Atomic %
Fe	0.1513	16.68	10.34
Ca	0.2369	25.01	21.61
Mg	0.0313	5.75	8.11
K	0.0076	0.82	0.70
Ti	0.0000	0.00	0.00
Na	0.0380	8.88	13.36
P	0.0603	7.77	8.73
Cl	0.1388	15.97	15.65
S	0.0000	0.00	0.00
Al	0.0927	14.58	18.69
Mn	0.0401	4.54	2.84
Total		**100.00**	**100.03**

Table I 37. Quantitative analysis of particle 3 clarifier 4 effluent sample at 48 hours

Date of Experiment: May 17, 1999

Element	Relative Atomic Number	Normal wt %	Atomic %
Fe	0.0000	0.00	0.00
Ca	0.2192	24.10	18.09
Mg	0.0627	10.13	12.61
K	0.0014	0.16	0.12
Ti	0.0000	0.00	0.00
Na	0.1219	18.94	24.76
P	0.0357	4.56	4.40
Cl	0.2314	26.51	22.51
S	0.0000	0.00	0.00
Al	0.1027	15.60	17.49
Total		**100.00**	**99.98**

Figure I 1. Overview of blank quartz coupon

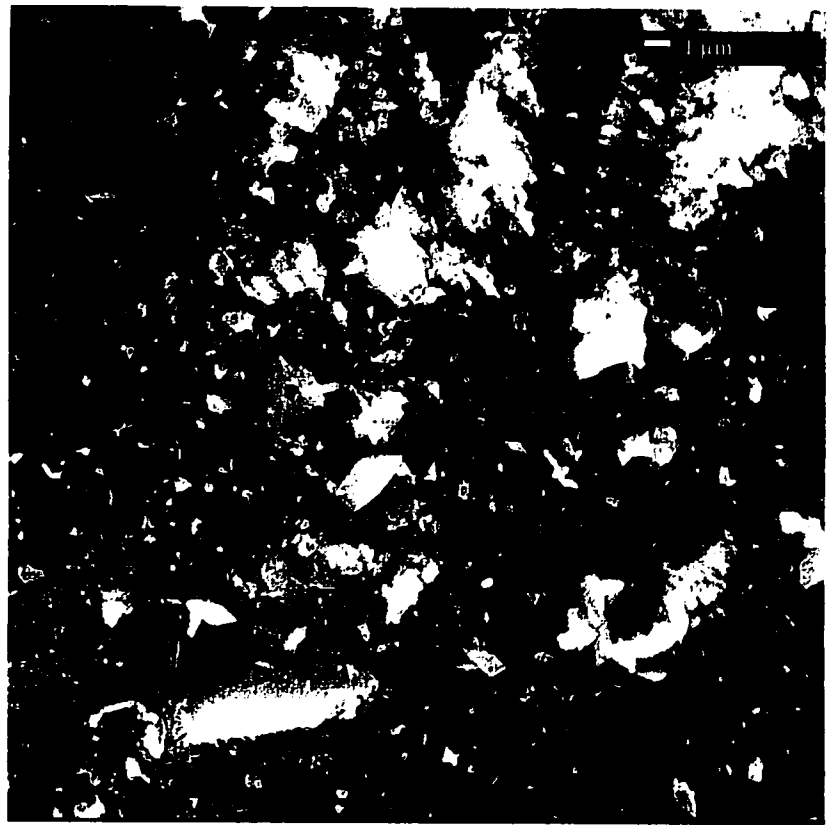

Figure I 2. Scratches on surface of blank

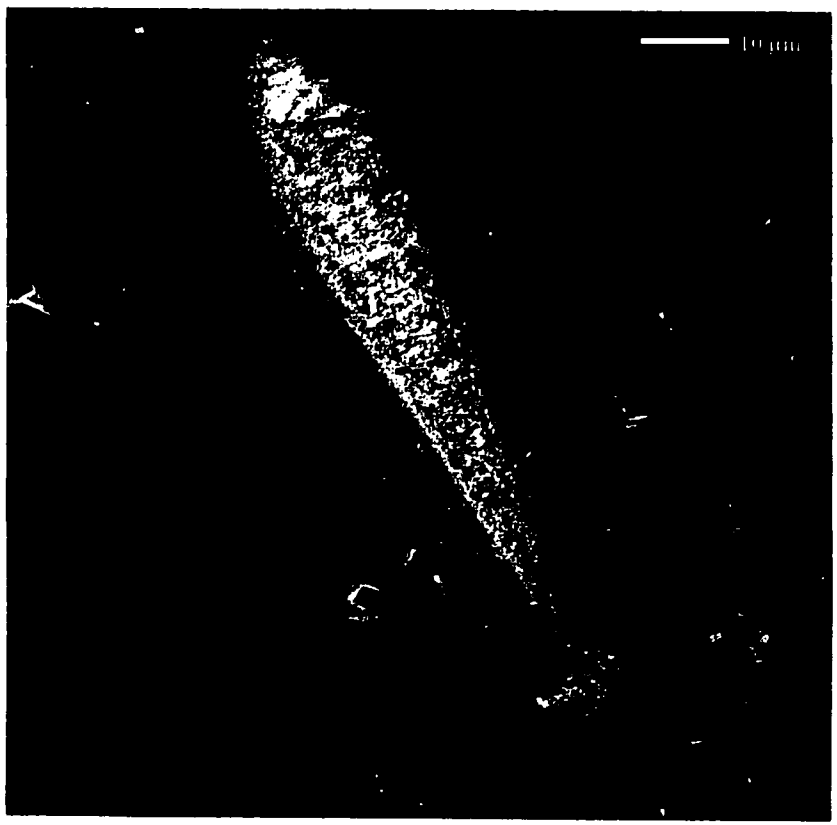

Figure I 3. Scratch on the surface of clean quartz coupon

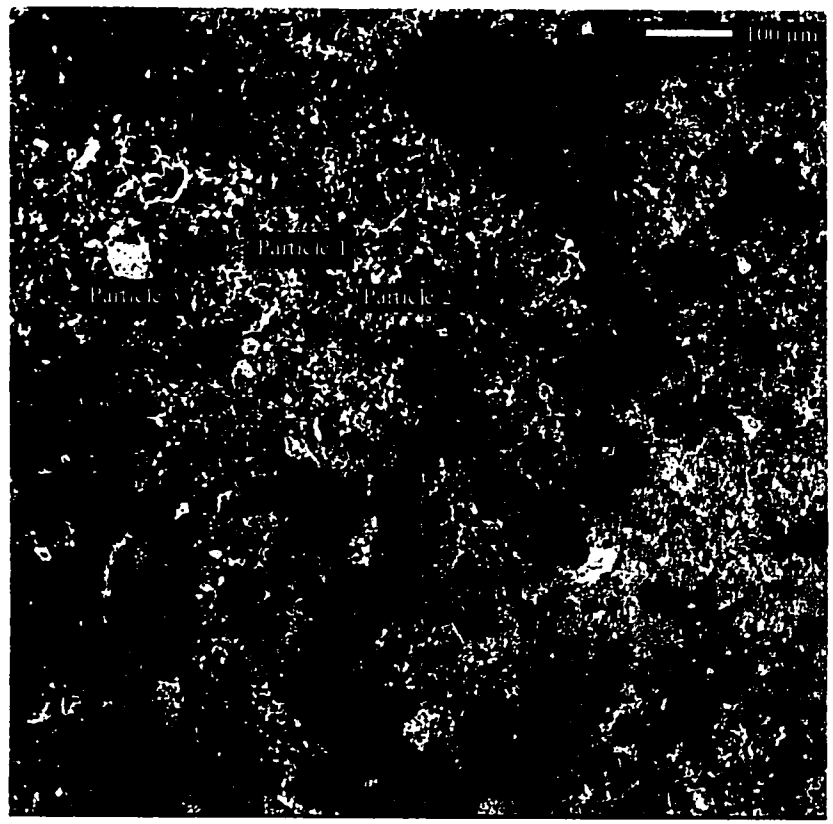

Figure I 4. Overview of surface of 1.5 mg/L Experiment 1 at 24 hours.

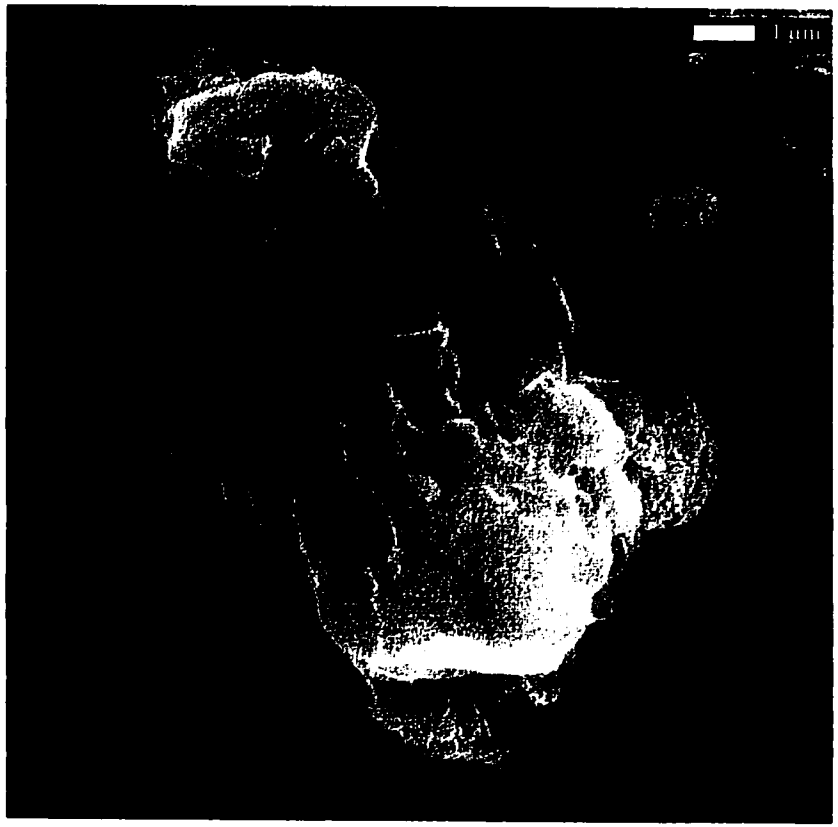

Figure I 5. Particle 1 on 1.5 mg/L Experiment 1 at 24 hours.

Figure I 6. Particle 2 on 1.5 mg/L Experiment 1 at 24 hours.

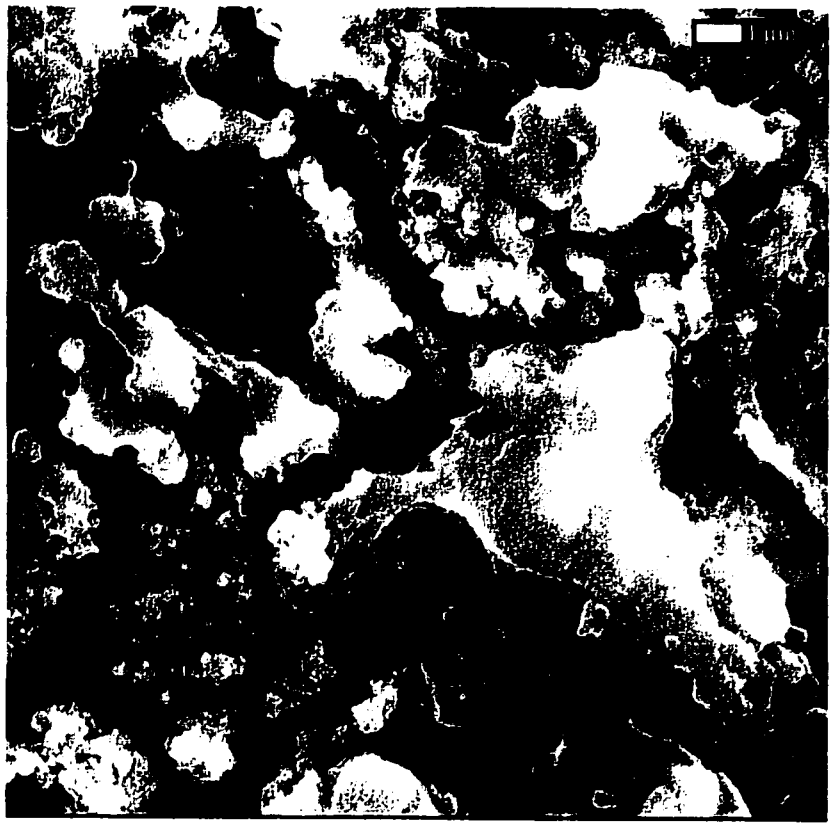

Figure I 7. Particle 3 on 1.5 mg/L Experiment 1 at 24 hours

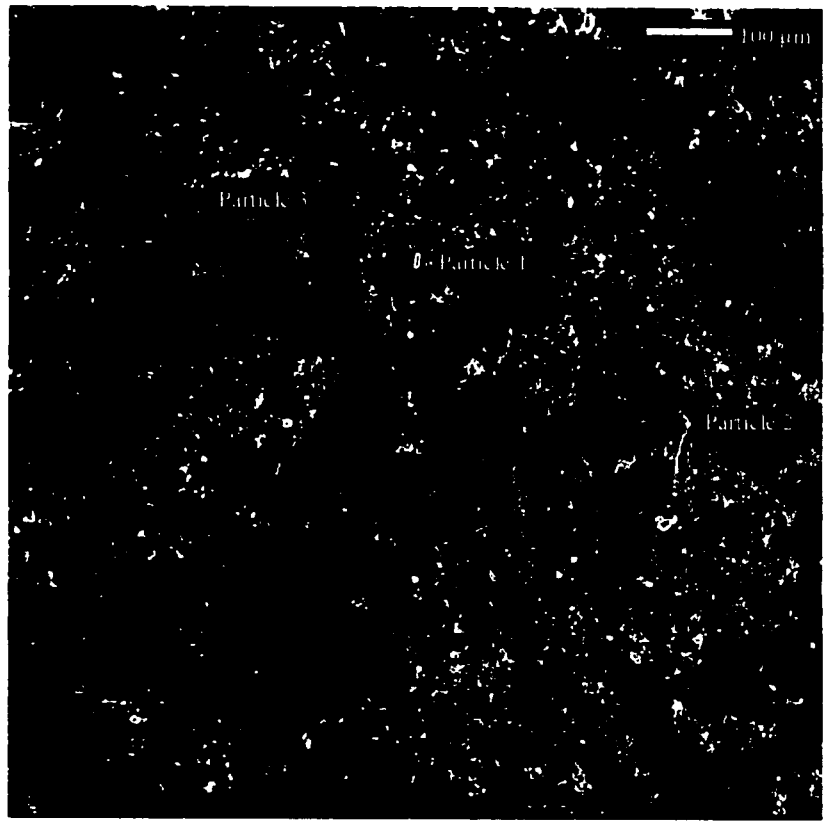

Figure I 8. Overview of surface of 1.5 mg/L Experiment 1 at 48 hours.

Figure I 9. Particle 1 on 1.5 mg/L Experiment 1 at 48 hours

Figure I 10. Particle 2 on 1.5 mg/L Experiment 1 at 48 hours

Figure I 11. Bacteria found at particle 3 on 1.5 mg/L Experiment 1 at 48 hours.

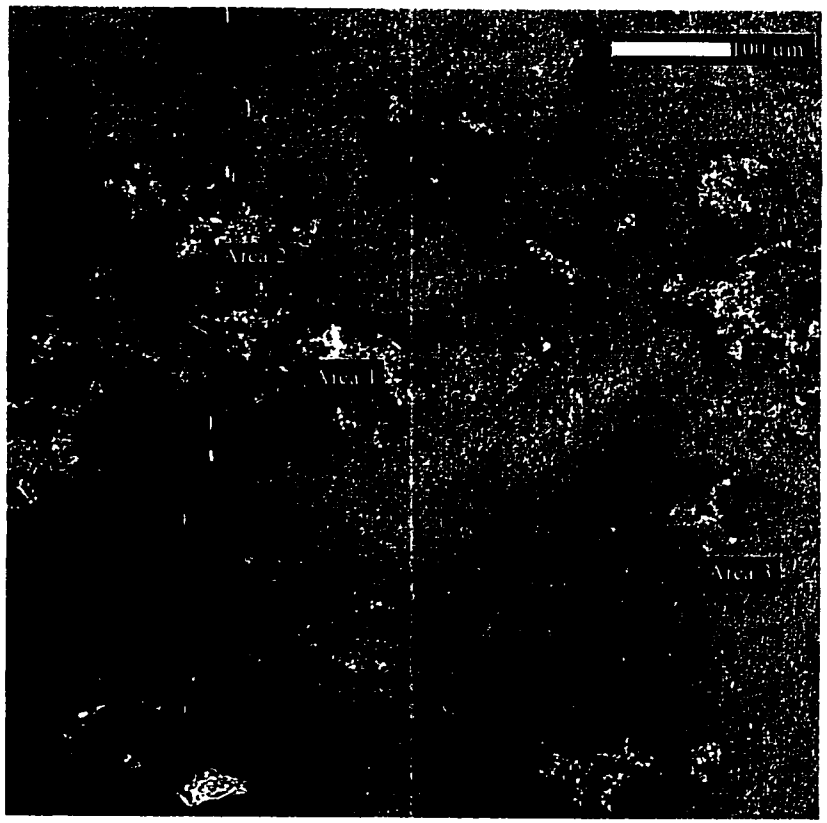

Figure I 12. Overview of surface of 1.5 mg/L Experiment 2 at 24 hours

Figure I 13. Area 1 on 1.5 mg/L experiment 2 at 24 hours

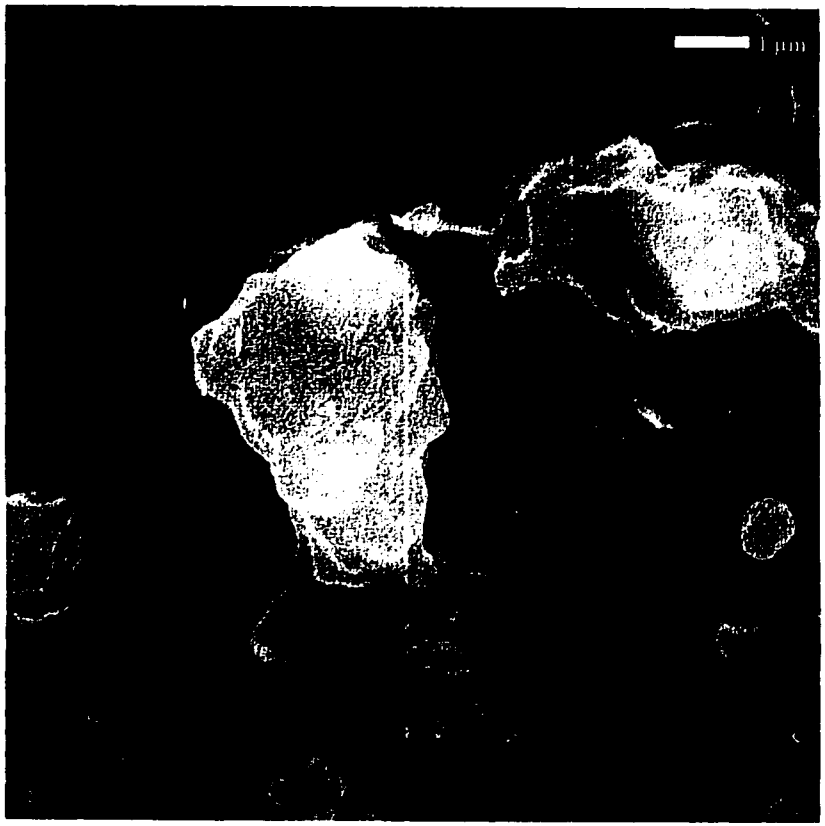

Figure I 14. Area 2 on 1.5 mg/L experiment 2 at 24 hours

Figure I 15. Area 3 on 1.5 mg/L experiment 2 at 24 hours

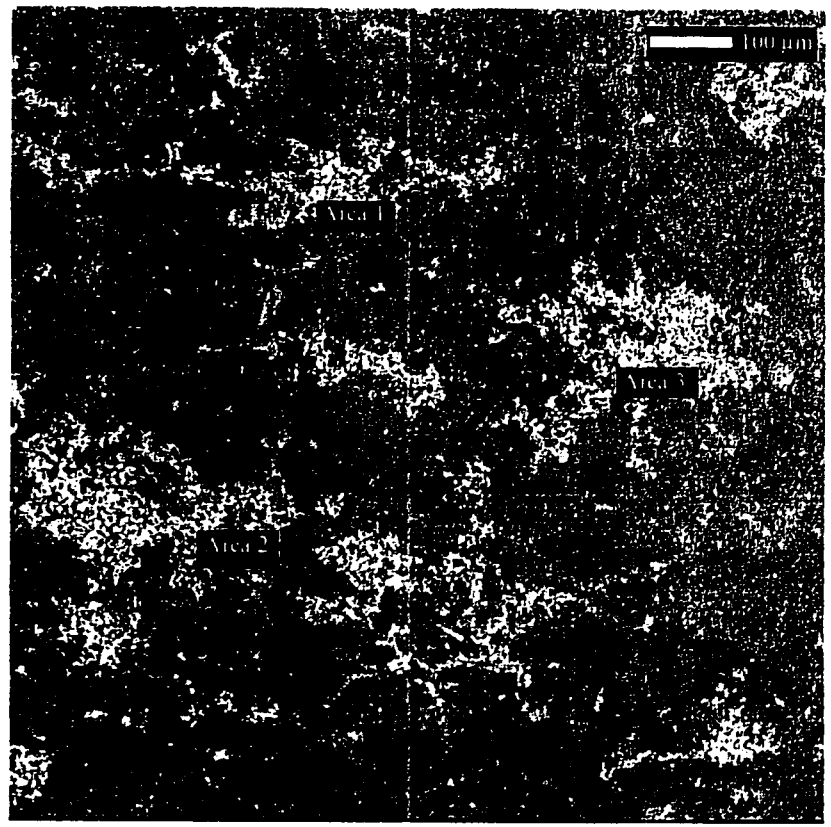

Figure I 16. 1.5 mg/L experiment 2 overview at 48 hours.

Figure I 17. Area 1 on 1.5 mg/L experiment 2 at 48 hours

Figure I 18. Area 2 on 1.5 mg/L experiment 2 at 48 hours

Figure I 19. Area 3 on 1.5 mg/L experiment 2 at 48 hours

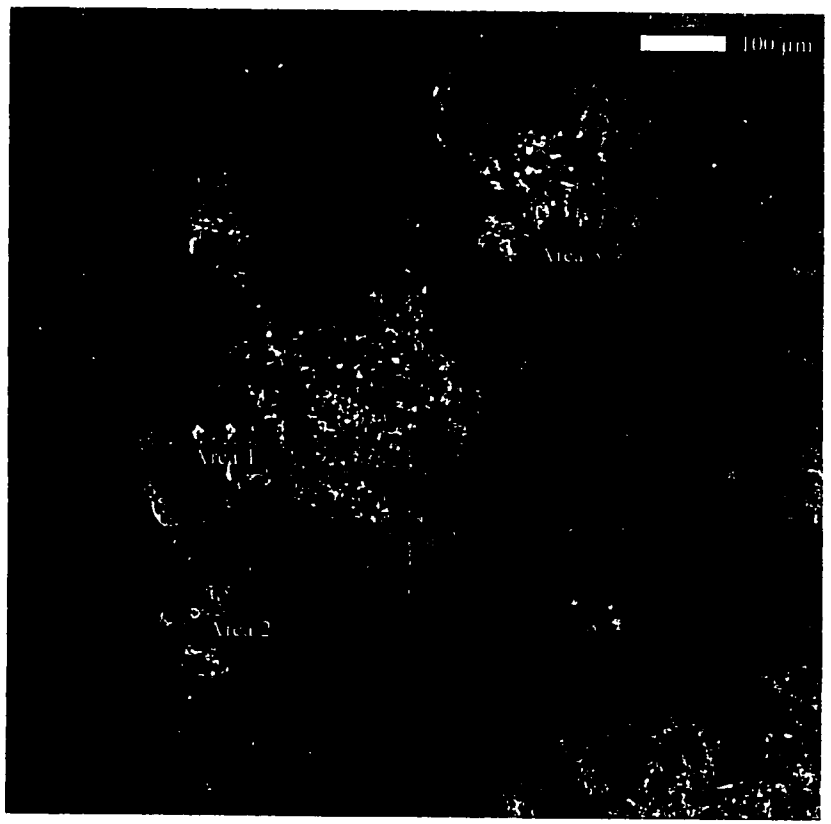

Figure I 20. 1.5 mg/L experiment 3 overview at 24 hours

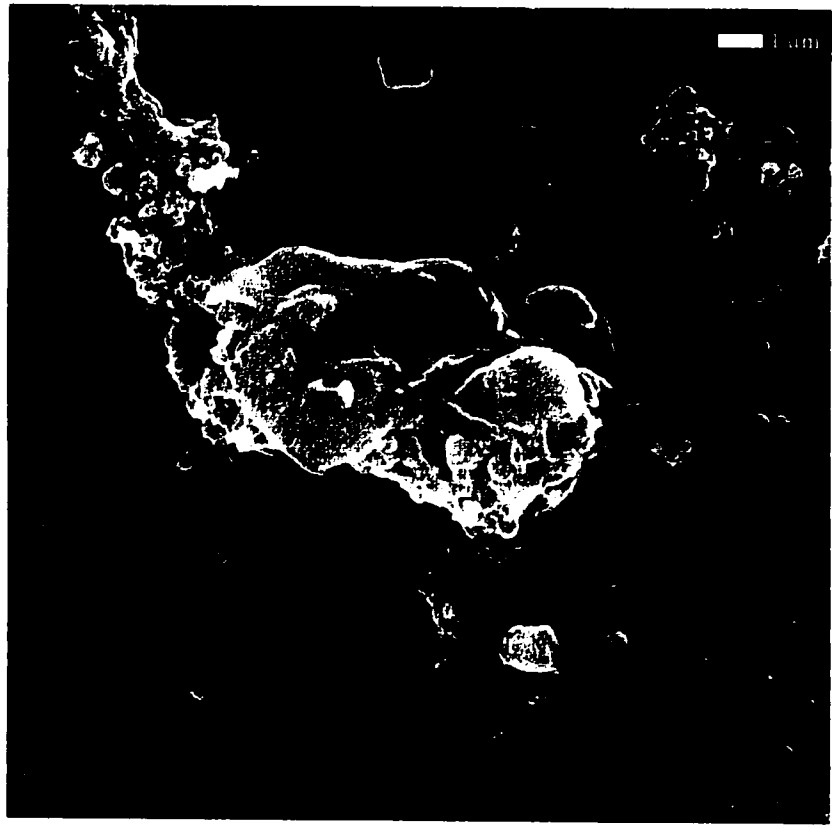

Figure I 21. Area 1 on 1.5 mg/L experiment 3 at 24 hours

Figure I 22. Area 2 on 1.5 mg/L experiment 3 at 24 hours.

Figure I 23. Area 3 on 1.5 mg/L experiment 3 at 24 hours.

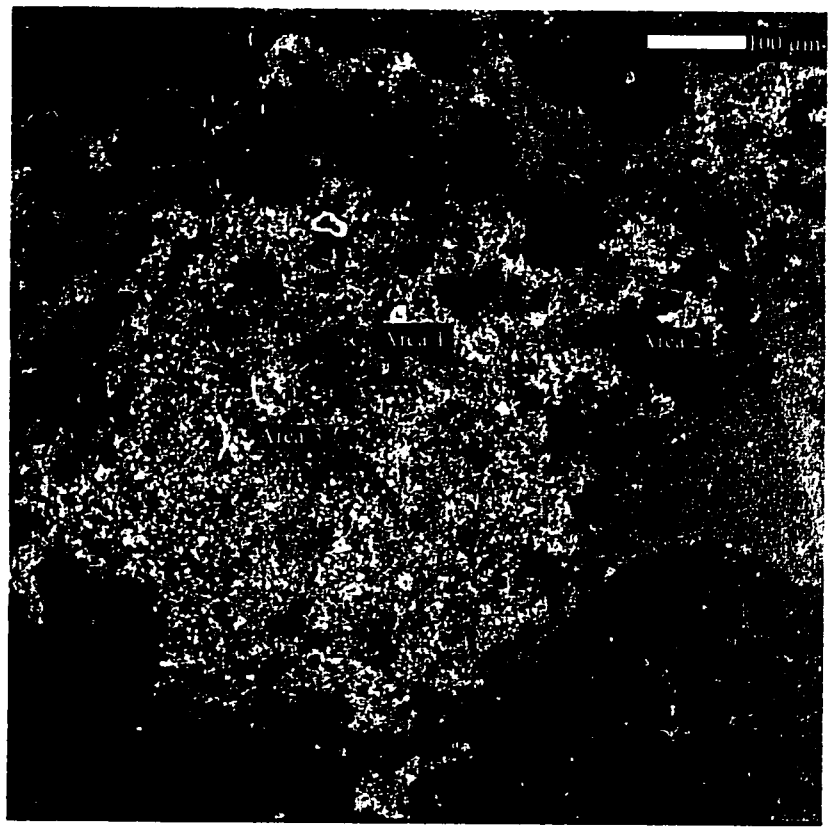

Figure I 24. 1.5 mg/L experiment 3 overview at 48 hours

Figure I 25. Area 1 on 1.5 mg/L experiment 3 at 48 hours

Figure I 26. Area 2 on 1.5 mg/L experiment 3 at 48 hours

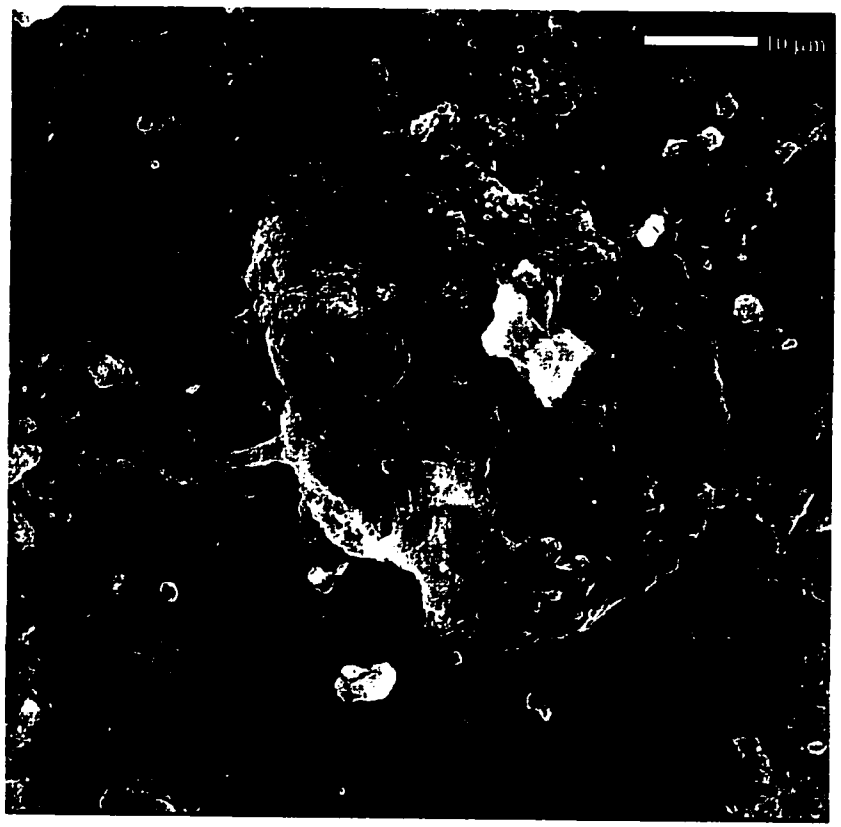

Figure I 27. Area 3 on 1.5 mg/L experiment 3 at 48 hours.

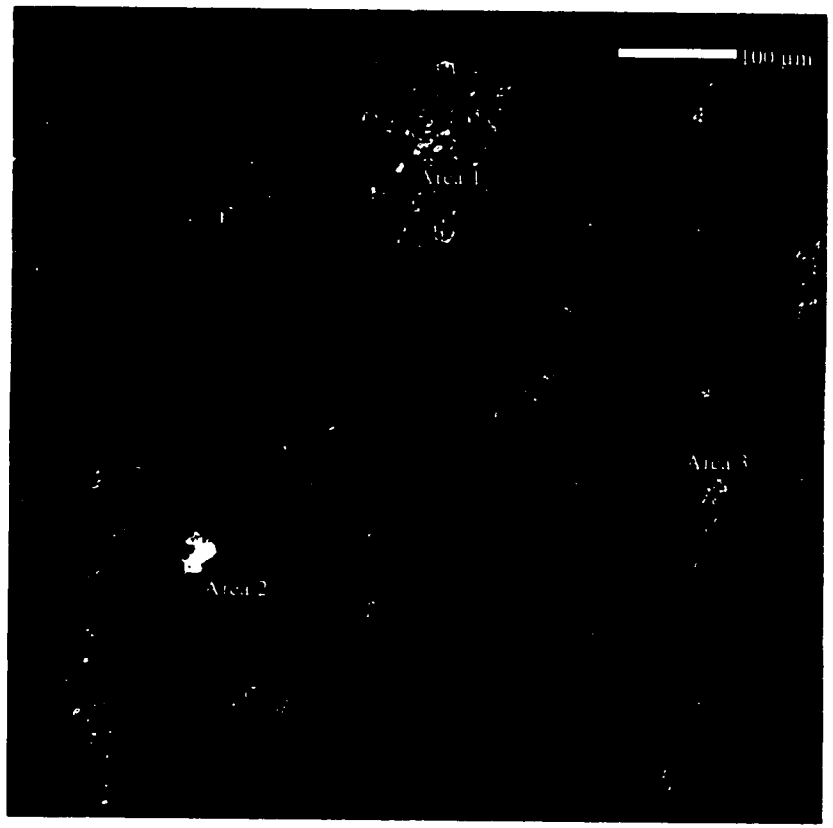

Figure I 28. Overview of 3.0 mg/L sample

Figure I 29. Area 1 on 3.0 mg/L sample at 24 hours

Figure I 30. Area 2 on 3.0 mg/L sample at 24 hours.

Figure I 31. Area 3 on 3.0 mg/L sample at 24 hours.

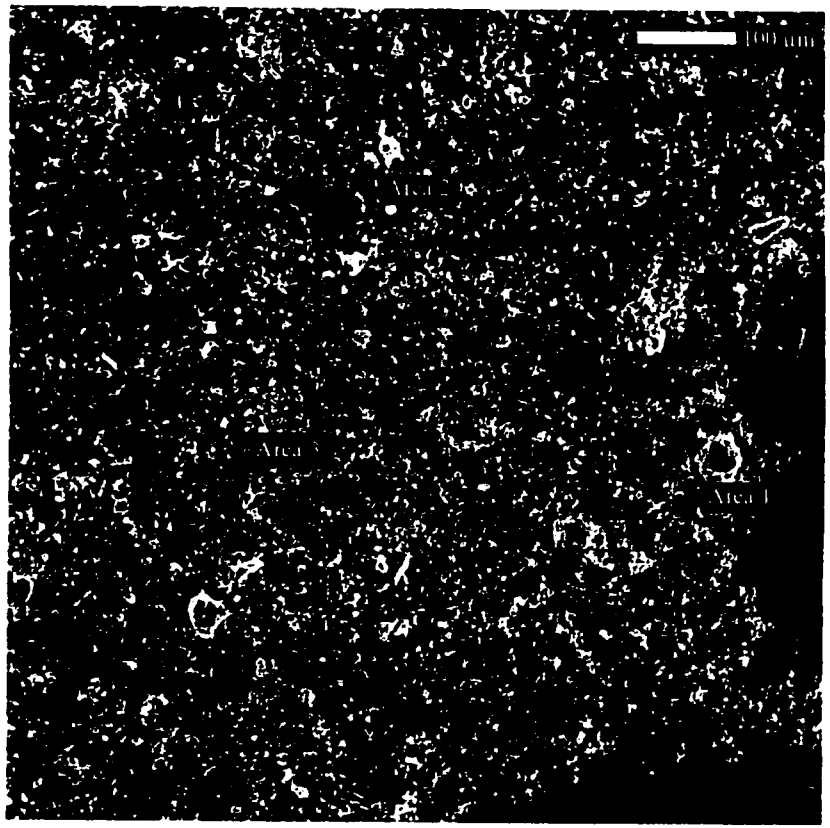

Figure I 32. Overview of 3.0 mg/L sample at 48 hours.

Figure I 33. Area 1 on 3.0 mg/L sample at 48 hours

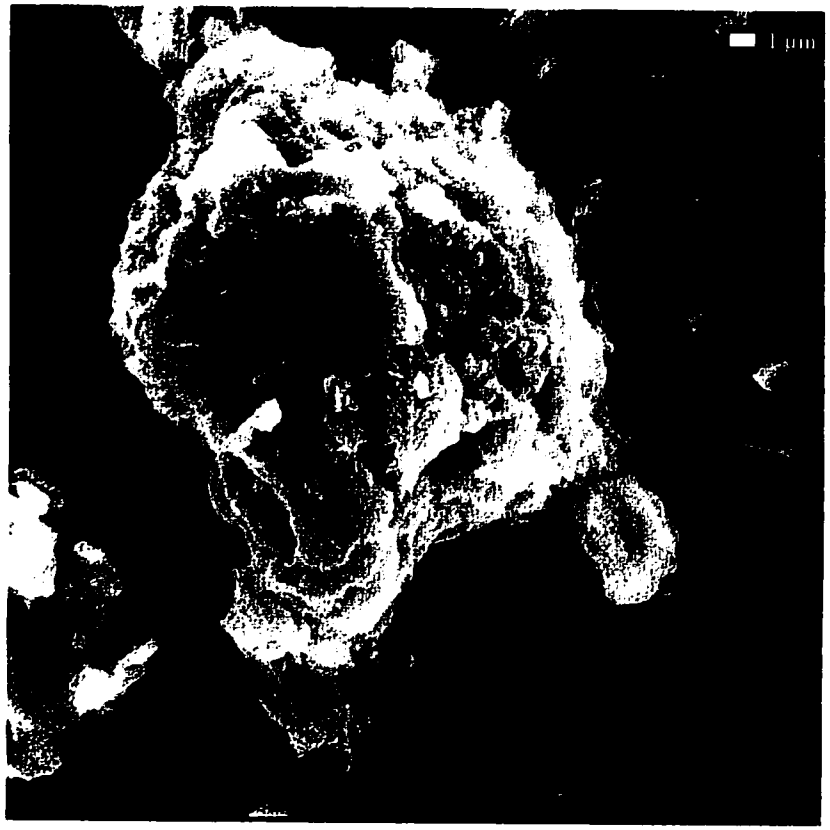

Figure I 34. Area 2 on 3.0 mg/L sample at 48 hours.

Figure I 35. Area 3 on 3.0 mg/L sample at 48 hours.

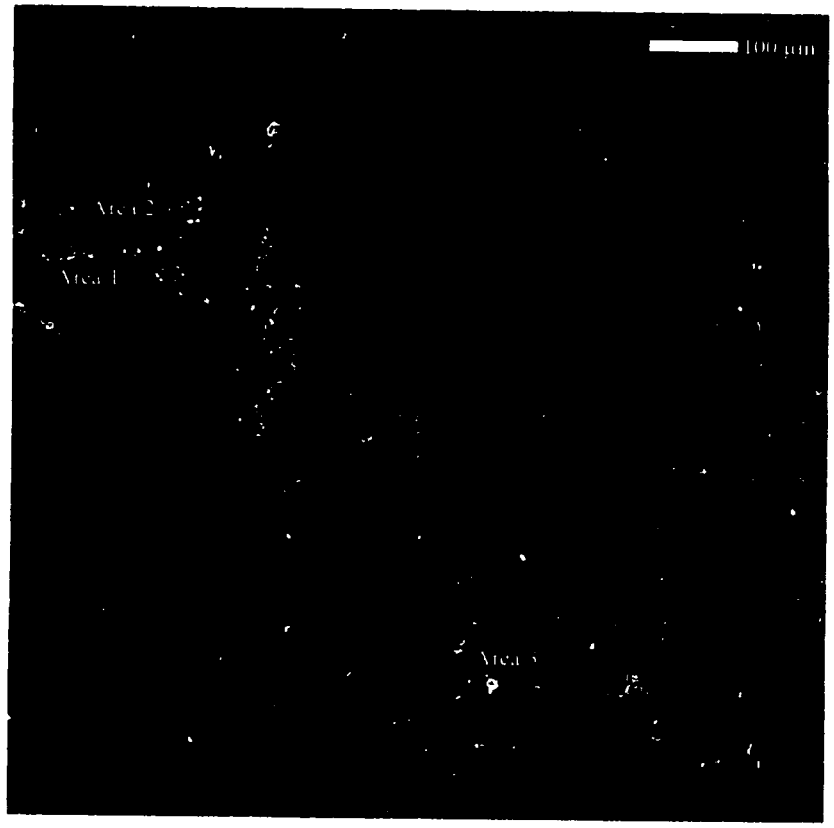

Figure I 36. Overview of clarifier 4 effluent sample at 24 hours

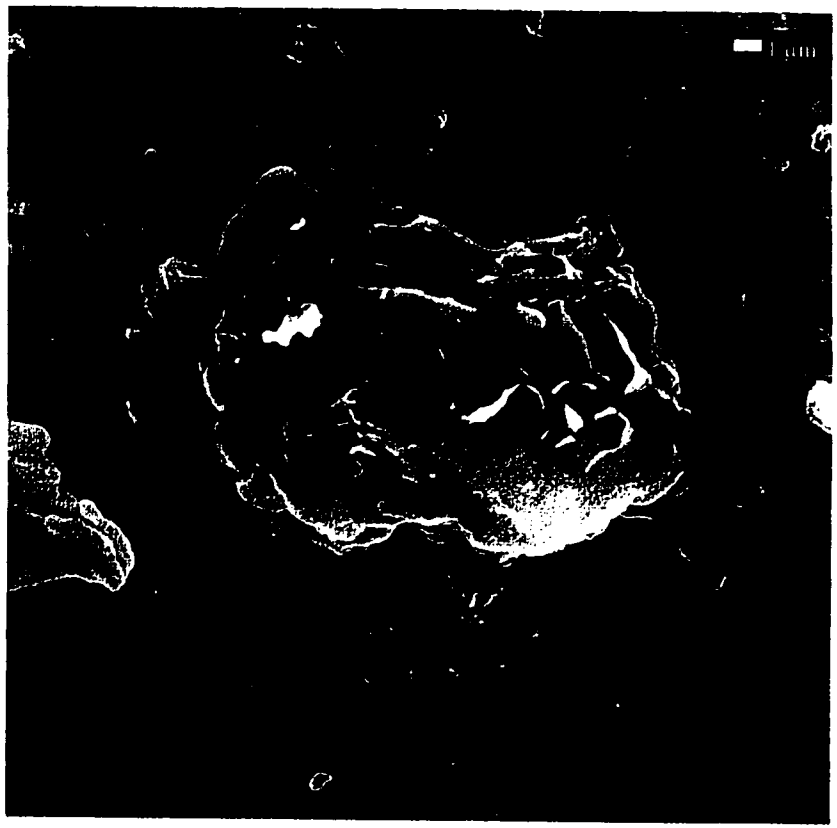

Figure I 37. Area 1 on clarifier 4 effluent sample at 24 hours.

Figure I 38. Area 2 on clarifier 4 effluent sample at 24 hours.

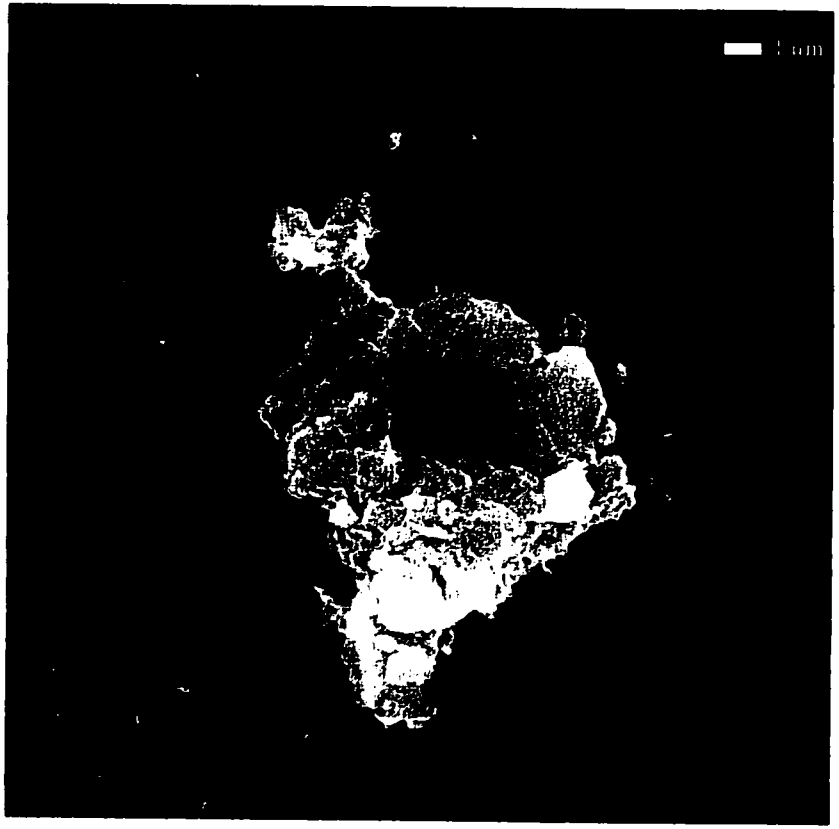

Figure I 39. Area 3 on clarifier 4 effluent sample at 24 hours.

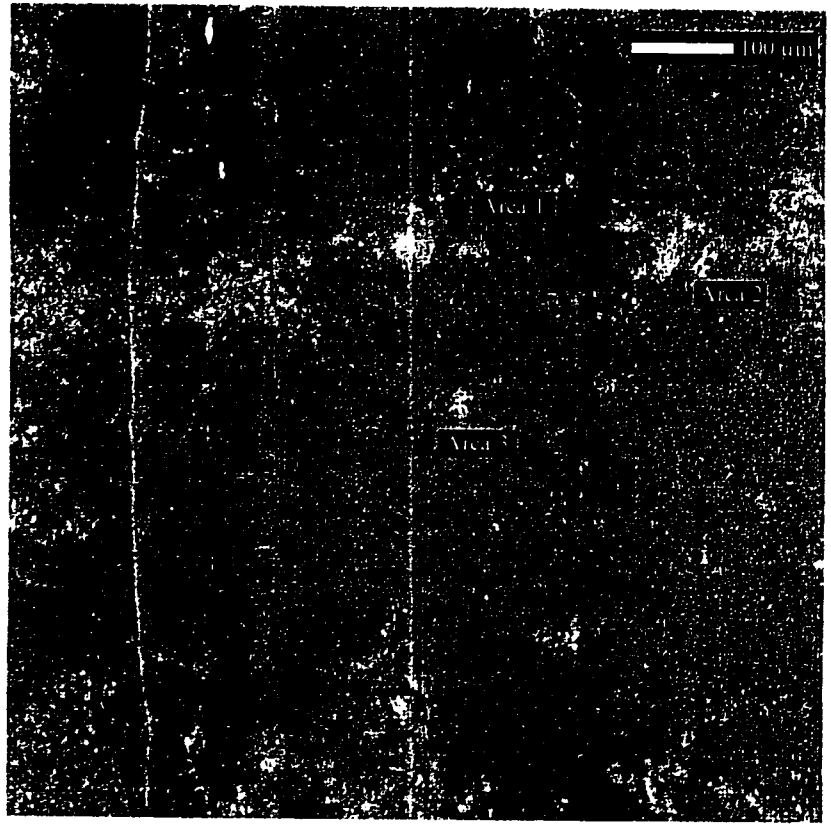

Figure I 40. Overview of clarifier 4effluent sample at 48 hours

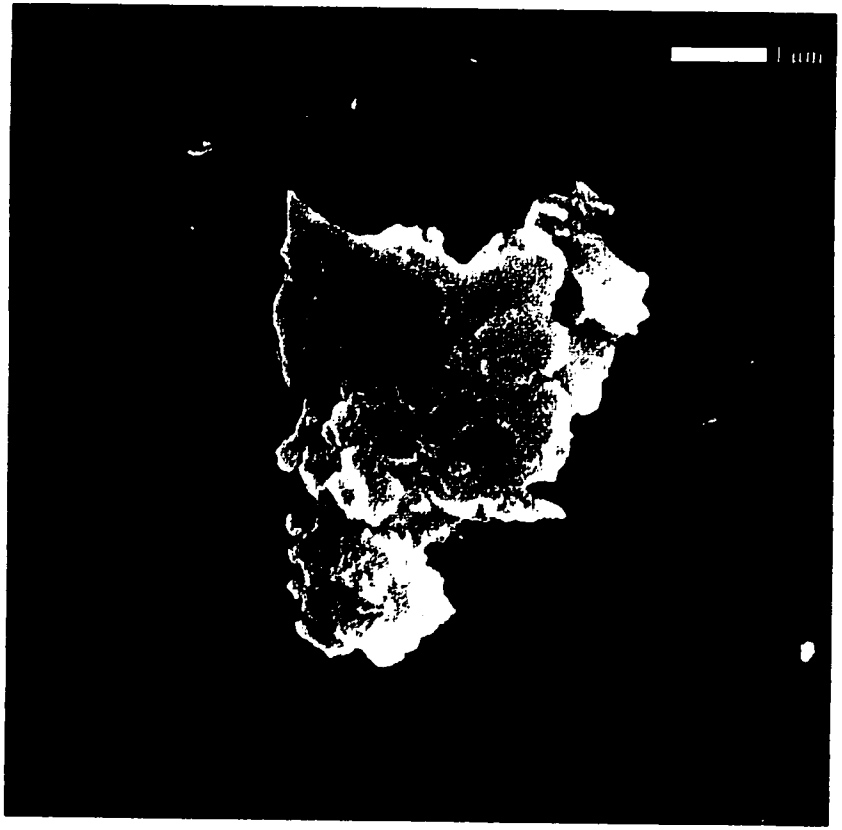

Figure I 41. Area 1 on clarifier 4 effluent sample at 48 hours.

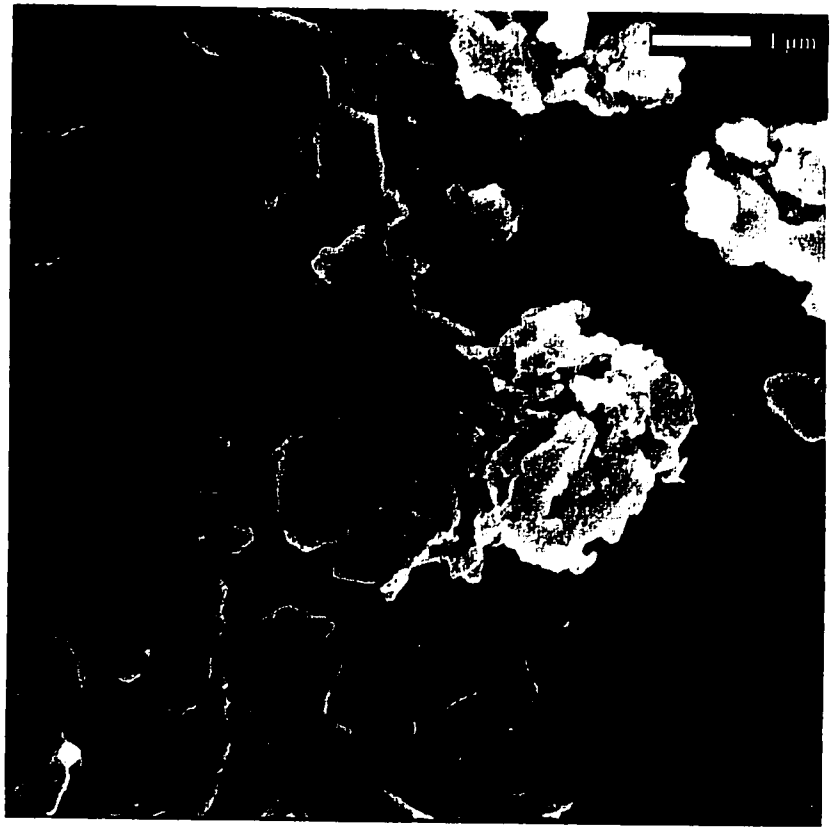

Figure I 42. Area 2 on clarifier 4 effluent sample at 48 hours

Figure I 43. Area 3 on clarifier 4 effluent at 48 hours.

Appendix J. Transmittance Data for Quartz Glass Pieces

Table J 1. Transmittance Data for Quartz glass pieces

Date of Experiment: April 29, 1999

	1.5 mg/L at 24 hours Experiment 1		1.5 mg/L at 48 hour Experiment 1		1.5 mg/L at 24 hours Experiment 2		1.5 mg/L at 48 hours Experiment 2	
Trial	Absorbance (254 nm)	%T	Absorbance (254 nm)	%T	Absorbance (254 nm)	%T	Absorbance (254 nm)	%T
1	0.126	74.6	0.042	90.8	0.034	92.4	0.075	84.3
2	0.126	74.6	0.176	66.6	0.024	94.7	0.069	85.1
3	0.118	76.1	0.042	90.0	0.065	86.1	0.050	89.2
4	0.126	74.6	0.045	90.4	0.056	87.8	0.061	86.8
5	0.120	75.9	0.178	66.4	0.024	94.7	0.078	83.6
6	0.119	76.0	0.192	64.2	0.052	88.8	0.055	88.1
Average	**0.123**	**75.3**	**0.113**	**78.1**	**0.042**	**90.7**	**0.064**	**86.1**

Table J 2. Transmittance Data for Quartz glass pieces

Date of Experiment: April 29, 1999

	1.5 mg/L at 24 hours Experiment 3		1.5 mg/L at 48 hours Experiment 3		3.0 mg/L at 24 hours		3.0 mg/L at 48 hours	
Trial	Absorbance (254 nm)	%T	Absorbance (254 nm)	%T	Absorbance (254 nm)	%T	Absorbance (254 nm)	%T
1	0.101	79.2	0.073	84.4	0.041	91.2	0.154	70.0
2	0.092	80.9	0.050	89.3	0.037	91.7	0.114	76.8
3	0.091	81.1	0.073	84.4	0.034	92.3	0.165	68.3
4	0.098	79.7	0.062	86.6	0.043	90.5	0.140	72.3
5	0.070	85.1	0.046	90.1	0.039	91.4	0.145	71.4
6	0.076	83.7	0.060	87.2	0.039	91.3	0.153	70.3
Average	**0.088**	**81.6**	**0.060**	**87.0**	**0.039**	**91.4**	**0.145**	**71.5**

Table J 3. Transmittance Data for Quartz glass pieces

Date of Experiment: April 29, 1999

	Treated Effluent at 24 hours		Treated Effluent at 48 hours	
Trial	Absorbance (254 nm)	%T	Absorbance (254 nm)	%T
1	0.043	90.4	0.030	93.3
2	0.012	97.1	0.033	92.7
3	0.043	90.4	0.021	95.1
4	0.029	93.8	0.023	94.6
5	0.022	95.0	0.027	93.9
6	0.044	90.3	0.022	95.1
Average	**0.032**	**92.8**	**0.026**	**94.1**

Appendix K. Independent Laboratory Results Table

K 1. 1.5 mg/L experiment 2 at 24 hours

Metals, Dissolved	Results (μg)	Detection limit (μg)	Mass per area (μg/mm^2)	Lamp scale (μg/lamp)
Aluminum (Al)	4.5	0.2	0.01500	1908
Barium (Ba)	0.071	0.002	0.00024	30.104
Beryllium (Be)	0.00	0.01	0.00000	0
Bismuth (Bi)	0.004	0.001	0.00001	1.696
Boron (B)	0.38	0.04	0.00127	161.12
Cadmium (Cd)	0.022	0.002	0.00007	9.328
Calcium (Ca)	11	1	0.03667	4664
Chromium (Cr)	0.481	0.008	0.00160	203.944
Cobalt (Co)	0.004	0.002	0.00001	1.696
Copper (Cu)	0.08	0.24	0.00027	33.92
Iron (Fe)	3.2	0.2	0.01067	1356.8
Lead (Pb)	0.137	0.002	0.00046	58.088
Magnesium (Mg)	1.8	0.2	0.00600	763.2
Manganese (Mn)	0.056	0.002	0.00019	23.744
Molybdenum (Mo)	0.003	0.002	0.00001	1.272
Nickel (Ni)	0.042	0.002	0.00014	17.808
Phosphorus (P)	2.5	0.2	0.00833	1060
Potassium (K)	3.0	0.2	0.01000	1272
Silver (Ag)	0.004	0.004	0.00001	1.696
Sodium (Na)	9	2	0.03000	3816
Strontium (Sr)	0.070	0.002	0.00023	29.68
Thallium (Ti)	0.000	0.001	0.00000	0
Tin (Sn)	0.067	0.004	0.00022	28.408
Uranium (U)	<0.002	0.002	0.00001	<0.848
Vanadium (V)	0.009	0.002	0.00003	3.816
Zinc (Zn)	0.43	0.04	0.00143	182.32

Table K 2. 1.5 mg/L experiment 2 48 hours

Metals, Dissolved	Results (μg)	Detection limit (μg)	Mass per area (μg/mm^2)	Lamp scale (μg/lamp)
Aluminum (Al)	6.1	0.2	0.02033	2582.33
Barium (Ba)	0.164	0.002	0.00055	69.43
Beryllium (Be)	<0.01	0.01	0.00003	4.23
Bismuth (Bi)	0.003	0.001	0.00001	1.27
Boron (B)	0.22	0.04	0.00073	93.13
Cadmium (Cd)	0.004	0.002	0.00001	1.69
Calcium (Ca)	23	1	0.07667	9736.67
Chromium (Cr)	0.608	0.008	0.00203	257.39
Cobalt (Co)	0.005	0.002	0.00002	2.12
Copper (Cu)	0.07	0.24	0.00024	30.90
Iron (Fe)	7.6	0.2	0.02533	3217.33
Lead (Pb)	0.031	0.002	0.00010	13.12
Magnesium (Mg)	4.1	0.2	0.01367	1735.67
Manganese (Mn)	0.117	0.002	0.00039	49.53
Molybdenum (Mo)	0.007	0.002	0.00002	2.96
Nickel (Ni)	0.062	0.002	0.00021	26.25
Phosphorus (P)	4.2	0.2	0.01400	1778.00
Potassium (K)	1.3	0.2	0.00433	550.33
Silver (Ag)	0.006	0.004	0.00002	2.54
Sodium (Na)	5	2	0.01667	2116.67
Strontium (Sr)	0.189	0.002	0.00063	80.01
Thallium (Ti)	<0.001	0.001	0.00000	0.42
Tin (Sn)	1.442	0.004	0.00481	610.45
Uranium (U)	0.002	0.002	0.00001	0.85
Vanadium (V)	0.012	0.002	0.00004	5.08
Zinc (Zn)	0.59	0.04	0.00197	249.77

Table K 3. 1.5 mg/L experiment 3 at 24 hours

Metals, Dissolved	Results (μg)	Detection limit (μg)	Mass per area (μg/mm^2)	Lamp scale (μg/lamp)
Aluminum (Al)	6.5	0.2	0.02167	2751.67
Barium (Ba)	0.206	0.002	0.00069	87.21
Beryllium (Be)	<0.01	0.01	0.00003	4.23
Bismuth (Bi)	0.005	0.001	0.00002	2.12
Boron (B)	0.19	0.04	0.00063	80.43
Cadmium (Cd)	0.003	0.002	0.00001	1.27
Calcium (Ca)	19	1	0.06333	8043.33
Chromium (Cr)	1.117	0.008	0.00372	472.86
Cobalt (Co)	<0.002	0.002	0.00001	0.85
Copper (Cu)	0.09	0.24	0.00030	38.10
Iron (Fe)	9.2	0.2	0.03067	3894.67
Lead (Pb)	0.041	0.002	0.00014	17.36
Magnesium (Mg)	5.1	0.2	0.01700	2159.00
Manganese (Mn)	0.130	0.002	0.00043	55.03
Molybdenum (Mo)	0.008	0.002	0.00003	3.39
Nickel (Ni)	0.080	0.002	0.00027	33.87
Phosphorus (P)	4.7	0.2	0.01567	1989.67
Potassium (K)	1.8	0.2	0.00600	762.00
Silver (Ag)	0.007	0.004	0.00002	2.96
Sodium (Na)	10	2	0.03333	4233.33
Strontium (Sr)	0.178	0.002	0.00059	75.35
Thallium (Ti)	<0.001	0.001	0.00000	0.42
Tin (Sn)	0.763	0.004	0.00254	323.00
Uranium (U)	0.002	0.002	0.00001	0.85
Vanadium (V)	0.013	0.002	0.00004	5.50
Zinc (Zn)	1.49	0.04	0.00497	630.77

Table K 4. 1.5 mg/l experiment 3 at 48 hours

Metals, Dissolved	Results (μg)	Detection limit (μg)	Mass per area (μg/mm^2)	Lamp scale (μg/lamp)
Aluminum (Al)	2.9	0.2	0.009667	1227.67
Barium (Ba)	0.076	0.002	0.000253	32.17
Beryllium (Be)	<0.01	0.01	0.000033	4.23
Bismuth (Bi)	0.002	0.001	0.000007	0.85
Boron (B)	0.14	0.04	0.000467	59.27
Cadmium (Cd)	0.011	0.002	0.000037	4.66
Calcium (Ca)	10	1	0.033333	4233.33
Chromium (Cr)	1.010	0.008	0.003367	427.57
Cobalt (Co)	<0.002	0.002	0.000007	0.85
Copper (Cu)	0.12	0.24	0.000383	48.68
Iron (Fe)	2.6	0.2	0.008667	1100.67
Lead (Pb)	0.020	0.002	0.000067	8.47
Magnesium (Mg)	2.3	0.2	0.007667	973.67
Manganese (Mn)	0.033	0.002	0.000110	13.97
Molybdenum (Mo)	0.017	0.002	0.000057	7.20
Nickel (Ni)	0.052	0.002	0.000173	22.01
Phosphorus (P)	2.0	0.2	0.006667	846.67
Potassium (K)	1.6	0.2	0.005333	677.33
Silver (Ag)	<0.004	0.004	0.000013	1.69
Sodium (Na)	8	2	0.026667	3386.67
Strontium (Sr)	0.073	0.002	0.000243	30.90
Thallium (Ti)	<0.001	0.001	0.000003	0.42
Tin (Sn)	1.130	0.004	0.003767	478.37
Uranium (U)	<0.002	0.002	0.000007	0.85
Vanadium (V)	0.005	0.002	0.000017	2.12
Zinc (Zn)	0.78	0.04	0.002600	330.20

Table K 5. Clarifier 4 effluent at 24 hours

Metals, Dissolved	Results (μg)	Detection limit (μg)	Mass per area (μg/mm^2)	Lamp scale (μg/lamp)
Aluminum (Al)	6.4	0.2	0.021333	2709.33
Barium (Ba)	0.228	0.002	0.000760	96.52
Beryllium (Be)	<0.01	0.01	0.000033	4.23
Bismuth (Bi)	0.006	0.001	0.000020	2.54
Boron (B)	0.15	0.04	0.000500	63.50
Cadmium (Cd)	0.002	0.002	0.000007	0.85
Calcium (Ca)	18	1	0.060000	7620.00
Chromium (Cr)	1.450	0.008	0.004833	613.83
Cobalt (Co)	<0.002	0.002	0.000007	0.85
Copper (Cu)	<0.01	0.24	0.000033	4.23
Iron (Fe)	14.0	0.2	0.046667	5926.67
Lead (Pb)	0.072	0.002	0.000240	30.48
Magnesium (Mg)	4.0	0.2	0.013333	1693.33
Manganese (Mn)	0.504	0.002	0.001680	213.36
Molybdenum (Mo)	0.007	0.002	0.000023	2.96
Nickel (Ni)	0.085	0.002	0.000283	35.98
Phosphorus (P)	5.8	0.2	0.019333	2455.33
Potassium (K)	1.6	0.2	0.005333	677.33
Silver (Ag)	0.011	0.004	0.000037	4.66
Sodium (Na)	7	2	0.023333	2963.33
Strontium (Sr)	0.169	0.002	0.000563	71.54
Thallium (Ti)	<0.001	0.001	0.000003	0.42
Tin (Sn)	1.110	0.004	0.003700	469.90
Uranium (U)	<0.002	0.002	0.000007	0.85
Vanadium (V)	0.013	0.002	0.000043	5.50
Zinc (Zn)	1.49	0.04	0.004967	630.77

Table K 6. Clarifier 4 effluent at 48 hours

Metals, Dissolved	Results (μg)	Detection limit (μg)	Mass per area (μg/mm^2)	Lamp scale (μg/lamp)
Aluminum (Al)	7.5	0.2	0.02500	3175.00
Barium (Ba)	0.487	0.002	0.00162	206.16
Beryllium (Be)	<0.01	0.01	0.00003	4.23
Bismuth (Bi)	0.005	0.001	0.00002	2.12
Boron (B)	0.19	0.04	0.00063	80.43
Cadmium (Cd)	<0.002	0.002	0.00001	0.85
Calcium (Ca)	21	1	0.06933	8805.33
Chromium (Cr)	1.290	0.008	0.00430	546.10
Cobalt (Co)	<0.002	0.002	0.00001	0.85
Copper (Cu)	<0.01	0.24	0.00003	4.23
Iron (Fe)	10.6	0.2	0.03533	4487.33
Lead (Pb)	0.061	0.002	0.00020	25.82
Magnesium (Mg)	4.9	0.2	0.01633	2074.33
Manganese (Mn)	0.508	0.002	0.00169	215.05
Molybdenum (Mo)	0.006	0.002	0.00002	2.54
Nickel (Ni)	0.074	0.002	0.00025	31.33
Phosphorus (P)	5.2	0.2	0.01733	2201.33
Potassium (K)	1.8	0.2	0.00600	762.00
Silver (Ag)	0.014	0.004	0.00005	5.93
Sodium (Na)	8	2	0.02667	3386.67
Strontium (Sr)	0.132	0.002	0.00044	55.88
Thallium (Ti)	<0.001	0.001	0.00000	0.42
Tin (Sn)	0.934	0.004	0.00311	395.39
Uranium (U)	<0.002	0.002	0.00001	0.85
Vanadium (V)	0.015	0.002	0.00005	6.35
Zinc (Zn)	1.03	0.04	0.00343	436.03